ADVANCING TRAVEL DEMAND MODELS: FROM INDIVIDUAL CHOICES TO EQUILIBRIUM ANALYSIS WITH MATHEMATICAL PROGRAMMING METHODS

YU GU

PhD

The Hong Kong Polytechnic University

2024

The Hong Kong Polytechnic University

Department of Civil and Environmental Engineering

Advancing travel demand models: From individual choices to equilibrium analysis with mathematical programming methods

Yu GU

A thesis submitted in partial fulfilment of the requirements for the degree of Doctor of Philosophy

September 2023

CERTIFICATE OF ORIGINALITY

I hereby declare that this thesis entitled “Advanced travel demand models for future transportation systems: From individual choice to network equilibrium” is my own work and that, to the best of my knowledge and belief, it reproduces no material previously published or written, nor material that has been accepted for the award of any other degree or diploma, except where due acknowledgement has been made in the text.

_____(Signed)

GU Yu (Name of student)

Abstract

In the era of emerging technologies, a variety of innovative transport policies and mobility services have been implemented and promoted in the transition to future transportation systems, such as road pricing, customized bus, e-hailing, bike sharing, and shared parking. The fusion of emerging technologies has created opportunities to not only improve the transportation service level but also provide unprecedented service features, which can exert a transformative impact on the multi-dimensional travel behavior and hence the multi-level travel demand pattern in multi-modal transportation systems.

Transportation planning, which is crucial to address the fundamental needs of emerging technologies, requires advanced network equilibrium models for accurate analysis of travel demands. Equilibrium models analyze aggregate travel demand considering the effect of interactions among travelers in the individual choice. The classical random utility models (RUMs), such as the multinomial logit model and its variants, have been primarily embedded in equilibrium models for reproducing individual travel choices with conventional mobility services. Despite allowing the computationally manageable mathematical programming (MP) formulation for equilibrium models, the embedded RUMs are restrictive in modeling the complex travel behavior with the features of emerging mobility services, including distinct magnitudes of travel disutility, provisions of loyalty subscription schemes, and mobility bundling strategies. In addition, the classical closed-form RUMs are mainly based on an additive utility function and restrictive assumptions that the random errors are identically and independently Gumbel distributed, which are inadequate to reflect the way individuals perceive travel disutility in emerging choice contexts. Although open-form choice models can address some of the issues, the lack of an analytical probability expression poses additional difficulties for model estimation, interpretation, and evaluation. Also, owing to the computationally burdensome evaluation of open-form probabilities, the equilibrium problem becomes intractable when the choice set contains more than a handful of alternatives in real-world applications using large-scale transportation networks.

This research aims to advance the travel demand modeling considering both the multi-dimensional travel choice behavior with emerging service features at the disaggregate level and the mobility operational features and interactions among travelers at the aggregate level. To achieve this goal, the objectives of this research lie in the developments of (1) advanced RUMs with relaxed model assumptions, alternate utility functional form, and alternate

distributional assumptions, to reproduce the heterogeneous multi-dimensional behavioral changes facing with different emerging mobility services, and (2) advanced equilibrium models with computationally manageable MP formulations while retaining consistent with the individual choices reproduced by the developed RUMs based on endogenous travel disutility.

The contributions of this research are summarized as follows:

(1) The properties and derivation of the state-of-the-art multiplicative random utility models (MRUMs) are investigated to facilitate the development of advanced travel choice models. On this basis, the applications of MRUM in accessibility and vulnerability assessment are proposed, facilitating the analyses of transportation system performances under both normal and abnormal conditions.

(2) Advanced RUMs are developed to reproduce individual travel choices in multi-modal transportation systems with emerging mobility services. Different from conventional travel choice models, the proposed models can simultaneously address various behavioral issues arisen with the introduction of emerging policy and mobility services. Specifically, the heterogeneous perceptions of travel distance, scale heterogeneity with respect to mobility service quality, perceptual correlation in path cost perceptions, mode correlation among similar travel modes, spatial correlation among adjacent locations and overlapped routes, effect of mobility bundling strategies, and repeated choice behavior arisen from loyalty subscription schemes, are considered to reflect the behavioral reactions to various emerging mobilities at different choice dimensions. Further, an innovative closed-form MRUM with alternate distributional assumptions is proposed, which can capture the choice context with an emerging travel alternative that has unprecedented service features. The innovative closed-form MRUM can provide new behavioral insights into various decision-making scenarios in the transition to future transportation system.

(3) Advanced network equilibrium models are developed to analyze aggregate travel demand patterns consistent with the individual travel choice behavior while considering interactions among travelers. Specifically, the proposed models respectively consider the equilibrium bi-criteria route choice in tolled networks, equilibrium mode choice in multi-modal systems with customized bus services, equilibrium of joint bundle and mode choice in multi-modal systems with various emerging mobility services, and equilibrium of joint destination and parking choice among spatially distributed locations with shared parking services. Benefiting from the properties of the developed RUMs, the proposed equilibrium models are formulated as equivalent MP problems. The MP formulation facilitates the

understanding and interpretation of the equilibrium models, enables the application to real-world case studies using convergent and efficient solution algorithms, and facilitates the sensitivity analysis-based evaluation of transportation system performances.

List of publications

Journal papers:

Travel choice model

Gu, Y., Chen, A., and Kitthamkesorn, S. (2022). Weibit choice models: Properties, mode choice applications and graphical illustrations. *Journal of Choice Modelling*, 100373. (The content in Sections 2.1.1–2.1.2 is mainly from this paper)

Gu, Y., Chen, A., Kitthamkesorn, S., and Jang, S. (2023). A binary choice model considering the oddball effect in transition to future transportation system. Under revision with *Communications in Transportation Research*. (The content in Chapter 4 is partly from this paper)

Gu, Y., Chen, A., Kitthamkesorn, S., and Jang, S. (2023). Alternate closed-form weibit-based model for assessing travel choice with an oddball alternative. Under revision with *Transportation Research Part B.* (The content in Chapter 4 is mainly from this paper)

Equilibrium analysis

Gu, Y., and Chen, A. (2023). Modeling mode choice of customized bus services with loyalty subscription schemes in multi-modal transportation networks. *Transportation Research Part C*, 147, 104012. (The content in Chapter 7 is mainly from this paper)

Gu, Y., Chen, A., and Kitthamkesorn, S. (2022). Accessibility-based vulnerability analysis of multi-modal transportation networks with weibit choice models. *Multimodal Transportation*, 1(3), 100029. (The content in Section 2.1.3 is mainly from this paper)

Gu, Y., and Chen, A. (2023). Considering path order and perceptual correlations in a tolled network with ordered GEV model. Under preparation. (The content in Chapter 6 is mainly from this paper)

Gu, Y., and Chen, A. (2023). Equilibrium analysis for emerging mobility services with loyalty bundle schemes. Under review with *Transportation Research Part B.* (The content in Chapter 9 is mainly from this paper)

Gu, Y., Chen, A., and Kitthamkesorn, S. (2023). Modeling shared parking services at spatially correlated locations through a weibit-based combined destination and parking choice equilibrium model. Under revision with *Transportation Research Part B.* (The content in Chapter 8 is mainly from this paper)

Transportation network performance under disruptions

Gu, Y., Chen, A., and Xu, X. (2023). Measurement and ranking of important link combinations in the analysis of transportation network vulnerability envelope buffers under multiple-link disruptions. *Transportation Research Part B,* 167, 118-144.

Gu, Y., Fu, X., Liu, Z., Xu, X. and Chen, A. (2020). Performance of transportation network under perturbations: Reliability, vulnerability, and resilience. *Transportation Research Part E*, 133, 101819.

Gu, Y., Chen, A., Xu, Y., and Kitthamkesorn, S. (2023). Modeling vulnerability envelope of urban rail transit networks under simultaneous disruptions of stations and line sections. Under revision with *Transportation Research Part C.*

Gu, Y., Ryu, S., Xu, Y., Chen, A., Chan, H., and Xu, X. (2023). A random-key genetic algorithm-based method for transportation network vulnerability envelope analysis under simultaneous multi-link disruptions. Under review with *Expert Systems with Applications*.

Acknowledgement

First and foremost, I would like to express my sincere gratitude to Prof. Anthony Chen for his endless patience, continuous support, and invaluable guidance throughout my PhD study. I was always inspired by his extensive knowledge, plentiful experience, and unique and profound way of thinking. Besides knowledge, his gentleness, self-motivated working attitude, and enthusiasm for education would substantially influence the rest of my career and life.

Thanks also go to my co-supervisor Prof. Defeng Sun for his kind support.

I am very grateful to Dr. Songyot Kitthamkesorn and Dr. Sunghoon Jang for their insightful comments and instructive suggestions on this research work.

Many thanks are also extended to the past and present members of transportation groups of the Hong Kong Polytechnic University for their cooperation in the past years.

Above all, my deepest gratitude goes to my parents for their endless love and unconditional support for my PhD study.

Table of contents

List of Figures

List of Tables

Acronyms

ARUM	Additive Random Utility Model
BSUE	Bi-Objective Stochastic User Equilibrium
CB	Customized Bus
CNL	Cross-Nested Logit
CNW	Cross-Nested Weibit
DCNW	Dogit-Cross-Nested Weibit
DNW	Dogit- Nested Weibit
GEV	Generalized Extreme Value
MNL	Multinomial Logit
MNL-O	Multinomial Logit with an Oddball alternative
MNW	Multinomial Weibit
MNW-O	Multinomial Weibit with an Oddball alternative
MRUM	Multiplicative Random Utility Model
MP	Mathematical Programming
IID	Independently and Identically Distributed
NL	Nested Logit
NW	Nested Weibit
OD	Origin-Destination
OGEV	Ordered GEV
OPSGEV	Ordered Path-Size GEV
PT	Public Transit
PTS	Perceived Time Surplus
PSL	Path-Size Logit
PSW	Path-Size/Parking-Size Weibit
RUM	Random Utility Model
SCW	Spatially Correlated Weibit
SUE	Stochastic User Equilibrium
UE	User Equilibrium

Chapter 1 Introduction

1.1 Background

Modeling individual travel choices and analyzing the corresponding aggregate equilibrium travel demands play an important role in the analysis and planning of transportation system. The choice modeling and equilibrium analysis of transportation systems are facing with new challenges in the era of emerging technologies, where various innovative transport policies and mobility services have been implemented and promoted, such as road pricing, customized bus (CB), shared parking, bike sharing, and e-hailing. They may not only enhance transportation system performances, but also reshape individual travel behaviors owing to their innovative service features, such as the distinct magnitudes of travel disutility, provision of loyalty subscription schemes, and new promotion strategies like mobility bundling. To facilitate the decision-making in the transition from current to future transportation systems, it is imperative to advance the individual travel choice and network equilibrium models to account for the disaggregate-level behavioral changes and its impact on aggregate travel demand stemmed from the emerging service features.

In the well-established four-step transportation planning method, individual travel behaviors are often modeled at four choice dimensions, including the travel choice (whether to travel), destination choice, mode choice, and route choice. The individual travel behavior can be simply reproduced as deterministic choices of the minimum-disutility travel alternative. However, this approach unrealistically assumes travelers to have perfect knowledge of the actual travel time, which is inadequate to capture the limited cognitive ability of travelers and may generate inaccurate results. The random utility models (RUMs) are developed and widely used to consider the stochasticity in travel choices (e.g., perception error of travel disutility). Based on the principle that travelers choose the alternatives which maximize their stochastic perceived travel utility (or equivalently, minimize the perceived travel disutility), RUMs can accurately obtain travel choice probabilities with sound behavioral foundations (Domencich and McFadden, 1975; Ben-Akiva and Lerman, 1985; Ortúzar and Willumsen, 2011).

The additive random utility models (ARUMs) are dominant in existing transportation research, where the perceived travel disutility is expressed as the sum of a deterministic disutility and a random perception error. Assuming random errors to follow the Gumbel and normal distributions respectively lead to the well-established logit and probit choice models (Domencich and McFadden, 1975; Daganzo, 1979). Compared with the probit model, the logit model is less flexible owing to its restrictive model assumptions, namely the random errors are assumed to be independently and identically Gumbel distributed (IID), making it difficult to capture the heterogeneity in travel perceptions and correlations among similar alternatives. Despite these limitations, the logit model has the merit of closed-form probability expression, making it more computationally manageable than the probit model and more commonly adopted in travel choice and equilibrium analyses (Prashker and Bekhor, 2004).

Based on the individual choices at the four dimensions, travel demands can be analyzed at the corresponding spatial levels, i.e., trip generation, trip distribution, modal split, and traffic assignment. Simply aggregating the individual choice probabilities may lead to an aggregation bias, as the choice probabilities resulting from exogeneous travel disutility will be inconsistent with the actual travel disutility under the realized travel demand pattern. Thus, it is necessary to consider the interactions among individuals in congested transportation networks. For instance, by integrating the flow-dependent travel time in different route choice models, the stochastic user equilibrium (SUE) models have been developed and applied in the traffic assignment problem (Daganzo and Sheffi, 1977; Sheffi, 1985; Prashker and Bekhor, 2004). The road travel time is endogenously generated as a function of road traffic volume, which guarantees the consistency between travel choice and travel disutility.

In particular, the SUE model can be formulated as an equivalent mathematical programming (MP) problem when the conventional multinomial logit (MNL) choice model and its extensions are incorporated (Fisk, 1980; Prashker and Bekhor, 2004). The MP formulation is valuable as it is easily understandable and highly interpretable based on the explicit objective function, constraints, decision variables, and Kuhn–Tucker

optimality conditions. Further, many convergent and efficient solution algorithms are enabled by the MP formulation, where the objective function helps find the searching direction and updating step size, as well as the stopping criteria for convergence examination (Patriksson, 1994). Beyond the traffic assignment level, the SUE models with MP formulation have been extended to combined travel demand models that simultaneously consider any combinations of the four demand analysis levels (Oppenheim, 1995). Thus, the equilibrium models serve as an important component in transportation system analysis and decision-making processes (Bell and Iida, 1997; Yang and Huang, 2005; Ortúzar and Willumsen, 2011).

However, existing logit-based equilibrium models with MP formulation inherit the limitations from closed-form logit models, namely the inadequacy to simultaneously address the heterogeneity and similarity issues, which are important concerns in capturing the complex multi-dimensional behavioral responses to the emerging service features. Although the two issues can be addressed via open-form choice models like probit and mixed logit models, the lack of analytical choice probability poses additional difficulty to their application in equilibrium analyses. As travel disutility is a function of travel demand in congested networks, the equilibrium model can be viewed as a fixed-point problem where choice probabilities exist on both sides of the equation. Solving such models often requires an iterative procedure to update the demand pattern with choice probabilities evaluated at each iteration. Owing to the computationally burdensome evaluation of open-form choice probabilities, the equilibrium travel demand models become intractable when the choice set contains more than a handful of alternatives, particularly impractical for large-scale transportation networks with thousands or even millions of routes. The computational burden will become even heavier in the network design problem embedded with a network equilibrium model, which can be formulated as a bi-level program with an equilibrium traffic assignment model at the lower level, or a single-level mathematical programming with equilibrium constraints (Yang and Bell, 1998). In summary, existing equilibrium analyses are inadequate for analyzing travel demands in the era of emerging technologies. This calls

for advancing both the individual choice model and equilibrium model for system analysis and decision-making in the transition to future transportation networks.

Besides extending the logit-based models with an additive utility function, the multiplicative random utility models (MRUMs) have been proposed based on the multiplicative disutility function. Compared with the ARUM, MRUM is consistent with the psychophysical laws that can better reflect the way travelers perceive different magnitudes of disutility (Fosgerau and Bierlaire, 2009; Chakroborty et al., 2021). By assuming Weibull distributed perception errors, the closed-form weibit choice model was recently developed to inherently address the heterogeneity issue and can be extended to consider more complex similarity issues at different choice dimensions (Castillo et al., 2008; Kitthamkesorn and Chen, 2013, 2017). Therefore, it is beneficial to advance the weibit-based MRUM and develop corresponding equilibrium models to simultaneously address different behavioral issues with various emerging mobility services while retaining the valuable MP formulation.

1.2 Research objectives

This research aims to advance the travel demand modeling in transition to the future transportation system with emerging mobility services. The advancements are to be made from two modeling perspectives, namely (1) the individual choice modeling to better consider complex multi-dimensional travel choice behaviors at the disaggregate level, and (2) the equilibrium modeling with MP formulations for travel demand analysis considering interactions among travelers and operational features of emerging mobilities at the aggregate level. The specific objectives to achieve this aim are as follows:

1. To investigate the properties of distributional assumptions made for the closed-form additive and multiplicative RUMs, to facilitate the development of advanced travel choice models with considerations of complex behavioral issues.
2. To develop an alternate closed-form MRUM for modeling choice contexts with the oddball effect, where an “oddball” alternative with emerging service features exists

in the choice set and competes with conventional alternatives with only common service features.

3. To develop an advanced route choice model and the corresponding traffic assignment models for tolled networks, where the path correlations are considered with respect to both travel time and monetary costs, the two choice criteria that are likely to be considered in the road network with road pricing schemes.

4. To develop an advanced mode choice model and the corresponding equilibrium model for multi-modal transportation systems with CB services while considering the effect of loyalty CB subscription schemes and operational features of CB services.

5. To develop an advanced joint bundle and mode choice model and the corresponding equilibrium model for the analysis of multi-modal transportation systems with various emerging mobilities, considering the effects of flexible mobility bundling strategies and loyalty bundle schemes.

6. To develop an advanced joint destination and parking choice model and the corresponding combined travel demand model for the transportation system with shared parking services, where the spatial correlations are considered at both choice dimensions, including the substitution effect among adjacent locations and the overlap among parking spaces of neighboring destinations.

1.3 Thesis organization

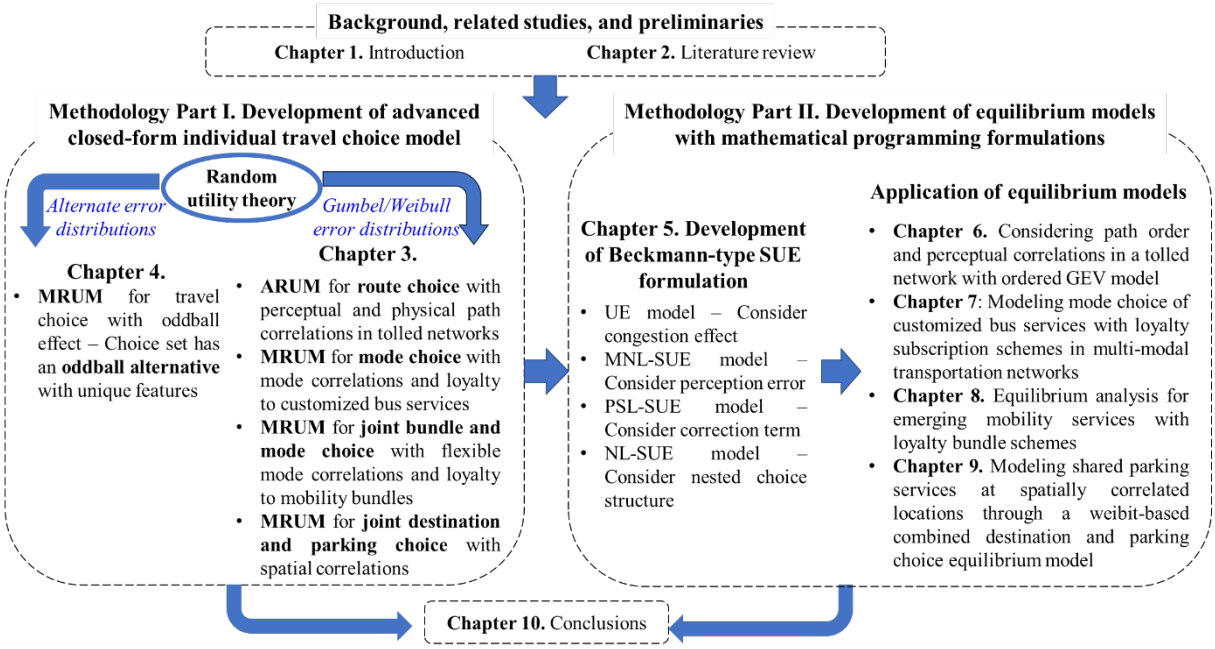

Figure 1.1. Thesis organization

The thesis organization is shown in Figure 1.1. The remainder of this thesis is as follows:

- Chapter 2 overviews related studies on the research topics considered in this thesis, including: (1) closed-form individual travel choice models with illustrations of their development and applications based on the random utility theory, and (2) equilibrium models with MP formulation for different levels of aggregate travel demand analyses.

➢ The first part of the proposed methodology includes Chapters 3-4, which focuses on the development of advanced closed-form individual choice models for emerging choice contexts based on the random utility theory.

- Chapter 3 develops advanced "Luce-form" choice models with closed-form probability expressions for reproducing individual travel behaviors at multiple dimensions of emerging choice contexts. The developed models include an ordered path-size generalized extreme value (OPSGEV) route choice model, a dogit-nested weibit (DNW) mode choice model, a dogit-cross-nested weibit (DCNW) model for the joint mobility bundle and mode choice, and a spatially correlated weibit-parking-size weibit (SCW-PSW) model for the joint destination and parking choice.

- Chapter 4 develops a closed-form choice model based on an alternate distributional assumption to specifically account for the "oddball" alternative in choice set (e.g., an emerging mobility service), which has unique service features compared with the other regular alternatives (e.g., conventional travel modes).

➢ The second part of the proposed methodology includes Chapters 5-9, which focuses on the development of advanced equilibrium models with MP formulation. The developed equilibrium models are consistent with the advanced individual choice models developed in Chapter 3, while interactions among travelers and operational service features of emerging mobilities are endogenously considered for aggregate-level travel demand analyses.

- Chapter 5 illustrates the development of the Beckmann-type MP formulation for general equilibrium models, including the deterministic UE model, the basic logit SUE model, and various extensions of the logit SUE model corresponding to the advancements in individual choice models.
- Chapter 6 develops the OPSGEV SUE model for traffic assignment in tolled road networks, which is consistent with the OPSGEV route choice model considering both perceptual and physical path correlations.
- Chapter 7 develops the DNW equilibrium modal split model for multi-modal transportation systems with CB services, which considers the effect of passenger loyalty and constraints on CB service demand.
- Chapter 8 develops an equilibrium analysis framework for various emerging mobility services consistent with the DCNW choice model, which considers the effect of mobility bundling and loyalty subscription schemes in both aggregate travel demand analyses and system performance evaluations.
- Chapter 9 develops an SCW-PSW combined travel demand model for investigating the effects of shared parking services on the joint destination and parking choice at adjacent locations with spatial correlations.
- Chapter 10 presents concluding remarks and directions for future research.

Chapter 2 Literature review and preliminaries

This chapter reviews related studies and provides preliminaries for the thesis in two parts, i.e., the random utility models (RUMs) for travel choice modeling at the individual level, and the equilibrium models for travel demand analysis at the aggregate level. This chapter is structured as follows. Section 2.1 overviews the development and application of RUMs with "Luce-form" probabilities and their generalizations. Section 2.2 overviews the development of network equilibrium models with MP formulation that are consistent with the class of Luce-form RUMs discussed in Section 2.1.

2.1 Random utility models with Luce-form probability

In transportation research, an understanding of individual travel choices is critical for estimating and forecasting travel demand at different spatial levels. RUMs are the mainstream of travel choice models, where travelers are considered to make decisions that maximize/minimize their perceived travel utility/disutility (Haghani et al., 2021). To model the stochasticity in travel choice behavior, the perceived travel utility/disutility is often considered as a random variable that can be separable into a deterministic term denoting the actual travel utility/disutility, and a random term denoting the travel perception error. Based on the functional relationship between the deterministic and random terms, RUMs used in transportation studies can be classified as (1) the additive RUM (ARUM) where the perceived utility is the sum of deterministic and random terms, and (2) the multiplicative RUM (MRUM) where the perceived disutility is the product of deterministic and random terms.

With different distributional assumptions for the random error term, different choice models can be developed. In the literature, the normal and Gumbel distributions are dominant in ARUMs (Domencich and McFadden, 1975; Daganzo, 1979), while the distributions defined at the positive domain (e.g., the Log-normal, Fréchet, and Weibull distributions) are used in MRUMs (Fosgerau and Bierlaire, 2009; Mattsson et al., 2014). Specifically, by assuming random errors to identically and independently follow the

"Luce class" distribution, the well-established Luce-form models can be developed (Luce and Suppes, 1965; Lindberg, 2012):

$$P_i = \frac{w_i}{\sum_{j \in I} w_j}, \tag{2.1}$$

where w_i denotes the positive "strict utility" term associated with alternative i.

Luce-form models are beneficial owing to their simple and closed-form choice probability expressions. Compared with the choice models with open-form probability, the analytical solution to Luce-form models enables exact and efficient estimation methods such as the maximum likelihood method. While the open-form models must be estimated using the simulation method (Train, 2003) or numerical approximation method (e.g., Bhat, 1995), which requires large computational burden and may lead to estimation errors due to simulation errors or approximation errors. Also, the estimation of open-form models suffers from the reproducibility issue, i.e., the estimation result may not be replicated through different numerical methods or in different trials of the simulation method, which leads to unreliable model interpretation and behavioral insights (Diethelm, 2012). Also, the closed-form choice probability plays a critical role in defining the solution properties and the generalization of model outcomes (Mondal and Bhat, 2021). Furthermore, the analytical model solution largely reduces the computational burden of choice probability evaluation and significantly facilitates applications in higher-level optimization problems, such as the equilibrium analysis of transportation systems. Therefore, this section focuses on the mostly used Luce-form ARUMs and MRUMs, i.e., logit and weibit models, as well as their generalizations that address more complex behavioral issues.

2.1.1 Logit-based additive RUM

The additive utility function is adopted in logit-based models:

$$V_i = v_i + \varepsilon_i, \tag{2.2}$$

where V_i denotes the perceived travel utility, v_i and ε_i are respectively the deterministic utility and random error of alternative *i*. Assuming ε_i as IID Gumbel variables leads to the multinomial logit (MNL) model. Section 2.1.1.1 illustrates properties of the Gumbel distribution and the development of binary and multinomial logit models on this basis.

2.1.1.1 Properties of the Gumbel distribution and development of MNL model

Table 2.1 presents the probability density function (PDF), cumulative distribution function (CDF), and six properties of the Gumbel distribution (η, θ) with location parameter η and scale parameter θ (Ben-Akiva and Lerman, 1985).

Table 2.1. Properties of the Gumbel distribution

Property	Gumbel (η, θ) (η: location parameter; θ: scale parameter)
PDF	$f(x) = \theta \exp\left\{-\theta(x-\eta) - \exp\left[-\theta(x-\eta)\right]\right\}$
CDF	$F(x) = \exp\left\{-\exp\left[-\theta(x-\eta)\right]\right\}$
1. Mode	η
2. Mean	$\eta + \gamma/\theta$
3. Variance	$\pi^2/6\theta^2$
4. **Linear** transformation of variable	If X is Gumbel distributed with parameters (η, θ), then $X + \nu$ is also Gumbel distributed with parameters $(\eta + \nu, \theta)$
5. Comparison of variables	**Absolute difference** between two independent Gumbel distributed variables X_1 and X_2 with the same scale parameter θ follows the **Logistic distribution** with CDF as follows: $F = \frac{1}{1+\exp\left\{\theta \cdot \left[(x_2 - x_1) - (\eta_2 - \eta_1)\right]\right\}}$
6. Stableness under **maximization**	The **maximum** of N independent Gumbel-distributed variables $X_1, ..., X_N$ with parameters (η_1, θ), …, (η_N, θ) is Gumbel distributed with parameters $\left(\frac{1}{\theta}\ln\sum_{i=1}^{N}\exp(\theta \cdot \eta_i), \theta\right)$

The first three properties indicate the statistical features of the Gumbel distribution, i.e., mode, mean, and variance. Given the value of scale parameter θ, the mean of a Gumbel variable is determined by the location parameter (where γ is the Euler constant), while the variance is fixed disregarding the value of mean. Property 4 shows that the linear transformation of a Gumbel variable merely changes its location parameter without influencing the value of scale parameter, implying the applicability of the Gumbel distribution to ARUMs. By adding different deterministic utility to the Gumbel error term of each travel alternative, the total perceived travel utility is still Gumbel distributed with the same scale parameter among all alternatives.

Properties 5 and 6 facilitates the development of logit choice model. The binary logit choice probability can be derived making use of Property 5. The probability of choosing alternative *i* over alternative *j* can be expressed as the probability that alternative *i* has a larger perceived travel utility than alternative *j*:

$$\begin{aligned} P_i &= \text{Prob}\left(V_i > V_j\right) \\ &= \text{Prob}\left(v_i + \varepsilon_i > v_j + \varepsilon_j\right). \\ &= \text{Prob}\left(\varepsilon_j - \varepsilon_i \le v_i - v_j\right) \end{aligned} \tag{2.3}$$

From Property 5, $\varepsilon_j - \varepsilon_i$ is Logistically distributed. The binary choice probability can then be derived based on the CDF of the Logistic distribution:

$$\begin{aligned} P_i &= F_L\left(v_i - v_j\right) \\ &= \frac{1}{1+\exp\left[\theta\left(v_j - v_i\right)\right]} \\ &= \frac{\exp\left(\theta v_i\right)}{\exp\left(\theta v_i\right)+\exp\left(\theta v_j\right)}. \\ &= \frac{1}{\exp\left[\theta\underbrace{\left(v_j - v_i\right)}_{\text{absolute diff}}\right]} \end{aligned} \tag{2.4}$$

From Eq. (2.4), the logit choice probability is dependent on the *absolute* difference in travel utility and the scale parameter θ. The scale parameter can be interpreted as the dispersion parameter indicating the degree of uncertainty in perceiving travel utility.

The binary logit choice probability shown in Eq. (2.4) can be extended to the multinomial case using Property 6 of the Gumbel distribution. The MNL probability of choosing alternative *i* in a multinomial choice set *I* is the probability that the perceived travel utility of alternative *i* is larger than the maximum perceived utility of all other alternatives in set *I*, which can be expressed as

$$\begin{aligned} P_i &= P\left[V_i > \max_{j \neq i \in I}\left(V_j\right)\right] \\ &= P\left[v_i + \varepsilon_i > \max_{j \neq i \in I}\left(v_j + \varepsilon_j\right)\right] \end{aligned} . \tag{2.5}$$

Based on Property 6, $\max_{j \neq i \in I}\left(v_j + \varepsilon_j\right)$ is Gumbel distributed with location parameter $\frac{1}{\theta}\ln \sum_{j \neq i \in I} \exp\left(\theta \cdot v_j\right)$ and scale parameter θ. Hence the multinomial choice probability can be obtained following the binary case:

$$\begin{aligned} P_i &= \frac{\exp\left(\theta v_i\right)}{\exp\left(\theta v_i\right) + \exp\left[\theta \cdot \frac{1}{\theta}\ln \sum_{j \neq i \in I} \exp\left(\theta v_j\right)\right]} \\ &= \frac{\exp\left(\theta v_i\right)}{\exp\left(\theta v_i\right) + \sum_{j \neq i \in I} \exp\left(\theta v_j\right)} \\ &= \frac{\exp\left(\theta v_i\right)}{\sum_{j \in I} \exp\left(\theta v_j\right)} \end{aligned} . \tag{2.6}$$

From Eq. (2.6), MNL model has the Luce-form choice probability as presented in Eq. (2.1), where the strict utility term w_i is an exponential function of the deterministic utility v_i, i.e., $\exp\left(\theta v_i\right)$.

2.1.1.2 Extended closed-form logit models

Despite the computationally manageable closed-form probability expression, the MNL model has limitations arisen from its restrictive IID assumption. The independently distributed assumption makes the MNL model inadequate to capture correlations among similar alternatives. On the other hand, the MNL model cannot capture travelers' heterogeneous perceptions owing to the fixed perception variance arisen from the identically distributed assumption and properties of the Gumbel distribution.

Due to the analytical tractability of the MNL model, various closed-form extensions of the logit model have been developed to handle the first limitation: the inability to model correlation among travel alternatives. These models either (1) add correction terms reflecting alternative correlations in the deterministic part of utility function, or (2) use a more flexible nested choice structure incorporating additional random errors to reflect alternative correlations in the stochastic part of utility function.

(1) Extended logit models with correction terms

One mainstream of the closed-form extended logit models is to introduce correction terms that penalize the similarity among alternatives. This method is mainly applied to the route choice problem where alternative correlation is often represented by the overlaps among paths. Cascetta et al (1996) proposed the C-logit model that subtracts a positive commonality factor (CF) from the deterministic utility to penalize the degree of path overlapping, which can be expressed as

$$V_i = v_i - CF_i + \varepsilon_i \,. \tag{2.7}$$

The value of CF can be derived based on the proportion of overlapped length of each path. The path with a higher degree of overlapping will have a larger value of commonality, leading to a lower deterministic utility and a lower choice probability, which reflects the effect of path overlapping:

Similarly, the path-size logit (PSL) model considers the effect of path overlapping by introducing a path-size (PS) factor to the path utility function (Ben-Akiva and Bierlaire, 1999):

$$V_i = v_i + \frac{1}{\theta} \ln PS_i + \varepsilon_i . \tag{2.8}$$

The PS factor is derived from the concept of elemental and aggregate alternatives based on the random utility theory (Ben-Akiva and Lerman, 1985). Each path *i* is considered as an aggregate alternative composed by elemental alternatives with a size of PS_i. The paths having no overlaps are considered as "full" alternatives with a size of 1, which does not influence the path utility. While the overlapped paths cannot be considered as a distinctive alternative and have sizes $0<PS_i<1$, which leads to a negative correction term that penalizes the path overlapping. Various approaches have been proposed to derive the value of PS factor based on the length of overlapped fraction (Ben-Akiva and Bierlaire, 1999; Ramming, 2002; Hoogendoorn-Lanser, 2005). Alternatively, Bovy et al. (2008) proposed the path size correction factor, which is derived as an approximation of the nested choice models described below. Duncan et al. (2020) proposed the adaptive PSL model with a PS factor that further weighs the contributions of excessively long paths while consistent with the relative path attractiveness.

(2) Extended logit models with a nested choice structure

The other mainstream of closed-form extended logit models is the generalized extreme value (GEV) family of models based on a nested choice structure with multiple choice levels (McFadden, 1978). The nested logit (NL) model is the mostly used GEV model, where similar travel alternatives at the lower (conditional) choice level are collected in the same upper-level nest (marginal level) and share a common part of travel utility perception (Ben-Akiva and Lerman, 1985). Figure 2.1 shows an example choice structure of the two-level NL model.

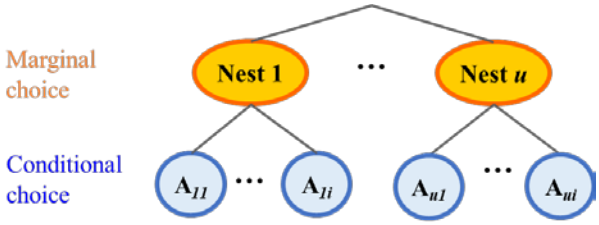

Figure 2.1. Example choice structure of NL model

The utility function of alternative i in nest u is expressed as follows:

$$V_i = v_{ui} + \varepsilon_{ui} + v_u + \varepsilon_u , \tag{2.9}$$

where v_{ui} and v_u respectively denote the individual deterministic utility of alternative i and the common deterministic utility of nest u. ε_{ui} and ε_u are random errors at the conditional and marginal choice levels, respectively.

The NL choice probability can then be expressed as the product of marginal choice probability P_u and conditional choice probability $P_{i|u}$ derived following the derivation of MNL model:

$$\begin{aligned} P_i &= P_u \cdot P_{i|u} \\ &= \frac{\exp\left[\theta_u \left(v_u + \Gamma_u\right)\right]}{\sum_{t \in U} \exp\left[\theta_u \left(v_t + \Gamma_t\right)\right]} \cdot \frac{\exp\left(\theta_k v_i\right)}{\sum_{j \in I_u} \exp\left(\theta_k v_j\right)} , \end{aligned} \tag{2.10}$$

where θ_u and θ_k are scale parameters at the marginal and conditional choice levels, respectively. Γ_u denotes the composite utility obtained at the conditional choice level, which is derived based on Property 6 of the Gumbel distribution:

$$\Gamma_u = \frac{1}{\theta_k} \ln \sum_{i \in I_u} \exp\left(\theta_k v_i\right). \tag{2.11}$$

Although the NL model can account for correlations among alternatives in the same nest, the nests are independent of each other, i.e., the correlation among alternatives in different nests cannot be handled. The cross-nested logit (CNL) model has been proposed to consider more flexible correlation structures by allowing overlaps

among nests, i.e., a single alternative can be collected in different nests to model its correlations to different groups of alternatives (Vovsha, 1997). The cross-nested choice structure can be specified for modeling different alternative correlations, such as the ordered GEV (OGEV) model for modeling order correlations among similarly ranked alternatives (Small, 1987), the paired-combinatorial logit (PCL) model for modeling correlations between each pair of alternatives (Chu, 1989), and the spatially correlated logit (SCL) for modeling spatial correlations between adjacent locations (Bhat and Guo, 2004). The CNL model can be further generalized to estimate more flexible competition effect among alternatives via more flexible model parameters (generalized nested logit (GNL) model, Wen and Koppelman 2001), or by incorporating more choice levels (network GEV model, Daly and Bierlaire, 2006).

2.1.2 Weibit-based multiplicative RUM

The extended logit models mainly focus on the similarity issue stemming from the independently distributed assumption; while the second limitation, i.e., the inability to handle heterogeneous travel perceptions due to the identically distributed assumption, is seldom discussed in closed-form logit models. Galvez (2001) developed the "Powit" model with a power function-based Luce-form choice probability. Castillo et al. (2008) independently proposed and derived the weibit model based on the Weibull distribution, which has the same form of the Powit model, to address the heterogeneity issue when modeling route choices. Unlike the MNL model, which uses the additive utility function, the basic multinomial weibit (MNW) model is based on a *multiplicative* form of the *disutility* function (Fosgerau and Bierlaire, 2009):

$$V_i = v_i \cdot \varepsilon_i , \tag{2.12}$$

where v_i denotes the deterministic *disutility* of alternative *i*. Assuming the error term ε_i to be IID Weibull variables leads to the multinomial weibit (MNW) model. The multiplicative error structure presented in Eq. (2.12) evaluates the *relative* differences in disutility, which has been found to outperform the additive utility function used in

logit models in various choice contexts, such as travel mode choice, expressway road choice, and railway itinerary choice (Fosgerau and Bierlaire, 2009; Kurauchi and Ido, 2017; Li et al., 2020; Wen et al., 2021).

2.1.2.1 Properties of the Weibull distribution and development of MNW model

This section illustrates properties of the Weibull distribution and development of binary and multinomial weibit models on this basis. Analogous to the properties of the Gumbel distribution presented in Table 2.1 (Ben-Akiva and Lerman, 1985), Table 2.2 presents the PDF, CDF, and six properties of the Weibull distribution (α, β) with scale parameter α and shape parameter β.

Table 2.2. Properties of the Weibull distribution

Property	Weibull (α, β) (α : scale parameter; β : shape parameter)
1. Mode	$\begin{cases} \alpha \cdot \left(\frac{\beta - 1}{\beta} \right)^{\frac{1}{\beta}} & \beta > 1 \\ 0 & \beta \le 1 \end{cases}$
2. Mean	$\alpha \cdot \Gamma\left(1 + \frac{1}{\beta}\right)$
3. Variance	$\alpha^2 \left[\Gamma\left(1 + \frac{2}{\beta}\right) - \Gamma^2\left(1 + \frac{1}{\beta}\right) \right]$
4. **Multiplicative** transformation of variable	If *X* is Weibull distributed with parameters (α, β), then *kX* is also Weibull distributed with parameters ($k\alpha, \beta$)
5. Comparison of variables	**Relative difference** of two independent Weibull distributed variables X_1 and X_2 with the same shape parameter β follows the **Log-logistic distribution** with CDF**:** $F = \frac{1}{1 + \left[\left(\frac{x_1}{x_2} \right) \Big/ \left(\frac{\alpha_1}{\alpha_2} \right) \right]^{-\beta}}$
6. Stableness under **minimization**	The **minimum** of *N* independent Weibull distributed variables $X_1, ..., X_N$ with parameters (α_1, β), …, (α_N, β) is Weibull distributed with parameters $\left(\left[\sum_i (\alpha_i)^{-\beta} \right]^{-\frac{1}{\beta}}, \beta \right)$

The first three properties are statistical features of the Weibull distribution. Compared to the Gumbel distribution with a fixed variance independent of the mean, the Weibull distribution has a variance determined by the scale parameter α and shape parameter β (Property 3), which is a function dependent on the mean derived from Property 2. This implies that unlike the Gumbel distribution, the Weibull distribution has non-identical variances that depend on the alternative disutility, which facilitate to reflect the heterogeneous travel disutility perceptions of distinct travel alternatives.

Property 4 shows that the multiplicative transformation of a Weibull variable merely changes its scale parameter without influencing the value of shape parameter, implying the applicability of the Weibull distribution to MRUMs. By multiplying the Weibull distributed error term with a deterministic disutility of each travel alternative, the total perceived travel utility is still Weibull distributed while retaining the same shape parameter among all alternatives.

Analogous to the logit model, the weibit model can be developed using Properties 5 and 6 of the Weibull distribution. The binary weibit choice probability can be derived making use of Property 5. Unlike the *absolute* difference-based Property 5 of the Gumbel distribution, Property 5 of the Weibull distribution relates to the *relative* difference between two random variables, which is suitable for the MRUM with a multiplicative error structure. The probability of choosing alternative *i* over alternative *j* can be expressed as the probability that alternative *i* has a lower perceived travel disutility than alternative *j*:

$$\begin{aligned} P_i &= P\left(v_i \cdot \varepsilon_i \le v_j \cdot \varepsilon_j\right) \\ &= P\left[\left(\varepsilon_i / \varepsilon_j\right) \le \left(v_j / v_i\right)\right]. \end{aligned} \tag{2.13}$$

From Property 5, $\varepsilon_i / \varepsilon_j$ is Log-logistically distributed. The binary choice probability can be obtained based on the CDF of the Log-logistic distribution as follows:

$$
\begin{aligned}
P_i &= \frac{1}{1+\left(v_j / v_i\right)^{-\beta}} \\
&= \frac{\left(v_i\right)^{-\beta}}{\left(v_j\right)^{-\beta}+\left(v_i\right)^{-\beta}} . \\
&= \frac{1}{1+\underbrace{\left(v_j / v_i\right)}_{\text{relative diff}}^{-\beta}}
\end{aligned}
\tag{2.14}
$$

The weibit choice probability is dependent on the *relative* difference in travel disutility and the shape parameter β. The shape parameter can be interpreted as the dispersion parameter of weibit model, which indicates the degree of uncertainty in perceiving travel disutility.

The MNW model can be derived by combining the binary weibit choice probability with Property 6 of the Weibull distribution. The MNW probability of choosing alternative *i* in a multinomial choice set *I* is the probability that the perceived travel disutility of alternative *i* is lower than the minimum perceived disutility among all other alternatives in set *I*, which can be expressed as

$$
\begin{aligned}
P_i &= P\left[V_i \le \min_{j \ne i \in I}\left(V_j\right)\right] \\
&= P\left[v_i \cdot \varepsilon_i \le \min_{j \ne i \in I}\left(v_j \cdot \varepsilon_j\right)\right],
\end{aligned}
\tag{2.15}
$$

where $\min_{j \ne i \in I}\left(v_j \cdot \varepsilon_j\right)$ is Weibull distributed with the same shape parameter β and scale parameter $\left[\sum_{j \ne i \in I}\left(v_j\right)^{-\beta}\right]^{-\frac{1}{\beta}}$. The multinomial choice probability can be obtained following the binary case:

$$
\begin{aligned}
P_i &= \frac{\left(v_i\right)^{-\beta}}{\left\{\left[\sum_{j \ne i \in I}\left(v_j\right)^{-\beta}\right]^{-\frac{1}{\beta}}\right\}^{-\beta}+\left(v_i\right)^{-\beta}} . \\
&= \frac{\left(v_i\right)^{-\beta}}{\sum_{j \in I}\left(v_j\right)^{-\beta}}
\end{aligned}
\tag{2.16}
$$

Like the widely used MNL model, MNW model also retains the Luce-form choice probability as presented in Eq. (2.1). Instead of the exponential function used in the MNL model, a power function of disutility v_i, $\left(v_i\right)^{-\beta}$, is used to express the strict utility term w_i in the MNW model.

2.1.2.2 Extended closed-form weibit model – Nested weibit model

This section presents extended weibit models that further relax the independently distributed assumption. In the literature, the weibit model can be advanced using the techniques of extending logit models (as presented in Section 2.1.1.2) to account for correlations among travel alternatives, such as the PSW model (Kitthamkesorn and Chen, 2013) and NW model (Kitthamkesorn and Chen, 2017). Together with the inherent ability to consider heterogeneous travel perceptions, the advanced weibit models can simultaneously address both the similarity and heterogeneity issues arising from the IID assumptions while retaining a closed-form probability expression. As the development of PSW model is similar to the PSL model, this section focuses on the development and properties of the NW model.

(1) Development of NW model

The NW model adopts the nested choice structure of the NL model, where similar alternatives are collected in the same nest. From the choice structure, the NW disutility of alternative i in nest u includes disutility at both the upper and lower levels in a multiplicative form, which can be written as

$$V_i = v_{ui} \cdot \varepsilon_{ui} \cdot v_u \cdot \varepsilon_u . \tag{2.17}$$

The perceived disutility of choosing alternative i in nest u is decomposed into two parts, the individual part related to alternative i and the common part related to nest u. In Eq. (2.17), v_{ui} and v_u represent the deterministic individual disutility of alternative i and common disutility of alternatives in nest u; ε_{ui} and ε_u are the related random error

terms. Analogous to the development of the NL model (Ben-Akiva and Lerman, 1985), the following distributional assumptions are made for the NW model: (1) ε_{ui} and ε_u are independent; (2) ε_{ui} are independently Weibull distributed with shape parameter β_k ; (3) ε_u are independently distributed such that $\varepsilon_u \cdot \varepsilon^*_{m|u}$ follows the Weibull distribution with shape parameter β_u, where $\varepsilon^*_{m|u}$ is the random error associated with $\min_{i \in I_u} \left(v_{ui} \cdot \varepsilon_{ui} \right)$.

The NW choice probability can then be expressed as the product of marginal probability and conditional probability:

$$P_i = P_u \cdot P_{i|u} . \tag{2.18}$$

The marginal probability of choosing nest *u* can be expressed as

$$\begin{aligned} P_u &= P\left[v_u \cdot \varepsilon_u \cdot \min_{i \in I_u} \left(v_{ui} \cdot \varepsilon_{ui} \right) \le v_w \cdot \varepsilon_w \cdot \min_{j \in I_w} \left(v_{wj} \cdot \varepsilon_{wj} \right), \forall w \ne u \in U \right] \\ &= P\left[\left(\varepsilon_u \cdot \varepsilon^*_{ui} \right) \Big/ \left(\varepsilon_w \cdot \varepsilon^*_{wj} \right) \le \left(v_w \cdot v^*_{wj} \right) \Big/ \left(v_u \cdot v^*_{ui} \right), \forall w \ne u \in U \right] \end{aligned} . \tag{2.19}$$

From Property 6 of the Weibull distribution, the term v^*_{ui} denoting the expectation of $\min_{i \in I_u} \left(v_{ui} \cdot \varepsilon_{ui} \right)$ can be expressed as

$$v^*_{ui} = \left[\sum_{i \in I_u} \left(v_{ui} \right)^{-\beta_k} \right]^{-\frac{1}{\beta_k}} . \tag{2.20}$$

From distributional assumption (3) of the NW model, the marginal choice probability can be obtained following the derivation of the MNW model with shape parameter β_u:

$$\begin{aligned} P_u &= \frac{\left(v_u \cdot v^*_{ui} \right)^{-\beta_u}}{\sum_{w \in U} \left(v_w \cdot v^*_{wj} \right)^{-\beta_u}} \\ &= \frac{\left(v_u \right)^{-\beta_u} \cdot \left[\sum_{i \in I_u} \left(v_{ui} \right)^{-\beta_k} \right]^{\frac{\beta_u}{\beta_k}}}{\sum_{w \in U} \left(v_w \right)^{-\beta_u} \cdot \left[\sum_{j \in I_w} \left(v_{wj} \right)^{-\beta_k} \right]^{\frac{\beta_u}{\beta_k}}} \end{aligned} . \tag{2.21}$$

The conditional probability of choosing alternative *i* given that nest *u* is chosen can be expressed as

$$\begin{aligned} P_{i|u} &= P\left[v_{ui} \cdot \varepsilon_{ui} \le v_{uj} \cdot \varepsilon_{uj}, \forall j \ne i \in I_u \right] \\ &= P\left[\varepsilon_{ui} / \varepsilon_{uj} \le v_{uj} / v_{ui}, \forall j \ne i \in I_u \right] \end{aligned}. \tag{2.22}$$

From distributional assumption (2) of the NW model, the conditional choice probability can be obtained following the derivation of the MNW model with shape parameter β_k:

$$P_{i|u} = \frac{(v_{ui})^{-\beta_k}}{\sum_{j \in I_u,} (v_{uj})^{-\beta_k}}. \tag{2.23}$$

The ratio of the shape parameters at different levels, β_u / β_k, can be estimated as a whole number for practical purposes (Ben-Akiva and Lerman, 1985). Hence, the dissimilarity parameter $\varphi_u = \beta_u / \beta_k$ can be introduced to indicate the degree of competition effect among alternatives in nest *u*. For normalization, we can set $\beta_k = 1$ and $\varphi_u = \beta_u$. By definition, $\beta_u < \beta_k$ and $\beta_u, \beta_k > 0$, φ_u is bounded by 0 and 1. Assuming no nest-specific disutility, i.e., $v_u = 1, \forall u \in U$, the NW model can be alternatively expressed as

$$P_i = \frac{v_{ui}^{-\frac{1}{\varphi_u}} \cdot \left[\sum_{i \in I_u} (v_{ui})^{-\frac{1}{\varphi_u}} \right]^{\varphi_u - 1}}{\sum_{w \in U} \left[\sum_{j \in I_w} (v_{wj})^{-\frac{1}{\varphi_u}} \right]^{\varphi_u}}. \tag{2.24}$$

(2) Variance and covariance of NW model

Although the nested choice structures of the NW and NL models are identical, the former model has different performances owing to the mode disutility-dependent variances and covariances. Figure 2.2 illustrates the difference between the variance-covariance matrices of the two models based on a travel choice example with two nests

and five alternatives. The nested choice structure can lead to a block-diagonal variance-covariance matrix, i.e., there is zero covariance between alternatives belonging to different nests. According to the identically distributed assumption and statistical properties of the Gumbel distribution, the variances of the NL model are fixed, which equal $\frac{\pi^2}{6}$ assuming $\theta_u = 1$ for the total error term $\varepsilon_{ui} + \varepsilon_u$ of alternative *i*. In addition, the covariances between alternatives *i* and *j* in the same nest *u* are also identical, as the correlation coefficient is a function of the dissimilarity parameter only, i.e., $\rho_{ij} = 1 - \varphi_u{}^2$ and $\text{cov}_{ij} = \sigma_i \sigma_j \cdot \rho_{ij} = \frac{\pi^2}{6} \cdot \left(1 - \varphi_u{}^2\right)$ (Ben-Akiva and Lerman, 1985).

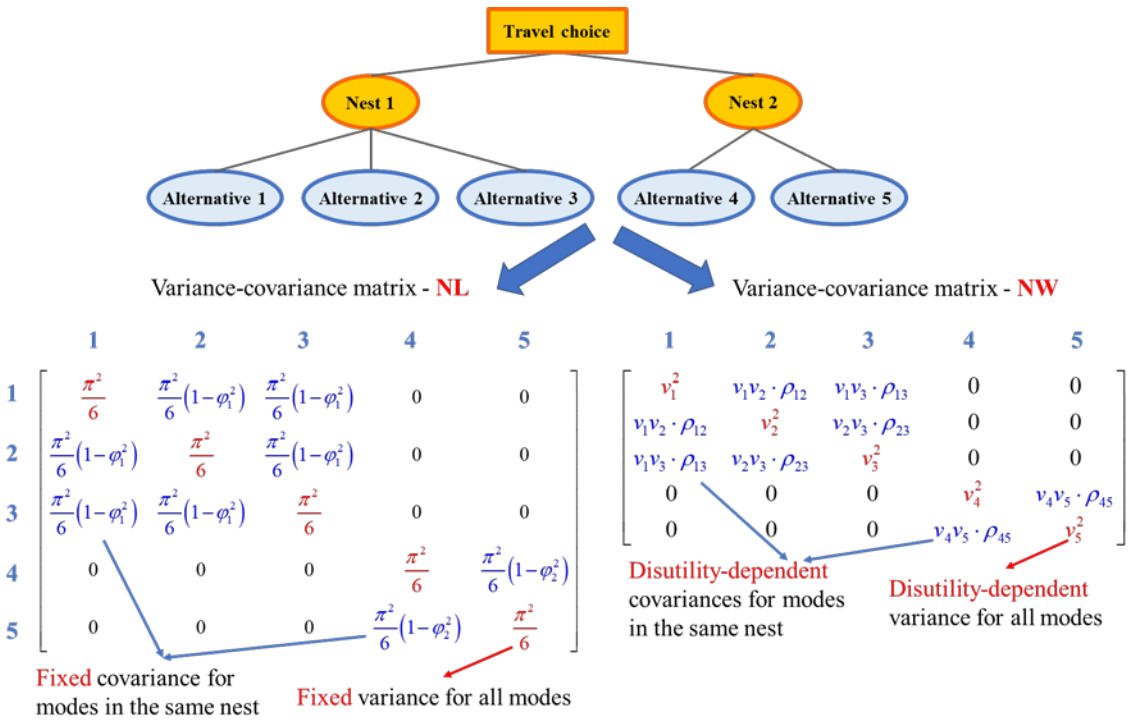

Figure 2.2. Variance-covariance structures of the NL and NW models

On the other hand, based on the statistical properties of the Weibull distribution, the NW model has disutility-dependent variances. Specifically, by normalizing the shape parameter $\beta_u = 1$ for the total random error $\varepsilon_{ui} \cdot \varepsilon_u$ of alternative *i* in nest *u*, the variance of alternative *i* is

$$\sigma_i^2 = \left(v_i\right)^2, \tag{2.25}$$

where $v_i = v_{ui} \cdot v_u$ is the total deterministic disutility. The NW covariance of alternatives *i* and *j* in the same nest *u* is

$$\begin{aligned} \mathrm{cov}_{ij} &= E\left[V_i \cdot V_j\right] - E\left[V_i\right] \cdot E\left[V_j\right] \\ &= E\left[v_i \cdot \varepsilon_{ui} \cdot \varepsilon_u \cdot v_j \cdot \varepsilon_{uj} \cdot \varepsilon_u\right] - E\left[v_i \cdot \varepsilon_{ui} \cdot \varepsilon_u\right] \cdot E\left[v_j \cdot \varepsilon_{uj} \cdot \varepsilon_u\right]. \\ &= v_i \cdot v_j \cdot \left\{E\left[\varepsilon_{ui} \cdot \varepsilon_{uj} \cdot {\varepsilon_u}^2\right] - E\left[\varepsilon_{ui} \cdot \varepsilon_u\right] \cdot E\left[\varepsilon_{uj} \cdot \varepsilon_u\right]\right\} \end{aligned} \tag{2.26}$$

By assumption, ε_{ui} are independent variables, ε_{ui} and ε_u are independent of each other, hence the correlation coefficient can be written as

$$\begin{aligned} \rho_{ij} &= \frac{\mathrm{cov}_{ij}}{\sigma_i \sigma_j} \\ &= E\left[\varepsilon_{ui} \cdot \varepsilon_{uj} \cdot {\varepsilon_u}^2\right] - E\left[\varepsilon_{ui} \cdot \varepsilon_u\right] \cdot E\left[\varepsilon_{uj} \cdot \varepsilon_u\right], \\ &= E\left[\varepsilon_{ui}\right] \cdot E\left[\varepsilon_{uj}\right] \cdot \left\{E\left[{\varepsilon_u}^2\right] - E^2\left[\varepsilon_u\right]\right\} \end{aligned} \tag{2.27}$$

where $E\left[\varepsilon_{ui}\right]$ and $E\left[\varepsilon_u\right]$ can be obtained based on the assumptions that ε_{ui} follow the Weibull distribution $\left(1, \beta_k\right)$ and ε_u follow the Weibull distribution (1,1):

$$E\left[\varepsilon_{ui}\right] = \Gamma\left(1 + \frac{1}{\beta_k}\right) = \Gamma\left(1 + \varphi_u\right), \tag{2.28}$$

$$E\left[\varepsilon_{ui} \cdot \varepsilon_u\right] = \Gamma\left(1 + \frac{1}{1}\right) = 1, \tag{2.29}$$

$$E\left[\varepsilon_u\right] = \frac{E\left[\varepsilon_{ui} \cdot \varepsilon_u\right]}{E\left[\varepsilon_{ui}\right]} = \frac{1}{\Gamma\left(1 + \varphi_u\right)}. \tag{2.30}$$

$E\left[{\varepsilon_u}^2\right]$ can be obtained based on the variance of the total error term $\varepsilon_{ui} \cdot \varepsilon_u$:

$$\begin{aligned} D\left(\varepsilon_{ui} \cdot \varepsilon_u\right) &= E\left[\left(\varepsilon_{ui}\right)^2 \cdot \left(\varepsilon_u\right)^2\right] - E^2\left[\varepsilon_{ui} \cdot \varepsilon_u\right] \\ &= E\left[\left(\varepsilon_{ui}\right)^2\right] \cdot E\left[\left(\varepsilon_u\right)^2\right] - 1 \qquad , \\ &= 1 \end{aligned} \tag{2.31}$$

where $E\left[\left(\varepsilon_{ui}\right)^2\right]$ can be expressed as follows:

$$\begin{aligned} E\left[\left(\varepsilon_{ui}\right)^2\right] &= D\left[\left(\varepsilon_{ui}\right)^2\right] + E^2\left[\varepsilon_{ui}\right] \\ &= \Gamma\left(1+2\varphi_u\right) - \Gamma^2\left(1+\varphi_u\right) + \Gamma^2\left(1+\varphi_u\right). \\ &= \Gamma\left(1+2\varphi_u\right) \end{aligned} \tag{2.32}$$

Substituting Eq. (2.32) into Eq. (2.31) leads to the expression of $E\left[\varepsilon_u{}^2\right]$:

$$\begin{aligned} &\Gamma\left(1+2\varphi_u\right)\cdot E\left[\left(\varepsilon_u\right)^2\right] - 1 = 1 \\ &\Rightarrow E\left[\left(\varepsilon_u\right)^2\right] = \frac{2}{\Gamma\left(1+2\varphi_u\right)} = \frac{2}{2\varphi_u\cdot\Gamma\left(2\varphi_u\right)} = \frac{1}{\varphi_u\cdot\Gamma\left(2\varphi_u\right)} \end{aligned}. \tag{2.33}$$

Substituting Eqs. (2.28), (2.30), (2.33) into Eq. (2.27) gives the correlation coefficient:

$$\begin{aligned} \rho_{ij} &= \Gamma^2\left(1+\varphi_u\right)\cdot\left\{\frac{1}{\varphi_u\cdot\Gamma\left(2\varphi_u\right)} - \left[\frac{1}{\Gamma\left(1+\varphi_u\right)}\right]^2\right\} \\ &= \frac{\Gamma\left(1+\varphi_u\right)\cdot\varphi_u\Gamma\left(\varphi_u\right)}{\varphi_u\cdot\Gamma\left(2\varphi_u\right)} - 1 \\ &= \frac{\Gamma\left(1+\varphi_u\right)\cdot\Gamma\left(\varphi_u\right)}{\Gamma\left(2\varphi_u\right)} - 1 \end{aligned} \quad . \tag{2.34}$$

Therefore, the correlation coefficient is positive and depends on the dissimilarity parameter φ_u. The covariance of alternatives *i* and *j* in the same nest *u* is a function of their disutility and the correlation coefficient. This implies that the NW model allows alternatives to have disutility-dependent degrees of correlation in the same nest, which can simultaneously consider the heterogeneity issue while addressing the similarity issue based on the nested choice structure.

2.1.2.3 Relationship between the weibit and logit models

This section illustrates the characteristics of the weibit model based on the comparison with the widely used logit model in terms of model development, probability expressions, and properties.

(1) Comparison of model development

Figure 2.3 graphically compares the derivations of the MNL and MNW models using a trinomial choice problem. Consider a case with three alternatives, A1, A2, and A3, which independently follow the Gumbel/Weibull distributions with the same scale/shape parameter. The disutility of the three alternatives is set to 2, 4, and 6, respectively. The scale parameter of the Gumbel distributions is set to 1. The shape parameter of the Weibull distribution is set to 3.3. The choice probability of A1 in the multinomial case can be obtained by comparing A1 with the alternative A*, which denotes the maximum utility or the minimum disutility of alternatives A2 and A3. Property 6 shows that the Gumbel/Weibull distribution is stable under the maximum/minimum operation, i.e., the alternative A* remains Gumbel/Weibull distributed with the same scale/shape parameter. Hence, Property 5 can be used to derive the choice probability of A1 as the binary choice between A1 and A*.

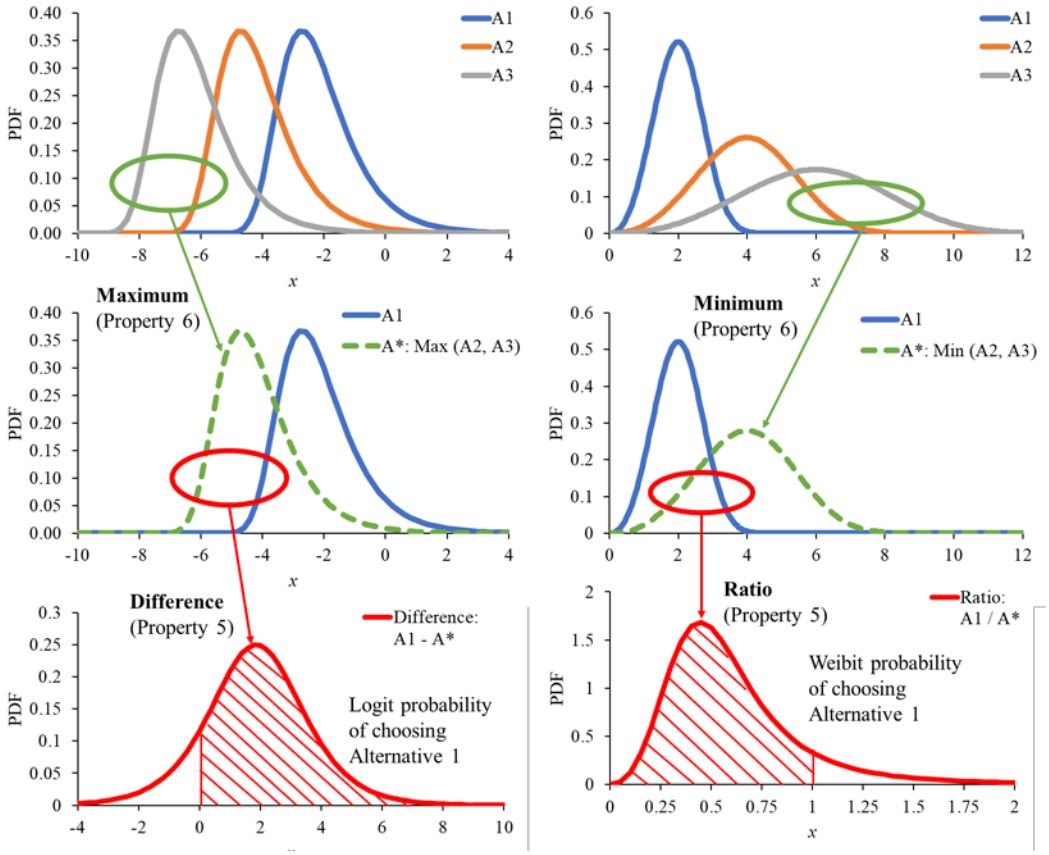

(a) logit model (b) weibit model

Figure 2.3. Derivation of multinomial choice models

(2) Comparison of probability functions

Figure 2.4 illustrates this relationship between the weibit and logit models based on the general "*logit-type*" probability function as discussed by Brathwaite and Walker (2018):

$$P_i = \frac{\exp\left[S\left(v_i\right)\right]}{\sum_{j \in I} \exp\left[S\left(v_j\right)\right]}. \tag{2.35}$$

The MNL model can be expressed by directly using $\theta \cdot v_i$ to represent $S(v_i)$, where the scale parameter is often set as $\theta = 1$. $S(v_i)$ of the MNW model is in a logarithmic form: $S(v_i) = -\beta \cdot \ln(v_i)$. The weibit model can thus be deemed as a logarithmic transformation of the logit model (Castillo et al., 2008; Fosgerau and Bierlaire, 2009).

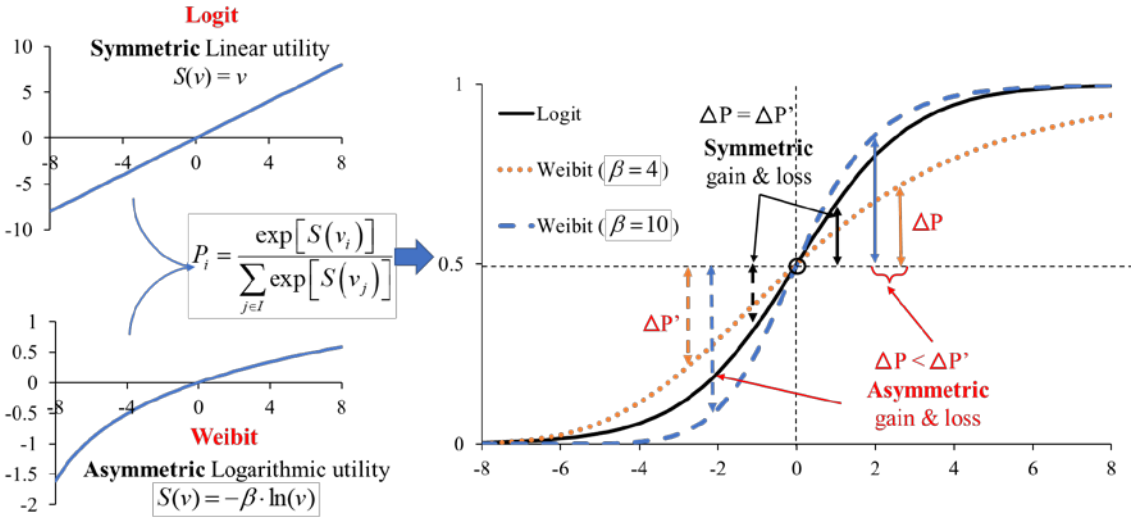

Figure 2.4. Relationship between logit and weibit choice models

As can be seen from Figure 2.4, the logarithmic form of utility function leads to the asymmetric probability curve of the weibit model, which is governed by the shape parameter β . Unlike the symmetric logit model providing an equal rate of increasing/decreasing choice probability with equal gains/losses, the weibit model gives a higher decrease than increase in probability when alternative utility is

decreasing/increasing to the same degree. The asymmetric property might be preferred in the evaluation of travel behavior, which is beneficial for analyses of transportation system accessibility and vulnerability as described in Section 2.1.3.

(3) Comparison of model properties

Owing to the differences in model development and probability function discussed above, the weibit model has distinct properties and performances than the logit model. Figure 2.5 compares the performances of the weibit and logit models. An illustrative binary mode choice example is presented in the typical short and long networks shown in Figure 2.5(a). The two modes are assumed to have the same absolute travel disutility difference but different magnitudes of mode disutility in the two networks (10 and 15 versus 100 and 105). As shown in Figure 2.5(b), because the logit model has a fixed variance, the PDFs of the perceived travel utility have the same shape for different networks. Using the absolute difference-based binary logit model, the same choice probability is derived for the two networks (Figure 2.5(c)). On the other hand, the disutility-dependent Weibull perception variances lead to different PDF shapes and hence distinct mode choice probabilities for the two networks (Figures 2.5(d) and 2.5(e)). Therefore, the weibit model can inherently address the heterogeneity issue embedded in the logit model.

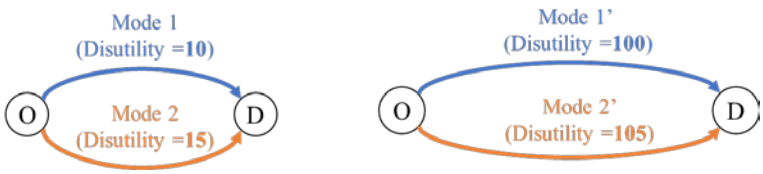

(a) Short (left) and long (right) networks

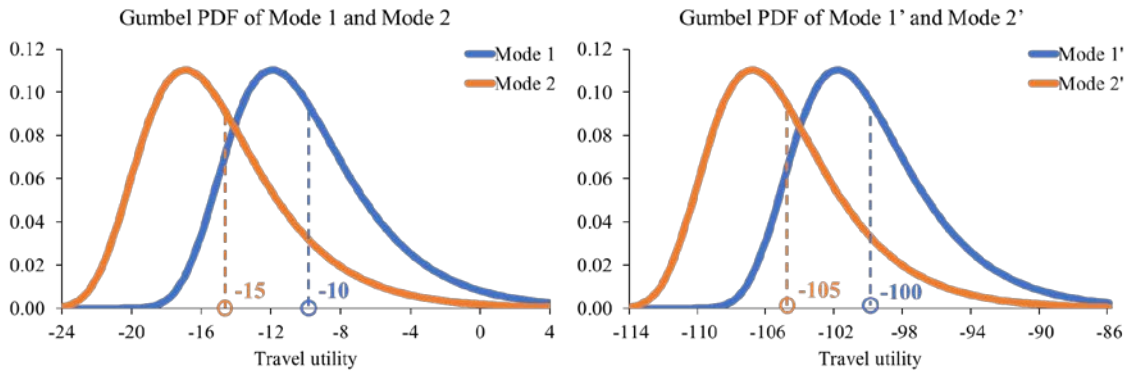

(b) PDF of Gumbel distributed travel utility perception

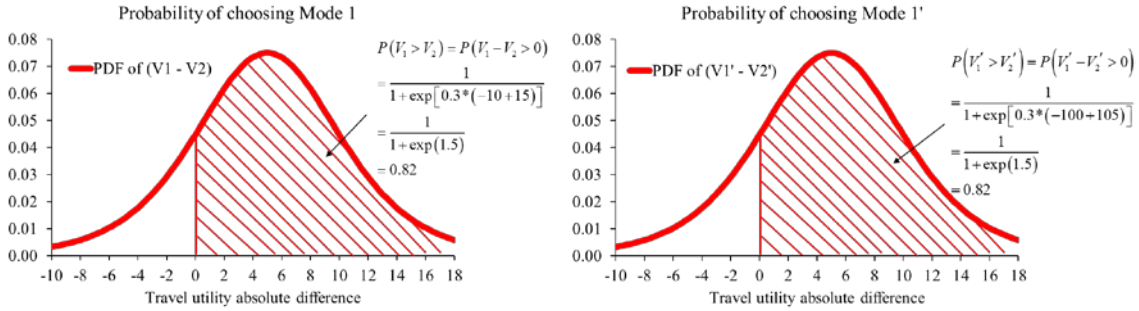

(c) Logit choice probability of Mode 1/Mode 1′

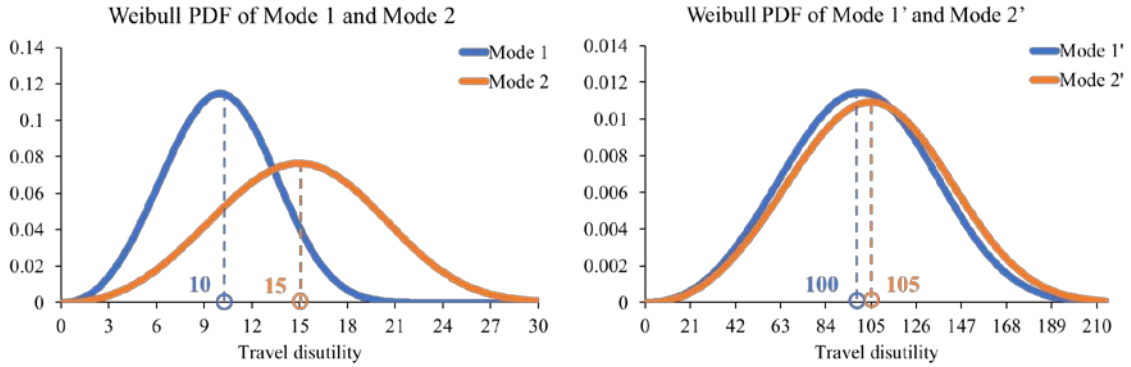

(d) PDF of Weibull distributed travel disutility perception

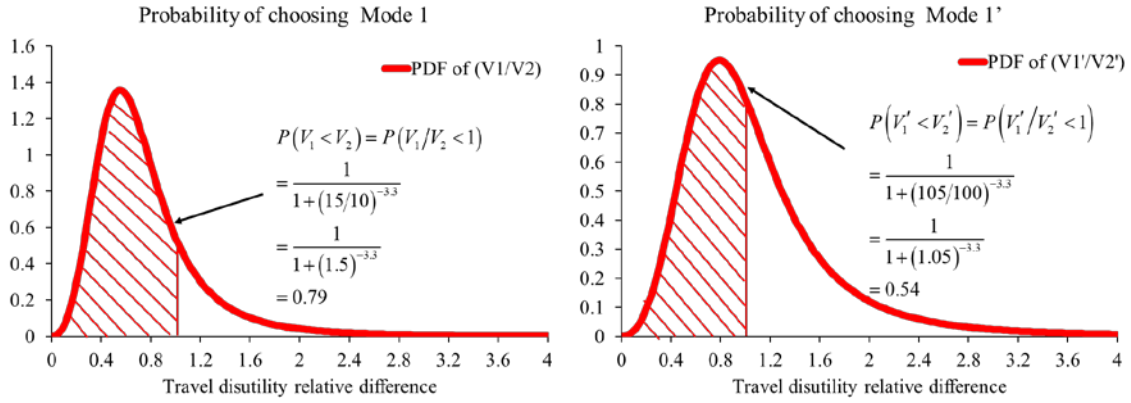

(e) Weibit choice probability of Mode 1/Mode 1′

Figure 2.5. Comparison between weibit and logit models in short and long networks

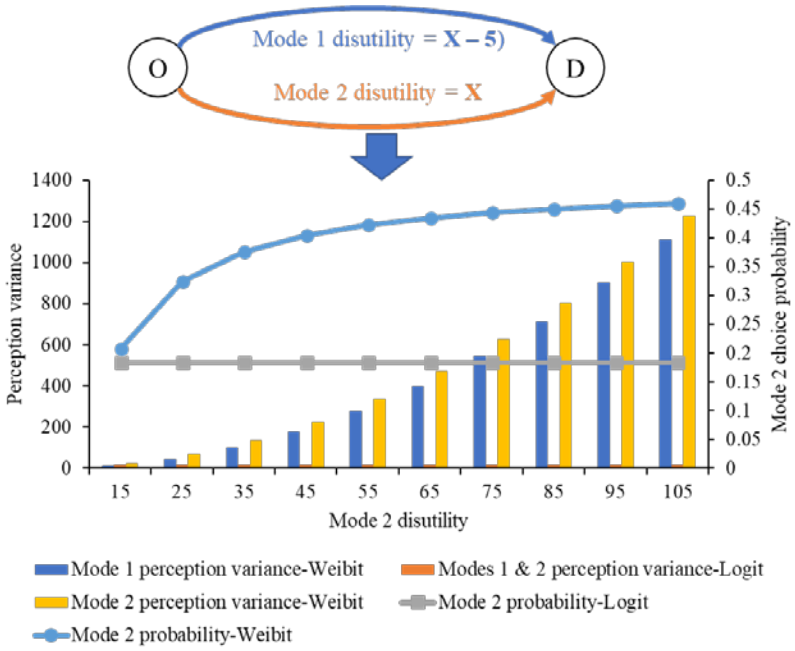

Figure 2.6. Illustration of the difference between perception variance and choice probability of weibit and logit models

Figure 2.6 further illustrates the different performances of the weibit and logit models based on a more general case where the travel disutility of mode 2 is X, and that of mode 1 is $(X - 5)$. The logit model has a fixed perception variance for the two modes, which results in the unchanged model choice probability disregarding the varying magnitudes of mode disutility. The weibit model, on the other hand, generates different perception variances for the two modes that are changing with the variation in mode disutility, which leads to the mode choice probability dependent on the disutility of both modes. This weibit outcomes seem to conform with real-world conditions, as the same difference in the travel disutility is likely to have a more significant effect in a short network but can be ignored in a long network. It shows the potential of the weibit model to outperform the logit model for considering heterogeneous perceptions of travel disutility when modeling the choice between distinct travel alternatives in future multi-modal transportation systems.

(4) Comparison of model elasticities

This section investigates the direct and cross elasticities of logit-based and weibit-based models to further explore the differences between these models. We assume that the alternative disutility is a linear function of a series of attributes:

$$v_i = \sum_{k \in K_i} \omega_k \tau_k^i, \forall i \in I , \tag{2.36}$$

where τ_k^i denotes the k^{th} attribute of alternative *i*, and ω_k is the coefficient associated with τ_k^i . The direct elasticity measures the effect of a change in an attribute of alternative *i* on the choice probability of alternative *i*, which can be written as

$$E_{\tau_k^m}^{P_m} = \frac{\partial P_m}{\partial \tau_k^m} \cdot \frac{\tau_k^m}{P_m}, \forall k \in K_m, m \in M . \tag{2.37}$$

On the other hand, the cross elasticity measures the effect of a change in an attribute of alternative *i* on the choice probability of another alternative *j*, which can be written as

$$E_{\tau_k^i}^{P_j} = \frac{\partial P_j}{\partial \tau_k^i} \cdot \frac{\tau_k^i}{P_j}, \forall k \in K_i, i, j \in I . \tag{2.38}$$

The direct and cross elasticities of the MNL, MNW, NL, NW, CNL models, as well as the cross-nested weibit (CNW) model that will be developed in Section 3.3.2.1, are compared in Table 2.3. The NW and CNW models based on nested choice structures have larger elasticities than the MNW model when more than one nest exists. Furthermore, the cross elasticities among alternatives in the same nest are larger than those among alternatives in different nests, which suggests that alternatives are more sensitive to changes in alternatives in the same nest than in alternatives outside the nest. The effects of nested and cross-nested structures on the weibit choice probability are in line with those for logit models summarized by Wen and Koppelman (2001).

The major difference between logit models and weibit models is that the elasticities of weibit models also depend on the alternative disutility v_i, which implies that as the alternative disutility increases, a unit change in the attribute may affect the choice probability less. This feature allows the weibit models to also consider the effect

of distinct magnitudes of alternative disutility on choice behavior, i.e., the heterogeneous perceptions of different alternatives. This is consistent with the intuition that the same degree of change might seem less significant for an alternative with a higher original disutility than for an alternative with a lower disutility. Since the term v_i is used to denote the utility in logit models and the disutility in weibit models, the elasticities of the two groups of models have opposite signs.

Table 2.3. Direct and cross elasticities of logit-based models and weibit-based models

	Direct elasticity	Cross elasticity
MNL	$\theta\omega_k\tau_k^i\cdot\left(1-P_i^{\mathbf{MNL}}\right)$	$-\theta\omega_k\tau_k^i\cdot P_i^{\mathbf{MNL}}$
MNW	$-v_i^{-1}\cdot\beta\omega_k\tau_k^i\cdot\left(1-P_i^{\mathbf{MNW}}\right)$	$.v_i^{-1}\cdot\beta\omega_k\tau_k^i\cdot P_i^{\mathbf{MNW}}.$
NL	$\omega_k\tau_k^i\cdot\left[\left(1-P_{ui}^{\mathbf{NL}}\right)+\left(\frac{1-\varphi_u}{\varphi_u}\right)\left(1-P_{i\|u}^{\mathbf{NL}}\right)\right]$	$\begin{cases}-\omega_k\tau_k^i\cdot P_{ui}^{\mathbf{NL}}, & i\in I_u, j\notin I_u\\ -\omega_k\tau_k^i\cdot\left[P_{ui}^{\mathbf{NL}}+\left(\frac{1-\varphi_u}{\varphi_u}\right)P_{i\|u}^{\mathbf{NL}}\right], & i,j\in I_u\end{cases}$
NW	$-v_i^{-1}\cdot\omega_k\tau_k^i\cdot\left[\left(1-P_{ui}^{\mathbf{NW}}\right)+\left(\frac{1-\varphi_u}{\varphi_u}\right)\left(1-P_{i\|u}^{\mathbf{NW}}\right)\right]$	$\begin{cases}v_i^{-1}\cdot\omega_k\tau_k^i\cdot P_{ui}^{\mathbf{NW}}, & i\in I_u, j\notin I_u\\ v_i^{-1}\cdot\omega_k\tau_k^i\cdot\left[P_{ui}^{\mathbf{NW}}+\left(\frac{1-\varphi_u}{\varphi_u}\right)P_{i\|u}^{\mathbf{NW}}\right], & i,j\in I_u\end{cases}$
CNL	$\omega_k\tau_k^i\cdot\frac{\sum_{u\in U}P_u^{\mathbf{CNL}}\cdot P_{i\|u}^{\mathbf{CNL}}\cdot\left[\left(1-P_{ui}^{\mathbf{CNL}}\right)+\left(\frac{1-\varphi_u}{\varphi_u}\right)\left(1-P_{i\|u}^{\mathbf{CNL}}\right)\right]}{P_{ui}^{\mathbf{CNL}}}$	$\begin{cases}-\omega_k\tau_k^i\cdot P_{ui}^{\mathbf{CNL}}, & i\in I_u, j\notin I_u\\ \omega_k\tau_k^i\cdot\left[P_{ui}^{\mathbf{CNL}}+\frac{\sum_{u\in U}P_u^{\mathbf{CNL}}\cdot P_{i\|u}^{\mathbf{CNL}}\cdot\left(\frac{1-\varphi_u}{\varphi_u}\right)P_{j\|u}^{\mathbf{CNL}}}{P_{ui}^{\mathbf{CNL}}}\right], & i,j\in I_u\end{cases}$
CNW	$-v_i^{-1}\cdot\omega_k\tau_k^i\cdot\frac{\sum_{u\in U}P_u^{\mathbf{CNW}}\cdot P_{i\|u}^{\mathbf{CNW}}\cdot\left[\left(1-P_{ui}^{\mathbf{CNW}}\right)+\left(\frac{1-\varphi_u}{\varphi_u}\right)\left(1-P_{i\|u}^{\mathbf{CNW}}\right)\right]}{P_{ui}^{\mathbf{CNW}}}$	$\begin{cases}v_i^{-1}\cdot\omega_k\tau_k^i\cdot P_{uj}^{\mathbf{CNW}}, & i\in I_u, j\notin I_u\\ -v_i^{-1}\cdot\omega_k\tau_k^i\cdot\left[P_{ui}^{\mathbf{CNW}}+\frac{\sum_{u\in U}P_u^{\mathbf{CNW}}\cdot P_{i\|u}^{\mathbf{CNW}}\cdot\left(\frac{1-\varphi_u}{\varphi_u}\right)P_{j\|u}^{\mathbf{CNW}}}{P_{ui}^{\mathbf{CNW}}}\right], & i,j\in I_u\end{cases}$

2.1.3 Utility-based accessibility and vulnerability analysis

This section introduces the applications of logit and weibit models in transportation system accessibility and vulnerability analyses based on the random utility theory. Accessibility is a critical concept widely used for assessing transportation systems under normal conditions, which describes the potential for users to reach spatially distributed opportunities, assessed from the perspective of either individuals or locations using a variety of measures. This section focuses on the utility-based measure stemmed from the random utility theory, which assesses accessibility as the utility travelers gain from the travel alternatives provided in the transportation system. Compared with other accessibility indices, the utility-based measure is advantageous as it has sold behavioral interpretations from the perspective of travelers and is consistent with the choice behavior modelled in travel demand models. In addition, the utility-based accessibility measure uses monetary terms to reflect changes in accessibility, thus can be directly used for cost-benefit analysis in decision-making (Van Wee, 2016; Winkler, 2016).

Vulnerability is an important measure of the operability of a transportation system under abnormal conditions, quantifying the network's susceptibility to disruptions (Berdica, 2002). Transportation system vulnerability is often measured based on the consequences of serious disruptions, e.g., removal of infrastructure and transportation services, in terms of degradation in certain performance measures (Jenelius et al., 2006). This section focuses on the accessibility-based vulnerability analysis, which assesses system vulnerability based on the reduction in utility-based accessibility measure after the removal of network components (e.g., nodes and links) (Jenelius et al., 2006; Chen et al., 2007; Jansuwan and Chen, 2015; Xu et al., 2021). Benefiting from the utility-based accessibility measure, the system vulnerability can be comprehensively analyzed considering changes on both the supply side (e.g., network topology) and the demand side (e.g., the complex choice behavior and travel demand patterns) (Mattsson and Jenelius, 2015; Taylor, 2017; Gu et al., 2020).

In this section, the logit-based accessibility and vulnerability measures based on choice models are first reviewed with discussions on their properties and limitations. Advanced accessibility and vulnerability analyses are then proposed based on the state-of-the-art weibit models. Benefiting from the appealing properties of weibit choice model (Section 2.1.2), the proposed weibit-based measures are inherently suitable for assessing the *relative* variation in system performance and are appropriate to assess the vulnerability of networks with distinct scales. The weibit-based measures are further advanced in consistent with extended weibit choice models, which can simultaneously address the similarity and heterogeneity issues embedded in the traditional logit-based transportation system analyses.

2.1.3.1 Logit-based vulnerability measure

We first briefly demonstrate the traditional logit-based accessibility and vulnerability measures stemming from the MNL choice model. Based on Property 6 of the Gumbel distribution (Table 2.1), the maximum perceived utility of a set of Gumbel distributed travel alternatives is still Gumbel distributed. The expected maximum utility gained from the travel choice set I can then be expressed in an additive form in line with the additive error structure in the logit model (Williams, 1977):

$$E\left(\max_i \{V_i, \forall i \in I\}\right) = A^L + C^L , \tag{2.39}$$

where C^L is a constant and A^L is the logsum measure expressed as follows:

$$A^L = \frac{1}{\theta} \ln \sum_{i \in I} \exp(\theta v_i) . \tag{2.40}$$

Logsum is used as the accessibility measure, which can be interpreted as the consumer surplus. The variation in logsum can be applied to assess the social benefit in specific planning scenarios with development of certain transportation infrastructure or policy (Williams, 1977; Ben-Akiva and Lerman, 1985; De Jong et al., 2007).

The transportation system vulnerability can be measured based on the *absolute difference* between post- and pre-disruption logsum measures:

$$\Delta A^L = A_0^L - A^{L'} = \frac{1}{\theta}\left[\ln\sum_{i\in I}\exp(-\theta\tau_i{}') - \ln\sum_{i\in I}\exp(-\theta\tau_i^0)\right], \qquad (2.41)$$

where τ_i^0, $\tau_i{}'$, A_0^L, $A^{L'}$ respectively denote the travel disutility (opposite of utility) of alternative *i* and the logsum before and after disruption. ΔA^L can be directly used as the vulnerability measure and can be interpreted as a kind of "average" degradation in the expected maximum travel utility. In line with the absolute utility difference–dependent logit choice probability, the logsum can accurately reflect the vulnerability when there is an absolute utility degradation of each travel alternative, i.e.,

$$\tau_i{}' = \tau_i^0 + \Delta A^L, \qquad (2.42)$$

$$A^{L'} = -\frac{1}{\theta}\ln\sum_{i\in I}\exp\left(-\theta\tau_i{}'\right) = -\frac{1}{\theta}\ln\sum_{i\in I}\exp\left[-\theta\left(\tau_i^0 + \Delta A^L\right)\right]. \qquad (2.43)$$

To account for the proportional degradation in network performance, the vulnerability measure V^L has also been widely used to derive the relative reduction in logsum after disruption:

$$V^L = \frac{\Delta A^L}{A_0^L}\ . \qquad (2.44)$$

However, owing to the IID assumptions embedded in the logit choice model, the logit-based vulnerability measure is still insufficient for reflecting the relative degradation in post-disruption network performance in networks with distinct scales and/or similar travel alternatives.

2.1.3.2 Issues associated with logit-based vulnerability measure

The logit-based vulnerability measure is affected by several issues stemming from the IID assumption of the logit choice model. In particular, the identically distributed

assumption causes difficulty in application to transportation networks with distinct scales and hinders the reflection of relative changes in network performance. The independently distributed assumption leads to the underestimation of the importance of independent travel alternatives. These issues will be discussed in this section.

(1) Distinct network scale

The Gumbel distributed random perception error with scale parameter θ gives a fixed perception variance $\sigma^2 = \pi^2/6\theta^2$ (Table 2.1). In this regard, a single value of θ may not be sufficient to reproduce the travel utility perception and travel choice probabilities for networks with distinct scales (Chen et al., 2012). This limitation may lead to biased logsum measures and vulnerability analysis outcomes.

Figure 2.7 illustrates the effect of network scale on the outcome of logit-based vulnerability analysis based on short and long networks shown in Figure 2.7(a). The scale parameter is set as $\theta = 0.3$. The vulnerabilities under the removals of Alternative 1 and Alternative 2 are separately assessed to examine the importance of each alternative. Figure 2.7(b) depicts the distribution of perceived travel utility and the logsum under each scenario (colored digits in bold). Figure 2.7(c) summarizes the vulnerability assessment outcomes including the absolute logsum differences based on Eq. (2.41), the relative logsum reduction derived from Eq. (2.44), and the relative importance of the two alternatives calculated as the ratio between the absolute logsum differences after removal of each alternative. The higher relative importance of Alternative 1 (or 1′) indicates that the removal of Alternative 1 (or 1′) will cause greater damage to the network than the removal of Alternative 2 (or 2′). The absolute difference in logsum is not sufficient to compare the vulnerability of different networks with heterogeneous scales. Although the relative reduction in logsum can partly handle the effect of distinct network scales, the outcome network vulnerability and the component importance are still inconsistent with the actual change in network scale.

(a) Short and long networks

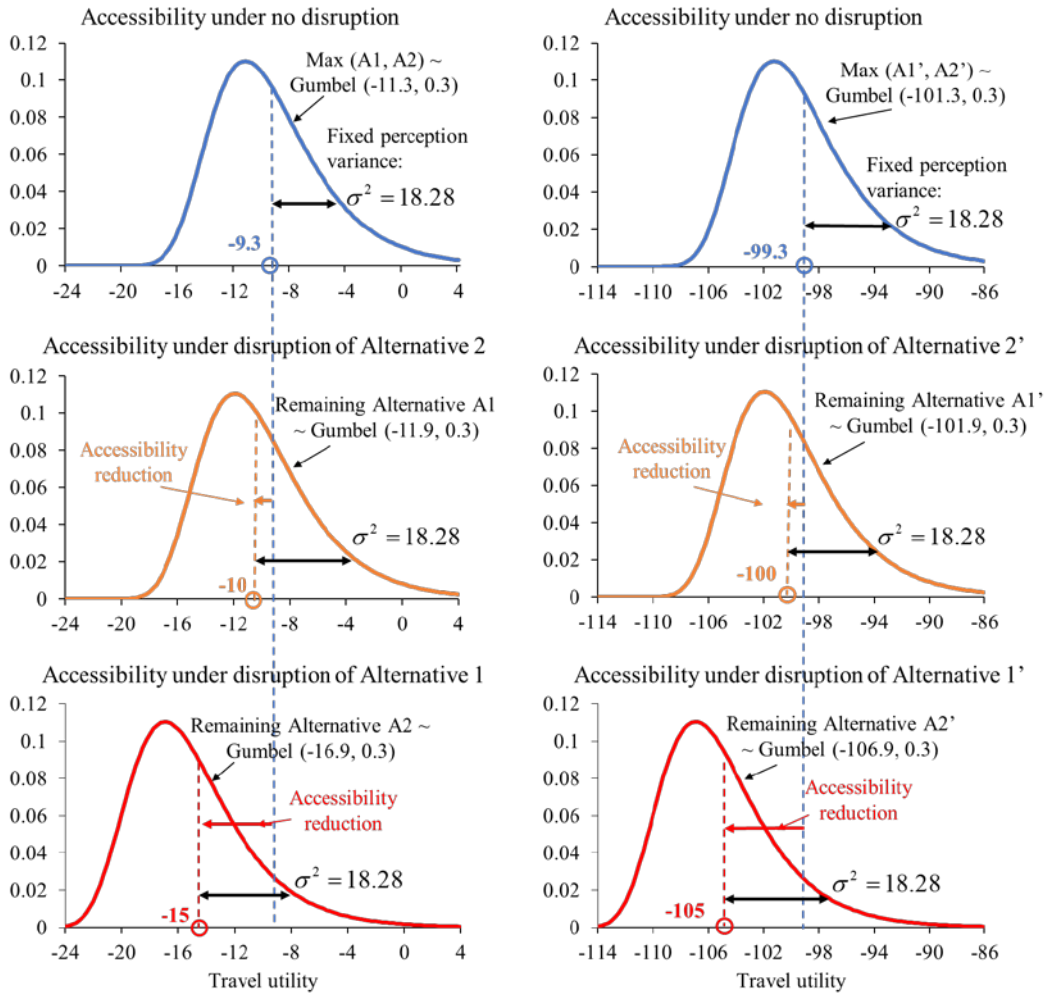

(b) Logit-based vulnerability analysis for short (left) and long (right) networks

Logsum-based vulnerability - Shorter network			
Disrupted alternative	**Absolute difference**	Relative reduction	Relative importance (A1/A2)
Alternative 1	5.67	61%	**8.45**
Alternative 2	0.67	7%	

Logsum-based vulnerability - Longer network			
Disrupted alternative	**Absolute difference**	Relative reduction	Relative importance (A1/A2)
Alternative 1	5.67	5.7%	**8.45**
Alternative 2	0.67	0.7%	

(c) Logit-based vulnerability outcomes of short (left) and long (right) networks

Figure 2.7. Effect of network scales on logit-based vulnerability analysis

The inadequacy of logit-based model to account for the difference in network scales may prohibit the applicability of logsum measures to vulnerability analysis, in

that the network scale, i.e., the magnitude of the network travel disutility, can change significantly under serious disruptions. Furthermore, the inability to correctly handle distinct network scales will hinder the comparison of vulnerability between different networks and influence the transferability of the vulnerability analysis outcomes.

(2) Relative network performance degradation

This section illustrates the inadequacy of the logit-based measure to reflect the relative degradation in network performance. As the logit model is unable to reflect the relative disutility difference in choice probability (Kitthamkesorn and Chen, 2013), the resulting logsum may lead to biased vulnerability outcome under relative performance degradation.

Consider a case with two alternatives with travel disutility τ_1 and τ_2. The logsum of the two alternatives can be expressed as below:

$$\begin{aligned} A &= \frac{1}{\theta}\ln\left[\exp\left(-\theta\tau_1\right)+\exp\left(-\theta\tau_2\right)\right] \\ &= -\tau_1+\frac{1}{\theta}\ln\left\{1+\exp\left[-\theta\left(\tau_2-\tau_1\right)\right]\right\} \end{aligned}. \tag{2.45}$$

Assume that under disruption, the ratios between the post- and pre-disruption cost of all alternatives are $\nu>1$, i.e., the post-disruption travel costs become $\nu\tau_1$ and $\nu\tau_2$. It is reasonable to expect that the post-disruption accessibility A' becomes $\nu\cdot A$:

$$\begin{aligned} A' &= \nu\cdot\frac{1}{\theta}\ln\left[\exp\left(-\theta\tau_1\right)+\exp\left(-\theta\tau_2\right)\right] \\ &= -\nu\tau_1+\nu\cdot\frac{1}{\theta}\ln\left\{1+\exp\left[-\theta\left(\tau_2-\tau_1\right)\right]\right\} \end{aligned}. \tag{2.46}$$

However, if we incorporate the post-disruption travel disutility to derive the logsum measure, a value different from A' will be obtained:

$$A^{L'} = \frac{1}{\theta}\ln\left[\exp\left(-\theta\cdot\nu\tau_1\right)+\exp\left(-\theta\cdot\nu\tau_2\right)\right] = -\nu\tau_1+\frac{1}{\theta}\ln\left\{1+\exp\left[-\theta\cdot\nu\left(\tau_2-\tau_1\right)\right]\right\} \quad (2.47)$$

The difference between the logit-based post-disruption accessibility, $A^{L'}$, and the reference value, A', can be expressed as follows:

$$A^{L'} - A' = \frac{1}{\theta}\ln\left\{1+\exp\left[-\theta\cdot\nu\left(\tau_2-\tau_1\right)\right]\right\} - \nu\cdot\frac{1}{\theta}\ln\left\{1+\exp\left[-\theta\left(\tau_2-\tau_1\right)\right]\right\}. \quad (2.48)$$

The term $A^{L'} - A'$ is monotonically increasing with $\tau_2 - \tau_1 > 0$ and monotonically decreasing with $\tau_2 - \tau_1 < 0$. When $\tau_2 - \tau_1 \to +\infty$ or $\tau_2 - \tau_1 \to -\infty$, $A^{L'} - A' = 0$. Therefore, the term $A^{L'} - A'$ is always non-positive, i.e., the post-disruption accessibility is always underestimated by logsum. An illustrative example with scale parameter $\theta = 0.3$ is shown in Figure 2.8. The blue line shows the values of term $A^{L'} - A'$ under different disutility differences ($\tau_2 - \tau_1$). The gap between the blue line and the x axis denotes the overestimated absolute reduction in accessibility (i.e., overestimated vulnerability), which reaches the maximum when $\tau_2 - \tau_1 = 0$. Note that the overestimated vulnerability is also influenced by the value of θ. As θ approaches infinity, the overestimated vulnerability approaches zero.

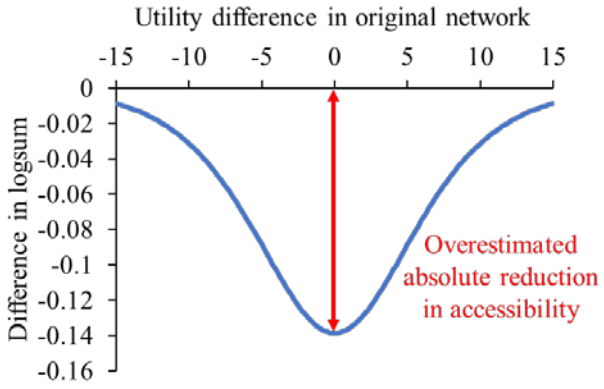

Figure 2.8. Overestimated vulnerability owing to logit-based measure

(3) Similar travel alternatives

Because of the independence assumption in the MNL model, the widely used MNL-based logsum measure ignores the correlation among similar travel alternatives; thus, it may generate biased choice probability and vulnerability analysis outcomes. Figure 2.9 presents an illustrative example of the effect of alternative similarity on vulnerability analysis in the context of mode choice.

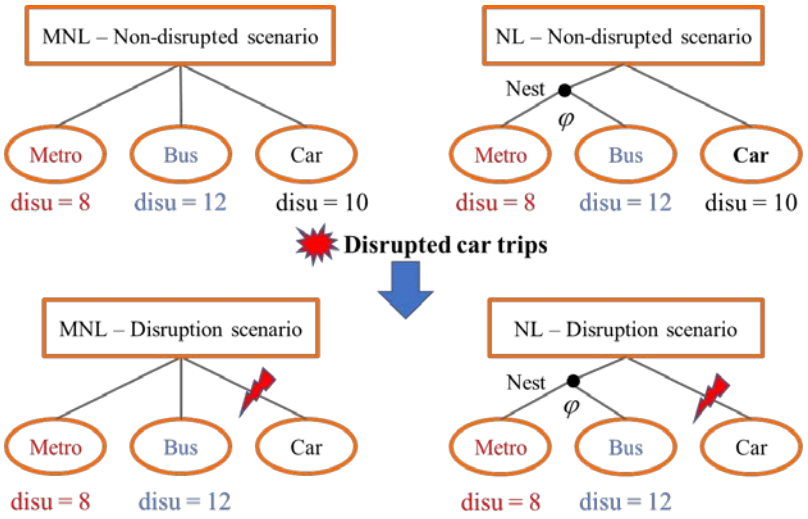

(a) Mode choice scenario

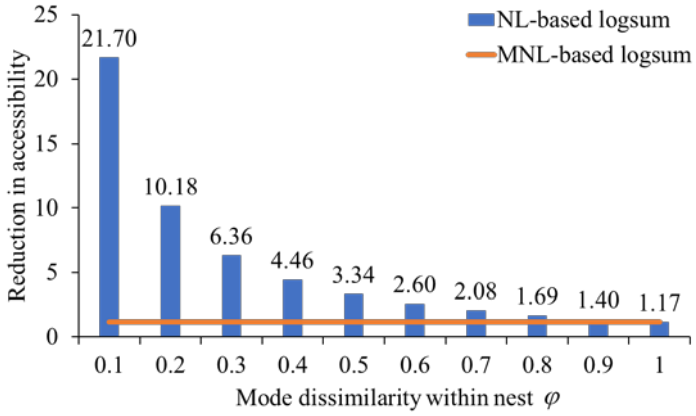

(b) Comparison between logsum reductions from the NL and MNL models

Figure 2.9. Effect of similarity on the logit-based vulnerability measure

Three modes are considered in the illustrative example: metro, bus, and private car. The accessibility reduction owing to the removal of the car mode is assessed. The MNL model, which neglects mode correlation, is compared with the NL model, in which similar alternatives are nested together (e.g., metro and bus are nested as transit

modes). The mode correlation is modeled by a dissimilarity parameter φ satisfying $0 < \varphi < 1$. A lower value of φ indicates a higher correlation between alternatives in the same nest. The NL model collapses to the MNL model when $\varphi = 1$. From Figure 2.9(b), the NL model leads to a greater reduction in accessibility with the decrease in the dissimilarity parameter, which implies that the neglect of correlation may lead to underestimation of the importance of an independent mode (the car mode in this case).

2.1.3.3 Weibit-based accessibility and vulnerability measure

To address the aforementioned issues associated with the logit-based measure, this section proposes accessibility-based vulnerability measures stemming from the weibit-based choice model, which is also derived based on the random utility theory. Based on Property 6 of Weibull distribution (Table 2.2), the minimum disutility of a set of Weibull distributed travel alternatives is still Weibull distributed, with the same shape parameter but different scale parameters. The expected minimum disutility gained from the travel choice set *I* can be expressed as:

$$E\left(\min_i \{V_i, \forall i \in I\}\right) = A^W \cdot C^W, \tag{2.49}$$

where C^W is a constant dependent on the shape parameter β, and A^W is the weibit-based accessibility measure, which can be expressed as follows:

$$A^W = \left[\sum_{i \in I} (\tau_i)^{-\beta}\right]^{-1/\beta}. \tag{2.50}$$

Different from the logsum which takes the log of the denominator of the logit choice probability, the weibit-based accessibility measure takes the root of the denominator of the weibit choice probability. The proposed weibit-based vulnerability measure is derived based on the ratio between the post- and pre-disruption weibit-based accessibility, ΔA^W:

$$V^W = \Delta A^W = \left[\sum_{i\in I}\left(\tau_i'\right)^{-\beta}\right]^{-1/\beta} \Big/ \left[\sum_{i\in I}\left(\tau_i^0\right)^{-\beta}\right]^{-1/\beta}. \tag{2.51}$$

A higher value of the vulnerability measure V^W indicates a larger increase in disutility under disruption, namely, a larger system performance degradation. ΔA^W can then be interpreted as the average increase rate in alternative travel disutility:

$$A^{W\prime} = \left[\sum_{i\in I}\left(v_i'\right)^{-\beta}\right]^{-1/\beta} = \left[\sum_{i\in I}\left(v_i^0 \cdot \Delta A^W\right)^{-\beta}\right]^{-1/\beta}. \tag{2.52}$$

Different from the logit model, the weibit model allows alternative-specific perception variances and has a relative disutility difference-dependent choice probability (Section 2.1.2). Thus, the weibit-based vulnerability measure is inherently suitable to reflect the performance degradation when there is a relative degradation in the service level of each travel alternative. Figure 2.10 illustrates the effect of the proposed weibit-based measure. The short and long networks depicted in Figure 2.7(a) are used to present an illustrative example. The vulnerabilities under the removals of Alternatives 1 and 2 are separately assessed to examine the importance of each alternative. Figure 2.10(a) depicts the distribution of perceived travel disutility, perception variance, and the weibit-expected disutility under each scenario (colored digits in bold). Figure 2.10(b) summarizes the vulnerability assessment outcomes, including the relative differences in the weibit-expected disutility shown in Figure 2.10(a) and the relative importance of the two alternatives denoted by the ratio between the performance degradations after removal of each alternative. With alternative-specific perception variances, the weibit-based measure can derive different vulnerabilities (relative differences) for different alternatives in different networks. Furthermore, the relative importance of Alternative 1 and 1′ is consistent with the disutility ratio between Alternative 1/1′ and Alternative 2/2′.

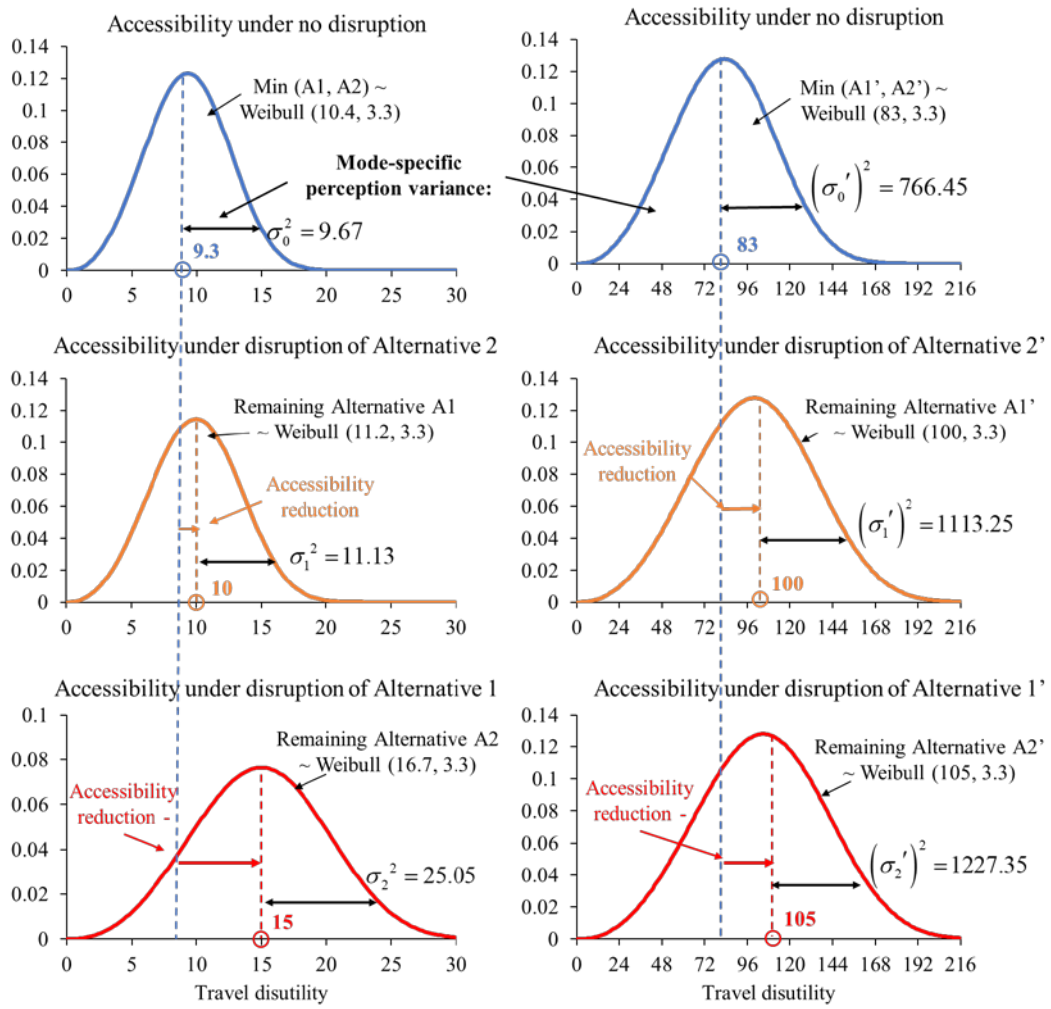

(a) Vulnerability analysis based on weibit-expected disutility

Weibit-based vulnerability - Shorter network		
Disrupted alternative	Relative difference	Relative importance (A1/A2)
Alternative 1	1.61	**1.50**
Alternative 2	1.07	

Weibit-based vulnerability - Longer network		
Disrupted alternative	Relative difference	Relative importance (A1/A2)
Alternative 1	1.265	**1.05**
Alternative 2	1.205	

(b) Weibit-based vulnerability analysis outcomes of short and long networks

Figure 2.10. Effect of weibit-based vulnerability analysis

In summary, the weibit-based vulnerability measure allows a comparison between outcomes from networks with distinct scales and overcomes the issues of the logit-based measure associated with heterogeneous network scales and relative change in network performance. However, the measure based on the MNW model is still affected by the similarity issue (3) in Section 2.1.3.2. To deal with this limitation, the advanced

weibit models introduced in Section 2.1.2.2 can be incorporated in the accessibility-based vulnerability measure.

2.1.3.4 Accessibility and vulnerability measures based on extended weibit models

This section presents the accessibility and vulnerability measures derived from extended weibit models, which can simultaneously address the similarity and heterogeneity issues in logit-based measures. The PSW model commonly used in route choice problems and the NW model commonly used in mode choice problems are adopted to exemplify the derivation of accessibility measures.

(1) PSW-based accessibility measure

In the PSW model, a PS factor PS_k^{rs} is introduced to the disutility function of path k between OD pair rs:

$$V_k^{rs} = \left(PS_k^{rs}\right)^{-\frac{1}{\beta_k}} \cdot \tau_k^{rs} \cdot \varepsilon_k^{rs}, \forall k \in K^{rs}, rs \in RS, \tag{2.53}$$

which leads to the PSW choice probability as follows:

$$P_k^{rs} = \frac{PS_k^{rs} \cdot \left(\tau_k^{rs}\right)^{-\beta_k}}{\sum_{k \in K^{rs}} PS_k^{rs} \cdot \left(\tau_k^{rs}\right)^{-\beta_k}}, \forall k \in K^{rs}, rs \in RS. \tag{2.54}$$

The PS factor is a correction term that only influences the deterministic disutility. Thus, the accessibility measure based on the PSW model can be obtained based on Property 6 of the Weibull distribution (Table 2.2) following Eq. (2.50):

$$A_k^W = \left[\sum_{k \in K^{rs}} PS_k^{rs} \cdot \left(\tau_k^{rs}\right)^{-\beta_k}\right]^{-\frac{1}{\beta_k}}, \forall k \in K^{rs}, rs \in RS. \tag{2.55}$$

(2) NW-based accessibility measure

As illustrated in Section 2.1.2.2, the NW model adopts a nested structure and a multiplicative error structure (Eq. (2.17)). As an example, a two-level NW mode choice

model is considered in this section, where individual modes belonging to the same type of mobility service are collected in the same nest. Travelers are considered to make marginal choice of service type and conditional choice of individual mode belonging to the selected type of service. The NW-based accessibility measures are then separately derived from different choice levels. First, the accessibility measure of service type *u* between OD pair *rs* can be obtained as the expected minimum disutility from the conditional choice level:

$$A_{rsu}^{W} = \left[\sum_{m \in M_u^{rs}} \left(\tau_{um}^{rs} \right)^{-\beta_u} \right]^{-\frac{1}{\beta_u}}, \forall u \in U^{rs}, rs \in RS . \tag{2.56}$$

Due to the nested structure of the NW model, the accessibility at the marginal choice level is dependent on the accessibility at the conditional level. If there exists no nest-specific disutility, the accessibility measure between OD pair *rs* can be obtained as the expected minimum disutility from the marginal choice level:

$$A_{rs}^{W} = \left[\sum_{u \in U^{rs}} \left(A_{rsu}^{W} \right)^{-\beta_{rs}} \right]^{-\frac{1}{\beta_{rs}}}, \forall rs \in RS . \tag{2.57}$$

Based on the advanced weibit-based accessibility measures shown in Eqs. (2.55)–(2.57), the corresponding accessibility-based vulnerability measures can be obtained as the relative difference between the post- and pre-disruption accessibility following Eq. (2.51).

2.2 Network equilibrium models with MP formulation

Network equilibrium models have been exhaustedly studied for aggregate-level travel demand analysis, where individual travel choice models can be integrated to reproduce the disaggregate-level travel behavior. Instead of the travel choice models that derive choice probabilities based on exogeneous travel disutility v, equilibrium models consider the interactions among travelers via endogenous travel disutility dependent on travel demand, i.e. $v=v(q)$. At the equilibrium, the travel demand pattern is consistent with the travel choices derived based on the demand-dependent travel disutility. Hence, the equilibrium condition can be represented as a fixed-point problem with the travel demand existing on both sides of the equation:

$$\mathbf{q} = D \cdot \mathbf{P}\left(\mathbf{v}\left(\mathbf{q}\right)\right), \tag{2.58}$$

where D denotes the total travel demand in transportation system. $\mathbf{q}$, $\mathbf{v}$, and $\mathbf{P}$ denote the vectors of investigated travel demand, travel disutility, and travel choice probability, respectively. Different equilibrium models have been developed based on different choice models reproducing choice probability $\mathbf{P}$. In the literature, equilibrium models are mainly applied in traffic assignment problems, which assign OD travel demands onto links following certain selfish route choice behavior in congested networks. Figure 2.11 summarizes the network equilibrium models with Beckmann-type MP formulation.

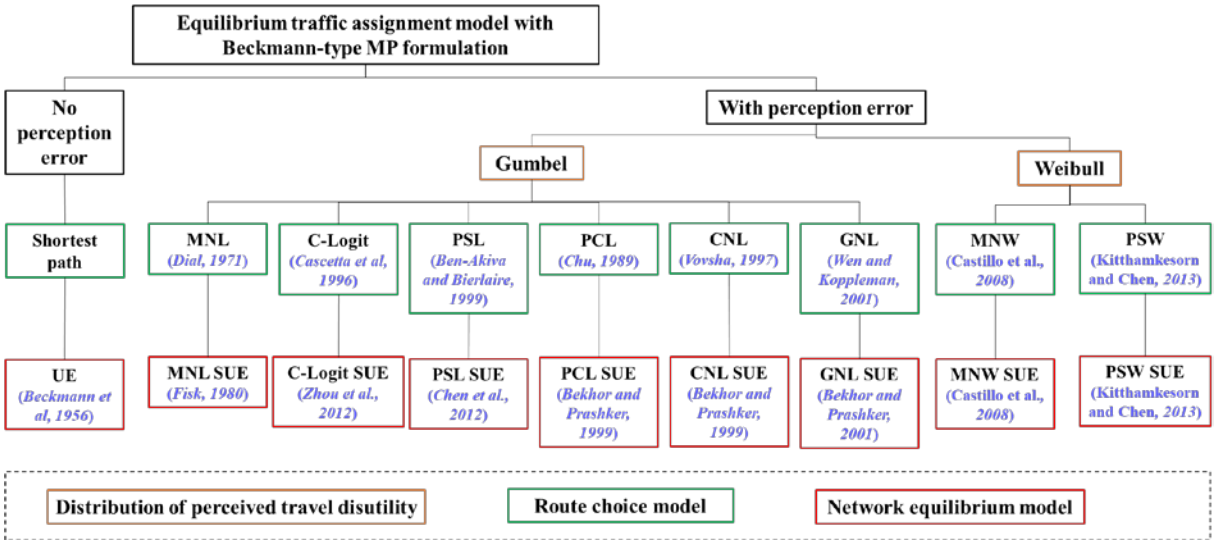

Figure 2.11. Summary of network equilibrium models with MP formulation

In the deterministic network equilibrium analysis, travelers are assumed to have perfect knowledge of transportation systems and no perception error. All travelers choose the paths with the minimum travel disutility between each OD pair, which leads to the user equilibrium (UE) assignment following Wardrop's first principle (Wardrop, 1952). Beckmann et al. (1956) formulated the UE model as a mathematical programming (MP) problem with a convex objective function and linear constraints. Beckmann's MP formulation guarantees the equivalence and uniqueness of solutions while facilitating model interpretation and development of convergent and efficient solution algorithms.

The other line of equilibrium model is the stochastic user equilibrium (SUE) principle suggested by Daganzo and Sheffi (1977). Instead of unrealistically assuming travelers to have perfect knowledge of transportation system, the SUE problem considers imperfect knowledge and hence perception errors on travel disutility. At SUE, travelers are assumed to choose the paths with the minimum perceived travel disutility, where the perceived travel disutility is assumed to follow certain distribution, e.g., the normal distribution, Gumbel distribution, and Weibull distribution. The normal distributed perception error results in the multinomial probit (MNP) SUE model (Daganzo and Sheffi, 1977). Maher (2001) extended the unconstrained SUE formulation to the elastic demand version, which can be applied to both types of perception error distributions, i.e., both probit-based and logit-based SUE problems Rosa and Maher (2002) investigated the MNP SUE-ED problem with multiple user classes. Meng and Liu (2011, 2012) and Meng et al. (2014) extended The MNP SUE model has been further extended to consider specific issues including elastic demand (Maher, 2001), multiple user classes (Rosa and Maher, 2002), link interactions (Meng and Liu, 2011), continuously distributed value of time (Meng et al., 2012), and link capacity constraints (Meng et al., 2014). However, studies on the MNP SUE model are relatively limited owing to the absence of an MP model formulation and a closed-form expression of MNP choice probability, which largely increases the computational burden for simulating the route choice probability in large-scale networks.

Comparing with other types of SUE model formulations, such as the variational inequality, nonlinear complementary problem, and fixed-point formulations, the MP formulation is desirable owing to its various appealing properties: readily interpretable and easily understandable optimality conditions; solvable by existing convergent and

efficient algorithms; and the convex objective function that can be used to obtain appropriate step size and stop criterion for the solution procedure (Kitthamkesorn and Chen, 2017). Therefore, the MP formulation has been widely adopted by SUE studies for various applications, and thus is the focus of the proposed research. This section reviews the SUE models with Beckmann-type MP formulation based on different route choice models, followed by the extensions to combined demand that incorporate higher choice dimensions in equilibrium analysis. The method of developing Beckmann-type SUE formulations based on different choice models will be introduced in Section 5.

2.2.1 SUE models with MP formulation

2.2.1.1 Logit-based SUE models

Assuming Gumbel distributed path disutility perception errors leads to the MNL route choice model, which is most adopted in SUE problems (Dial, 1971). Owing to the Luce-form logit choice probability, the MNL SUE model can be represented by a Beckmann-type MP formulation, where an entropy term is additionally incorporated to account for the stochasticity in route choice behavior at the aggregate level (Fisk, 1980). Despite the appealing properties of having an MP formulation, the MNL SUE model inherits limitations from the MNL choice model, namely the inadequacy to consider the heterogeneous travel disutility perception and correlations among paths (e.g., path overlaps) (Chen et al., 2012).

To deal with the limitations of the MNL SUE model, many extended logit choice models introduced in Section 2.1.1.2 have been integrated to deal with path correlations. The extended logit models with correction term can be integrated by adding an objective term with respect to the path disutility correction, such as the C-logit SUE model (Zhou et al., 2012) and PSL SUE model (Chen et al., 2012). On the other hand, the extended logit models with nested choice structure can be integrated by specifying decision variables corresponding to the adopted structure and adding entropy terms with respect to different choice levels in the objective function. For instance, Bekhor and Prashker (1999) developed the MP formulation of the PCL SUE and CNL SUE models; Bekhor and Prashker (2001) develops the GNL SUE model formulation. However, the heterogeneity issue cannot be inherently addressed by the extended logit SUE models. Chen et al. (2012) proposed to scale the logit dispersion parameter θ for

each OD pair (i.e., a common scaled dispersion parameter for the route set between each OD pair), which showed the scaled logit models can outperform the unscaled ones by distinguishing the magnitudes of trip lengths between different OD pairs. However, scaling the dispersion parameters for different OD pairs may be cumbersome as there are many OD pairs in a typical large-scale transportation network (e.g., a medium-sized network known as the Winnipeg network has 154 zones, 2535 links, and 4345 OD pairs).

2.2.1.2 Weibit-based SUE models

The weibit-based SUE model has been recently proposed that inherently addresses the heterogeneity issue embedded in logit-based SUE models. In a pioneering work, Castillo et al. (2008) proposed the SUE problem based on the MNW route choice model, which accounts for the heterogeneity issue via route-specific perception variances and relative difference-dependent probability. Many equilibrium analyses have been developed to advance the MNW SUE model based on extended weibit choice models that further relax the independently distributed assumptions. For instance, Kitthamkesorn and Chen (2013, 2014) used the path-size factor of the PSL model to develop the PSW model, applying it to the SUE problem using the constrained convex program in 2013 and the unconstrained nonlinear program in 2014. Kitthamkesorn et al. (2015) extended the PSW SUE model to the elastic OD demand case to explain the interaction between supply and demand. Xu et al. (2015) developed the hybrid weibit-logit model to take advantage of both the relative difference-based weibit model and the absolute difference-based logit model in the traffic assignment.

Another stream of studies focused on the theoretical analysis and practical applications of weibit-based SUE models. For example, Yao and Chen (2014) analyzed the stochastic assignment paradox based on the logit and weibit choice models. Cheng et al. (2022) explored the stochastic assignment paradox using the multiplicative hybrid weibit-logit model. Wang et al. (2021a) analytically and empirically investigated the effect of traveler's prior knowledge or information on the performance of weibit-based SUE models. Weibit models have also been applied to various traffic assignment and

related network design problems. For example, link-based stochastic network loading algorithms have been customized for applying the weibit-based SUE models to road traffic assignment (Kitthamkesorn and Chen, 2014; Sharifi et al., 2015; Liu et al., 2017). Kitthamkesorn et al. (2021) further considered the MNW travel choice behavior in the design of park and ride facilities. Weibit route choice can also be incorporated in day-to-day traffic assignment (Ye, 2022), which can be applied to network vulnerability analysis (Xu et al., 2021) and road congestion pricing (Qu et al., 2021). Xie et al. (2020) applied the weibit model to schedule-based stochastic passenger assignment for train schedule optimization in a high-speed railway network.

2.2.2 Combined travel demand model

The SUE models discussed in Section 2.2.1 focus on the level of traffic assignment with respect to the route choice dimension. Efforts have also been made to develop combined travel demand models that flexibly incorporate more levels in the sequent four-step model dimensions with respect to other choice dimensions, i.e., trip generation, trip distribution, and modal split (Safwat and Magnanti, 1988; Oppenheim, 1995; Boyce and Bar-Gera, 2004; Zhou et al., 2009). Different from the sequent four-step model considering different choice dimensions in a separate manner, the combined model can reproduce the joint travel, destination, mode, and route choice in a consistent way based on the random utility theory. Besides considering all four choice dimensions, many combined models focus on some of the interacting dimensions for specific applications, such as the combined distribution and assignment (CDA) model and the combined modal split and traffic assignment (CMSTA) model.

(1) Combined distribution and assignment model

The CDA model considers the joint destination and route choice, where the destination choice is reproduced based on the OD travel cost consistent with the route choice behavior. Tomlin (1971) proposed an MP formulation of CDA model using an entropy term standing for the equilibrium trip distribution based on the gravity model, while the route choice follows the system optimal principle. Florian et al. (1975) further developed an CDA model considering selfish route choice behaviors, in which the route

choice is modeled following the UE principle. However, the gravity-based trip distribution model used in such CDA models can also be interpreted from the perspective of the random utility theory as an MNL destination choice, which is inconsistent with the deterministic UE route choice. Efforts have been made to guarantee the consistency between destination and route choices by integrating the logit-based SUE traffic assignment model (e.g., Oppenheim 1995). Yao et al (2014) further developed a general unconstrained formulation for the CDA model. Further extensions have been made to incorporate specific considerations, such as multiple user and vehicle classes (Friesz, 1981; Lam and Huang, 1992), variable destination cost (Oppenheim, 1993), different types of location choices (Yang and Meng, 1998), capacity constraints (Tam and Lam, 2000), and network uncertainty (Yim et al., 2011).

Several efforts have been made to advance the CDA model by incorporating advanced destination and route choice models. For example, Chu (2011) adopted the dogit model for reproducing destination choice with both compulsory and discretionary trip purposes. Yao et al. (2014) adopted the spatially correlated logit model to account for the similarity among spatially adjacent locations. The PSL model was also adopted for route choice with consideration of path overlaps.

(2) Combined modal split and traffic assignment model

The CMSTA model considers both mode choice and route choice together. The mode choice is influenced by the aggregate cost stemmed from the equilibrium route choice. Similar to the development of CDA models, many CMSTA models first combine the stochastic mode choice following the binary logit choice model and the deterministic route choice following the UE principle (Florian, 1977; Florian and Nguyen, 1978; Abdulaal and LeBlanc, 1979). The CMSTA model was then extended to consider multiple modes (Oppenheim, 1995) and stochastic route choice (Oppenheim, 1995; Wu and Lam, 2003).

Many advanced choice models have been integrated in the CMSTA model for considering various behavioral issues. For instance, Kitthamkesorn et al. (2016) developed the NL-CNL CMSTA model to simultaneously consider the similarity issues at both dimensions, where the mode correlation is considered via the NL model and the path overlap is considered by the CNL model. Liu et al. (2018) developed a CNL-UE CMSTA model to specifically account for the similarity between the park & ride service

and other travel modes. Wang et al. (2020a) developed a dogit-PSL CMSTA model, where the dogit model is adopted to consider mode choice captivity and the PSL model is adopted to account for path overlap. Du et al. (2022) developed a CNL-PSL CMSTA model for network capacity analysis, where the CNL model is adopted for the mode choice with various emerging mobility services. Besides the extended logit-based CMSTA models that are inadequate to reflect heterogeneous travel perceptions, Kitthamkesorn and Chen (2017) proposed an advanced weibit-based CMSTA model to simultaneously consider similarity and heterogeneity issues at both mode and route choice dimensions. The NW model was developed for the mode choice behavior, whereas the route choice was reproduced using the PSW model.

Methodology Part I. Modeling individual travel choices: Development of advanced random utility models with emerging choice behavior

Chapter 3 Closed-form choice models based on “Luce class” of error distributions

This chapter focuses on the development of advanced individual choice models with random errors identically following the “Luce class” distributions, which leads to the generalized “Luce-form” choice probabilities that are efficient for probability evaluation. For applications in emerging choice contexts with different innovative transport policies or mobility services, the independently distributed assumption is relaxed in different manners to consider various correlations among travel alternatives in the emerging transportation system.

In particular, Section 3.1 develops an ordered path-size generalized extreme value model for the route choice in road networks with road tolls. Besides incorporating correction terms to penalize the physical correlation (overlap) among paths, a specific ordered nested choice structure is incorporated to account for the perceptual correlation among paths with closely ranked tolls. By taking advantage of the two ways of developing extended logit models as illustrated in Section 2.1.1.2, i.e., adding correction terms and introducing a nested choice structure, the developed model is able to address different path correlations in an integrated manner.

Section 3.2 develops a dogit-nested weibit mode choice model for multi-modal systems with customized bus services. Instead of the commonly used Gumbel error distribution, this section shows the MRUM development based on the Weibull error distribution, a “Luce class” distribution that fits the MRUM framework. Furthermore, a nested choice structure is introduced to model the mode similarity. The dogit mode, an alternative probabilistic choice system, is embedded in the MRUM framework to develop a closed-form choice model that considers the issue of passenger loyalty.

Section 3.3 develops a dogit-cross-nested weibit model for joint mobility bundle and mode choice with various emerging mobility services. On the basis of the advanced dogit-nested weibit model developed in Section 3.2, this model considers the effect of mobility bundling, an emerging marketing strategy for promoting emerging mobilities, on both the mode similarity issue and the passenger loyalty issue.

Section 3.4 develops a spatially correlated weibit–parking-size weibit model for joint destination and parking choice with shared parking services. In addition to the

single-dimensional choice behaviors considered in Sections 3.1-3.3, this section develops a combined destination and parking choice model based on a hierarchical choice structure. The two ways of modeling correlations illustrated in Section 2.1.1.2 are adapted based on the features of different choice dimensions considered. The developed model is still within the weibit-based MRUM framework. Thus, it retains the computationally efficient generalized "Luce-form" choice probability that facilitates further applications in the equilibrium analysis in real-world networks.

3.1 Route choice in tolled networks

3.1.1 Background and related studies

Route choice models play a critical role in travel demand analysis. Besides the extensively used multinomial logit (MNL) model which has a closed-form probability expression but fails to capture the correlation among paths, various extended logit models have been developed and adapted for the route choice in the stochastic user equilibrium (SUE) analysis (Prashker and Bekhor, 2004). The commonly used extended logit route choice models include:

- C-Logit (Cascetta et al, 1996): Add a correction term representing the utility reduction due to commonality with overlapped paths.
- Path-size logit (PSL, Ben-Akiva and Bierlaire, 1999): Add a factor representing the "size" of an overlapped path compared with a "full" path without overlapping.
- Paired combinatorial logit (Chu, 1989): Use a nested choice structure with each pair of overlapped paths collected in the same nest.
- Cross-nested logit (Vovsha, 1997): Use a nested choice structure with all paths passing the same link collected in the same nest.

In summary, the existing logit-based route choice models are dominated by the consideration of physical correlation among paths, namely the path overlap associated with the length or travel time attribute of each path. However, few studies have considered the *perceptual path correlation* triggered by other attributes that can also exert significant effects on route choice behaviors (Frejinger and Bierlaire, 2007). For

example, the path order based on the ranking of monetary travel cost, which is an important attribute in conjunction with travel time, has been considered in the route choice in tolled networks (Leurent, 1993; Glavic et al., 2017; Xie et al., 2021). There are likely correlations among the random utility components of adjacently ordered alternatives (Small, 1987). *Specifically, in the tolled network with a ranking of toll, there may exist path order correlation, i.e., the perceptual correlation among paths with adjacent orders of toll.* Figure 3.1 illustrates this issue based on a route choice example between an OD pair in Hong Kong, where the navigation software suggests three paths using three cross-harbor tunnels with a ranking of tolls (WHC for Western Harbour Crossing, CHT for Cross-Harbour Tunnel, and EHC for Eastern Harbour Crossing, respectively). In addition to the physical overlaps among the three alternatives, travelers choose routes considering the tradeoff between cost and time based on the perceptual correlation between paths with close rankings of toll, which has been overlooked in the route choice literature. For instance, Paths 2 and 3 are perceptually correlated as they both rank low in road tolls (first and second, respectively), thus are likely to be considered as competing alternatives by price-sensitive travelers. Therefore, in addition to the physical path overlap, the perceptual path order correlation is also imperative to be incorporated in the route choice model for tolled networks.

This section aims to model the route choice in tolled networks while specifically accounting for the effect of road toll ordering and path order correlations. The integration of path order information is based on the discovery that the ordered generalized extreme value (OGEV) model (Small, 1987) can naturally account for the correlation among ordered choice alternatives, which matches the route choice with a known ranking of toll. On this basis, an advanced route choice model is developed to consider perceptual and physical path correlations simultaneously.

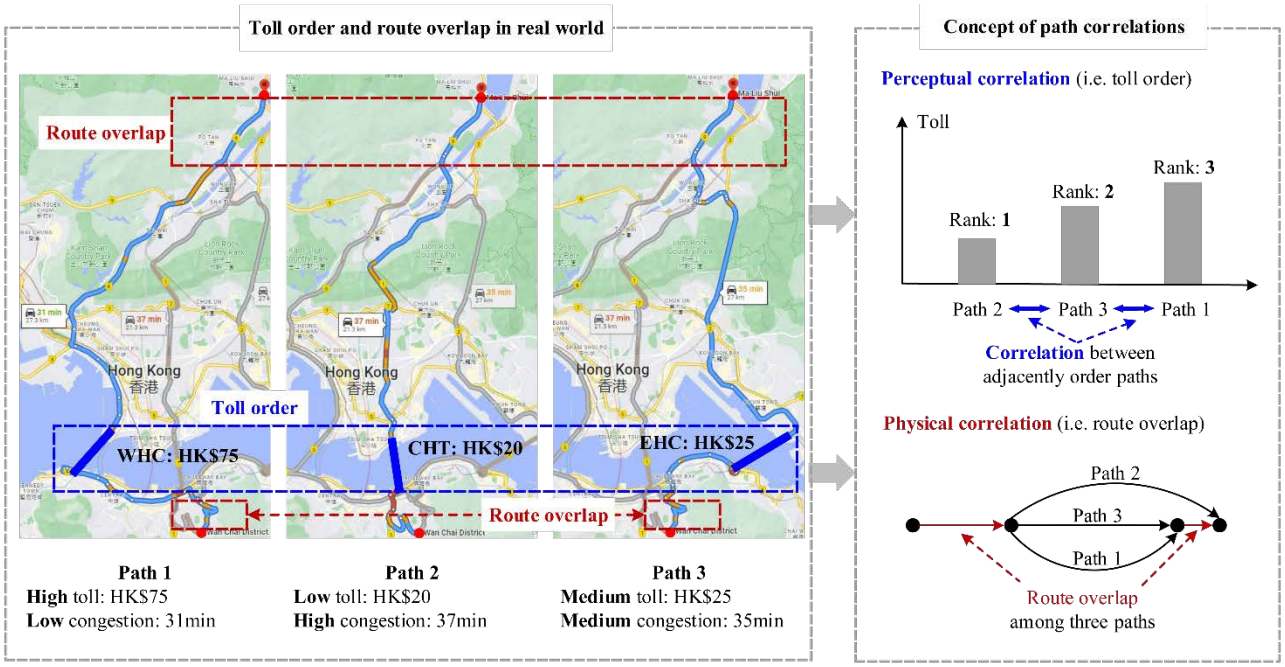

Figure 3.1. An illustration of path perceptual and physical correlations in the Hong Kong road network

3.1.2 Route choice considering perceptual correlation and physical overlap

In this section, the OGEV model, which is suitable for incorporating the ordering information of choice alternatives, is extended to the ordered path-size generalized extreme value (OPSGEV) model for modeling both the perceptual order correlation and the physical overlap in the route choice problem. The perceived path travel utility function is defined for accounting for different correlations via different deterministic disutility and random error terms:

$$V_{uk}^{rs} = \underbrace{v_k^{rs}}_{\substack{Systematic \\ utility}} + \underbrace{\frac{1}{\theta_k} PS_k^{rs}}_{\substack{Path \\ overlap}} + \underbrace{\frac{1}{\theta_u} w_{uk}^{rs}}_{\substack{Path\ order \\ correlation}} + \underbrace{\varepsilon_{uk}^{rs} + \varepsilon_u^{rs}}_{\substack{Error \\ components}}, \forall k \in K_u^{rs}, u \in U^{rs}, rs \in RS, \quad (3.1)$$

where RS, U^{rs}, and K_u^{rs} denotes the set of OD pairs, the path subsets between OD pair rs, and the paths in subset u between OD pair rs, respectively; v_k^{rs} is the systematic path utility measuring the tradeoff between travel time and road toll; ε_{uk}^{rs} and ε_u^{rs} are error components associated with the individual path and the subset of adjacently ordered

paths, respectively. Following the development of the nested logit model (Ben-Akiva and Lerman, 1985), three distributional assumptions are made: (1) ε_{uk}^{rs} and ε_{u}^{rs} are independent; (2) ε_{uk}^{rs} are independently and identically distributed (IID) Gumbel variables with scale parameter θ_k; (3) ε_{u}^{rs} are distributed so that $\varepsilon_{uk}^{rs}+\varepsilon_{u}^{rs}$ are IID Gumbel variables with scale parameter θ_u.

PS_k^{rs} denotes the path-size (PS) factor, which penalizes the physical correlation (overlap) among individual paths together with scale parameter θ_k (Ben-Akiva and Bierlaire, 1999). The PS factor is measured based on the total path length and the lengths of links shred by different paths as follows:

$$PS_k^{rs}=\sum_{a\in A_k^{rs}}\frac{l_a}{l_k}\cdot\frac{1}{\sum_{k\in K^{rs}}\delta_{a,k}^{rs}},\forall k\in K^{rs},rs\in RS, \tag{3.2}$$

where l_a and l_k are the length of link a and path k, respectively; A_k^{rs} denotes the set of links on path k; $\delta_{a,k}^{rs}$ is the binary variable indicating the link-path incidence relationship, $\delta_{a,k}^{rs}=1$ if link a is on path k, otherwise $\delta_{a,k}^{rs}=0$. Paths with a heavy overlap have a smaller PS factor, indicating a higher penalty on path utility. Other functional forms of PS factor can also be included (see Bovy et al., 2008; Prato, 2009).

The allocation parameter w_{uk}^{rs} denotes the membership of path k in path subset u between OD pair rs, which influences the competition effect between path k and its adjacently ordered paths. The allocation parameter w_{uk}^{rs} and scale parameter θ_u together reflect the path order correlation. To guarantee unbiased model specification, w_{uk}^{rs} can be normalized as $\sum_{u\in U^{rs}}w_{uk}^{rs}=1$ (Abbe et al., 2007). In the standard OGEV model, w_{uk}^{rs} can be specified as $\frac{1}{M+1}$, where M denotes the number of adjacently ordered paths that are considered correlated to each path and M+1 is the maximum number of paths in a subset (Small, 1987).

Based on the utility function (3.1) and the three distributional assumptions, the OPSGEV model can be analytically derived. Figure 3.2 illustrates the simultaneous

consideration of path correlations arising from toll ranking and physical overlap in the proposed OPSGEV model. The path order correlations are considered via the nesting structure at the marginal choice level, while the path overlaps are modeled via the utility correction terms at the conditional choice level. The OPSGEV probability P_k^{rs} is a product of the marginal choice probability of subset *u* and the conditional probability of choosing path *k* from subset *u*.

$$P_k^{rs} = \sum_{u=k}^{k+M} P(u) \cdot P(k|u), \forall k \in K^{rs}, rs \in RS, \tag{3.3}$$

where K^{rs} denotes the path set between OD pair *rs*. The marginal and conditional choice probabilities, $P(u)$ and $P(k|u)$, can be expressed as follows.

$$P(u) = \frac{\left[\sum_{k \in K_t} PS_k^{rs} \cdot \left(w_{uk}^{rs}\right)^{\frac{\theta_k}{\theta_u}} \exp\left(\theta_k v_k^{rs}\right)\right]^{\frac{\theta_u}{\theta_k}}}{\sum_{u=1}^{|K|+M} \left[\sum_{l \in K_u} PS_l^{rs} \cdot \left(w_{ul}^{rs}\right)^{\frac{\theta_k}{\theta_u}} \exp\left(\theta_k v_k^{rs}\right)\right]^{\frac{\theta_u}{\theta_k}}}, \forall u \in U^{rs}, rs \in RS, \tag{3.4}$$

$$P(k|u) = \frac{PS_k^{rs} \cdot \left(w_{uk}^{rs}\right)^{\frac{\theta_k}{\theta_u}} \exp\left(\theta_k v_k^{rs}\right)}{\sum_{l \in K_u} PS_l^{rs} \cdot \left(w_{ul}^{rs}\right)^{\frac{\theta_k}{\theta_u}} \exp\left(\theta_k v_k^{rs}\right)}, \forall k \in K_u, u \in U^{rs}, rs \in RS. \tag{3.5}$$

Define the dissimilarity parameter $\rho = \theta_u / \theta_k$ that indicates the order correlation among paths in the same subset, which is positive and ranges from zero to one as $0 < \theta_u < \theta_k$ (Ben-Akiva and Lerman, 1985). A lower value of ρ indicates a higher degree of correlation, i.e., an increased competition among adjacently ordered paths. With a normalization of $\theta_k = 1$, the OPSGEV probability can be analytically expressed by substituting Eqs. (3.4) and (3.5) to Eq. (3.3) and replacing θ_u, θ_k with ρ:

$$P_k^{rs} = \sum_{u=k}^{k+M} \frac{PS_k^{rs} \cdot \left(w_{uk}^{rs}\right)^{1/\rho} \exp\left(v_k^{rs}\right) \cdot \left[\sum_{k \in K_u} PS_k^{rs} \cdot \left(w_{uk}^{rs}\right)^{1/\rho} \exp\left(v_k^{rs}\right)\right]^{\rho-1}}{\sum_{u=1}^{|K|+M} \left[\sum_{l \in K_u} PS_l^{rs} \cdot \left(w_{ul}^{rs}\right)^{1/\rho} \exp\left(v_k^{rs}\right)\right]^{\rho}}, \forall k \in K^{rs}, rs \in RS. \tag{3.6}$$

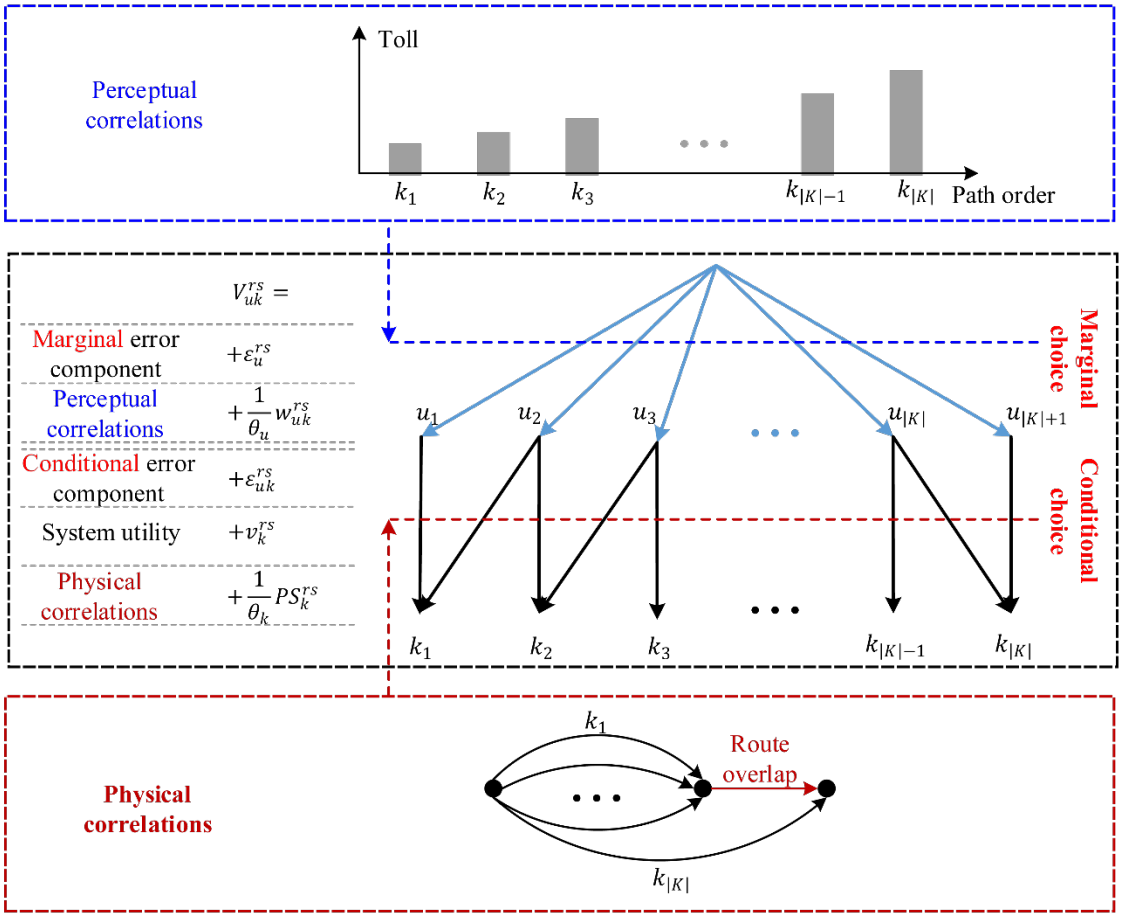

Figure 3.2. Illustration of the OPSGEV model with both perceptual and physical correlations

The effect of the OPSGEV model in considering both perceptual and physical path correlations is illustrated in Figure 3.3 via a three-path example.

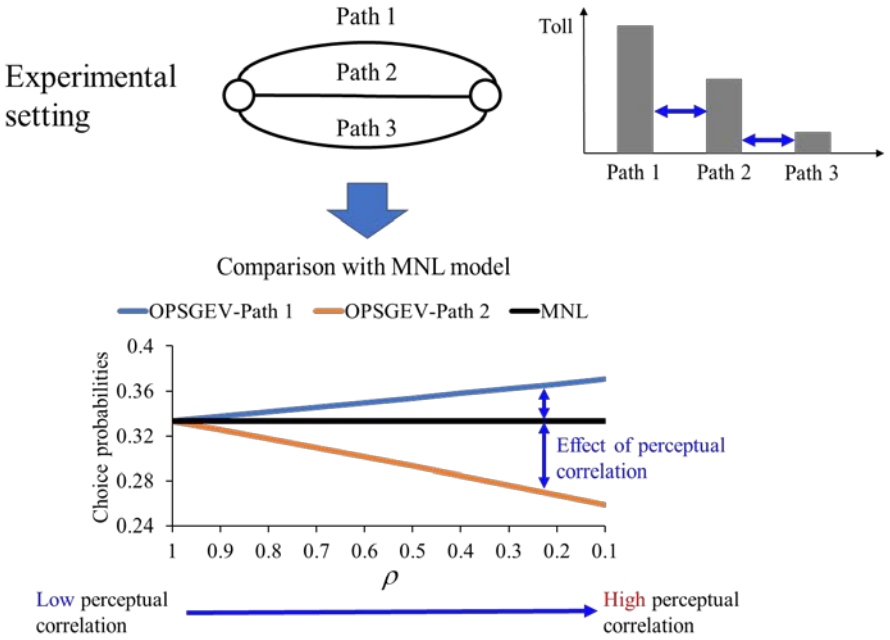

(a) Effect of considering perceptual correlation only

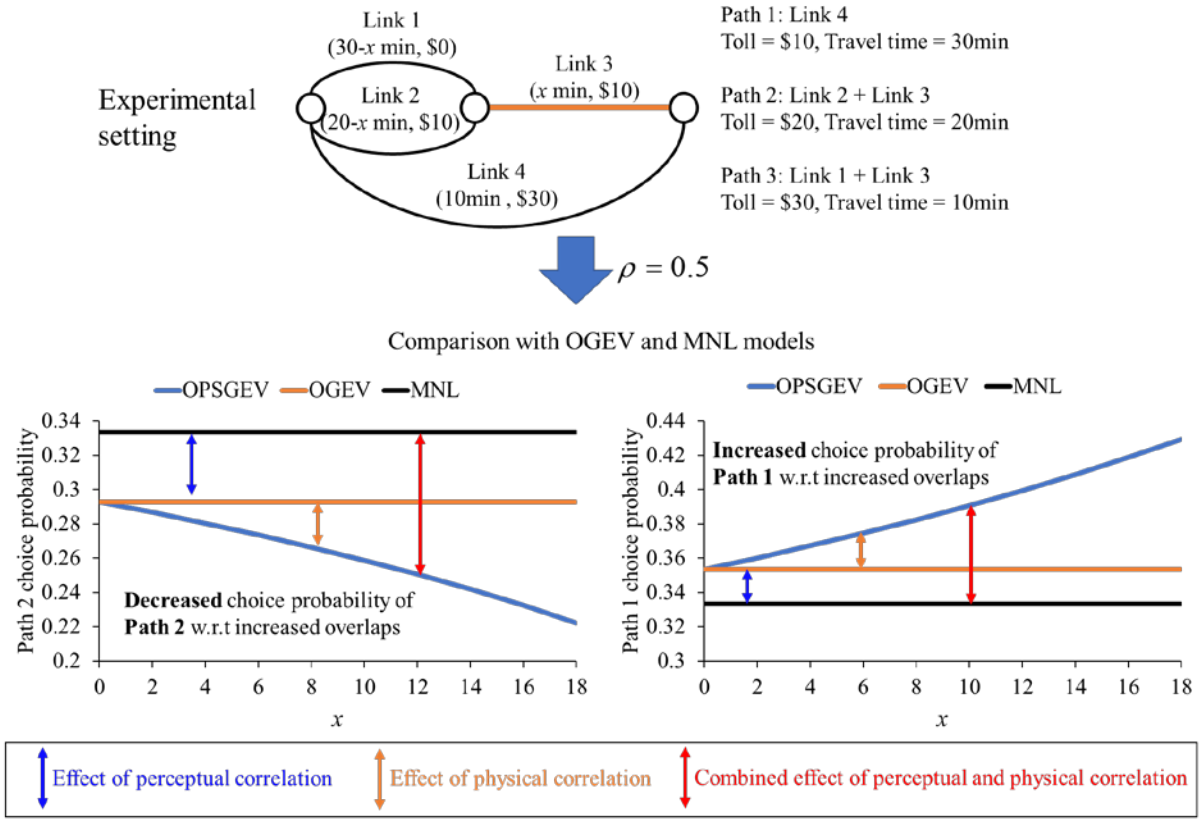

(b) Effect of considering both perceptual and physical correlations

Figure 3.3.Effect of considering path correlations based on OPSGEV model

Figure 3.3(a) explores the effect of ρ based on a comparison between the OPSGEV model and the commonly used MNL model, in scenarios with the same order of path toll and equal v_k^{rs} but different perceptual correlation among paths. Given a membership parameter w_{uk}^{rs}, the path order correlation is influenced by the dissimilarity parameter ρ as shown in Eq. (3.6). Unlike the MNL model which ignores path correlations and provides the same route choice probability (i.e., 1/3 for all three paths), the OPSGEV model can capture the difference in path order correlation by varying the values of dissimilarity parameter ρ. With the increase of ρ, the OPSGEV choice probability of less correlated paths increases (e.g., Path 1 correlated only with Path 2), while the highly correlated path (e.g., Path 2 correlated with both Paths 1 and 3) tends to have a lower choice probability due to its increasing competition among adjacently ranked paths. Figure 3.3(b) further compares the OPSGEV and OGEV models to illustrate the effect of considering the path overlap (Link 3). Path travel utility v_k^{rs} is specialized as a linear combination of time and toll. With an increasing length of Link 3, the choice probability of overlapped Paths 2 and 3 decreases, while the probability of non-overlapped Path 1 increases. The combined effect of considering the two types of path correlations is then presented based on the comparison between the OPSGEV and MNL models. In summary, the developed OPSGEV model can capture both types of path correlations, which can exert significant effects on route choice and are important for modeling the route choice in tolled networks.

3.2 Mode choice of customized bus services with loyalty subscription schemes

3.2.1 Background and related studies

Customized bus (CB) is an emerging on-demand transit mode that provides advanced, cost-effective, and environmentally friendly transportation services with innovative service features (Liu and Ceder 2015; Liu et al. 2016). This section aims to model travelers' mode choice behavior in multi-modal transportation systems considering the emerging behavioral issues arising from the operation of CB services.

CB services meet the requirements of passengers via allowing them to subscribe to CB lines with their preferred origin–destination (OD) stops and departure/arrival times. Compared with conventional transit modes, CB may decrease passengers' walking distance for access, and reduce their waiting time and in-vehicle travel time. In addition, CB services increase passenger loyalty by offering a loyalty scheme for long-term (e.g., monthly) subscription and eliminating in-vehicle crowding discomfort by guaranteeing a seat for every passenger. When comparing to the private car, CB services are more economical and environmentally friendly and are often allowed to travel in dedicated bus lanes to alleviate the effect of road congestion on in-vehicle travel time (Liu et al., 2016).

Another unique characteristic of CB services is that they require passengers to subscribe to book a seat. To attract passengers, CB operators offer two types of subscription schemes: (1) one-time subscription schemes, which enable subscribers to purchase a one-way ticket at the original price, and (2) loyalty subscription schemes, which enable subscribers to purchase a ticket for a long period (e.g., a monthly ticket) at a discounted price. For instance, the CB operators in Beijing offer 20%-discounted monthly subscriptions (Liu and Cedar, 2015). Subscribers to CB loyalty schemes must pay fares for the entire subscription period in advance and are therefore likely to subsequently travel only on CB lines, without considering other modes. This travel choice behavior is different from that of those who purchase one-time CB subscriptions, as the latter remain open to considering other modes in their choice set.

Previous travel choice analyses have typically modeled mode choice based on the disutility minimization rule, which compares the travel disutility of day-to-day or within-day subscriptions to one-time CB services with the utility of other travel modes (e.g., Djavadian and Chow, 2017; Gu et al., 2018; Li et al., 2018b; Huang et al., 2020b). However, this modeling method ignores passenger loyalty to CB services that is captured by loyalty subscription schemes with price incentives, which drives passengers to repeatedly purchase the same product/service without considering other alternatives.

Passenger loyalty has long been considered an important determinant of travel choice behavior and has been widely studied in transportation systems, such as logistics (e.g., Ellinger et al., 1999; Chang and Thai, 2016) and air transport (e.g., Chang and Hung, 2013; Vlachos and Lin, 2014). In the context of urban transportation networks, passenger loyalty is primarily investigated in the PT system (e.g., Li et al., 2018a; van Lierop et al., 2018). However, emerging shared-transportation modes are distinct from conventional PT modes, as shared modes can develop high passenger loyalty by offering loyalty schemes that have cheaper fares and higher usefulness for long-term users (Nguyen-Phuoc et al., 2020; Lee and Wong, 2021; Su et al., 2021). For example, CB services are an emerging sharing mode, and their long-term loyalty subscription schemes were shown to attract a stable and high number of loyal passengers (Wang et al., 2019). Wang et al. (2020b) also used empirical data collected in Dalian, China, to investigate the relationship between a monthly subscription scheme and passenger loyalty to CB services. However, most studies have empirically investigated the determinants of passenger loyalty, and little effort has been made to incorporate the choice behavior of loyal passengers into mode choice models. This under investigated aspect must be explored when modeling CB services with loyalty subscription schemes. As a loyalty subscription scheme can significantly increase passenger loyalty to CB services, distinct choice behaviors are exhibited by passengers with and without loyalty. Loyal passengers may repeatedly use CB services without considering other alternatives, whereas non-loyal passengers tend to use the mode that minimizes their

travel disutility. Therefore, passenger loyalty must be explicitly considered in the mode choice model.

Mode correlation and heterogeneity are also important for mode choice modeling, as they were found to significantly affect the decision-making of passengers who seek to minimize their disutility (Yan et al., 2019b). Efforts have recently been devoted to modeling mode choice in a network that offers both conventional and emerging modes of transport (e.g., Cantarella et al., 2015; Lu et al., 2015; Kitthamkesorn et al., 2016; Li et al., 2018b). However, many of these studies fail to simultaneously account for mode correlation and heterogeneity owing to the IID assumption embedded in the traditional multinomial logit (MNL) model. If mode correlation is not considered, the choice probability of similar modes may be overestimated (e.g., the red bus/blue bus problem). If heterogeneity is ignored, the mode choice probability will be derived from only the absolute differences between the mode disutility, which may be inaccurate if the magnitudes of service quality vary between modes. Many empirical studies adopt mixed logit models to simultaneously address the correlation and heterogeneity issues when investigating travel choice behaviors involving emerging on-demand modes (e.g., Choudhury et al., 2018; Xie et al., 2019; Yan et al., 2019a; Sweet, 2021). However, the mixed logit models lack the closed-form probability expression that enables the efficient and exact estimation of the choice model and provides a clear understanding of model outcomes. In addition, the lack of closed-form probability hinders the integration of mixed logit models in the network equilibrium model, which requires to iteratively approximate many open-form choice probabilities and significantly increase the computational burden. Existing studies on mode choice equilibrium mainly focus on addressing the mode correlation by using closed-form logit models with a hierarchical choice structure, e.g., the nested logit (NL) model, while few studies (Kitthamkesorn and Chen, 2017) have devised an equilibrium mode choice model to simultaneously address mode correlation and heterogeneity.

To address the above research gaps, this section aims to develop and advanced closed-form choice model for simultaneously considering the following behavioral

issues with the advent of CB services: (1) the passenger loyalty to CB services due to loyalty subscription schemes; (2) correlations among modes in multi-modal transportation systems; and (3) heterogeneous perceptions of different travel modes with distinct magnitudes of travel disutility.

To facilitate the presentation of the essential ideas, the notations used in this section are listed below.

Set

RS	Set of OD pairs.
U^{rs}	Set of types of modes between OD pair *rs*.
M_u^{rs}	Set of type *U* modes between OD pair *rs*.
M	Set of all modes.

Inputs and parameters

v_m^{rs}	Travel disutility of mode *m* between OD pair *rs*.
v_u^{rs}	Travel disutility of nest *u* between OD pair *rs*.
β_{um}^{rs}	Shape parameter of mode *m* under nest *u* between OD pair *rs*.
β_u^{rs}	Shape parameter of nest *u* between OD pair *rs*.
μ_m^{rs}	Loyalty proportion of mode *m* between OD pair *rs*.
η_m^{rs}	Loyalty parameter for mode *m* between OD pair *rs* in the dogit-based model.
$P_m^{rs\prime}$	Choice probability of mode *m* between OD pair *rs* in the previous period.
PS_k	A positive correction factor that penalizes the overlapped section on alternative *k* in the path-size weibit model.

Variables

λ_{um}^{rs}	Probability of choice passengers choosing mode *m* belonging to nest *u* between OD pair *rs*.
$\lambda_{m\|u}^{rs}$	Probability of choice passengers choosing mode *m* between OD pair *rs*, given that nest *u* is chosen.

λ_u^{rs}	Probability of choice passengers choosing nest *u* between OD pair *rs*.
λ_m^{rs}	Probability of choice passengers choosing mode *m* between OD pair *rs*.
$P_{l,m}^{rs}$	Choice probability of mode *m* between OD pair *rs* given that mode *l* is chosen previously.
P_m^{rs}	Probability of loyal passengers choosing mode *m* between OD pair *rs*.
v	Aggregate disutility gained from a set of choice alternatives.

3.2.2 Mode choice behavior with consideration of passenger loyalty, mode correlation, and mode heterogeneity

This section develops an advanced mode choice model that accounts for the characteristics of each mode, especially the emerging CB service with loyalty subscription schemes. As mentioned in Section 3.2.1, CB passengers subscribing to different schemes may behave distinctly. Thus, CB passengers are divided into two groups according to the scheme they subscribe to: (1) loyal passengers, who subscribe to a CB loyalty scheme (e.g., a monthly subscription), and (2) choice passengers, who subscribe to a one-time CB service. The characteristics of these two groups are depicted in Figure 3.4. Each column in Figure 3.4 denotes the choice sets of loyal and choice passengers for each trip in the whole period of a loyalty CB scheme. Loyal passengers pay in advance for CB services throughout the whole period of the loyalty scheme and are thus likely to only use CB services without considering any other modes, i.e., their choice set consists of only the CB mode for each trip. In contrast, choice passengers only pay for a one-time CB service each time they need it and thus make mode choices based on the generalized travel time of each mode, i.e., they consider the full choice set comprised of CB, private car, and conventional PT for each trip.

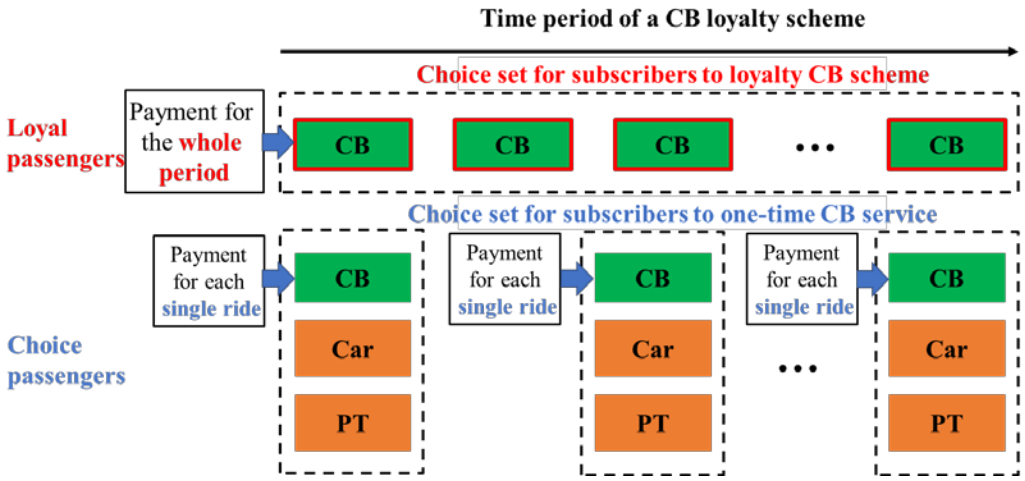

Figure 3.4. Characteristics of passengers subscribing to two different CB schemes

As discussed in Section 3.2.1, it is imperative to consider mode correlation and mode heterogeneity when modeling the behavior of choice passengers. In this section, we adopt the weibit-based model to account for mode heterogeneity, which allows mode-specific variations dependent on the perceived modal disutility. A nested choice structure is adopted to account for mode correlation, which collects similar modes into the same upper nest. The overall mode choice structure modeled in this section is shown in Figure 3.5. The proportion of loyal passengers, $\frac{\eta_m^{rs}}{\left(1+\sum_{m\in M}\eta_m^{rs}\right)}$, and that of choice passengers, $\lambda^{rs}=\frac{1}{\left(1+\sum_{m\in M}\eta_m^{rs}\right)}$, are derived based on a customer loyalty model as will be shown in Sections 3.2.2.3-3.2.2.4. The marginal mode type (upper nest) choice probability and conditional mode choice probability of choice passengers, λ_u^{rs} and $\lambda_{m|u}^{rs}$, are derived based on the nested weibit (NW) model in Section 3.2.2.1.

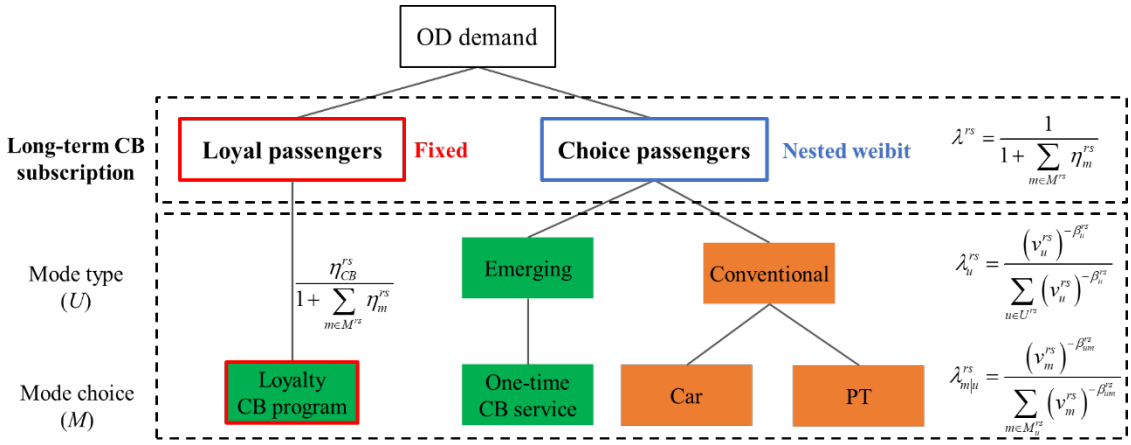

Figure 3.5. Overall structure for modeling mode choice with CB services

3.2.2.1 Mode choice of choice passengers

As discussed above, a NW model is adopted in this chapter to address mode correlation and mode heterogeneity and thereby reproduce the mode choice of choice passengers (Kitthamkesorn and Chen, 2017). As shown in Figure 3.5, the correlation between the conventional travel modes that are familiar to travelers, i.e., conventional PT and private car, is modeled in the same upper nest. In contrast, CB services are considered as a distinct emerging type of mode due to their innovative service characteristics. The NW choice probability of choice passengers, λ_{um}^{rs}, can be expressed as a product of the marginal probability of choosing mode type (upper nest) u, λ_{u}^{rs}, and the conditional probability of choosing mode m within nest u, $\lambda_{m|u}^{rs}$:

$$\lambda_{um}^{rs} = \lambda_{m|u}^{rs} \cdot \lambda_{u}^{rs}, \forall m \in M_u^{rs}, u \in U^{rs}, rs \in RS\,. \tag{3.7}$$

The conditional probability can be expressed based on the multinomial weibit (MNW) model (Castillo et al., 2008; Kitthamkesorn and Chen 2013):

$$\lambda_{m|u}^{rs} = \frac{\left(v_m^{rs}\right)^{-\beta_{um}^{rs}}}{\sum_{m \in M_u^{rs}} \left(v_m^{rs}\right)^{-\beta_{um}^{rs}}}, \forall m \in M_u^{rs}, u \in U^{rs}, rs \in RS\,, \tag{3.8}$$

where v_m^{rs} denotes the travel disutility of mode m between OD pair rs, β_{um}^{rs} is the shape parameter of the NW model at the conditional choice level (individual mode).

The marginal probability of nest choice is expressed as follows:

$$\lambda_u^{rs} = \frac{\left(v_u^{rs}\right)^{-\beta_u^{rs}}}{\sum_{u \in U_{rs}} \left(v_u^{rs}\right)^{-\beta_u^{rs}}}, \forall u \in U^{rs}, rs \in RS, \tag{3.9}$$

where β_u^{rs} is the shape parameter of the NW model at the marginal choice level (upper nest). The disutility of choosing nest *u* between OD pair *rs*, v_u^{rs}, can be obtained as the expected minimum disutility of choosing a mode within the nest, which is expressed as follows:

$$v_u^{rs} = \left[\sum_{m \in M_u^{rs}} \left(v_m^{rs}\right)^{-\beta_{um}^{rs}} \right]^{-\frac{1}{\beta_{um}^{rs}}}, \forall m \in M_u^{rs}, u \in U^{rs}, rs \in RS. \tag{3.10}$$

Substituting Eqs. (3.8–3.10) into Eq. (3.7) gives the NW mode choice probability, as follows:

$$\lambda_{um}^{rs} = \frac{\left(v_m^{rs}\right)^{-\beta_{um}^{rs}} \left[\sum_{m \in M_u^{rs}} \left(v_m^{rs}\right)^{-\beta_{um}^{rs}} \right]^{\frac{\beta_u^{rs}}{\beta_{um}^{rs}}-1}}{\sum_{u \in U_{rs}} \left[\sum_{m \in M_u^{rs}} \left(v_m^{rs}\right)^{-\beta_{um}^{rs}} \right]^{\frac{\beta_u^{rs}}{\beta_{um}^{rs}}}}, \forall m \in M_u^{rs}, u \in U^{rs}, rs \in RS. \tag{3.11}$$

By definition, β_u^{rs} is smaller than β_{um}^{rs}, i.e., $\beta_u^{rs} / \beta_{um}^{rs} < 1$, which indicates that modes belonging to the same type (upper nest) are more sensitive to each other than to the modes of different types.

3.2.2.2 Effect of considering mode correlation and heterogeneity

This section describes the effects of considering mode correlation and heterogeneity in the NW model. First, we illustrate the effect of using a weibit-based model to address the heterogeneity issue via the three-mode case depicted in Figure 3.6. Consider a choice set comprising two existing modes with similar levels of travel disutility (30 vs.

27). The logit and the weibit models provide similar modal splits for this set. Next, a new mode with a distinct service quality is introduced into the network. The NL and the NW models are then applied to estimate the choice probability of new mode at different magnitudes of disutility. The following can be concluded from Figure 3.6:

- The weibit model obtains similar outcomes to the commonly used logit model if the new mode offers a similar level of service to existing modes, which verifies the applicability of the weibit model for estimating mode choice.
- The weibit model better reflects the effect of heterogenous perceptions of mode service than the logit model. Specifically, even if the new mode offers a significantly higher level of service than existing modes, the logit model continues to estimate a non-negligible share for the existing modes. This is because the logit mode assumes there is an identical perception variance for all modes, even if they offer distinct levels of service. In contrast, the weibit model allows mode-specific perception variance dependent on mode disutility, in keeping with the heterogenous perceptions of varying mode service levels (Kitthamkesorn and Chen, 2017).

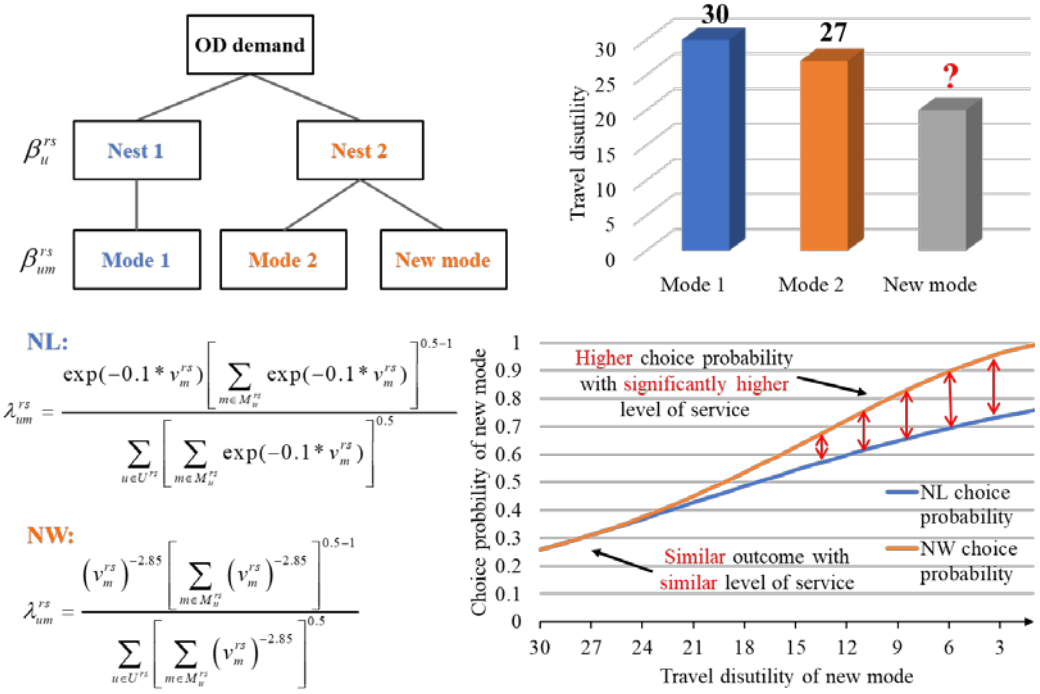

Figure 3.6. Effect of considering heterogeneity in mode choice

We illustrate the use of the NW model to consider mode correlation in Figure 3.7. In this case, it is assumed that the new mode has correlations with the existing mode 2, which is analogous to the well-known red bus/blue bus problem (Ben-Akiva and Lerman, 1985). The neglect of correlation between mode 2 and the new mode leads to underestimation of the choice probability of mode 1. By introducing a nested choice structure, the NW model can reflect different degrees of mode correlation in terms of the ratio between the shape parameters β_u^{rs} and β_{um}^{rs}. A higher value of $\beta_u^{rs}/\beta_{um}^{rs}$ indicates a lower degree of correlation between modes in the same nest.

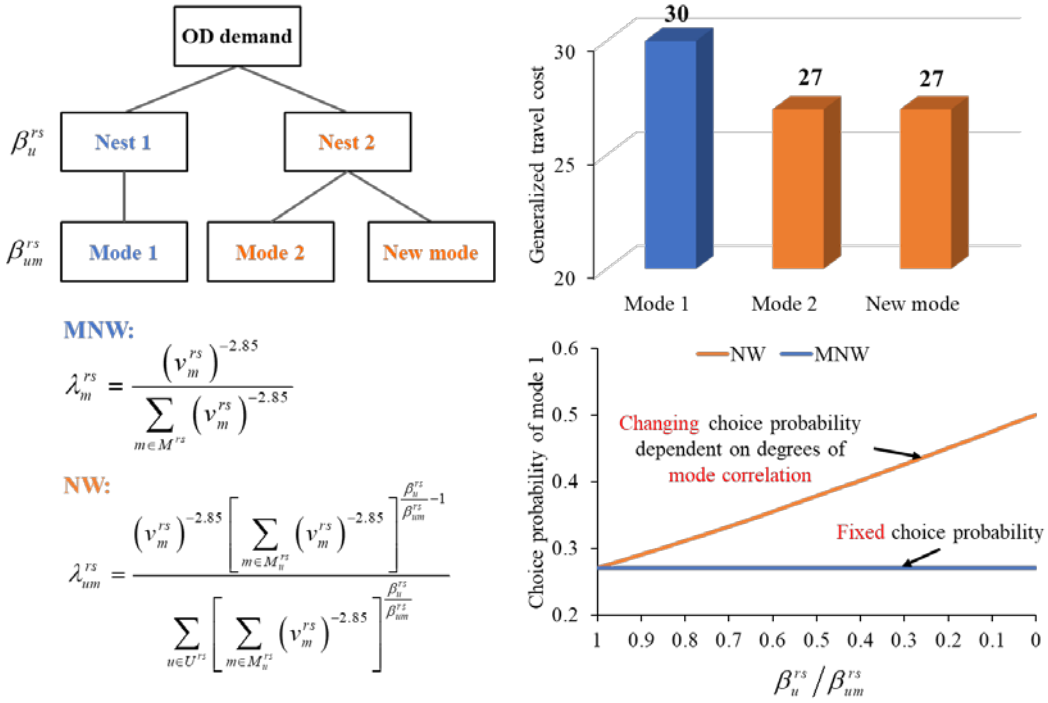

Figure 3.7. Effect of considering mode correlation

3.2.2.3 Mode choice with loyal CB passengers

We use the Colombo/Morrison (C/M) model (Colombo and Morrison, 1989), which is widely used to model customer loyalty in the context of marketing, to describe the choice behaviors of loyal passengers and choice passengers. Let μ_m^{rs} be the loyalty proportion, which can be interpreted as the proportion of previous passengers of mode

m that continue to use mode *m* between OD pair *rs*, despite the unattractiveness of this mode (Bordley, 1990). Let λ_m^{rs} denote the probability that choice passengers select mode *m*. Then, the choice probability of mode *m*, given that mode *l* is chosen previously, can be expressed as the probability that the choice passengers previously use mode *l* but currently choose mode *m*, as follows:

$$P_{l,m}^{rs} = \left(1-\mu_l^{rs}\right)\cdot\lambda_m^{rs}, \forall l \neq m \in M, rs \in RS . \tag{3.12}$$

This section focuses on the loyal passengers of CB services, i.e., only the CB services have a positive loyalty proportion μ_m^{rs}:

$$\begin{cases} \mu_m^{rs} \in [0,1), & m = CB \\ \mu_m^{rs} = 0, & m = bus, car \end{cases}. \tag{3.13}$$

Given that mode *m* is chosen in the previous period, the choice probability of mode *m* can be expressed as the sum of the probability that choice passengers will select mode *m* and the proportion of passengers loyal to mode *m*, as follows:

$$P_{m,m}^{rs} = \left(1-\mu_m^{rs}\right)\cdot\lambda_m^{rs} + \mu_m^{rs}, \forall m \in M, rs \in RS . \tag{3.14}$$

3.2.2.4 Interpreting loyalty of CB passengers using dogit-based model

This section incorporates passenger loyalty into the mode choice model. As proved by Bordley (1990), the C/M model with λ_m^{rs} expressed by the MNL choice probability can be interpreted as the dogit model, which is a well-established model that is widely used to consider captive mode choices (Gaudry and Dagenais, 1979; Wang et al., 2020a). In a similar way, we interpret the NW choice probability of choice passengers and the choice behavior of loyal passengers using a dogit–NW (DNW) model. This DNW model is expressed as follows:

$$P_{um}^{rs}=\underbrace{\frac{\eta_m^{rs}}{\left(1+\sum_{m\in M}\eta_m^{rs}\right)}}_{\text{Loyal passengers}}+\underbrace{\frac{1}{\left(1+\sum_{m\in M}\eta_m^{rs}\right)}}_{\text{Choice passengers}}\cdot\underbrace{\frac{\left(v_m^{rs}\right)^{-\beta_{um}^{rs}}\left[\sum_{m\in M_u^{rs}}\left(v_m^{rs}\right)^{-\beta_{um}^{rs}}\right]^{\frac{\beta_u^{rs}}{\beta_{um}^{rs}}-1}}{\sum_{u\in U_{rs}}\left[\sum_{m\in M_u^{rs}}\left(v_m^{rs}\right)^{-\beta_{um}^{rs}}\right]^{\frac{\beta_u^{rs}}{\beta_{um}^{rs}}}}}_{\text{Nested weibit choice probability}},\quad(3.15)$$

where η_m^{rs} represents the loyalty (or termed as captivity) parameter in the dogit model. The first term on the right-hand side of Eq. (3.15) denotes the mode share from the loyal passengers with a deterministic mode choice, and the second term denotes the mode share from the choice passengers with a random mode choice. This expression is based on the dogit model (Gaudry and Dagenais, 1979; Wang et al., 2020a) but with the MNL choice probability replaced by the NW choice probability in the second term on the RHS. The DNW model presented in Eq. (3.15) can also be expressed as follows:

$$P_{um}^{rs}=\frac{\eta_m^{rs}\cdot\sum_{u\in U^{rs}}\left[\sum_{m\in M_u^{rs}}\left(v_m^{rs}\right)^{-\beta_{um}^{rs}}\right]^{\frac{\beta_u^{rs}}{\beta_{um}^{rs}}}+\left(v_m^{rs}\right)^{-\beta_{um}^{rs}}\left[\sum_{m\in M_u^{rs}}\left(v_m^{rs}\right)^{-\beta_{um}^{rs}}\right]^{\frac{\beta_u^{rs}}{\beta_{um}^{rs}}-1}}{\sum_{u\in U^{rs}}\left[\sum_{m\in M_u^{rs}}\left(v_m^{rs}\right)^{-\beta_{um}^{rs}}\right]^{\frac{\beta_u^{rs}}{\beta_{um}^{rs}}}\cdot\left(1+\sum_{m\in M}\eta_m^{rs}\right)}.\quad(3.16)$$

We have the following proposition.

Proposition 3.1. Given the choice probability of mode *m* in the previous period, the mode choice behavior of choice passengers and loyal passengers shown in Eqs. (3.11)–(3.14) can be interpreted using the DNW model.

Proof. Let $P_m^{rs\prime}$ denote the choice probability of mode *m* in the previous period. The mode choice probability considering loyal passengers and the nested choice structure of choice passengers can be written as follows:

$$P_{um}^{rs}=\mu_m^{rs}P_m^{rs\prime}+\lambda_{um}^{rs}\cdot\sum_{l\in M}\left(1-\mu_l^{rs}\right)P_l^{rs\prime},\forall m\in M_u^{rs},u\in U^{rs},rs\in RS,\quad(3.17)$$

where the term λ_m^{rs} used in Eqs. (3.12)–(3.14) is replaced by the NW choice probability λ_{um}^{rs} given in Eq. (3.11). As proposed by Bordley (1990), the new parameter η_m is defined as follows, based on the proportion of loyal passengers and previous choice probabilities:

$$\eta_m^{rs} = \frac{\mu_m^{rs} P_m^{rs\prime}}{\sum_{l \in M} \left(1 - \mu_l^{rs}\right) P_l^{rs\prime}}, \forall m \in M, rs \in RS . \tag{3.18}$$

The following two relationships can be derived from Eq. (3.18):

$$\begin{aligned} 1 + \sum_{m \in M} \eta_m^{rs} &= \frac{\sum_{l \in M} \left(1 - \mu_l^{rs}\right) P_l^{rs\prime} + \sum_{l \in M} \mu_l^{rs} P_l^{rs\prime}}{\sum_{l \in M} \left(1 - \mu_l^{rs}\right) P_l^{rs\prime}} \\ &= \frac{1}{\sum_{l \in M} \left(1 - \mu_l^{rs}\right) P_l^{rs\prime}} \end{aligned}, \tag{3.19}$$

$$\mu_m^{rs} P_m^{rs\prime} = \eta_m^{rs} \cdot \sum_{l \in M} \left(1 - \mu_l^{rs}\right) P_l^{rs\prime}, \forall m \in M, rs \in RS . \tag{3.20}$$

Mode choice probability P_{um} can then be expressed as:

$$\begin{aligned} P_{um}^{rs} &= \eta_m^{rs} \cdot \sum_{l \in M} \left(1 - \mu_l^{rs}\right) P_l^{rs\prime} + \lambda_{um}^{rs} \cdot \sum_{l \in M} \left(1 - \mu_l^{rs}\right) P_l^{rs\prime} \\ &= \left(\eta_m^{rs} + \lambda_{um}^{rs}\right) \cdot \sum_{l \in M} \left(1 - \mu_l^{rs}\right) P_l^{rs\prime} \\ &= \left(\eta_m^{rs} + \lambda_{um}^{rs}\right) \cdot \frac{1}{1 + \sum_{m \in M} \eta_m^{rs}} \end{aligned} . \tag{3.21}$$

Substituting the NW probability λ_{um}^{rs} given in Eq. (3.11) into Eq. (3.21), the DNW choice probability can be obtained as expressed in Eq. (3.15). This completes the proof. Figure 3.8 graphically illustrates the general interpretation of passenger loyalty using the dogit-based choice model.

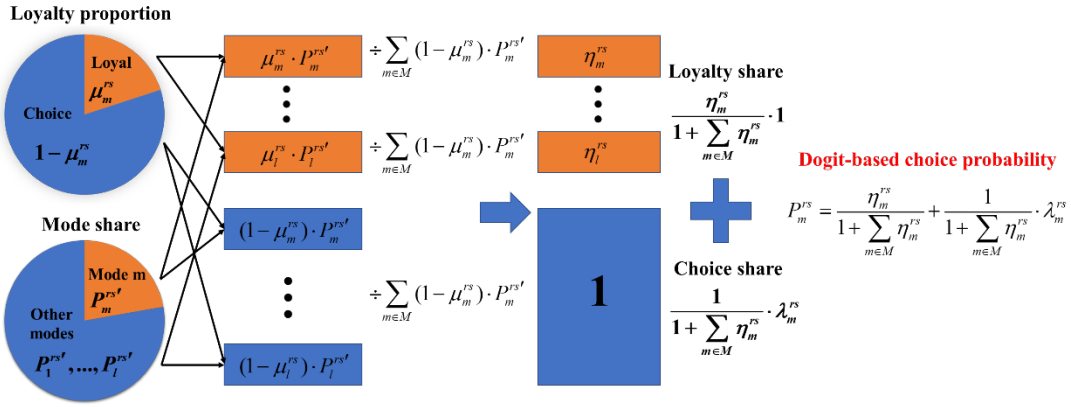

Figure 3.8. Interpretation of passenger loyalty using the dogit-based choice model

3.2.2.5 Alternative interpretations of passenger loyalty

In addition to the interpretation using the DNW model as shown in Section 3.2.2.4, we present an alternative interpretation of passenger loyalty when there lacks exogenous information on previous choice probability $P_m^{rs\prime}$. By replacing $P_m^{rs\prime}$ with current choice probability P_m^{rs} in Eq. (3.17), the mode choice probability can be expressed as follows:

$$P_{um}^{rs} = \mu_m^{rs} P_m^{rs} + \lambda_{um}^{rs} \cdot \sum_{l \in M} \left(1 - \mu_l^{rs}\right) P_l^{rs}, \forall m \in M_u^{rs}, u \in U^{rs}, rs \in RS . \qquad (3.22)$$

We have the following proposition.

Proposition 3.2. Without considering the choice probability of mode *m* in the previous period, the mode choice behavior of choice passengers and loyal passengers shown in Eq. (3.22) can be either in a similar form to the DNW model, or interpreted via Eq. (3.23) as follows:

$$P_{um}^{rs} = \frac{\left[\sum_{m \in M_u^{rs}} \left(v_m^{rs}\right)^{-\beta_{um}^{rs}}\right]^{\frac{\beta_u^{rs}}{\beta_{um}^{rs}}}}{\sum_{u \in U^{rs}} \left[\sum_{m \in M_u^{rs}} \left(v_m^{rs}\right)^{-\beta_{um}^{rs}}\right]^{\frac{\beta_u^{rs}}{\beta_{um}^{rs}}}} \cdot \frac{\left(v_m^{rs}\right)^{-\beta_{um}^{rs}} \Big/ \left(1 - \mu_m^{rs}\right)}{\sum_{m \in M_u^{rs}} \left(v_m^{rs}\right)^{-\beta_{um}^{rs}} \Big/ \left(1 - \mu_m^{rs}\right)} . \qquad (3.23)$$

Proof. We first derive the expression in Eq. (3.23). Without loss of generality, λ_{um}^{rs} is replaced with λ_m^{rs} in Eq. (3.22), from which the following relationships can be derived:

$$\left(1-\mu_m^{rs}\right)\cdot P_m^{rs}=\lambda_m^{rs}\cdot\sum_{l\in M}\left(1-\mu_l^{rs}\right)P_l^{rs}\ , \tag{3.24}$$

$$P_m^{rs}=\frac{\lambda_m^{rs}}{1-\mu_m^{rs}}\cdot\sum_{l\in M}\left(1-\mu_l^{rs}\right)P_l^{rs}\ . \tag{3.25}$$

Summing up both sides of Eq. (3.25) for all modes leads to following expressions:

$$1=\sum_{m\in M}\frac{\lambda_m^{rs}}{1-\mu_m^{rs}}\cdot\sum_{l\in M}\left(1-\mu_l^{rs}\right)P_l^{rs}\ , \tag{3.26}$$

$$\sum_{l\in M}\left(1-\mu_l^{rs}\right)P_l^{rs}=\frac{1}{\sum_{m\in M}\frac{\lambda_m^{rs}}{1-\mu_m^{rs}}}\ . \tag{3.27}$$

Taking Eq. (3.27) into Eq. (3.25) gives the expression of mode choice probability:

$$P_m^{rs}=\frac{\lambda_m^{rs}}{1-\mu_m^{rs}}\cdot\frac{1}{\sum_{m\in M}\frac{\lambda_m^{rs}}{1-\mu_m^{rs}}}\ . \tag{3.28}$$

Substituting λ_m^{rs} by the NW choice probability (Eq. (3.11)), λ_{um}^{rs}, and considering the nested choice structure in Eq. (3.28), the choice probability expression given in Eq. (3.23) can be obtained.

Next, we show that the choice probability given in Eq. (3.23) can also be expressed in the form of Dogit-based model. Define parameter η_m^{rs} as follows (Bordley, 1990):

$$\eta_m^{rs}=\frac{\lambda_m^{rs}\cdot\mu_m^{rs}}{1-\mu_m^{rs}}, \tag{3.29}$$

which leads to the following relationship:

$$\begin{aligned}1+\sum_{m\in M}\eta_m^{rs}&=1+\sum_{m\in M}\lambda_m^{rs}\cdot\left(\frac{1}{1-\mu_m^{rs}}-1\right)\\&=1+\sum_{m\in M}\frac{\lambda_m^{rs}}{1-\mu_m^{rs}}-\sum_{m\in M}\lambda_m^{rs}\ .\\&=\sum_{m\in M}\frac{\lambda_m^{rs}}{1-\mu_m^{rs}}\end{aligned} \tag{3.30}$$

P_m^{rs} can be expressed as:

$$\begin{aligned} P_m^{rs} &= \lambda_m^{rs} \cdot \left(\frac{\mu_m^{rs}}{1-\mu_m^{rs}} + 1 \right) \cdot \frac{1}{1+\sum_{m \in M} \eta_m^{rs}} \\ &= \left(\eta_m^{rs} + \lambda_m^{rs} \right) \cdot \frac{1}{1+\sum_{m \in M} \eta_m^{rs}} \end{aligned} . \tag{3.31}$$

Specifying λ_m^{rs} as the NW choice probability (Eq. (3.11)) gives the DNW choice probability in Eqs. (3.15) and (3.16). Note that the specification of parameter η_m^{rs} in Eq. (3.29) is based on the value of λ_m^{rs}, which is dependent on modes other than *m*. Thus, the η_m^{rs} used in Eqs. (3.29)–(3.31) is different from the loyalty parameter in standard Dogit-based models. This completes the proof.

The difference between Eq. (3.23) and the original NW choice probability in Eq. (3.11) is the inclusion of the correction term $(1-\mu_m^{rs})$ in the conditional probability of choosing mode *m* given nest *u*. This correction term can be regarded as the decrease in the disutility of mode *m* due to passenger loyalty, which can be interpreted based on the concept of aggregate alternatives in the random utility theory. *Choosing mode m* can be considered as an aggregate alternative comprising two types of elemental alternatives, namely *choosing mode m because of loyalty*, and *choosing mode m because of its disutility*. It is assumed that the elemental alternatives have the same mean disutility v_m, and that the probability of choosing the aggregate alternative is equal to the probability of choosing any of the elemental alternatives. Let *v* denote the aggregate disutility gained from the two types of elemental alternatives. *v* can be expressed as the minimum expected disutility of elemental alternatives based on the Weibull distribution:

$$
\begin{aligned}
v &= \left(\sum_{m \in M_A} {v_m}^{-\beta} \right)^{-\frac{1}{\beta}} \\
&= \left(N \cdot {v_m}^{-\beta} \right)^{-\frac{1}{\beta}} \quad , \\
&= N^{-\frac{1}{\beta}} \cdot v_m
\end{aligned}
\tag{3.32}
$$

where $N^{-\frac{1}{\beta}}$ is a correction term ranging from 0 to 1, which represents the effect of the size of aggregate alternative (denoted as N, $N > 1$) on the decrease in disutility. Figure 3.9 illustrates the value of N in this study.

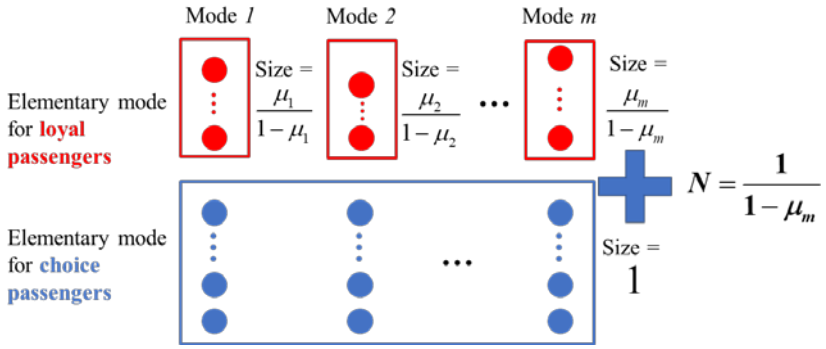

Figure 3.9. Illustration of correction term with respect to passenger loyalty

In a transportation system containing both loyal and choice passengers, loyal passengers only consider one mode in their choice set, which may lead to different values of N for different modes, given the variation in their loyalty to different modes. Considering modes 1, …, m with different proportions of loyal passengers $\mu_1, ..., \mu_m$, the ratio between loyal passengers and choice passengers in each mode is $\frac{\mu_1}{1-\mu_1}, ..., \frac{\mu_m}{1-\mu_m}$. The size of each elemental alternative for choice passengers is the same and is normalized as 1, the total size of aggregate alternative m (comprising choice and loyal passengers) can be expressed as $1 + \frac{\mu_m}{1-\mu_m} \cdot 1 = \frac{1}{1-\mu_m}$. By using $N = \frac{1}{1-\mu_m}$ in the utility function, the weibit-based mode choice probability can be expressed as:

$$P_m = \frac{\left[\left(1-\mu_m\right)^{\frac{1}{\beta}} \cdot v_m\right]^{-\beta}}{\sum_{l\in M}\left[\left(1-\mu_m\right)^{\frac{1}{\beta}} \cdot v_m\right]^{-\beta}} = \frac{\left(v_m\right)^{-\beta} \cdot \left(1-\mu_m\right)^{-1}}{\sum_{l\in M}\left[\left(v_l\right)^{-\beta} \cdot \left(1-\mu_l\right)^{-1}\right]}, \tag{3.33}$$

which gives the conditional mode choice probability stated in Eq. (3.23).

The form of probability function (3.33) is similar to the path-size weibit (PSW) model (Kitthamkesorn and Chen, 2013), which can be expressed as follows:

$$P_k = \frac{PS_k \cdot \left(v_k\right)^{-\beta}}{\sum_{l\in K} PS_l \cdot \left(v_l\right)^{-\beta}}. \tag{3.34}$$

PS_k is a positive correction factor lower than 1, which is a penalty term that decreases the choice probability of path *k* with increases in the number and length of overlapped paths (Ben-Akiva and Bierlaire, 1999; Ramming, 2002). In contrast, the term $1-\mu_m$ in Eq. (3.33) ranges from 0 to 1; thus, $\left(1-\mu_m\right)^{-1} > 1$ can be regarded as a bonus term that increases the choice probability of mode *m* with increases in the loyal proportion, μ_m.

3.3 Joint bundle and mode choice with various emerging mobility services

3.3.1 Background and related studies

In addition to focusing on the single customized bus (CB) service, this section extends the DNW model in Section 3.2 to further consider various shared and on-demand emerging mobility services operated in the multi-modal transportation system, such as ride-hailing (Wang and Yang, 2019), and bike sharing (Shui and Szeto, 2020). The emerging mobility services offer innovative and attractive service features, including different levels of service, limited capacity of service (Du et al., 2022), integration of mobilities in digital platforms (van den Berg et al., 2022; Zhou et al., 2022), and provision of long-term loyalty subscription schemes (Wang et al., 2020b; Chen et al., 2023). These features distinguish emerging mobility services from conventional travel modes, which are expected to influence individual travel choices. This calls for development of advanced travel choice models to capture the complex choice behaviors led by the innovative service features.

Emerging mobility services are often operated on digital platforms, where multiple mobility services operated by different providers can be simultaneously accessed by travelers. This enables the development of mobility bundles, in which different mobility services are packaged by the platform and offered to travelers with promotion strategies. Different from the conventional one-time ticket or pay-as-you-go (PAYG) scheme of a single mode, mobility bundles offer a long-term (e.g., monthly) loyalty bundle scheme that provides incentives and allows subscribers to use the bundled modes at lower costs (Nguyen-Phuoc et al., 2020; Tang et al., 2023). Thus, the bundling of mobilities can affect travelers' perception of bundled travel modes and lead to changes in individual choice behaviors owing to the bundle choice, which has attracted increasing research attention (Kriswardhana and Esztergar-Kiss, 2023). Caiati et al. (2020) and Jang et al. (2021) used the portfolio choice model to investigate the customized configuration of mobility bundles and the choice of mode within customized bundles. Many studies focus on the bundle and mode choices with fixed mobility bundles offered by service providers. The choices between the PAYG scheme and different mobility bundles are

mainly reproduced via logit-based models, including the closed-form multinomial logit (MNL) model (Ho et al., 2018; Tsouros et al., 2021; Hensher et al., 2021) and the open-form mixed logit models for considering more complex behavioral issues like heterogeneities and mode correlations (Matyas and Kamargianni, 2019; Ho et al., 2021; Feneri et al., 2022). However, the effect of traveler loyalty arising from bundle schemes is often ignored in choice modeling. Furthermore, there still lacks an individual choice model that can simultaneously address the heterogeneity and similarity issues with the operation of various emerging mobilities while retaining the valuable closed-form probability expression.

To address the above research gaps, a dogit-cross-nested weibit (DCNW) model is proposed for reproducing the individual joint bundle and mode choices. various complex behavioral issues stemmed from mobility bundling are specifically considered, including (1) travelers' loyalty to the subscription-based mobility bundles; and (2) heterogeneous perceptions and correlations among mobility services in different bundles provided by different operators.

To facilitate the presentation of the essential ideas, the notations used in this section are listed below.

Sets

R	Set of origin zones.
S	Set of destination zones.
U^{rs}	Set of mobility bundles/mode nests between OD pair *rs*.
M^{rs}	Set of modes operated between OD pair *rs*.
M_u^{rs}	Set of modes in nest *u* between OD pair *rs*.
B_u^{rs}	Set of loyalty schemes of bundle *u* between OD pair *rs*.

Inputs

v_{um}^{rs}	Travel disutility of mode *m* in nest *u* between OD pair *rs*.
τ_u^{rs}	Nest-specific cost of nest *u* between OD pair *rs*.

$P_{w,u}^{rs}$	Probability of choosing bundle *u* between OD pair *rs* in the current period given that bundle *w* is chosen in the previous period.
$P_u^{rs\prime}$	Choice probability of bundle *u* between OD pair *rs* in the previous period.
p_b	Proportion of travelers using loyalty scheme *b*.

Parameters

β_{um}^{rs}	Shape parameter at the conditional choice level between OD pair *rs*.
β_u^{rs}	Shape parameter at the marginal choice level between OD pair *rs*.
μ_{um}^{rs}	Membership of mode *m* in bundle *u* between OD pair *rs*.
ψ_u^{rs}	Loyalty proportion of bundle *u* between OD pair *rs*.
ψ_{bu}^{rs}	Loyalty proportion of scheme *b* of bundle *u* between OD pair *rs*.
η_u^{rs}	Loyalty parameter for bundle *u* between OD pair *rs* in the dogit model.
η_{bu}^{rs}	Loyalty parameter for scheme *b* of bundle *u* between OD pair *rs* in the dogit model.

Variables

P_m^{rs}	Choice probability of mode *m* between OD pair *rs*.
θ_m^{rs}	Probability of choice travelers to choose mode *m* between OD pair *rs*.
θ_u^{rs}	Marginal probability of choice travelers to choose nest *u* between OD pair *rs*.
$\theta_{m\|u}^{rs}$	Conditional probability of choice travelers to choose mode *m* in nest *u* between OD pair *rs*.
v_u^{rs}	Disutility of nest *u* between OD pair *rs*.
v_{bu}^{rs}	Disutility of loyalty scheme *b* of bundle *u* between OD pair *rs.*
$\left(v_{um}^{rs}\right)^*$	Composite disutility obtained of nest *u* between OD pair *rs*.
Acc_u^{rs}	Accessibility of nest *u* between OD pair *rs*.

3.3.2 Joint bundle and mode choice modeling for emerging mobility services with loyalty bundle schemes

This section proposes a DCNW choice model for emerging services with loyalty bundle schemes. Figure 3.10 exemplifies the overall choice structure of the proposed DCNW model. The proposed modeling structure considers both conventional (private car, private bike, bus, taxi) and emerging mobility services (e-hailing, CB, bike sharing), where each type of emerging mobility can be operated by multiple service providers, and each mobility service can be bundled by different platforms. As an example, Figure 3.10 includes e-hailing services by two different providers (i.e., e-hailing 1 and e-hailing 2) and mobility bundles on two platforms (i.e., Bundle 1 provided by a ride-hailing platform and Bundle 2 provided by a shared mobility platform).

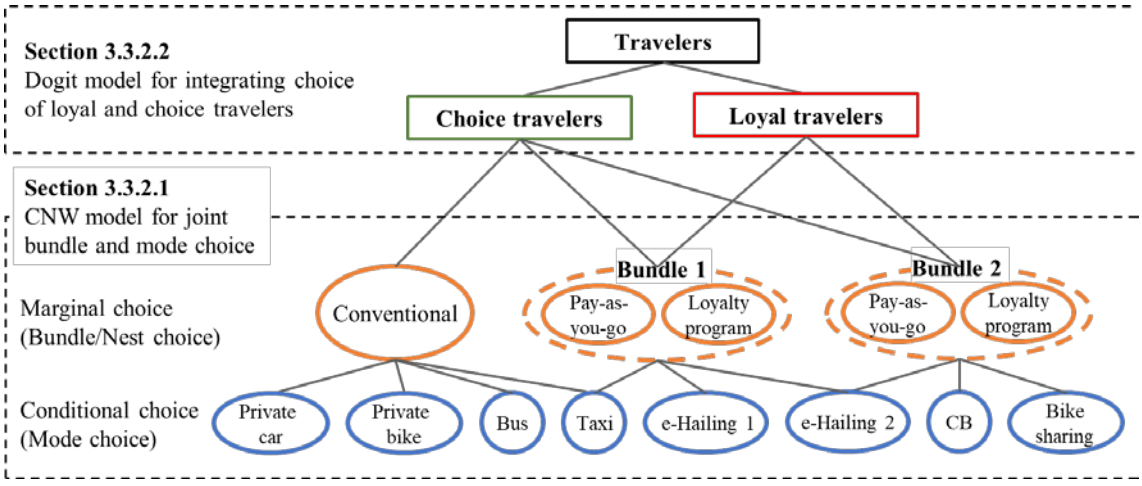

Figure 3.10. Overall structure for modeling emerging mobility services with loyalty bundle schemes

The bundle loyalty stemmed from loyalty bundle schemes is modeled considering the different choice behaviors of two types of travelers: (1) choice travelers, i.e., users of the PAYG bundle schemes that are considered with no loyalty and tend to choose from all the mobility bundles to minimize travel disutility, and (2) loyal travelers, i.e., users of the loyalty bundle schemes that tend to repeatedly choose their subscribed bundle without considering other alternative bundles. Thus, the two types of travelers

are considered to have the same conditional mode choice probability but different marginal bundle choice behaviors due to bundle loyalty. The DCNW model will be described from a bottom-up structure in this section. Section 3.3.2.1 first develops the cross-nested weibit (CNW) model for the joint bundle and mode choice of choice travelers based on the random utility theory. The dogit model for integrating the repeated bundle choice behavior of loyal travelers is then presented in Section 3.3.2.2.

3.3.2.1 Cross-nested weibit model for choice travelers

Analogous to Section 3.2, this section adopts the weibit-based model to account for the effect of the heterogeneous perceptions of emerging and conventional mobility services. The effect of bundling strategies on mode correlation is considered via the cross-nested choice structure of the CNW model as presented in Figure 3.11. The mobility services that can be accessed via the same bundle/platform are considered as correlated with each other and are collected in the same nest. The conventional modes are not packaged as a bundle but are considered within the same nest, as they are existing transportation services and are likely to share common features when perceived by travelers. The cross-nested choice structure is also flexible to model the correlation among bundles/nests, where travel modes can be integrated in multiple nests/bundles (e.g., taxi and e-hailing 2 in Figure 3.11). Furthermore, the proposed choice structure can jointly model the bundle and mode choices as well as the interaction therebetween. The choice of bundle/nest is considered at the upper (marginal choice) level, which determines the demand for conditional choices at the lower level. The conditional choice determines the composite mode disutility, which reciprocally influences the disutility of mobility bundle and hence the choice behaviors at the upper level. On this basis, the marginal and conditional choice probabilities can be determined based on the weibit models with shape parameters β_u^{rs} and β_{um}^{rs} at corresponding choice levels. Finally, the mode choice probability can be obtained by summarizing the choice probability of each service provider of that mode.

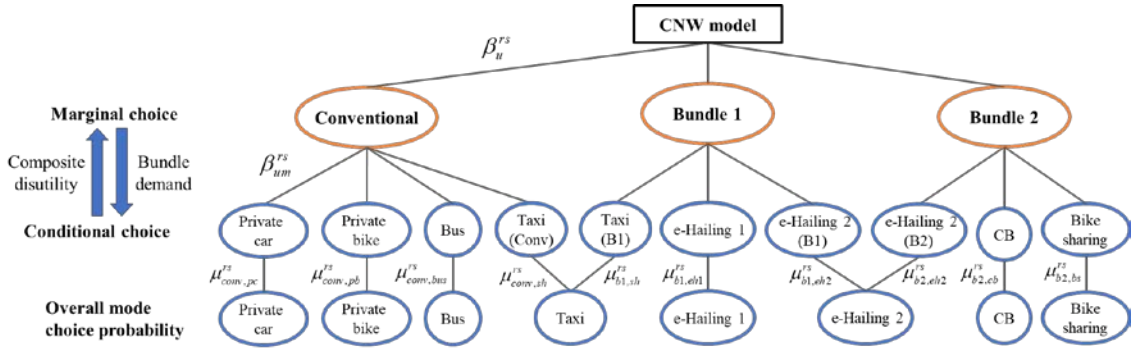

Figure 3.11. Choice structure of CNW model

The detailed formulation of the CNW model for modeling joint bundle and mode choices is illustrated below. The perceived mobility service disutility V_{um}^{rs} is expressed in a multiplicative form as follows:

$$V_{um}^{rs} = v_{um}^{rs} \cdot \left(\mu_{um}^{rs}\right)^{-\frac{1}{\beta_u^{rs}}} \cdot \varepsilon_{um}^{rs} \cdot \tau_u^{rs} \cdot \varepsilon_u^{rs}, \forall m \in M_u^{rs}, u \in U^{rs}, rs \in RS, \qquad (3.35)$$

where v_{um}^{rs} and τ_u^{rs} respectively denote the deterministic disutility of individual mode m and cost of nest/bundle u between OD pair rs; ε_{um}^{rs} and ε_u^{rs} are the corresponding error terms. ε_{um}^{rs} are assumed to independently and identically follow the Weibull distribution with shape parameter β_{um}^{rs}; ε_u^{rs} are assumed as independent random variables such that $\varepsilon_{um}^{rs} \cdot \varepsilon_u^{rs}$ follows the Weibull distribution with shape parameter β_u^{rs}. Parameter μ_{um}^{rs} indicates the membership of mode m in nest/bundle u, which is normalized as $\sum_{u \in U^{rs}} \mu_{um}^{rs} = 1$ (Abbe et al., 2007).

The CNW mode choice probability of choice travelers θ_m^{rs} can be expressed based on the product of the marginal probability of choosing bundle/nest u, θ_u^{rs}, and the conditional probability of choosing individual mode m, $\theta_{m|u}^{rs}$:

$$\theta_m^{rs} = \sum_{u \in U^{rs}} \theta_u^{rs} \cdot \theta_{m|u}^{rs}, \forall m \in M^{rs}, rs \in RS. \qquad (3.36)$$

The marginal choice probability can be obtained as the probability that bundle/nest *u* has the minimum perceived disutility among all bundles/nests:

$$\begin{aligned}\theta_u^{rs} &= P\left[v_u^{rs} \cdot \varepsilon_u^{rs} \le v_w^{rs} \cdot \varepsilon_w^{rs}, \forall w \ne u \in U^{rs} \right] \\ &= P\left[\tau_u^{rs} \cdot \left(v_{um}^{rs}\right)^* \cdot \varepsilon_u^{rs} \le \tau_w^{rs} \cdot \left(v_{wm}^{rs}\right)^* \cdot \varepsilon_w^{rs}, \forall w \ne u \in U^{rs} \right]. \\ &= P\left[\frac{\varepsilon_u^{rs}}{\varepsilon_w^{rs}} \le \frac{\tau_w^{rs} \cdot \left(v_{wm}^{rs}\right)^*}{\tau_u^{rs} \cdot \left(v_{um}^{rs}\right)^*}, \forall w \ne u \in U^{rs} \right]\end{aligned} \tag{3.37}$$

$\left(v_{um}^{rs}\right)^*$ denotes the composite disutility obtained at the conditional choice level, which is derived from the conditional choice model as will be shown in Eq. (3.41). When there is no nest/bundle-specific cost, $\tau_u^{rs} = 1$ and the marginal choice probability is

$$\theta_u^{rs} = \frac{\left(v_{um}^{rs}\right)^{*-\beta_u^{rs}}}{\sum_{w \in U^{rs}} \left(v_{wm}^{rs}\right)^{*-\beta_u^{rs}}}, \forall u \in U^{rs}, rs \in RS . \tag{3.38}$$

The conditional probability of choosing mode *m* in bundle/nest *u* can be obtained as the probability that individual mode *m* has the minimum perceived disutility among all modes in nest *u*, which can be expressed as

$$\begin{aligned}\theta_{m|u}^{rs} &= P\left[v_{um}^{rs} \cdot \left(\mu_{um}^{rs}\right)^{-\frac{1}{\beta_u^{rs}}} \cdot \varepsilon_{um}^{rs} \le v_{un}^{rs} \cdot \left(\mu_{un}^{rs}\right)^{-\frac{1}{\beta_u^{rs}}} \cdot \varepsilon_{un}^{rs}, \forall n \ne m \in M_u^{rs} \right] \\ &= P\left[\frac{\varepsilon_{um}^{rs}}{\varepsilon_{un}^{rs}} \le \frac{\mu_{un}^{rs\,-\frac{1}{\beta_u^{rs}}} \cdot v_{un}^{rs}}{\mu_{um}^{rs\,-\frac{1}{\beta_u^{rs}}} \cdot v_{um}^{rs}}, \forall n \ne m \in M_u^{rs} \right]\end{aligned} . \tag{3.39}$$

Based on the distributional assumption of ε_{um}^{rs} and properties of the Weibull distribution, the conditional choice probability is derived as

$$\theta_{m|u}^{rs} = \frac{\left(\mu_{um}^{rs\,-\frac{1}{\beta_u^{rs}}} \cdot v_{um}^{rs} \right)^{-\beta_{um}^{rs}}}{\sum_{n \in M_u^{rs}} \left(\mu_{un}^{rs\,-\frac{1}{\beta_u^{rs}}} \cdot v_{un}^{rs} \right)^{-\beta_{um}^{rs}}}, \forall m \in M_u^{rs}, u \in U^{rs}, rs \in RS . \tag{3.40}$$

Based on the conditional choice model presented above, the composite disutility $\left(v_{um}^{rs}\right)^{*}$ can be obtained as the expected minimum disutility from the individual modes within bundle/nest *u*, which can also be used as the utility-based accessibility measure for bundle/nest *u* between OD pair *rs*:

$$Acc_u^{rs} = \left(v_{um}^{rs}\right)^{*} = \left[\sum_{m \in M_u^{rs}} \left(\mu_{um}^{rs\,-\frac{1}{\beta_u^{rs}}} \cdot v_{um}^{rs}\right)^{-\beta_{um}^{rs}}\right]^{-\frac{1}{\beta_{um}^{rs}}}, \forall m \in M_u^{rs}, u \in U^{rs}, rs \in RS\,. \tag{3.41}$$

Substituting Eqs. (3.38), (3.40), and (3.41) into Eq. (3.36) gives the CNW choice probability of choice travelers:

$$\begin{aligned}\theta_{um}^{rs} &= \frac{\left[\sum_{m \in M_u^{rs}} \left(\mu_{um}^{rs\,-\frac{1}{\beta_u^{rs}}} \cdot v_{um}^{rs}\right)^{-\beta_{um}^{rs}}\right]^{\frac{\beta_u^{rs}}{\beta_{um}^{rs}}}}{\sum_{w \in U^{rs}} \left[\sum_{m \in M_u^{rs}} \left(\mu_{um}^{rs\,-\frac{1}{\beta_u^{rs}}} \cdot v_{um}^{rs}\right)^{-\beta_{um}^{rs}}\right]^{\frac{\beta_u^{rs}}{\beta_{um}^{rs}}}} \cdot \frac{\left(\mu_{um}^{rs\,-\frac{1}{\beta_u^{rs}}} \cdot v_{um}^{rs}\right)^{-\beta_{um}^{rs}}}{\sum_{n \in M_u^{rs}} \left(\mu_{un}^{rs\,-\frac{1}{\beta_u^{rs}}} \cdot v_{un}^{rs}\right)^{-\beta_{um}^{rs}}} \\ &= \frac{\left(\mu_{um}^{rs\,-\frac{1}{\beta_u^{rs}}} \cdot v_{um}^{rs}\right)^{-\beta_{um}^{rs}} \cdot \left[\sum_{m \in M_u^{rs}} \left(\mu_{um}^{rs\,-\frac{1}{\beta_u^{rs}}} \cdot v_{um}^{rs}\right)^{-\beta_{um}^{rs}}\right]^{\frac{\beta_u^{rs}}{\beta_{um}^{rs}}-1}}{\sum_{w \in U^{rs}} \left[\sum_{m \in M_u^{rs}} \left(\mu_{um}^{rs\,-\frac{1}{\beta_u^{rs}}} \cdot v_{um}^{rs}\right)^{-\beta_{um}^{rs}}\right]^{\frac{\beta_u^{rs}}{\beta_{um}^{rs}}}}\end{aligned}\,. \tag{3.42}$$

Eqs. (3.37) and (3.39) implies the marginal (bundle) and conditional (mode) choice probabilities are derived based on the relative differences in bundle and mode disutility. Compared to the logit models with absolute difference-based choice probability, the relative difference-based weibit choice probability can better reflect the heterogeneous perceptions of different magnitude of travel disutility (Kitthamkesorn and Chen, 2013, 2017). Furthermore, the disutility function (3.35) can account for a single mobility service in different bundles/nests, which enables the consideration of mode correlation among bundles under different bundling strategies. In summary, the developed CNW model can effectively consider the heterogeneity and similarity issues

with mobility bundling in modeling the joint bundle and mode choice behavior of choice travelers.

3.3.2.2 Dogit model for considering bundle loyalty

This section further incorporates the repeated choice behavior of loyal travelers via the dogit model, which can be integrated with the developed CNW choice model while retaining consistency with the widely used Colombo/Morrison (C/M) model (Colombo and Morrison, 1989; Bordley, 1990). Different from Section 3.2 that considers loyalty to single modes, this section models bundle loyalty considering both the incentives of multiple loyalty schemes and the composite mode disutility of each bundle. Figure 3.12 illustrates using the dogit model for integrating the bundle choice behavior of loyal travelers from a bottom-up structure.

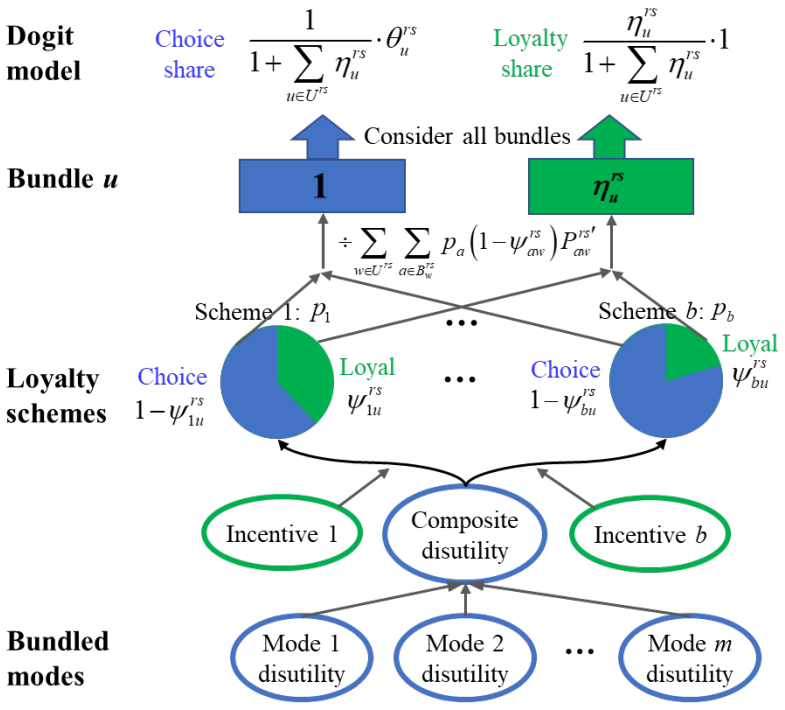

Figure 3.12. Illustration of dogit model for considering bundle loyalty

In the C/M model, loyal travelers are considered to repeatedly choose the same product from period to period. In the context of bundle choice, the choice proportion of

bundle u in the current period can then be expressed as the sum of the proportion sticking to bundle u, $P_{u,u}^{rs}$, and the proportion shifting from another bundle w, $P_{w,u}^{rs}$:

$$P_u^{rs} = P_u^{rs\prime} \cdot P_{u,u}^{rs} + \sum_{w \neq u \in U^{rs}} P_w^{rs\prime} \cdot P_{w,u}^{rs}, \forall u \in U^{rs}, rs \in RS, \tag{3.43}$$

where $P_u^{rs\prime}$ is the choice proportion of bundle u between OD pair rs in the previous period. Analogous to Section 3.2.2.3, $P_{u,u}^{rs}$, and $P_{w,u}^{rs}$ can be expressed as follows:

$$P_{w,u}^{rs} = \left(1 - \psi_w^{rs}\right) \cdot \theta_u^{rs}, \forall w \neq u \in U^{rs}, rs \in RS, \tag{3.44}$$

$$P_{u,u}^{rs} = \left(1 - \psi_u^{rs}\right) \cdot \theta_u^{rs} + \psi_u^{rs}, \forall u \in U^{rs}, rs \in RS. \tag{3.45}$$

where θ_u^{rs} is the bundle choice probability derived in Eq. (3.38) based on the random disutility minimization principle. ψ_u^{rs} denotes the proportion of loyal travelers who repeatedly choose bundle u without comparing the disutility of each bundle. Substituting Eqs. (3.44)–(3.45) into Eq. (3.43) gives the choice probability of bundle u:

$$P_u^{rs} = \psi_u^{rs} \cdot P_u^{rs\prime} + \theta_u^{rs} \cdot \sum_{w \in U^{rs}} \left(1 - \psi_w^{rs}\right) \cdot P_w^{rs\prime}, \forall u \in U^{rs}, rs \in RS. \tag{3.46}$$

Following Proposition 3.1, the dogit model is used to integrate the repeated bundle choice behavior represented in Eq. (3.46) as follows:

$$P_u^{rs} = \frac{\eta_u^{rs}}{1 + \sum_{w \in U^{rs}} \eta_w^{rs}} + \frac{1}{1 + \sum_{w \in U^{rs}} \eta_w^{rs}} \cdot \theta_u^{rs}, \forall u \in U^{rs}, rs \in RS, \tag{3.47}$$

where η_u^{rs} is the loyalty parameter of the dogit model as follows:

$$\eta_u^{rs} = \frac{\psi_u^{rs} \cdot P_u^{rs\prime}}{\sum_{w \in U^{rs}} \left(1 - \psi_w^{rs}\right) \cdot P_w^{rs\prime}}, \forall u \in U^{rs}, rs \in RS. \tag{3.48}$$

Alternatively, η_u^{rs} can be defined to account for a more general case where the bundle loyalty is imperfect, i.e., loyal travelers have different preferences to multiple loyalty bundle subscription schemes with different levels of incentives (Bordley, 1990):

$$\eta_u^{rs} = \frac{\sum_{b \in B_w^{rs}} p_b \cdot \psi_{bu}^{rs} P_{bu}^{rs\prime}}{\sum_{w \in U^{rs}} \sum_{a \in B_w^{rs}} p_a \left(1 - \psi_{aw}^{rs}\right) P_{aw}^{rs\prime}}, \forall u \in U^{rs}, rs \in RS, \tag{3.49}$$

where p_b is the proportion of subscribers to loyalty scheme *b*; ψ_{bu}^{rs} is the parameter denoting the proportion of loyal travelers to loyalty scheme *b*, which is defined in consistent with the weibit-based bundle choice model described in Eq. (3.38):

$$\psi_{bu}^{rs} = \frac{\left(v_{bu}^{rs}\right)^{-\beta_u^{rs}} - \left(v_u^{rs}\right)^{-\beta_u^{rs}}}{\sum_{w \in U^{rs}} \left(v_w^{rs}\right)^{-\beta_u^{rs}} + \left(v_{bu}^{rs}\right)^{-\beta_u^{rs}} - \left(v_u^{rs}\right)^{-\beta_u^{rs}}}, \forall u \in U^{rs}, rs \in RS. \tag{3.50}$$

v_{bu}^{rs} denotes the disutility perceived by the subscribers to the loyalty scheme *b* of bundle *u*, which can be obtained based on the service quality and discounts of bundled modes and is assumed to be lower than bundle disutility without preference (v_u^{rs}). In case that the previous choice probability $P_{bu}^{rs\prime}$ is unavailable, the overall loyalty parameter η_u^{rs} can be alternatively expressed as the weighted sum of the loyalty parameters to different loyalty schemes η_{bu}^{rs} (Bordley, 1990):

$$\eta_u^{rs} = \frac{\sum_{b \in B_w^{rs}} p_b \cdot \frac{\eta_{bu}^{rs}}{1 + \sum_{u \in U^{rs}} \eta_{bu}^{rs}}}{\sum_{b \in B_w^{rs}} \frac{p_b}{1 + \sum_{u \in U^{rs}} \eta_{bu}^{rs}}}, \forall u \in U^{rs}, rs \in RS, \tag{3.51}$$

where η_{bu}^{rs} is derived from the weibit-based bundle choice model as follows:

$$\eta_{bu}^{rs} = \frac{\left(v_u^{rs}\right)^{-\beta_u^{rs}} \cdot \left[\left(v_{bu}^{rs}\right)^{-\beta_u^{rs}} - \left(v_u^{rs}\right)^{-\beta_u^{rs}}\right]}{\left[\sum_{w \in U^{rs}} \left(v_w^{rs}\right)^{-\beta_u^{rs}}\right]^2}, \forall b \in B_u^{rs}, u \in U^{rs}, rs \in RS. \tag{3.52}$$

By summarizing Eqs. (3.36), (3.38), and (3.47), we can obtain the overall nest/bundle choice probability P_u^{rs} and hence the individual mode choice probability P_{um}^{rs} of the DCNW model as follows:

$$P_u^{rs} = \frac{\eta_u^{rs}}{1+\sum_{w\in U^{rs}} \eta_w^{rs}} + \frac{\eta_u^{rs}}{1+\sum_{w\in U^{rs}} \eta_w^{rs}} \cdot \frac{\left[\sum_{m\in M_u^{rs}} \left(\mu_{um}^{rs\,-\frac{1}{\beta_u^{rs}}} \cdot v_{um}^{rs}\right)^{-\beta_{um}^{rs}}\right]^{\frac{\beta_u^{rs}}{\beta_{um}^{rs}}}}{\sum_{w\in U^{rs}} \left[\sum_{m\in M_u^{rs}} \left(\mu_{um}^{rs\,-\frac{1}{\beta_u^{rs}}} \cdot v_{um}^{rs}\right)^{-\beta_{um}^{rs}}\right]^{\frac{\beta_u^{rs}}{\beta_{um}^{rs}}}}$$

$$= \frac{\eta_u^{rs} \cdot \sum_{w\in U^{rs}} \left[\sum_{m\in M_u^{rs}} \left(\mu_{um}^{rs\,-\frac{1}{\beta_u^{rs}}} \cdot v_{um}^{rs}\right)^{-\beta_{um}^{rs}}\right]^{\frac{\beta_u^{rs}}{\beta_{um}^{rs}}} + \left[\sum_{m\in M_u^{rs}} \left(\mu_{um}^{rs\,-\frac{1}{\beta_u^{rs}}} \cdot v_{um}^{rs}\right)^{-\beta_{um}^{rs}}\right]^{\frac{\beta_u^{rs}}{\beta_{um}^{rs}}}}{\left(1+\sum_{w\in U^{rs}} \eta_w^{rs}\right) \cdot \sum_{w\in U^{rs}} \left[\sum_{m\in M_u^{rs}} \left(\mu_{um}^{rs\,-\frac{1}{\beta_u^{rs}}} \cdot v_{um}^{rs}\right)^{-\beta_{um}^{rs}}\right]^{\frac{\beta_u^{rs}}{\beta_{um}^{rs}}}}, \tag{3.53}$$

$$P_{um}^{rs} = \frac{\eta_u^{rs} \cdot \sum_{w\in U^{rs}} \left[\sum_{m\in M_u^{rs}} \left(\mu_{um}^{rs\,-\frac{1}{\beta_u^{rs}}} \cdot v_{um}^{rs}\right)^{-\beta_{um}^{rs}}\right]^{\frac{\beta_u^{rs}}{\beta_{um}^{rs}}} + \left[\sum_{m\in M_u^{rs}} \left(\mu_{um}^{rs\,-\frac{1}{\beta_u^{rs}}} \cdot v_{um}^{rs}\right)^{-\beta_{um}^{rs}}\right]^{\frac{\beta_u^{rs}}{\beta_{um}^{rs}}}}{\left(1+\sum_{w\in U^{rs}} \eta_w^{rs}\right) \cdot \sum_{w\in U^{rs}} \left[\sum_{m\in M_u^{rs}} \left(\mu_{um}^{rs\,-\frac{1}{\beta_u^{rs}}} \cdot v_{um}^{rs}\right)^{-\beta_{um}^{rs}}\right]^{\frac{\beta_u^{rs}}{\beta_{um}^{rs}}}} \cdot \frac{\left(\mu_{um}^{rs\,-\frac{1}{\beta_u^{rs}}} \cdot v_{um}^{rs}\right)^{-\beta_{um}^{rs}}}{\sum_{n\in M_u^{rs}} \left(\mu_{un}^{rs\,-\frac{1}{\beta_u^{rs}}} \cdot v_{un}^{rs}\right)^{-\beta_{um}^{rs}}}$$

(3.54)

3.4 Joint destination and parking choice with shared parking services

3.4.1 Background and related studies

Shared parking is an emerging parking service that has recently received increasing interest in the sharing economy era. The shortage of parking spaces is often a serious transportation problem in congested metropolitan areas. Shared parking services encourage private parking lot owners to share unused residential parking lots, thereby increasing the utilization rate of private parking spaces, alleviating the parking supply shortage, and decreasing the cruising time required to search for parking spaces. Owing to these benefits, shared parking services are being widely implemented in many countries, such as Australia, China, the Netherlands, and France (Ardeshiri et al., 2021; Liu et al., 2022). The development of shared parking requires significant planning, policymaking in the areas of pricing and bidding (Xiao et al., 2018; Liu et al., 2021, 2022), platform design (Gao et al., 2022), and parking space allocation (Wang et al., 2022). To promote the development of shared parking, it is necessary to understand and model the effect of shared parking services on multi-dimensional individual travel choices, which is the focus of this section.

In addition to the parking choice, quality of parking services may influence travel disutility and behaviors at other choice dimensions (Lam et al., 2006; Jiang et al., 2014; Leurent and Boujnah, 2014; Liu, 2018; Liu et al., 2018). Specifically, the parking choice may affect the utility gained at the destination and hence interact with destination choice. In a pioneering work, Liu et al. (2021) modeled the effect of shared parking services on the combined destination and parking choice. The destination choice was reproduced based on the random utility theory through the multinomial logit (MNL) choice model, whereas the parking choice was modeled deterministically based on the user equilibrium (UE) principle. The destination choice directly determines the parking demand at each destination, whereas the parking disutility resulting from the parking choices reciprocally affects the destination attractiveness, and thus, the destination choice.

Nevertheless, research on modeling the joint destination and parking choice with shared parking services remains limited. To the best of the authors' knowledge, Liu et al. (2021) is the only work on this topic, and the following research gaps remain. (1) An inconsistency exists between the destination and parking choice dimensions in the model proposed by Liu et al. (2021). The MNL destination choice model considers the perception error of the destination attractiveness; in contrast, the UE-based parking choice model assumes that travelers have perfect traffic information and no perception error. (2) The MNL model cannot fully capture the heterogeneities in perceived destination and parking disutility, which are important to be considered in modeling both destination and parking choice behaviors (Barros et al., 2008; Ibeas et al., 2014). Furthermore, the MNL model is inadequate to capture the correlation in spatial dimensions (e.g., location adjacency), which has been found to have significant effects on the choice of spatially correlated alternatives (Bhat and Guo, 2004; Bekhor and Prashker, 2008; Sener et al., 2011; Perez-Lopez et al., 2020, 2022).

This section aims to develop an advanced closed-form random utility model to consistently consider the destination and parking choice behaviors and their interactions based on the random utility theory. The effects of heterogeneous travel perceptions and spatial correlations are specifically considered among closely spaced destination locations and parking lots at both destination and parking choice dimensions.

To facilitate the presentation of the essential ideas, the notations used in this section are listed below.

Sets

R	Set of origins.
S	Set of destinations.
$L_{s,sp}, L_{s,cp}$	Set of shared parking/curbside parking lots at destination s.
ST	Set of destination pairs.

Inputs and parameters

v_s^r	Total disutility of traveling from origin *r* to destination *s*.
$v_{s,sp}^r, v_{s,cp}^r$	Total disutility of traveling from origin *r* to destination *s* using shared parking/curbside parking.
$v_{s,sp}, v_{s,cp}$	Disutility of using shared parking/curbside parking at destination *s*.
$v_{s,st}^r$	Individual disutility of destination *s* in destination pair *st.*
τ_{st}^r	Common cost of destination pair *st.*
ψ_s	Attractiveness of destination *s.*
$\alpha_{s,st}^r$	Allocation parameter indicating the proportion of destination *s* in destination pair *st.*
β^r	Shape parameter with respect to the marginal destination choice level.
β_s	Shape parameter with respect to the conditional destination choice level.
μ	Dissimilarity parameter.
w_{st}	Spatial correlation between destinations *s* and *t*.
$PS_{s,sp}, PS_{s,cp}$	Parking-size factor of shared/curbside parking at destination *s.*
$N_{sp,i}, N_{cp,i}$	Parking space provided by parking lot *i* of shared/curbside parking.
$N_{s,sp}, N_{s,cp}$	Total shared/curbside parking space at destination *s*.
$\delta_{s,i}$	Indicator of whether parking lot *i* is used by destination *s*.
β_m	Shape parameter with respect to the parking choice.

Variables

A_s^r	Accessibility between OD pair *rs*.
P_s^r	Choice probability of destination *s* from origin *r*.
P_{st}^r	Marginal choice probability of destination pair *st* from origin *r*.
$P_{s,st}^r$	Conditional choice probability of destination *s* in destination pair *st* from origin *r*.
$P_{s,sp}^r, P_{s,cp}^r$	Choice probability of shared/curbside parking between OD pair *rs*.

3.4.2 Joint destination and parking choice with spatial correlation

3.4.2.1 Hierarchical destination and parking choice structure

The joint destination and parking choice is modeled on the hierarchical choice structure shown in Figure 3.13. The destination choice is modeled at the upper level, which determines the demand for the lower-level parking choice. The accessibility (composite disutility) obtained at the lower level is incorporated in the total disutility of traveling to a certain destination, which reciprocally influences the destination choice. The spatially correlated weibit (SCW) model is developed at the destination choice level to consider the spatial correlation among destinations, i.e., greater substitution occurs among adjacent destinations than among those located at large spatial distances. At the parking choice level, the parking-size weibit (PSW) model is developed to consider the overlaps among the parking space of adjacent destinations. The destination and parking choice models are described in Sections 3.4.2.2 and 3.4.2.3, respectively.

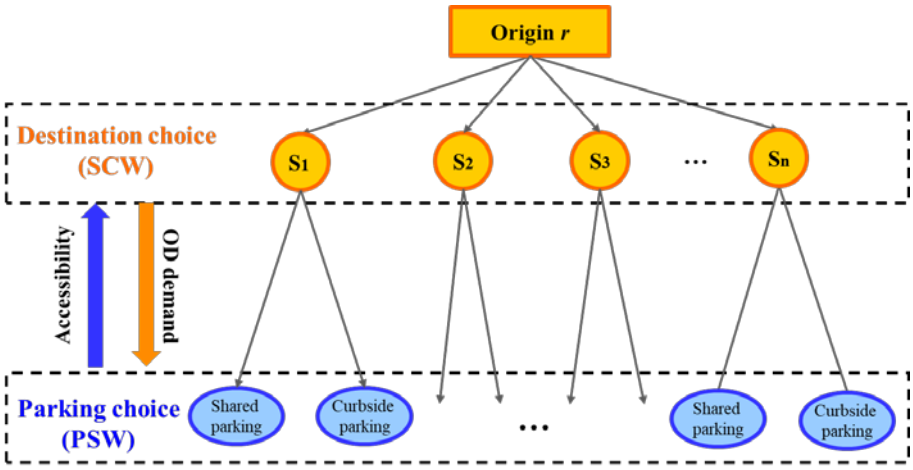

Figure 3.13. Joint destination and parking choice structure

3.4.2.2 Destination choice behavior

(1) Effect of weibit-based destination choice model

The logit-based model, which is widely used to model destination choices at the individual level, is associated with the aggregate gravity-type trip distribution model with a negative exponential deterrence function (Wilson, 1967). Notably, both the logit-

based model and the gravity model based on the exponential impedance function suffer from the following issues (Fotheringham and O'Kelly, 1989). (1) The model outcomes depend on the unit used for measuring the travel cost, which can influence the comparability of the outcomes. (2) The exponential impedance function cannot reflect the effect of the additive travel cost increase on destination demands. These problems are attributable to the fact that logit-based destination choice models implicitly assume homogenous perception variance in travel impedance, which might not be realistic when there exist multiple OD pairs with distinct scales of travel disutility.

The weibit-based destination choice model is adopted in this section to address the heterogeneity issue embedded in the logit-based model. The weibit-based model is equivalent to the gravity model with a negative power deterrence function, which is scale-independent and can effectively model destination choices that consider distinct trip distances (Choukroun, 1975, Xu et al., 2015). Figure 3.14 shows the effect of using a weibit model on considering heterogeneity by comparing the outcomes from the MNL and multinomial weibit (MNW) models in an illustrative example. Consider two OD pairs R-S_1 and R-S_2 with the same destination attractiveness but different OD travel impedances. Assuming a constant difference in the travel impedance, the choice probabilities from the two models are shown in the right panel of Figure 3.14. The destination choice probability yielded by the MNL model is constant and thus cannot capture the heterogeneous perceptions of OD travel disutility. In contrast, the MNW model can reflect the changes in OD travel disutility scale, with the effect of the disutility difference decreases with the increase in the disutility scale. This outcome is more realistic than that of the MNL model because travelers may become less sensitive to the same disutility difference at larger scales (Masin et al., 2009).

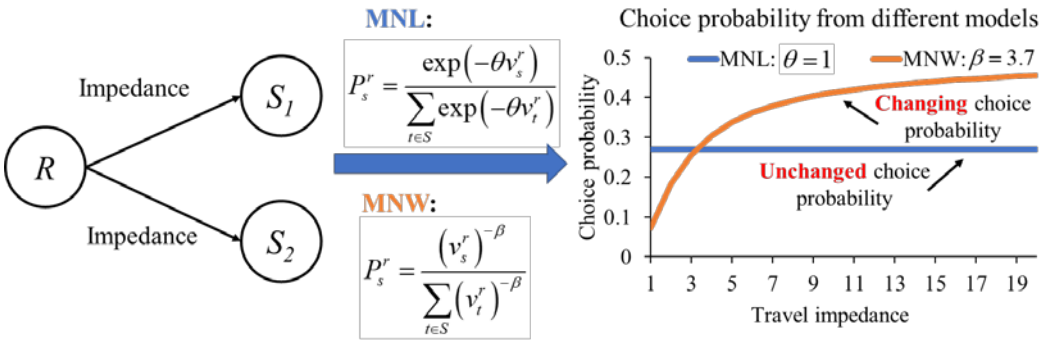

Figure 3.14. Effect of considering heterogeneity in destination choice

(2) SCW model formulation

To consider the spatial correlation among adjacent destinations together with the heterogeneity issue, the SCW model is developed based on the nested choice structure of the spatially correlated logit model (Bhat and Guo, 2004). Figure 3.15 illustrates the SCW choice structure for an example involving one origin and four adjacent destinations.

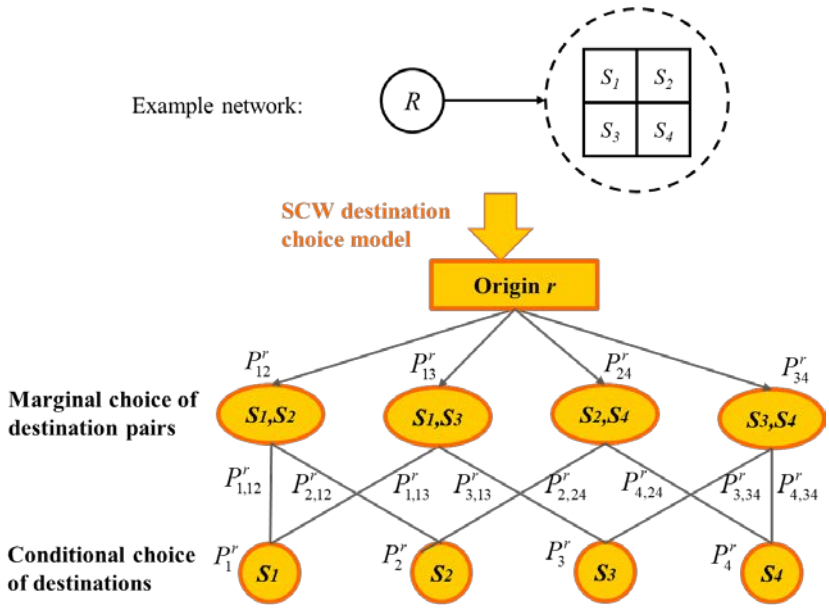

Figure 3.15. Choice structure of SCW model

Following the two-level choice structure shown in Figure 3.15, the perceived disutility of traveling from origin *r* to destination *s* belonging to destination pair *st* can be expressed as

$$V_{s,st}^{r} = \left(\alpha_{s,st}^{r}\right)^{-1} \cdot v_{s,st}^{r} \cdot \varepsilon_{s,st}^{r} \cdot \tau_{st}^{r} \cdot \varepsilon_{st}^{r}, \forall r \in R, st \in ST, \tag{3.55}$$

where $\alpha_{s,st}^{r}$ is the allocation parameter indicating the membership of destination *s* in pair *st*, which is positive and satisfies $\sum_{st \in ST} \alpha_{s,st}^{r} = 1$. $V_{s,st}^{r}$ is decomposed into two parts: (1) the individual disutility related to destination *s* with deterministic and random error terms $v_{s,st}^{r}$ and $\varepsilon_{s,st}^{r}$, respectively; and (2) the common cost related to destination pair *st* with deterministic and random error terms τ_{st}^{r} and ε_{st}^{r}, respectively.

Following three distributional assumptions are made for developing the SCW model: (1) $\varepsilon_{s,st}^{r}$ and ε_{st}^{r} are independent of each other; (2) $\varepsilon_{s,st}^{r}$ independently follows the Weibull distribution with shape parameter β_s; and (3) ε_{st}^{r} is distributed such that $\left(\varepsilon_{s,st}^{r}\right)^{*} \cdot \varepsilon_{st}^{r}$ follows the Weibull distribution with shape parameter β^{r}. $\left(\varepsilon_{s,st}^{r}\right)^{*}$ denotes the random error term associated with the minimum disutility of choosing a destination within the destination pair *st*, i.e., $\min_{s \in st}\left(U_{s,st}^{r}\right)$, where $U_{s,st}^{r} = \left(\alpha_{s,st}^{r}\right)^{-1} \cdot v_{s,st}^{r} \cdot \varepsilon_{s,st}^{r}$. Based on the hierarchical choice structure shown in Figure 3.15, the SCW probability of choosing destination *s* from origin *r* can be expressed based on the product of marginal and conditional choice probabilities:

$$P_{s}^{r} = \sum_{t \neq s \in S} P_{st}^{r} \cdot P_{s,st}^{r}, \forall r \in R, s \in S. \tag{3.56}$$

The marginal probability of choosing destination pair *st* from origin *r* can be derived based on the disutility minimization principle, as follows:

$$\begin{aligned} P_{st}^{r} &= P\left[\tau_{st}^{r} \cdot \varepsilon_{st}^{r} \cdot \min_{s \in st}\left(U_{s,st}^{r}\right) \leq \tau_{ij}^{r} \cdot \varepsilon_{ij}^{r} \cdot \min_{i \in ij}\left(U_{i,ij}^{r}\right), \forall ij \neq st \in ST\right] \\ &= P\left[\frac{\varepsilon_{st}^{r} \cdot \left(\varepsilon_{s,st}^{r}\right)^{*}}{\varepsilon_{ij}^{r} \cdot \left(\varepsilon_{i,ij}^{r}\right)^{*}} \leq \frac{\tau_{ij}^{r} \cdot \left(v_{i,ij}^{r}\right)^{*}}{\tau_{st}^{r} \cdot \left(v_{s,st}^{r}\right)^{*}}, \forall ij \neq st \in ST\right] \end{aligned}. \tag{3.57}$$

According to properties of the Weibull distributions, $\min_{s\in st}\left(U_{s,st}^{r}\right)$ is Weibull distributed with the same shape parameter β_s and the following scale parameter:

$$\left\{\left[\alpha_{s,st}^{r}\cdot\left(v_{s,st}^{r}\right)^{-1}\right]^{\beta_s}+\left[\alpha_{t,st}^{r}\cdot\left(v_{t,st}^{r}\right)^{-1}\right]^{\beta_s}\right\}^{-\frac{1}{\beta_s}}. \tag{3.58}$$

Based on distributional assumption (3), the marginal choice probability is

$$P_{st}^{r}=\frac{\left\{\tau_{st}^{r}\cdot\left\{\left[\alpha_{s,st}^{r}\cdot\left(v_{s,st}^{r}\right)^{-1}\right]^{\beta_s}+\left[\alpha_{t,st}^{r}\cdot\left(v_{t,st}^{r}\right)^{-1}\right]^{\beta^s}\right\}^{-\frac{1}{\beta_s}}\right\}^{-\beta^r}}{\sum_{s=1}^{|S|-1}\sum_{t=s+1}^{|S|}\left\{\tau_{st}^{r}\cdot\left\{\left[\alpha_{s,st}^{r}\cdot\left(v_{s,st}^{r}\right)^{-1}\right]^{\beta_s}+\left[\alpha_{t,st}^{r}\cdot\left(v_{t,st}^{r}\right)^{-1}\right]^{\beta_s}\right\}^{-\frac{1}{\beta_s}}\right\}^{-\beta^r}},\forall r\in R,st\in ST. \tag{3.59}$$

If no common disutility exists within each destination pair, $\tau_{st}^{r}=1,\forall st\in ST$ and can be omitted from Eq. (3.59).

Similarly, the conditional probability of choosing destination *s* given that destination pair *st* is chosen can be expressed as

$$\begin{aligned}P_{s,st}^{r}&=P\left[v_{s,st}^{r}\cdot\varepsilon_{s,st}^{r}\le v_{t,st}^{r}\cdot\varepsilon_{t,st}^{r},\forall t\ne s\in S\right]\\&=P\left[\varepsilon_{s,st}^{r}\big/\varepsilon_{t,st}^{r}\le v_{t,st}^{r}\big/v_{s,st}^{r},\forall t\ne s\in S\right]\end{aligned}. \tag{3.60}$$

Based on distributional assumption (2), $P_{s,st}^{r}$ can be derived as follows:

$$P_{s,st}^{r}=\frac{\left[\alpha_{s,st}^{r}\cdot\left(v_{s,st}^{r}\right)^{-1}\right]^{\beta_s}}{\left[\alpha_{s,st}^{r}\cdot\left(v_{s,st}^{r}\right)^{-1}\right]^{\beta_s}+\left[\alpha_{t,st}^{r}\cdot\left(v_{t,st}^{r}\right)^{-1}\right]^{\beta_s}},\forall r\in R,st\in ST. \tag{3.61}$$

Let the dissimilarity parameter μ denote the ratio between the shape parameters at the marginal and conditional choice levels, i.e., $\mu=\beta^r/\beta_s$. By definition, $\beta_s>\beta^r>0$, and μ is a positive parameter bounded by zero and one (Ben-Akiva and Lerman, 1985). For normalization, we set $\beta^r=1$ and $\beta_s=1/\mu$. The SCW probability given by Eqs. (3.56), (3.59), and (3.61) can be expressed as

$$P_s^r = \sum_{st \in ST} \frac{\left[\alpha_{s,st}^r \cdot \left(v_s^r\right)^{-1}\right]^{\frac{1}{\mu}} \cdot \left\{\left[\alpha_{s,st}^r \cdot \left(v_s^r\right)^{-1}\right]^{\frac{1}{\mu}} + \left[\alpha_{t,st}^r \cdot \left(v_t^r\right)^{-1}\right]^{\frac{1}{\mu}}\right\}^{\mu-1}}{\sum_{s=1}^{|S|-1} \sum_{t=s+1}^{|S|} \left\{\left[\alpha_{s,st}^r \cdot \left(v_s^r\right)^{-1}\right]^{\frac{1}{\mu}} + \left[\alpha_{t,st}^r \cdot \left(v_t^r\right)^{-1}\right]^{\frac{1}{\mu}}\right\}^{\mu}}, \forall r \in R, s \in S, \quad (3.62)$$

where $v_{s,st}^r$ is substituted by v_s^r.

The allocation parameter $\alpha_{s,st}^r$ can be derived as

$$\alpha_{s,st}^r = \frac{w_{st}}{\sum_{st \in ST} w_{st}}, \forall r \in R, st \in ST, \quad (3.63)$$

where w_{st} indicates the spatial correlation between destinations *s* and *t*. The spatial correlation can be derived based on the number of adjacent destinations, i.e., $w_{st} = 1$ if *s* and *t* are adjacent and 0 otherwise (Bhat and Guo, 2004).

(3) Effect of considering spatial correlation among destinations

A small network (Figure 3.16) is considered to illustrate the effect of spatial correlation among adjacent destinations and the way this problem is addressed by the SCW model. Three spatial distribution patterns of the four adjacent destinations are used to show the calculation of the allocation parameter $\alpha_{s,st}^r$, which influences the SCW destination choice probability.

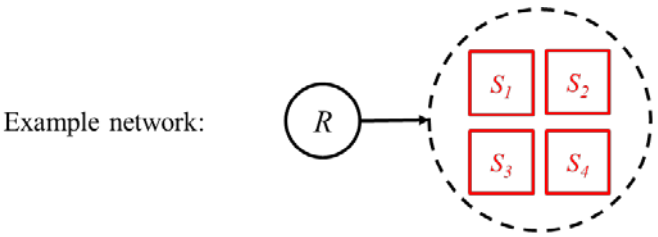

Spatial pattern 1

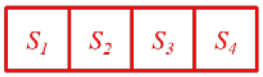

Allocation parameter $\alpha^{r}_{s,st}$

	S_1	S_2	S_3	S_4
S_1	0	1	0	0
S_2	0.5	0	0.5	0
S_3	0	0.5	0	0.5
S_4	0	0	1	0

Spatial pattern 2

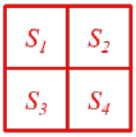

Allocation parameter $\alpha^{r}_{s,st}$

	S_1	S_2	S_3	S_4
S_1	0	0.5	0.5	0
S_2	0.5	0	0	0.5
S_3	0.5	0	0	0.5
S_4	0	0.5	0.5	0

Spatial pattern 3

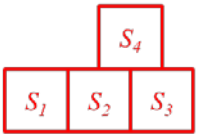

Allocation parameter $\alpha^{r}_{s,st}$

	S_1	S_2	S_3	S_4
S_1	0	1	0	0
S_2	0.33	0	0.33	0.33
S_3	0	0.5	0	0.5
S_4	0	0.5	0.5	0

Figure 3.16. Illustrative example of allocation parameter in SCW model

Figure 3.17 shows the effect of considering spatial correlation based on the SCW model. The demand for a destination is likely to be diverted by its neighbors. Assuming that the four adjacent destinations have the same utility and same travel impedance to the origin, the numbers of adjacent destinations and choice probabilities of these four destinations are presented in Figure 3.17. The MNW model is insensitive to the spatial allocation of the destinations. In contrast, the SCW model can reflect the differences among the allocation patterns. A destination with a larger number of adjacent destinations (i.e., higher spatial correlation) corresponds to a lower choice probability.

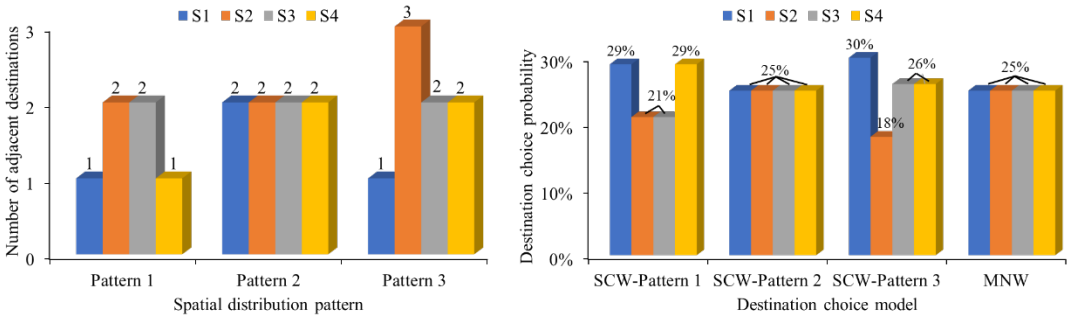

(a) Spatial correlations in the different patterns (b) Comparison of choice probabilities

Figure 3.17. Effect of considering spatial correlation via SCW model

3.4.2.3 Parking choice behavior

This section focuses on the choice between the two parking modes: curbside and shared parking services. To ensure behavioral consistency with the destination choice model, the weibit-based model is adopted at the parking choice level to inherently consider the effect of heterogeneity (i.e., heterogeneous perceptions of different parking disutility magnitudes) on parking choice behavior.

(1) Spatial correlation among parking spaces

In addition to spatial correlation at the destination choice level, it is important to also account for spatial correlation at the parking choice level, which stems from the overlap among parking spaces. Figure 3.18 demonstrates spatial correlation among parking spaces with the shared parking service as an example (which is similar for curbside parking). Consider the shared parking lots in the catchment areas of destinations s_1, s_2, and s_3. Several parking lots (i.e., l_1, l_2, l_3, and l_4) located between adjacent destinations can be reached by travelers at either destination. In particular, parking lot l_4 exhibits a significant overlap as it can be used by travelers at all three destinations. Thus, the overlapped parking lot must not be considered a "full parking alternative" for each destination, as it cannot contribute as much to the parking service as a distinct parking lot that only serves a single destination.

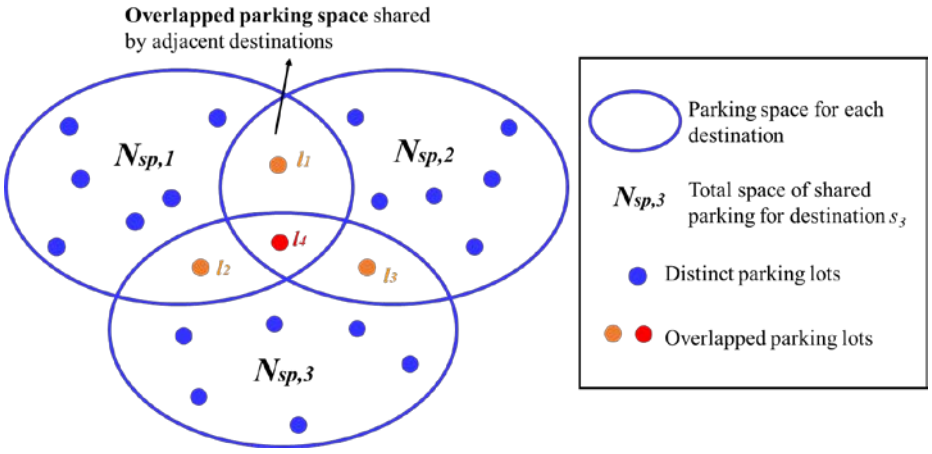

Figure 3.18. Spatial overlap among parking spaces

(2) PSW model formulation

The PSW model is developed to consider the effect of spatial correlation on parking disutility. A parking-size (*PS*) factor is introduced to penalize the overlapped parking space, which provides a smaller size of parking alternative than the distinct parking space that has the "full" size of parking alternative. The derivation and interpretation of the *PS* factor are analogous to those of the well-established path-size factors (Ben-Akiva and Bierlaire, 1999; Frejinger and Bierlaire, 2007). Following the theory for a choice model with aggregate alternatives (Ben-Akiva and Lerman, 1985), we consider each type of parking service (i.e., curbside parking and shared parking) at each destination as an aggregate alternative and each parking lot as an elemental alternative. Assuming that each aggregate alternative consists of sufficient elemental alternatives, each elemental alternative has the same mean disutility, and the random error of each elemental alternative independently follows the identical Weibull distribution, the disutility of an aggregate alternative can be expressed as

$$\begin{aligned} v &= \left(\sum_{i \in I} v_i^{-\beta} \right)^{-\frac{1}{\beta}} \\ &= \left(M \cdot v_i^{-\beta} \right)^{-\frac{1}{\beta}}, \\ &= M^{-\frac{1}{\beta}} \cdot v_i \end{aligned} \tag{3.64}$$

where v_i is the mean disutility of the elemental alternative i, β is the shape parameter, and M is the number of elemental alternatives. $M^{-\frac{1}{\beta}}$ represents the effect of alternative size on disutility of aggregate alternative. To account for the negative effect of overlap in the parking choice problem, we define the full size as 1 for each distinct parking lot and penalized size as $\frac{1}{\sum_{s \in S} \delta_{s,i}} < 1$ for each overlapped parking lot, where $\delta_{s,i}$ is a binary indicator of whether parking lot i can be used by destination s. Subsequently, we can derive the *PS* factor as the aggregate size of each type of parking service at destination s, which depends on the total weighted size of parking lots belonging to that parking

service. Taking the shared parking service as an example, the *PS* factor for shared parking at destination *s* can be expressed as

$$PS_{s,sp} = \sum_{i \in L_{s,sp}} \frac{N_{sp,i}}{N_{s,sp}} \cdot \frac{1}{\sum_{s \in S} \delta_{s,i}}, \forall s \in S , \tag{3.65}$$

where $N_{s,sp}$ and $N_{sp,i}$ denote the total shared parking space at destination *s* and the shared parking space provided by parking lot *i*, respectively. The perceived shared parking disutility can be expressed as

$$V_{s,sp} = \left(PS_{s,sp} \right)^{-\frac{1}{\beta_m}} \cdot v_{s,sp} \cdot \varepsilon_{s,sp}, \forall s \in S . \tag{3.66}$$

where $v_{s,sp}$ and $\varepsilon_{s,sp}$ are the deterministic disutility and random error term of shared parking service at destination *s*, respectively. β_m is the shape parameter at the parking choice level. The perceived curbside parking disutility $V_{s,cp}$ can be derived by substituting the corresponding *PS* factor, deterministic disutility and random error term (i.e., $PS_{s,cp}$, $v_{s,cp}$, and $\varepsilon_{s,cp}$) into Eq. (3.66), where the *PS* factor of the curbside parking service at destination *s*, $PS_{s,cp}$, can be derived by substituting $N_{s,cp}$ and $N_{cp,i}$ in Eq. (3.65). Based on the principle of random disutility minimization, the choice probability of shared parking/curbside parking service can be expressed as the probability that shared parking/curbside parking service has the minimum perceived parking disutility at destination *s*. Taking shared parking probability as an example,

$$\begin{aligned} P_{s,sp}^{r} &= P\left[V_{sp}^{s} \le V_{cp}^{s} \right] \\ &= P\left[\left(PS_{s,sp} \right)^{-\frac{1}{\beta_m}} \cdot v_{s,sp} \cdot \varepsilon_{s,sp} \le \left(PS_{s,cp} \right)^{-\frac{1}{\beta_m}} \cdot v_{s,cp} \cdot \varepsilon_{s,cp} \right]. \\ &= P\left[\frac{\varepsilon_{s,sp}}{\varepsilon_{s,cp}} \le \frac{\left(PS_{s,cp} \right)^{-\frac{1}{\beta_m}} \cdot v_{s,cp}}{\left(PS_{s,sp} \right)^{-\frac{1}{\beta_m}} \cdot v_{s,sp}} \right] \end{aligned} \tag{3.67}$$

Following the same logic as that of deriving the binary weibit model (Section 2.1.2.1) and incorporating the in-vehicle travel cost to calculate the OD travel disutility $v_{s,sp}^{r}$, the PSW choice probability of shared parking service can be derived as follows:

$$P_{s,sp}^{r} = \frac{\left(v_{s,sp}^{r}\right)^{-\beta_m} \cdot PS_{s,sp}}{\left(v_{s,sp}^{r}\right)^{-\beta_m} \cdot PS_{s,sp} + \left(v_{s,cp}^{r}\right)^{-\beta_m} \cdot PS_{s,cp}}, \forall rs \in RS . \quad (3.68)$$

The same derivation is applicable to evaluating the PSW choice probability of curbside parking service.

Based on the property of the Weibull distribution, the composite travel disutility at the parking choice level derived based on the PSW model can be expressed as follows:

$$A_{s}^{r} = \left[\left(v_{s,sp}^{r}\right)^{-\beta_m} \cdot PS_{s,sp} + \left(v_{s,cp}^{r}\right)^{-\beta_m} \cdot PS_{s,cp}\right]^{-\frac{1}{\beta_m}}, \forall rs \in RS . \quad (3.69)$$

Note that A_{s}^{r} can also be considered as the accessibility measure (as illustrated in Section 2.1.3) and is incorporated into the total disutility considered at the destination choice level (Eq. (3.55)). Thus, A_{s}^{r} connects the destination choice and parking choice and reflects the interaction between the two choice dimensions while consistent with the random utility theory.

Chapter 4 Closed-form weibit-based choice model for assessing oddball effect with alternate distributional assumptions

This chapter proposes a weibit-based model that relaxes the identically distributed assumption to model the choice set with a single "oddball" alternative that has unique attributes to other conventional alternatives. While retaining the closed-form probability expression, the proposed model handles the oddball alternative using a multiplicative random disutility function assuming Weibull distributed random components. The proposed model thus allows alternative-specific perception variances for both the conventional and oddball alternatives and a flexible variance ratio between them. This gives the proposed model high flexibility to consider various heterogeneity issues, including the heterogeneity among conventional alternatives, heterogeneity between conventional and oddball alternatives, and heterogeneity between the unique and common attributes of the oddball alternative. The empirical application of the proposed model is explored to figure out its practical performance. The proposed model could further provide new behavioral insights into various decision-making scenarios of transportation networks, such as transportation mode choices in the current era of emerging technologies and destination choices in urban agglomerations.

4.1 Introduction

With significant progress in transportation technologies and rapid lifestyle changes, travelers are likely to consider innovative transportation alternatives that have different attributes to the conventional alternatives, which are thus labeled "*oddball*" in the choice set. For example, emerging technologies such as autonomous vehicles are set to be added to the multi-modal transportation network, which will lead to new travel modes with uncommon service features, such as automated navigation, that cannot be obtained from conventional travel modes. In another case, with the development of urban agglomeration, more travelers now tend to choose destinations located in neighboring cities (Huang et al., 2020c). Differing from the traditional destination

choices within a city, choosing a destination in a neighboring city involves inter-city trips that may lead to unique opportunities for work, education, and entertainment.

The oddball alternative with unique attributes can be handled via alternative-specific random components in open-form choice models, such as the heteroscedastic extreme-value (HEV) model (Bhat, 1995). However, these models often require additional model parameters and lack a closed-form probability expression, which pose additional difficulties to model estimation, interpretation, and evaluation. Furthermore, the closed-form choice probability is valuable for the applications to higher-level optimization problems where the stochastic choice behavior of travelers is embedded. In contrast, conventional closed-form travel choice models, such as the multinomial logit (MNL) model and generalized extreme value (GEV) (e.g., the nested logit, NL) models, can significantly reduce the computational requirement for choice probability evaluation and are frequently adopted in travel demand forecasting and network design studies. However, MNL and GEV models mainly assume identically Gumbel distributed total random errors and an identical variance across alternatives with distinct magnitudes of disutility, which are inadequate to capture the oddball effect (Ben-Akvia and Lerman, 1985; Prashker and Bekhor, 2004; Koppelman and Sethi, 2008). Therefore, it is imperative to develop a closed-form choice model that can explicitly assess travel choice behavior with the new oddball alternatives of modern transportation networks.

In a pioneering study, Recker (1995) proposed a multinomial logit model with an oddball alternative (hereafter referred to as the MNL-O model), which explicitly accounts for the random utility associated with the unique features of a single oddball alternative while retaining a closed-form probability expression, with the oddball alternative's unique attributes considered separately in random components. The closed-from probability expression allows a straightforward interpretation of the relationship between the observed variables and choice probabilities, enabling the efficient and precise maximum likelihood estimation approach to be applied, eliminating the computational burden of needing additional numerical or simulation approaches for the probability evaluation (Koppelman, 2008; Mondal and Bhat, 2021).

With these advantages, the closed-form MNL-O model could be applied to distinguish the oddball alternative in econometric studies or be incorporated into transportation models that require efficient computation of many choice probabilities, such as the well-established network equilibrium models (Prashker and Bekhor, 2004).

However, the MNL-O model inherits some limitations from the MNL model with an additive utility function. First, it assumes an identical perception variance for all conventional alternatives, which is inadequate for addressing the heterogeneity issue. Second, although a different perception variance is assumed for the oddball alternative, it is still fixed and independent of alternative utility, keeping the variance ratio between oddball and conventional alternatives fixed. This could lead to an unrealistic expectation that the common and unique features of the oddball alternative have equal and fixed contributions to the random utility of the oddball alternative with the service level disregarded. Finally, the choice probabilities of the MNL-O model are dependent on the absolute differences in utility, which are inadequate to model distinct magnitudes of alternative utility in large-scale networks. These limitations make it difficult for the MNL-O model to reflect the heterogeneous perceptions of various travel modes or the distinct trip lengths associated with different destinations, which could hinder its application to the complex decision-making scenarios in modern transportation systems.

This chapter proposes an alternate weibit-based model for assessing travel choice with an oddball alternative, addressing the inherent heterogeneity issues in the MNL-O model while retaining the closed-form probability expression. Based on the multiplicative disutility function with Weibull distributed random components, the proposed model allows disutility-dependent variances for all alternatives. Thus, the model can naturally consider various heterogeneity issues, including the heterogeneous perceptions of conventional alternatives, heterogeneous perceptions of unique and common attributes of the oddball alternative, and distinct service features of conventional and oddball alternatives. Also, the multiplicative error structure adopted in the proposed model coincides with the psychophysical laws on how individuals perceive different magnitudes of travel disutility, and thus can have better behavioral

interpretations than the additive error structure in commonly used logit models (Chakroborty et al., 2021; Nirmale and Pinjari, 2023). Herein, derivations of closed-form choice probabilities of both conventional and oddball alternatives are proposed. The perception variances and elasticities with respect to both conventional and oddball alternatives are also analytically derived, illustrating the appealing theoretical properties of the proposed model.

The remainder of this chapter is organized as follows. Section 4.2 briefly reviews the formulation, properties, and limitations of Recker's MNL-O model. In Section 4.3, a weibit-based model with an oddball alternative is then developed, with detailed derivations of closed-form choice probabilities of both conventional and oddball alternatives provided. The theoretical properties and advantages of the proposed model are then thoroughly discussed via comparisons with some existing closed-form travel choice models that also focus on addressing the heterogeneity issues. Section 4.4 investigates the empirical performance of the proposed model. Finally, Section 4.5 concludes the chapter, discusses potential applications of the proposed model, and provides some directions for future research.

4.2 Problem statement

To facilitate the presentation of the essential ideas, the notations used are listed in Section 4.2.1. Recker's (1995) logit choice model with an oddball alternative is then introduced in Section 4.2.2, together with a discussion on its properties and limitations.

4.2.1 Notations

Sets

A	Set of all travel alternatives
A-r	Set of conventional travel alternatives without the oddball alternative
I	Set of common attributes shared by all alternatives
J	Set of unique attributes of the oddball alternative
$\boldsymbol{\tau}_k$	Set of attribute levels of alternative k

Parameters and variables

γ	Euler's constant
$P(k\|A)$	Choice probability of alternative k in choice set A
$R_{MNL\text{-}O}$	Variance ratio of the MNL-O model
$R_{MNW\text{-}O}$	Variance ratio of the MNW-O model
$E_{\tau_k^i}^{P(k\|A)}$	Direct elasticity of alternative k with respect to attribute i
$E_{\tau_l^i}^{P(k\|A)}$	Cross elasticity of alternative k with respect to attribute i of alternative l
V_k	Total perceived utility/disutility of alternative k
$\overline{V}_r$	Perceived utility/disutility of the common attributes of oddball alternative r
$\tilde{V}_r$	Perceived utility/disutility of the unique attributes of oddball alternative r
v_k	Total system utility/disutility of alternative k
$\overline{v}_r$	System utility/disutility of the common attributes of oddball alternative r
$\tilde{v}_r$	System utility/disutility of the unique attributes of oddball alternative r
ε_k	Random error associated with the common attributes of alternative k
ξ_r	Random error associated with the unique attributes of oddball alternative r
τ_k^i	Level of attribute i of alternative k
$\overline{\tau}_k^i$	Level of common attribute i of alternative k
$\tilde{\tau}_r^j$	Level of unique attribute j of oddball alternative r
ω^i	Coefficient of attribute i
λ	Location parameter of the Weibull distribution
α_k	Scale parameter of the Weibull distribution of alternative k
β	Shape parameter of the Weibull distribution
η_k	Location parameter of the Gumbel distribution of alternative k
θ	Scale parameter of the Gumbel distribution

4.2.2 Basis for Recker's logit choice model with an oddball alternative

4.2.2.1 Additive perceived utility of oddball alternative

A homogeneous choice set *A* is assumed in the MNL model, in which each conventional alternative shares a common set of attributes $\overline{\boldsymbol{\tau}} = \left\{\overline{\tau}^1, \overline{\tau}^2, \ldots, \overline{\tau}^m\right\}$. Let $\boldsymbol{\tau}_{\mathbf{k}} = \overline{\boldsymbol{\tau}}_{\mathbf{k}} = \left\{\overline{\tau}_k^1, \overline{\tau}_k^2, \ldots, \overline{\tau}_k^m\right\}$ denote the level of attributes of the k^{th} alternative. Then, a linear-in-parameters specification is assumed for the deterministic utility of *k*: $v_k = \overline{v}_k = \sum_{i \in I} \omega^i \overline{\tau}_k^i$. The additive utility function of conventional alternative *k* is

$$V_k = v_k + \varepsilon_k, \forall k \in A, \tag{4.1}$$

where ε_k is the random error term that is assumed to be independently and identically distributed (IID) Gumbel variable with the same scale parameter θ, i.e., $\varepsilon_k \sim G\left(\eta_k, \theta\right)$.

However, not all alternatives necessarily share the same set of attributes. Recker (1995) further considered a single oddball alternative, which additionally possessed a unique set of attributes $\tilde{\boldsymbol{\tau}} = \left\{\tilde{\tau}^{m+1}, \tilde{\tau}^{m+2}, \ldots, \tilde{\tau}^n\right\}$ in addition to the common attributes $\overline{\boldsymbol{\tau}}$. Suppose that the r^{th} alternative is the oddball in the choice set. Then, let $\overline{v}_r = \sum_{i \in I} \omega^i \overline{\tau}_r^i$ and ε_r respectively denote the deterministic utility and random error that are associated with the common attributes of the oddball alternative. Let $\tilde{v}_r = \sum_{j \in J} \omega^j \tilde{\tau}_r^j$ and ξ_r respectively denote the deterministic utility and random error that are associated with its unique attributes. Hence, the additive utility function of the oddball alternative is

$$V_r = \overline{V}_r + \tilde{V}_r = \left(\overline{v}_r + \varepsilon_r\right) + \left(\tilde{v}_r + \xi_r\right). \tag{4.2}$$

By assuming ε_r and ξ_r are IID Gumbel variables, i.e., $\varepsilon_r \sim G\left(\eta_{r1}, \theta\right)$ and $\xi_r \sim G\left(\eta_{r2}, \theta\right)$ (Recker, 1995), the oddball alternative differs from conventional alternatives in that its random error term is a summation of two IID Gumbel variables.

4.2.2.2 Formulation of logit choice model with an oddball alternative

Based on the additive utility function and distributional assumptions given in Section 4.2.2.1, the MNL-O model can be developed. Letting $v_r = \overline{v}_r + \tilde{v}_r$ denote the total deterministic utility and setting $\theta = 1$, the choice probabilities of the oddball and conventional alternatives can be derived as follows (Recker, 1995):

$$\begin{aligned} P_{MNL-O}\left(k\middle|A\right) &= \frac{e^{v_k+\eta_k}}{\sum_{l\neq r\in A} e^{v_l+\eta_l}} \cdot \left[1-\phi_r^L \cdot e^{\phi_r^L} \cdot E_1\left(\phi_r^L\right)\right] \\ &= P_{MNL}\left(k\middle|A-r\right) \cdot \left[1-\phi_r^L \cdot e^{\phi_r^L} \cdot E_1\left(\phi_r^L\right)\right], \forall k \neq r \in A \end{aligned} \quad , \tag{4.3}$$

$$P_{MNL-O}\left(r\middle|A\right) = \phi_r^L \cdot e^{\phi_r^L} \cdot E_1\left(\phi_r^L\right), \tag{4.4}$$

where $\phi_r^L = \frac{e^{v_r+\eta_{r1}+\eta_{r2}}}{\sum_{l\neq r\in A} e^{v_l+\eta_l}}$. $E_1\left(x\right) = \int_x^{+\infty} \frac{e^{-x}}{x} dx$ is the exponential integral, the value of which has already been tabulated (Harris, 1957).

4.2.2.3 Properties and limitations of the logit-based approach

The MNL-O model is demonstrated in Figure 4.1 via a comparison with the basic MNL model. The MNL-O model tends to estimate a higher choice probability of the oddball alternative, while the MNL model always results in a higher choice probability for a conventional alternative (Recker, 1995). In addition, Eqs. (4.3) and (4.4) clearly show that the independence from irrelevant alternatives (IIA) property no longer holds for the oddball alternative in the MNL-O model. Instead, the IIA property only remains within the subset of conventional alternatives in the MNL-O model.

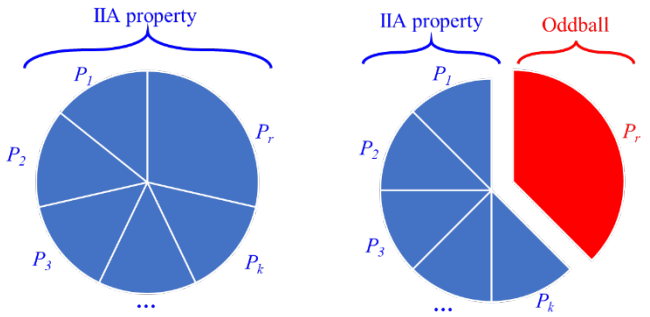

(a) MNL model (b) MNL-O model

Figure 4.1. Oddball choice probability derived from different models.

Figure 4.2 illustrates the different ways to consider an oddball alternative in the MNL and MNL-O models. As shown in Figure 4.2(a), the MNL model treats the oddball alternative in the same way as conventional alternatives. Because of the IID assumption and the properties of the Gumbel distribution, the MNL model has a fixed perception variance of $\pi^2/6\theta^2$ for all alternatives given the scale parameter θ. By comparison, the MNL-O model associates the oddball alternative with an additional random error term, which implies a higher uncertainty owing to the unique attributes that distinguishes the oddball alternative from conventional alternatives (Figure 4.2(b)). Because the random errors of common and unique attributes are assumed to be IID Gumbel variables (Recker, 1995), the variance of the oddball alternative is

$$D_{MNL-O}(V_r) = D(\bar{V}_r + \tilde{V}_r) = D(\bar{V}_r) + D(\tilde{V}_r) = \pi^2/6\theta^2 + \pi^2/6\theta^2 = \pi^2/3\theta^2 . \quad (4.5)$$

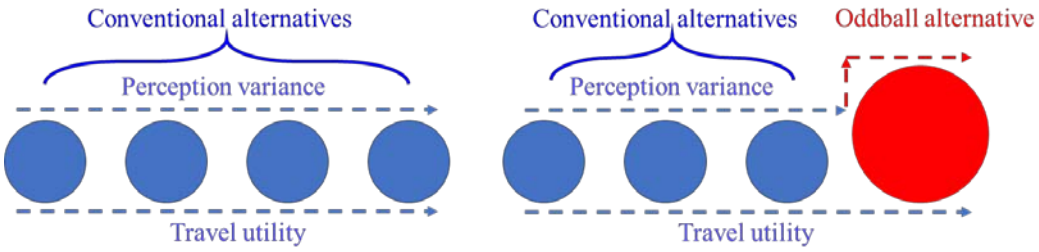

(a) MNL model (b) MNL-O model

Figure 4.2. Choice sets considered in different logit-based models.

Remark. In the MNL-O model, the assumption of identical variance remains within the subset of conventional alternatives. Although a different variance is assumed for the oddball alternative, it is still fixed and independent of the common and unique features. This leads to a fixed variance ratio between oddball and conventional alternatives:

$$R_{MNL-O} = \frac{\pi^2/3\theta^2}{\pi^2/6\theta^2} = 2\,. \tag{4.6}$$

In summary, despite its ability to specifically handle the oddball alternative, the MNL-O model still inherits some limitations from the MNL model. First, the identical and fixed perception variance among conventional alternatives is inadequate for modeling the heterogeneity issue among alternatives with distinct scales of utility. Second, the fixed variance ratio may not fully capture the different contributions of common and unique features to the choice of an oddball alternative. Third, the issues discussed above result in a choice probability function dependent on absolute utility differences, which might generate unrealistic travel choice probabilities when applied to transportation networks with distinct trips lengths or service levels (Kitthamkesorn and Chen, 2013).

4.3 Weibit-based model for assessing travel choice with an oddball alternative

This chapter proposes a closed-form weibit-based model to explicitly address the inherent heterogeneity issues in the MNL-O model. In contrast to the additive utility assumed in the logit-based models, the weibit-based model adopts a multiplicative form of disutility function (Fosgerau and Bierlaire, 2009). Taking the basic multinomial weibit (MNW) model as an example, the random perceived disutility can be expressed by the multiplication of the deterministic disutility v_k and the random error ε_k:

$$V_k = v_k \cdot \varepsilon_k, \forall k \in A. \tag{4.7}$$

The random errors are assumed IID Weibull variables with the same parameter, i.e., $\varepsilon_k \sim W(\alpha_k, \beta)$. α_k, and β are scale and shape parameters of the Weibull distribution.

Thus, the properties of the Weibull distribution enable the MNW model to inherently address the heterogeneity issue by allowing disutility-dependent perception variances (Castillo et al., 2008). As shown in Figure 4.3(a), the perception variance of each alternative is proportional to its squared mean disutility. However, the identical proportionality between variance and squared mean disutility is unsuitable for distinguishing the oddball alternative from conventional alternatives. To address this issue, a multinomial weibit model with an oddball alternative (MNW-O) is developed in Section 4.3.1 to account for the oddball alternative's unique features with a distinct proportionality between variance and mean disutility (as shown in Figure 4.3(b)).

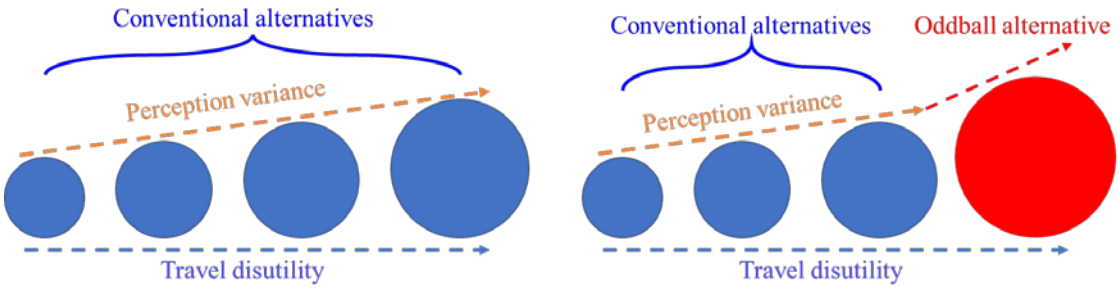

(a) MNW model (b) MNW-O model

Figure 4.3. Choice set considered in different weibit-based models.

4.3.1 Model formulation

Consistent with the MNW model, the proposed MNW-O model is also based on a multiplicative specification of disutility perception. The conventional alternatives share the same disutility function with the MNW model, as given in Eq. (4.7), while the disutility function of the oddball alternative additionally includes the perceived disutility of its unique features, which is expressed as

$$V_r = \overline{V}_r \cdot \tilde{V}_r = \left(\overline{v}_r \cdot \varepsilon_r\right) \cdot \left(\tilde{v}_r \cdot \xi_r\right), \tag{4.8}$$

where $\overline{v}_r$ and ε_r respectively denote the deterministic disutility and random error that are associated with the common attributes of the oddball alternative, and $\tilde{v}_r$ and ξ_r

respectively denote the deterministic disutility and random error that are associated with its unique attributes. Following the principle of disutility minimization, the MNW-O choice probability of a conventional or oddball alternative is equivalent to the probability that the chosen alternative has lower disutility than all other alternatives, which can be expressed as

$$\begin{aligned} P_{MNW-O}\left(k\middle|A\right) &= P\left(v_k\cdot\varepsilon_k \le v_l\cdot\varepsilon_l, \forall l\ne k, r\in A; v_k\cdot\varepsilon_k \le v_r\cdot\varepsilon_r\cdot\xi_r\right) \\ &= P\left(\varepsilon_l \ge \frac{v_k\cdot\varepsilon_k}{v_l}, \forall l\ne k, r\in A; \varepsilon_r \ge \frac{v_k\cdot\varepsilon_k}{v_r\cdot\xi_r}\right) \end{aligned}, \tag{4.9}$$

$$\begin{aligned} P_{MNW-O}\left(r\middle|A\right) &= P\left(v_r\cdot\varepsilon_r\cdot\xi_r \le v_k\cdot\varepsilon_k, \forall k\ne r\in A\right) \\ &= P\left(\varepsilon_k \ge \frac{v_r\cdot\varepsilon_r\cdot\xi_r}{v_k}, \forall k\ne r\in A\right) \end{aligned}, \tag{4.10}$$

where $v_r = \overline{v}_r\cdot\tilde{v}_r$ denotes the total system disutility of the oddball alternative *r*. The random errors, including ε_k, ε_r, and ξ_r, are assumed to be IID Weibull variables with the same shape parameter, β : $\varepsilon_k \sim W\left(0,\alpha_k,\beta\right)$, $\varepsilon_r \sim W\left(0,\alpha_{r1},\beta\right)$, and $\xi_r \sim W\left(0,\alpha_{r2},\beta\right)$. Thus, by defining $\phi_r^W = \frac{\left(v_r\cdot\alpha_{r1}\cdot\alpha_{r2}\right)^{-\beta}}{\sum_{l\ne r\in A}\left(v_l\cdot\alpha_l\right)^{-\beta}}$, the following two propositions are reached.

Proposition 4.1. The choice probability of conventional alternative *k* from the MNW-O model is:

$$\begin{aligned} P_{MNW-O}\left(k\middle|A\right) &= \frac{\left(v_k\cdot\alpha_k\right)^{-\beta}}{\sum_{l\ne r\in A}\left(v_l\cdot\alpha_l\right)^{-\beta}}\cdot\left[1-\phi_r^W\cdot e^{\phi_r^W}\cdot E_1\left(\phi_r^W\right)\right] \\ &= P_{MNW}\left(k\middle|A-r\right)\cdot\left[1-\phi_r^W\cdot e^{\phi_r^W}\cdot E_1\left(\phi_r^W\right)\right], \forall k\ne r\in A \end{aligned}. \tag{4.11}$$

Proof. The MNW-O choice probability of conventional alternative *k* expressed in Eq. (4.9) can be derived as follows based on the independence assumption:

$$P(k|A)=\int_{-\infty}^{+\infty}\int_{-\infty}^{+\infty}\tilde{f}_r(\xi_r)\cdot f_k(\varepsilon_k)\cdot\prod_{l\neq k,r\in A}P\left(\varepsilon_l\geq\frac{v_k\cdot\varepsilon_k}{v_l}\right)\cdot P\left(\varepsilon_r\geq\frac{v_k\cdot\varepsilon_k}{v_r\cdot\xi_r}\right)d\varepsilon_k d\xi_r$$
$$=\int_{-\infty}^{+\infty}\int_{-\infty}^{+\infty}\tilde{f}_r(\xi_r)\cdot f_k(\varepsilon_k)\cdot\prod_{l\neq k,r\in A}\left[1-F_l\left(\frac{v_k\cdot\varepsilon_k}{v_l}\right)\right]\cdot\left[1-\bar{F}_r\left(\frac{v_k\cdot\varepsilon_k}{v_r\cdot\xi_r}\right)\right]d\varepsilon_k d\xi_r \quad (4.12)$$

where f_k and $\tilde{f}_r$, are the PDFs of ε_k and ξ_r, F_l and $\bar{F}_r$ are the CDFs of ε_l and ε_r. Based on the Weibull distributional assumption, $P(k|A)$ can be derived as

$$P(k|A)=\int_0^{+\infty}\frac{\beta}{\alpha_{r2}}\left(\frac{\xi_r}{\alpha_{r2}}\right)^{\beta-1}e^{-\left(\frac{\xi_r}{\alpha_{r2}}\right)^{\beta}}d\xi_r\int_0^{+\infty}\frac{\beta}{\alpha_k}\left(\frac{\varepsilon_k}{\alpha_k}\right)^{\beta-1}e^{-\left(\frac{\varepsilon_k}{\alpha_{r2}}\right)^{\beta}}\cdot e^{-\sum_{l\neq k,r\in A}\left(\frac{v_k\cdot\varepsilon_k}{v_l\cdot\alpha_l}\right)^{\beta}}\cdot e^{-\left(\frac{v_k\cdot\varepsilon_k}{v_r\cdot\xi_r\cdot\alpha_{r1}}\right)^{\beta}}d\varepsilon_k \quad (4.13)$$

The double integral in Eq. (4.13) can be evaluated sequentially based on the integration by substitution. Let $u=e^{-\left(\frac{\varepsilon_k}{\alpha_{r2}}\right)^{\beta}}$, we have

$$P(k|A)=\int_0^{+\infty}\frac{\beta}{\alpha_{r2}}\left(\frac{\xi_r}{\alpha_{r2}}\right)^{\beta-1}e^{-\left(\frac{\xi_r}{\alpha_{r2}}\right)^{\beta}}d\xi_r\int_0^1 u^{\sum_{l\neq k,r\in A}\left(\frac{v_k\cdot\varepsilon_k}{v_l\cdot\alpha_l}\right)^{\beta}}\cdot u^{\left(\frac{v_k\cdot\alpha_k}{v_r\cdot\xi_r\cdot\alpha_{r1}}\right)^{\beta}}du \quad (4.14)$$

Let $w=u^{1+\sum_{l\neq k,r\in A}\left(\frac{v_k\cdot\varepsilon_k}{v_l\cdot\alpha_l}\right)^{\beta}}=u^{\sum_{l\neq r\in A}\left(\frac{v_k\cdot\varepsilon_k}{v_l\cdot\alpha_l}\right)^{\beta}}$, we have

$$P(k|A)=\int_0^{+\infty}\frac{\beta}{\alpha_{r2}}\left(\frac{\xi_r}{\alpha_{r2}}\right)^{\beta-1}e^{-\left(\frac{\xi_r}{\alpha_{r2}}\right)^{\beta}}d\xi_r\int_0^1\frac{1}{\sum_{l\neq r\in A}\left(\frac{v_k\cdot\varepsilon_k}{v_l\cdot\alpha_l}\right)^{\beta}}\cdot w^{\frac{\left[(v_k\cdot\alpha_k)/(v_r\cdot\xi_r\cdot\alpha_{r1})\right]^{\beta}}{\sum_{l\neq r\in A}\left(\frac{v_k\cdot\varepsilon_k}{v_l\cdot\alpha_l}\right)^{\beta}}}dw$$
$$=\frac{(v_k\cdot\alpha_k)^{-\beta}}{\sum_{l\neq r\in A}(v_l\cdot\alpha_l)^{-\beta}}\cdot\int_0^{+\infty}\frac{\beta}{\alpha_{r2}}\left(\frac{\xi_r}{\alpha_{r2}}\right)^{\beta-1}e^{-\left(\frac{\xi_r}{\alpha_{r2}}\right)^{\beta}}\cdot\frac{1}{\frac{\left[(v_k\cdot\alpha_k)/(v_r\cdot\xi_r\cdot\alpha_{r1})\right]^{\beta}}{\sum_{l\neq r\in A}\left[(v_k\cdot\alpha_k)/(v_l\cdot\alpha_l)\right]^{\beta}}+1}d\xi_r$$
$$=\frac{(v_k\cdot\alpha_k)^{-\beta}}{\sum_{l\neq r\in A}(v_l\cdot\alpha_l)^{-\beta}}\cdot\int_0^{+\infty}\frac{\beta}{\alpha_{r2}}\left(\frac{\xi_r}{\alpha_{r2}}\right)^{\beta-1}e^{-\left(\frac{\xi_r}{\alpha_{r2}}\right)^{\beta}}\cdot\frac{\sum_{l\neq r\in A}(v_l\cdot\alpha_l)^{-\beta}}{(v_r\cdot\xi_r\cdot\alpha_{r1})^{-\beta}+\sum_{l\neq r\in A}(v_l\cdot\alpha_l)^{-\beta}}d\xi_r \quad (4.15)$$

Let $\phi_r^W = \frac{\left(v_r \cdot \alpha_{r1} \cdot \alpha_{r2}\right)^{-\beta}}{\sum_{l \neq r \in A} \left(v_l \cdot \alpha_l\right)^{-\beta}}$, with $\int_0^{+\infty} \frac{\beta}{\alpha_{r2}} \left(\frac{\xi_r}{\alpha_{r2}}\right)^{\beta-1} e^{-\left(\frac{\xi_r}{\alpha_{r2}}\right)^{\beta}} d\xi_r = 1$, Eq. (4.15) can be rewritten as

$$
\begin{aligned}
P\left(k \middle| A\right) &= \frac{\left(v_k \cdot \alpha_k\right)^{-\beta}}{\sum_{l \neq r \in A} \left(v_l \cdot \alpha_l\right)^{-\beta}} \cdot \int_0^{+\infty} \frac{\beta}{\alpha_{r2}} \left(\frac{\xi_r}{\alpha_{r2}}\right)^{\beta-1} e^{-\left(\frac{\xi_r}{\alpha_{r2}}\right)^{\beta}} \cdot \left[1 - \frac{\left(v_r \cdot \xi_r \cdot \alpha_{r1}\right)^{-\beta}}{\left(v_r \cdot \xi_r \cdot \alpha_{r1}\right)^{-\beta} + \sum_{l \neq r \in A} \left(v_l \cdot \alpha_l\right)^{-\beta}}\right] d\xi_r \\
&= \frac{\left(v_k \cdot \alpha_k\right)^{-\beta}}{\sum_{l \neq r \in A} \left(v_l \cdot \alpha_l\right)^{-\beta}} \cdot \left[1 - \int_0^{+\infty} \frac{\beta}{\alpha_{r2}} \left(\frac{\xi_r}{\alpha_{r2}}\right)^{\beta-1} e^{-\left(\frac{\xi_r}{\alpha_{r2}}\right)^{\beta}} \cdot \frac{\phi_r^W}{\phi_r^W + \left(\xi_r / \alpha_{r2}\right)^{\beta}} d\xi_r\right]
\end{aligned}
$$

(4.16)

Let $x = \phi_r^W + \left(\xi_r / \alpha_{r2}\right)^{\beta}$, then

$$
P\left(k \middle| A\right) = \frac{\left(v_k \cdot \alpha_k\right)^{-\beta}}{\sum_{l \neq r \in A} \left(v_l \cdot \alpha_l\right)^{-\beta}} \cdot \left[1 - \int_{\phi_r^W}^{+\infty} e^{-\left(x - \phi_r^W\right)} \cdot \frac{\phi_r^W}{x} dx\right]. \tag{4.17}
$$

Substituting $E_1\left(x\right) = \int_x^{+\infty} \frac{e^{-x}}{x} dx$ into Eq. (4.17) gives the MNW-O choice probability of the conventional alternative shown in Eq. (4.11). This completes the proof.

Proposition 4.2. The choice probability of oddball alternative *r* from the MNW-O model is

$$
P_{MNW-O}\left(r \middle| A\right) = \phi_r^W \cdot e^{\phi_r^W} \cdot E_1\left(\phi_r^W\right). \tag{4.18}
$$

Proof. Based on the independence assumption, the MNW-O choice probability of oddball alternative *r* expressed in Eq. (4.10) can be derived as follows:

$$
\begin{aligned}
P\left(r \middle| A\right) &= \int_{-\infty}^{+\infty} \int_{-\infty}^{+\infty} f_r\left(\varepsilon_r\right) \cdot \tilde{f}_r\left(\xi_r\right) \cdot \prod_{k \neq r \in A} P\left(\frac{v_r \cdot \varepsilon_r \cdot \xi_r}{v_k}\right) d\varepsilon_r d\xi_r \\
&= \int_{-\infty}^{+\infty} \int_{-\infty}^{+\infty} f_r\left(\varepsilon_r\right) \cdot \tilde{f}_r\left(\xi_r\right) \cdot \prod_{k \neq r \in A} \left[1 - F_k\left(\frac{v_r \cdot \varepsilon_r \cdot \xi_r}{v_k}\right)\right] d\varepsilon_r d\xi_r
\end{aligned} \tag{4.19}
$$

Based on the identically Weibull distributed assumption, $P(r|A)$ can be derived as

$$P(r|A)=\int_0^{+\infty}\frac{\beta}{\alpha_{r2}}\left(\frac{\xi_r}{\alpha_{r2}}\right)^{\beta-1}e^{-\left(\frac{\xi_r}{\alpha_{r2}}\right)^{\beta}}d\xi_r\int_0^{+\infty}\frac{\beta}{\alpha_{r1}}\left(\frac{\varepsilon_r}{\alpha_{r1}}\right)^{\beta-1}e^{-\left(\frac{\varepsilon_r}{\alpha_{r1}}\right)^{\beta}}\cdot e^{-\sum_{k\neq r\in A}\left(\frac{v_r\cdot\varepsilon_r\cdot\xi_r}{v_k\cdot\alpha_k}\right)^{\beta}}d\varepsilon_r\,. \quad (4.20)$$

Let $u=e^{-\varepsilon_r/\alpha_{r1}}$, Eq. (4.20) can be written as

$$\begin{aligned}P(r|A)&=\int_0^{+\infty}\frac{\beta}{\alpha_{r2}}\left(\frac{\xi_r}{\alpha_{r2}}\right)^{\beta-1}e^{-\left(\frac{\xi_r}{\alpha_{r2}}\right)^{\beta}}d\xi_r\int_0^1 u^{\sum_{k\neq r\in A}\left(\frac{v_r\cdot\xi_r\cdot\alpha_{r1}}{v_k\cdot\alpha_k}\right)^{\beta}}du\\&=\int_0^{+\infty}\frac{\beta}{\alpha_{r2}}\left(\frac{\xi_r}{\alpha_{r2}}\right)^{\beta-1}e^{-\left(\frac{\xi_r}{\alpha_{r2}}\right)^{\beta}}\frac{1}{1+\sum_{k\neq r\in A}\left(\frac{v_r\cdot\xi_r\cdot\alpha_{r1}}{v_k\cdot\alpha_k}\right)^{\beta}}d\xi_r\,.\end{aligned} \quad (4.21)$$

Let $w=1+\sum_{k\neq r\in A}\left(\frac{v_r\cdot\xi_r\cdot\alpha_{r1}}{v_k\cdot\alpha_k}\right)^{\beta}=1+\frac{\sum_{k\neq r\in A}\left(v_k\cdot\alpha_k\right)^{-\beta}}{\left(v_r\cdot\alpha_{r1}\cdot\alpha_{r2}\right)^{-\beta}}\cdot\left(\frac{\xi_r}{\alpha_{r2}}\right)^{\beta}$, Eq. (4.21) can be written as

$$P(r|A)=\frac{\left(v_r\cdot\alpha_{r1}\cdot\alpha_{r2}\right)^{-\beta}}{\sum_{k\neq r\in A}\left(v_k\cdot\alpha_k\right)^{-\beta}}\cdot\int_1^{+\infty}\frac{e^{-(w-1)\cdot\frac{\left(v_r\cdot\alpha_{r1}\cdot\alpha_{r2}\right)^{-\beta}}{\sum_{k\neq r\in A}\left(v_k\cdot\alpha_k\right)^{-\beta}}}}{w}dw\,. \quad (4.22)$$

With $E_1(\mu)=\int_1^{+\infty}\frac{e^{-\mu\cdot x}}{x}dx$ (Gradshteyn and Ryzhik, 2007), substituting $\phi_r^W=\frac{\left(v_r\cdot\alpha_{r1}\cdot\alpha_{r2}\right)^{-\beta}}{\sum_{l\neq r\in A}\left(v_l\cdot\alpha_l\right)^{-\beta}}$ into Eq. (4.22) gives the MNW-O choice probability of the oddball alternative in Eq. (4.18). This completes the proof.

Thus, Eqs. (4.11) and (4.18) demonstrate that the MNW-O choice probabilities have a similar form to probabilities of the MNL-O model given in Eqs. (4.3) and (4.4), which enables the proposed MNW-O model to address the oddball effect. The difference lies in the expression of term ϕ_r. The ϕ_r^L in the MNL-O model is dependent

on an exponential function, which implies an absolute difference–based choice probability expression. By comparison, the MNW-O model adopts a power function–based ϕ_r^W, implying that the MNW-O choice probability is dependent on the relative differences of travel disutility. This difference suggests that the MNW-O model inherits its ability to consider the heterogeneity issue from the MNW model (Kitthamkesorn and Chen, 2013). This property is discussed in detail in Section 4.3.2.

4.3.2 Model properties

This section discusses the properties of the proposed MNW-O model. First, the properties inherited from the MNL-O model are discussed, i.e., the logical consistency conditions and asymptotic values, in Section 4.3.2.1. Then, the perception variance of the conventional and oddball alternatives in the proposed MNW-O model are provided in Section 4.3.2.2. Finally, the theoretical advantages the proposed model gains from the properties of weibit-based models are discussed in Sections 4.3.2.3 to 4.3.2.5, including its more flexible perception variances, its ability to consider the heterogeneity issue, and its disutility-dependent model elasticities.

4.3.2.1 Logical consistency conditions and asymptotic values

This section shows the proposed MNW-O model has similar logical consistency and asymptotic properties to the MNL-O model. The exponential integral incorporated in the choice probability expression is known to have the following limits:

$$\lim_{x\to+\infty} E_1(x) = \frac{e^{-x}}{x}, \tag{4.23}$$

$$\lim_{x\to 0} E_1(x) = -\gamma - \ln x, \tag{4.24}$$

where γ is Euler's constant. Clearly, the MNW-O model can satisfy the logical consistency conditions for discrete choice models, i.e., for every alternative *k*,

$0 \le P_{MNW-O}\left(k\middle|A\right) \le 1$ and $\sum_{k\in A} P_{MNW-O}\left(k\middle|A\right) = 1$. The MNW-O choice probabilities of the oddball alternative are further derived at asymptotic values in two important cases.

Case 1. Disutility of oddball alternative approaches zero: $v_r \to 0^+$

In this case, the oddball alternative is extremely superior with negligible travel disutility. Because $\lim_{v_r\to 0^+} \phi_r^w \to +\infty$, the choice probability of the oddball alternative is

$$\lim_{v_r\to 0^+} P_{MNW-O}\left(r\middle|A\right) = \lim_{\phi_r^w\to+\infty} \phi_r^w \cdot e^{\phi_r^w} \cdot \frac{e^{-\phi_r^w}}{\phi_r^w} = 1, \tag{4.25}$$

and the choice probabilities of the conventional alternatives are

$$\lim_{v_r\to 0^+} P\left(k\middle|A\right) = \lim_{\phi_r^w\to+\infty} \frac{\left(v_k\cdot\alpha_k\right)^{-\beta}}{\sum_{l\ne r\in A}\left(v_l\cdot\alpha_l\right)^{-\beta}} \cdot \left(1-\phi_r^w\cdot e^{\phi_r^w}\cdot\frac{e^{-\phi_r^w}}{\phi_r^w}\right) = 0. \tag{4.26}$$

In this case, the choice probability of the oddball alternative approaches one, which is consistent with the conventional discrete choice models when there is an alternative dominating the choice set with extremely high utility/low disutility.

Case 2. Disutility of oddball alternative approaches infinity: $v_r \to +\infty$

When the oddball alternative is extremely inferior with high disutility, i.e., $v_r \to +\infty$, then $\lim_{v_r+\infty} \phi_r^w \to 0^+$ and the choice probability of the oddball alternative becomes

$$\lim_{v_r\to+\infty} P_{MNW-O}\left(r\middle|A\right) = \lim_{\phi_r^w\to 0^+} \phi_r^w \cdot e^{\phi_r^w} \cdot \left(-\gamma - \ln\phi_r^w\right) = 0, \tag{4.27}$$

and the choice probability of conventional alternative is

$$\lim_{v_r \to +\infty} P_{MNW-O}\left(k \middle| A\right) = \lim_{\phi_r^w \to 0^+} \frac{\left(v_k \cdot \alpha_k\right)^{-\beta}}{\sum_{l \neq r \in A} \left(v_l \cdot \alpha_l\right)^{-\beta}} \cdot \left[1 - \phi_r^w \cdot e^{\phi_r^w} \cdot \left(-\gamma - \ln \phi_r^w\right)\right] = \frac{\left(v_k \cdot \alpha_k\right)^{-\beta}}{\sum_{l \neq r \in A} \left(v_l \cdot \alpha_l\right)^{-\beta}} \quad . \quad (4.28)$$

In this case, because the IIA property is held within the set of conventional alternatives, the MNW-O model degenerates to the MNW model when the oddball alternative has extremely high disutility and negligible choice probability.

4.3.2.2 Perception variances

This section provides the perception variance of conventional and oddball alternatives in the proposed MNW-O model. The conventional alternatives in the MNW-O model share the same form of variance as in the MNW model, which can be expressed as

$$D\left(V_k\right) = E^2\left(V_k\right) \cdot \left[\kappa\left(\beta\right) - 1\right], \quad (4.29)$$

where $E\left(V_k\right)$ denotes the mean disutility and $\kappa\left(\beta\right) = \frac{\Gamma\left(1 + 2/\beta\right)}{\Gamma^2\left(1 + 1/\beta\right)}$.

Remark. The variance of the conventional alternative is proportional to the squared mean disutility. The proportionality is $\kappa\left(\beta\right) - 1$, which is dependent on the shape parameter β and remains the same for all the conventional alternatives.

Proposition 4.3. The perception variance of the oddball alternative in the MNW-O model is proportional to the squared mean disutility of both its common and unique features. The proportionality is dependent on the shape parameter β and differs from the proportionality of conventional alternatives.

Proof. The perception variance of the oddball alternative can be expressed as

$$
\begin{aligned}
D_{MNW-O}\left(V_r\right) &= D\left(\overline{V}_r \cdot \tilde{V}_r\right) \\
&= E\left\{\left[\left(\overline{V}_r \cdot \tilde{V}_r\right) - E\left(\overline{V}_r \cdot \tilde{V}_r\right)\right]^2\right\}.
\end{aligned} \tag{4.30}
$$

With the independence assumption, Eq. (4.30) becomes

$$
\begin{aligned}
D_{MNW-O}\left(V_r\right) &= E\left(\overline{V}_r^2 \cdot \tilde{V}_r^2\right) - E^2\left(\overline{V}_r \cdot \tilde{V}_r\right) \\
&= E\left(\overline{V}_r^2\right) \cdot E\left(\tilde{V}_r^2\right) - E^2\left(\overline{V}_r\right) \cdot E^2\left(\tilde{V}_r\right) \\
&= \left[D\left(\overline{V}_r\right) + E^2\left(\overline{V}_r\right)\right] \cdot \left[D\left(\tilde{V}_r\right) + E^2\left(\tilde{V}_r\right)\right] - E^2\left(\overline{V}_r\right) \cdot E^2\left(\tilde{V}_r\right)
\end{aligned} \tag{4.31}
$$

Substituting Eq. (4.29) into Eq. (4.31),

$$
\begin{aligned}
D_{MNW-O}\left(V_r\right) &= \left[E^2\left(\overline{V}_r\right) \cdot \kappa\left(\beta\right)\right] \cdot \left[E^2\left(\tilde{V}_r\right) \cdot \kappa\left(\beta\right)\right] - E^2\left(\overline{V}_r\right) \cdot E^2\left(\tilde{V}_r\right) \\
&= E^2\left(\overline{V}_r\right) \cdot E^2\left(\tilde{V}_r\right) \cdot \left[\kappa^2\left(\beta\right) - 1\right] \\
&= E^2\left(V_r\right) \cdot \left[\kappa^2\left(\beta\right) - 1\right]
\end{aligned} \tag{4.32}
$$

Thus, the variance of the oddball alternative is a function of both the shape parameter and the mean disutility, and the proportionalities of the oddball and conventional alternatives are different, i.e., $\kappa^2\left(\beta\right) - 1 \neq \kappa\left(\beta\right) - 1$.

Proposition 4.4. The variance ratio between the oddball and conventional alternatives in the MNW-O model is flexible. The variance ratio is no lower than two when the oddball and conventional alternatives have the same mean disutility.

Proof. The variance ratio between the oddball and conventional alternatives in the MNW-O model is

$$
R_{MNW-O} = \frac{E^2\left(V_r\right) \cdot \left[\kappa^2\left(\beta\right) - 1\right]}{E^2\left(V_k\right) \cdot \left[\kappa\left(\beta\right) - 1\right]}. \tag{4.33}
$$

$R_{MNW\text{-}O}$ is therefore flexible, which is dependent on both the squared mean disutility of oddball and conventional alternatives and the shape parameter, β. Then, the variance

ratio is derived with the same mean disutility. By definition, β is positive, hence $\Gamma\left(1+2/\beta\right)>0$ and $\Gamma\left(1+1/\beta\right)>0$. Therefore,

$$\frac{d\kappa\left(\beta\right)}{d\beta}=\frac{2}{\beta^2}\cdot\frac{\Gamma\left(1+2/\beta\right)}{\Gamma^2\left(1+1/\beta\right)}\cdot\left[\psi\left(1+1/\beta\right)-\psi\left(1+2/\beta\right)\right]<0, \tag{4.34}$$

where $\psi\left(x\right)=\dfrac{\Gamma'\left(x\right)}{\Gamma\left(x\right)}$ is the digamma function. Thus, when $\beta>0$, $\kappa\left(\beta\right)$ is a decreasing function with respect to β. The asymptotic value of $\kappa\left(\beta\right)$ is

$$\lim_{\beta\to+\infty}\kappa\left(\beta\right)=\lim_{\beta\to+\infty}\frac{\Gamma\left(1+2/\beta\right)}{\Gamma^2\left(1+1/\beta\right)}=1. \tag{4.35}$$

Therefore, $\kappa\left(\beta\right)\geq 1$ within the domain of β. The variance ratio between the oddball and conventional alternatives with the same mean disutility is

$$R_{MNW-O}=\frac{\kappa^2\left(\beta\right)-1}{\kappa\left(\beta\right)-1}=\kappa\left(\beta\right)+1, \tag{4.36}$$

which is no lower than two, completing the proof.

The higher variance ratio between the oddball and conventional alternatives indicates that the oddball alternative is considered to have a higher uncertainty than conventional alternatives. Proposition 4.4 reveals that the proposed MNW-O model provides a disutility-dependent variance ratio, which highlights the heterogeneous perceptions of the common and unique features and is more realistic than the fixed variance ratio provided by the MNL-O model. When the oddball and conventional alternatives have the same disutility, the variance ratio in the MNW-O model decreases with the increase of β. This property is also intuitive, as a larger value of β can be interpreted as better knowledge of the transportation system, which reduces uncertainty.

4.3.2.3 Demonstration of the heterogeneous perception variances

This section demonstrates the disutility-dependent perception variances and non-identical variance ratio provided in Propositions 4.3 and 4.4. The effects these properties have on handling the heterogeneity issue in choice modeling is then illustrated for networks with different scales of travel disutility.

(1) Demonstration of perception variances with respect to alternative disutility

Figure 4.4 shows an example of the perception variance of an oddball alternative with respect to travel disutility in the MNL, MNL-O, MNW and MNW-O models. The following properties can be observed from Figure 4.4:

(a) Given the scale parameter θ, constant and utility-independent perception variances are used in the logit-based models, which indicates its inability to reflect the heterogeneous perceptions of utility for different alternatives or attributes.

(b) By contrast, the weibit-based models have disutility-dependent perception variances. Specifically, in the MNW-O model, the oddball alternative has a different variance to the conventional ones, implying that the MNW-O model can consider the heterogeneities with respect to these alternatives in different ways.

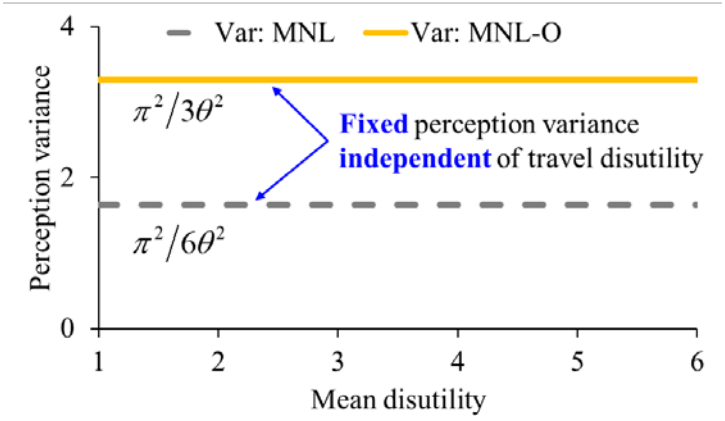

(a) Logit-based models with $\theta = 1$

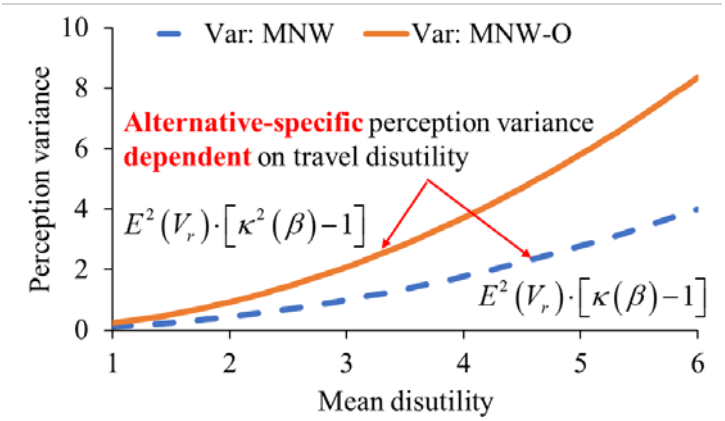

(b) Weibit-based models with $\beta = 3.7$

Figure 4.4. Perception variance of the oddball alternative with respect to its mean disutility in different models.

(2) Demonstration of perception variances with respect to the shape parameter

Figure 4.5 further explores the perception variance with respect to the shape parameter in weibit-based models and the variance ratio between oddball and conventional alternatives in the MNW-O model. Two conclusions can be drawn from Figure 4.5:

(a) With the same disutility, the perception variance of an oddball alternative is always larger in the MNW-O model than in the MNW model. This indicates the MNW-O model considers the oddball alternative to have higher uncertainty than conventional alternatives, which is consistent with the feature of the MNL-O model.

(b) An increasing shape parameter, β, causes the perception variances of the oddball alternatives in both models and the variance ratio in the MNW-O model to decrease. When $\beta \to +\infty$, the variance ratio between the oddball and conventional alternatives approaches two, which is the variance ratio in the MNL-O model. The variances of both the MNW and MNW-O models approach zero with $\beta \to +\infty$, implying that when travelers have perfect knowledge of all travel alternatives then they deterministically choose the alternative with the lowest disutility.

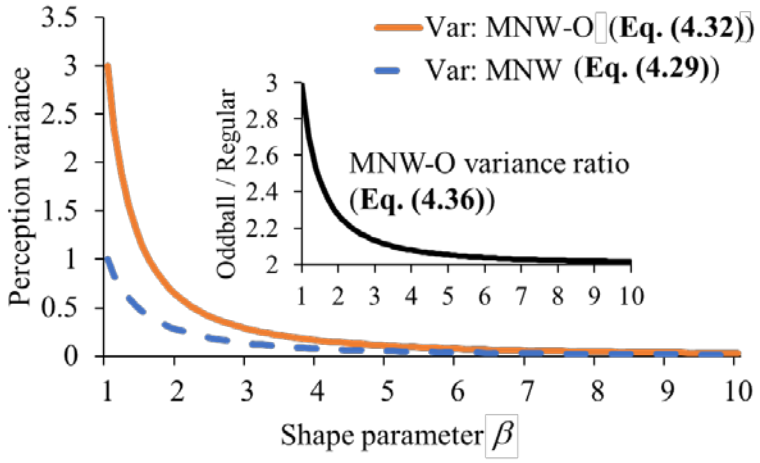

Figure 4.5. Perception variance of the oddball alternative with respect to the shape parameter in different models.

(3) Effect of considering the heterogeneity issue

Based on the non-identical perception variances and flexible variance ratio given in Propositions 4.3 and 4.4, the MNW-O model inherits the ability to consider the heterogeneity issue from the MNW model and could outperform the MNL-O model in networks with distinct scales of travel disutility. Consider a trinomial choice problem with two conventional alternatives that have the same disutility v_k, and one oddball alternative with disutility v_r. Then, assume a constant disutility difference between the conventional and oddball alternatives: $v_r = v_k - 5$. Figure 4.6 shows the evolution of the oddball choice probabilities derived from different models with v_r varying from 0 to 100, leading to the following observations:

(a) The MNL-O model provides a constant choice probability for varying scales of disutility, which can be attributed to its absolute difference-dependent choice probability function. This result seems unrealistic in this case because the constant difference between the oddball and conventional alternatives should become increasingly negligible when the scale of disutility becomes larger.

(b) The weibit models can indicate the effect of variation in the disutility scale via their variation in choice probability. This property makes the MNW-O model provide more realistic outcomes than the MNL-O model, which is consistent with the difference identified between MNW and MNL models in short and long networks

(Kitthamkesorn and Chen, 2013).

(c) Given the same system disutility, the MNW-O model tends to calculate a higher oddball choice probability than the MNW model, which is consistent with the difference between MNL-O and MNL models (Recker, 1995).

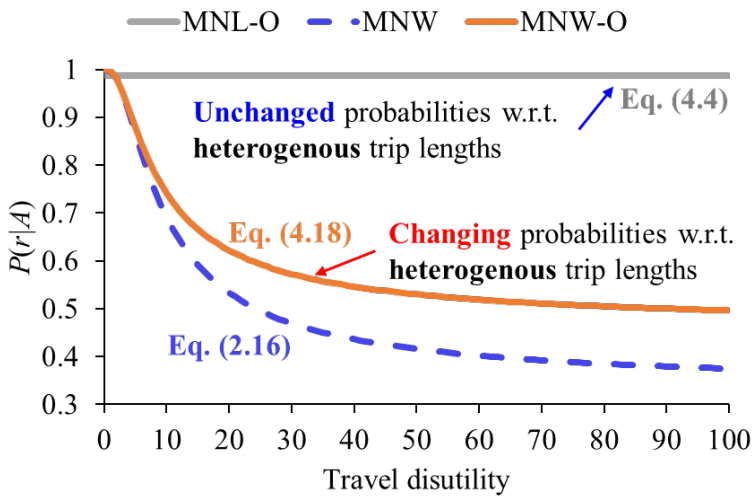

Figure 4.6. Effect of heterogeneity on oddball choice probability.

4.3.2.4 Model elasticities

This section compares the elasticities of the proposed model with related models, including the MNL, MNL-O, and MNW models. The direct elasticity of $P\left(k\middle|A\right)$ with respect to attribute *i* of alternative *k* can be expressed as

$$E_{\tau_k^i}^{P(k|A)} = \frac{\partial P\left(k\middle|A\right)}{\partial \tau_k^i} \cdot \frac{\tau_k^i}{P\left(k\middle|A\right)}, \forall \tau_k^i \in \boldsymbol{\tau}_\mathbf{k}, k \in A. \tag{4.37}$$

The cross elasticity of alternative *k* with respect to attribute *i* of alternative *l* is

$$E_{\tau_l^i}^{P(k|A)} \frac{\partial P\left(l\middle|A\right)}{\partial \tau_l^i} \cdot \frac{\tau_l^i}{P\left(l\middle|A\right)}, \forall \tau_k^i \in \boldsymbol{\tau}_\mathbf{k}, k, l \in A. \tag{4.38}$$

With $\frac{dE_1\left(x\right)}{dx} = -\frac{e^{-x}}{x}$, the direct and cross elasticities are derived for the MNL-O and MNW-O models that involve the exponential integral in their choice probability

functions. Because of the different probability expressions, the direct and cross elasticities with respect to conventional and oddball alternatives are derived separately.

Table 4.1 compares the direct and cross elasticities of the MNL, MNL-O, MNW, and MNW-O models, highlighting the following properties:

(a) Analogous to the elasticities of the MNW model (Table 2.3), the elasticities of the MNW-O model are also dependent on the alternative disutility. This property makes an alternative with higher disutility less sensitive to an equivalent perturbation than alternatives with lower disutility, which indicates the ability of the MNW-O model to account for the heterogeneity issues, as discussed in Section 3.2.3. Moreover, the elasticities of both the MNW and MNW-O models share the opposite signs to their logit-based counterparts. This is because the term *v* denotes utility in logit-based models, whereas it denotes disutility in weibit-based models.

(b) Both the direct and cross elasticities of the MNW-O model involve terms related to the oddball alternative *r*. This indicates that the effects of an oddball alternative on the choice probabilities are specifically considered in the MNW-O model. By contrast, the MNL and MNW models do not make this distinction and only account for conventional alternatives.

(c) In the MNL and MNW models, the cross elasticities for all alternatives *k* with respect to a change in alternative *l* remain constant, implying that the IIA property holds for all alternatives in the choice set. By comparison, the MNL-O and MNW-O models possess different cross elasticities when the oddball alternative *r* is involved, i.e., $E_{\tau_l^i}^{P(r|A)}$ differs from $E_{\tau_l^i}^{P(k|A)}$ and is dependent on a term related to oddball alternative *r*. This indicates that the IIA property is circumvented between the oddball and conventional alternatives.

Table 4.1. Comparison of direct and cross elasticities of MNL, MNW, MNL-O, and MNW-O models

Model	Direct elasticity	Cross elasticity
MNL	$\theta \cdot \omega^i \tau_k^i \cdot \left[1 - P_{MNL}\left(k \middle| A\right)\right]$	$-\theta \cdot \omega^i \tau_l^i \cdot P_{MNL}\left(l \middle| A\right)$
MNW	$-\left(\nu_k\right)^{-1} \cdot \beta \omega^i \tau_k^i \cdot \left[1 - P_{MNW}\left(k \middle| A\right)\right]$	$\left(\nu_l\right)^{-1} \cdot \beta \cdot \omega^i \tau_l^i \cdot P_{MNW}\left(l \middle| A\right)$
MNL-O	Direct elasticity of conventional alternative k, $E_{\tau_k^i}^{P(k\|A)}$: $\theta \cdot \omega^i \tau_k^i \cdot \left\{1 - P_{MNL}\left(k \middle| A - r\right) \cdot \left[\left(1 + \phi_r^L\right) - \frac{P_{MNL-O}\left(r \middle| A\right)}{1 - P_{MNL-O}\left(r \middle| A\right)}\right]\right\}$ Direct elasticity of oddball alternative r, $E_{\tau_r^i}^{P(r\|A)}$: $\theta \cdot \omega^i \tau_r^i \cdot \left[\left(1 + \phi_r^L\right) - \frac{\phi_r^L}{P_{MNL-O}\left(r \middle| A\right)}\right]$	Cross elasticity of conventional alternative k with respect to attribute i of conventional alternative l, $E_{\tau_l^i}^{P(k\|A)}$: $-\theta \cdot \omega^i \tau_l^i \cdot P_{MNL}\left(l \middle| A - r\right) \cdot \left[\left(1 + \phi_r^L\right) - \frac{P_{MNL-O}\left(r \middle| A\right)}{1 - P_{MNL-O}\left(r \middle| A\right)}\right]$ Cross elasticity of conventional alternative k with respect to attribute i of oddball alternative r, $E_{\tau_r^i}^{P(k\|A)}$: $\theta \cdot \omega^i \tau_r^i \cdot \left[\phi_r^L - \frac{P_{MNL-O}\left(r \middle| A\right)}{1 - P_{MNL-O}\left(r \middle| A\right)}\right]$ Cross elasticity of oddball alternative r with respect to attribute i of conventional alternative l, $E_{\tau_l^i}^{P(r\|A)}$: $-\theta \cdot \omega^i \tau_l^i \cdot P_{MNL}\left(l \middle| A - r\right) \cdot \left[\left(1 + \phi_r^L\right) - \frac{\phi_r^L}{P_{MNL-O}\left(r \middle| A\right)}\right]$

MNW-O	Direct elasticity of conventional alternative k, $E_{\tau_k^i}^{P(k\|A)}$: $-(v_k)^{-1}\cdot\beta\cdot\omega^i\tau_k^i\cdot\left\{1-P_{MNW}(k\|A-r)\cdot\left[(1+\phi_r^W)-\frac{P_{MNW-O}(r\|A)}{1-P_{MNW-O}(r\|A)}\right]\right\}$ Direct elasticity of oddball alternative r, $E_{\tau_r^i}^{P(r\|A)}$: $-(v_r)^{-1}\cdot\beta\cdot\omega^i\tau_r^i\cdot\left[(1+\phi_r^W)-\frac{\phi_r^W}{P_{MNW-O}(r\|A)}\right]$	Cross elasticity of conventional alternative k with respect to attribute i of conventional alternative l, $E_{\tau_l^i}^{P(k\|A)}$: $(v_l)^{-1}\cdot\beta\cdot\omega^i\tau_l^i\cdot P_{MNW}(l\|A-r)\cdot\left[(1+\phi_r^W)-\frac{P_{MNW-O}(r\|A)}{1-P_{MNW-O}(r\|A)}\right]$ Cross elasticity of conventional alternative k with respect to attribute i of oddball alternative r, $E_{\tau_r^i}^{P(k\|A)}$: $-(v_r)^{-1}\cdot\beta\cdot\omega^i\tau_r^i\cdot\left[\phi_r^W-\frac{P_{MNW-O}(r\|A)}{1-P_{MNW-O}(r\|A)}\right]$ Cross elasticity of oddball alternative r with respect to attribute i of conventional alternative l, $E_{\tau_l^i}^{P(r\|A)}$: $(v_l)^{-1}\cdot\beta\cdot\omega^i\tau_l^i\cdot P_{MNW}(l\|A-r)\cdot\left[(1+\phi_r^W)-\frac{\phi_r^W}{P_{MNW-O}(r\|A)}\right]$

4.4 Empirical application

The proposed MNW-O model is applied to the Swissmetro data set (Bierlaire et al., 2001) that has been widely used in transportation studies (e.g., Fosgerau and Bierlaire, 2009; Li, 2011; Mabit, 2017; Sifringer et al., 2020; Han et al., 2022). The data set described mode choice scenarios among three alternative modes: train, car, and Swissmetro. We have selected the respondents who have access to all three mode alternatives in the choice set. The Swissmetro is an emerging travel mode that can be considered as an oddball alternative with unique attributes (i.e., headway and seat availability). The number of observations is 3987. A brief description of the used data set can be found in Table 4.2.

Table 4.2. Description of the Swissmetro data set

Alternatives	Attributes
Train	Travel cost, Travel time
Car	Travel cost, Travel time
Swissmetro (oddball)	Travel cost, Travel time, Headway, Seats availability

The alternative utility can be formulated as:

$$v_k = \overline{v}_r = \omega^c \cdot travel\ cost + \omega^t \cdot travel\ time, \tag{4.39}$$

$$\tilde{v}_r = \omega^h \cdot headway + \omega^s \cdot seats\ availability, \tag{4.40}$$

where ω are the parameters to be estimated.

4.4.1 Estimation results

We compare the estimation results of the MNW-O model against MNL and other advanced choice models, including the NL model that relaxes the independently distributed assumption, the MNL-O model for capturing one oddball alternative in the choice set, the HEV model (Bhat, 1995) that is flexible to relax the identically

distributed assumption for all alternatives, and the MNW model that inherently allows disutility-dependent perception variances for all individuals. All the models are estimated using Apollo (Hess and Palma, 2019)[1]. Following Fosgerau and Bierlaire (2009), the coefficient of travel cost is normalized to minus unity and the scale/shape parameters of the logit/weibit-based models are estimated. Two socio-demographic attributes, namely gender (male or female) and age (over 54 or not), were considered in the model estimation. The alternative specific constants were not significantly estimated, therefore excluded. The estimation results are reported in Table 4.3.

Among the four logit-based models (MNL, NL, HEV, and MNL-O), the HEV model shows a better model fit than others. This result makes sense as the HEV model considers more generalized heteroscedasticity in the error variance between alternatives. The NL model allows covariances among similar alternatives and performs better than the basic MNL model. However, it still assumes an identical variance for all alternatives and is inadequate to account for the oddball effect. Although the MNL-O model also considers heteroscedasticity, it focuses on the non-identical variance of the oddball alternative and is less flexible than the HEV model. On the other hand, the weibit-based models (MNW and MNW-O) show better model fits than the logit-based models. This may be because the weibit-based models adopt the multiplicative error structure, which allows disutility-dependent perception variances (See Figure 4.4) and can better reflect the way travelers perceive travel disutility (Chakroborty et al., 2021; Nirmale and Pinjari, 2023). Finally, the proposed MNW-O model shows a better model fit than all other competing models. It suggests that the MNW-O model can successfully capture both the oddball effect and the heterogeneous perceptions of different alternatives and service features in the Swissmetro data set.

[1] To estimate the HEV and MNW-O models, we extend the input code in Apollo to represent their choice probabilities by integrating external functions in the R library, i.e., the Gaussian quadrature function for the HEV model (following the estimation procedure suggested by Bhat, 1995) and the exponential integral function for the MNW-O model.

Table 4.3. Estimation results

	MNL	NL	HEV	MNL-O	MNW	MNW-O
Attributes	Estimates (t-value)	Estimates (t-value)	Estimates (t-value)	Estimates (t-value)	Estimates (t-value)	Estimates (t-value)
Travel time	-1.582 (-16.91)	-1.026 (-13.29)	-1.681 (-10.88)	-1.298 (-14.02)	-1.655 (-14.00)	-1.793 (-9.59)
Headway	-0.028 (-8.02)	-0.019 (-4.93)	-0.035 (-5.95)	-0.054 (-10.56)	-0.024 (-7.32)	-0.036 (-15.73)
Seats availability	0.392 (2.24)	0.186 (-2.12)	0.350 (3.20)	0.599 (2.53)	0.329 (2.72)	0.755 (18.75)
Male	0.147 (1.62)	0.123 (2.93)	0.334 (3.09)	0.460 (4.94)	0.430 (7.86)	0.581 (10.85)
Age_Old	-0.197 (-3.09)	-0.069 (-1.70)	-0.104 (-1.61)	-0.441 (-5.03)	-0.229 (-4.09)	-0.302 (-3.60)
Scale	0.114 (18.57)	0.083 (14.86)	-	0.126 (16.67)	-	-
Scale_Car	-	-	0.097 (11.16)	-	-	-
Scale_Train	-	-	0.089 (12.70)	-	-	-
Scale_SM	-	-	0.052 (12.99)	-	-	-
Logsum	-	0.852 (13.47)	-	-	-	-
Shape	-	-	-	-	3.628 (33.10)	2.766 (28.71)
Model fit						
Final LL	-3625.77	-3620.26	-3589.91	-3609.07	-3562.96	-3552.31
Adj. rho-squared	0.171	0.172	0.179	0.175	0.185	0.188
BIC	7301.28	7298.56	7246.15	7267.88	7175.66	7154.36

In addition, we applied statistical tests proposed by Vuong (1989) and Clarke (2003) to compare the models. Both tests are common in that their null hypothesis

indicates the competing models are equally close to the actual model. On the other hand, they are distinguished in that the Vuong test assumes the asymptotic normality of the log-likelihood ratio between the two competing models, while the Clarke test is distribution-free considering the sum of the signs of the log-likelihood difference for each observation.

The statistic of the Voung test is

$$z_{Voung} = \frac{\sum_i \left[L_{mi}\left(\boldsymbol{\omega}_m\right) - L_{m'i}\left(\boldsymbol{\omega}_{m'}\right) \right]}{\sqrt{\frac{1}{n}\sum_i \left[L_{mi}\left(\boldsymbol{\omega}_m\right) - L_{m'i}\left(\boldsymbol{\omega}_{m'}\right) \right]^2 - \left\{ \frac{1}{n}\sum_i \left[L_{mi}\left(\boldsymbol{\omega}_m\right) - L_{m'i}\left(\boldsymbol{\omega}_{m'}\right) \right] \right\}^2}}, \tag{4.41}$$

where $L_{mi}\left(\boldsymbol{\omega}_m\right)$ is a loglikelihood value by a model *m* for an observation *i*.

On the other side, the Clarke test is

$$z_{Clarke} = \frac{2 \cdot \sum_i sgn\left[L_{mi}\left(\boldsymbol{\omega}_m\right) - L_{m'i}\left(\boldsymbol{\omega}_{m'}\right) \right] - n}{\sqrt{n}}, \tag{4.42}$$

where *n* is the number of observations and *sgn* denotes the sign function. Common to both tests, a large negative value of *z* means that model *m*′ statistically outperforms model *m*.

Table 4.4. Results of Voung and Clarke tests

Model 1	Model 2	Tests	
		Voung	Clarke
MNL	MNW-O	-85.229	-42.673
NL	MNW-O	-52.105	-30.988
HEV	MNW-O	-27.308	-20.330
MNL-O	MNW-O	-38.296	-36.934
MNW	MNW-O	-14.165	-12.283

Table 4.4 shows the values of test statistics z_{Voung} and z_{Clarke} for the comparison between the MNW-O model and other competing models. Consistent with the model

fit results, both tests clearly confirm that the proposed MNW-O model is superior to all other models. These results demonstrate that the proposed MNW-O model has a clear advantage of simultaneously capturing the oddball effect and the disutility-dependent perception variance, while the competing models can either consider only one of the two issues (HEV, MNL-O, and MNW models) or none of them (NL and MNL models).

4.4.2 Validation results

To validate the estimation results, a cross-validation test was conducted. First, we randomly created five subsets of data which includes about 20% of all observations. Of the five subsets, four were used as a training set to estimate models. Then the parameter estimates were applied to the remaining single subset (as a test set). This process is repeated 5 times to guarantee all subsets were used as the testing set.

Table 4.5. Results of cross-validation test

(a) Training sets

	Avg. Adj. rho-squared	Avg. BIC
MNL	0.169	5847.90
NL	0.171	5843.28
HEV	0.175	5800.24
MNL-O	0.174	5819.47
MNW	0.182	5745.64
MNW-O	0.186	5725.08

(b) Testing sets

	Avg. Adj. rho-squared	Avg. BIC
MNL	0.134	1465.15
NL	0.139	1463.47
HEV	0.148	1454.27
MNL-O	0.148	1455.19
MNW	0.157	1433.64
MNW-O	0.163	1425.77

Table 4.5 shows the results of the cross-validation test. The estimation results in training sets are consistent with the general interpretation of the results from the full

data set. The MNW-O model is superior to all other models in terms of the model fit measures in all cases. The results in testing sets based on prediction performance also reveal the consistent outperformance of the MNW-O model against the competing models. In summary, we can conclude that the MNW-O model outperforms the competing models in the Swissmetro data set with respect to both model fit and prediction performance. It is therefore important to consider the heterogenous perceptions of not only the conventional alternatives but also the unique features of oddball alternative to better understand the choice behavior with an oddball alternative.

Table 4.6. Elasticities of MNW-O model[2]

Class 1	Alternatives	Elasticities		
		Train	Car	Swissmetro
Travel cost	Train	*-0.775*	0.239	0.147
	Car	0.094	*-0.581*	0.051
	Swissmetro	0.074	0.074	*-0.624*
Travel time	Train	*-0.174*	0.022	0.045
	Car	0.049	*-0.391*	0.033
	Swissmetro	0.055	0.055	*-0.410*
Headway	Swissmetro	0.204	0.204	*-1.308*
Seat availability	Swissmetro	0.181	0.181	*-1.026*

Table 4.6 reveals the results of elasticities in the MNW-O model based on Table 4.1. The direct elasticities are italicized in the table to distinguish from the cross elasticities. As discussed in Section 4.3.2.4., the IIA property is not valid between conventional and oddball alternatives. Therefore, the cross elasticities with respect to change in an attribute of oddball alternative are equal between conventional alternatives, while the cross elasticities with respect to change in an attribute of a conventional alternative is not the same between conventional and oddball alternatives. The results indicate that the choice probability of the oddball alternative (Swissmetro) is more sensitive to the changes in the unique attributes (headway and seats availability) than in the common attributes (travel cost and travel time).

[2] Direct elasticities are italicized.

4.5 Conclusions

This chapter proposed a weibit-based model to assess choice behavior when there is an oddball alternative with unique features in the choice set. This proposed approach retains the closed-form choice probability expression, which ensures the computational efficiency of the probability evaluation and model estimation while facilitating model interpretation. Inspired by Recker's (1995) MNL-O model, the proposed MNW-O model can specifically handle the oddball alternative as well as the asymptotic values and logical consistency conditions. Furthermore, the proposed MNW-O model also provides improved performance by enabling disutility-dependent perception variances for both the conventional and oddball alternatives and allowing a flexible variance ratio between them. These advantageous properties lead to relative difference-based choice probabilities, which allow the proposed model to further consider various heterogeneity issues that are ignored in the MNL-O model but are important for applications in modern transportation systems. The applicability of the proposed model is empirically demonstrated in a mode choice case study based on the Swissmetro data set (Bierlaire et al., 2001). The statistical results revealed that considering the advantageous properties of the MNW-O model is important for the understanding and prediction of choice behavior when an oddball alternative is included in choice set.

The proposed model has numerous potential applications. In the context of mode choice, the MNW-O model is suitable for modeling the decision-making scenario where an emerging travel mode is introduced to a multi-modal transportation system. The emerging mode is likely to be associated with new attributes that are not familiar to travelers, which brings additional uncertainty and should be treated as an oddball alternative (Song, 2019). For instance, connected and autonomous vehicles (CAVs) are planned to be introduced to transportation systems in the future. CAVs are expected to provide unprecedented service features, such as avoidance of potential crashes due to the smooth driving and effective utilization of in-vehicle travel time due to the fully autonomous driving technologies. Such unique attributes may provide incremental travel utility but also a higher perceived uncertainty. Thus, it would be suitable to model

the CAVs as an oddball alternative and predict the market penetration via the proposed MNW-O model. Alternatively, the rapid development of urban agglomeration can make traveling to locations in neighboring cities more frequent, providing travelers with extra opportunities via inter-city trips, which may also form an important oddball alternative in the destination choice problem (Huang et al., 2020c). Additionally, the effect of heterogeneity has been extensively recognized as an important issue in destination choice behavior (e.g., Schmid et al., 2019). The proposed model is thus applicable to assessing travelers' decision-making among destination locations within an urban agglomeration that have distinct travel distances, different service levels, and unique opportunities.

The proposed model opens up the following potential research directions for future studies: (1) further handling the independence assumption and the IIA property remaining in the subset of conventional alternatives; (2) considering the oddball alternative with decremental utility perception of their unique features that lower the choice probability, e.g., the range anxiety of electric vehicle drivers; and (3) analogous to the development of mixed logit models (McFadden and Train, 2000), generalizing the proposed model by mixing the Weibull distributed error term with additional error terms with various distributional assumptions, e.g., the Fréchet distribution, the Log-logistic distribution, and the family of Log-normal distributions (Varela et al., 2018; Xie et al., 2020; Nirmale and Pinjari, 2023). On this basis, the outcome models may reproduce more general oddball effects based on the more flexible total error distributions while benefiting from the multiplicative error structure, which is consistent with the psychophysical laws of how individuals perceive attribute levels with varying magnitudes (Chakroborty et al., 2021).

Methodology Part II. Modeling aggregate travel demand: Development of equilibrium models in future transportation systems

Chapter 5 From disaggregate travel choice to aggregate network equilibrium: Development of Beckmann-type equilibrium model formulation based on generalized Luce-form RUMs

5.1 Beckmann's MP formulation for UE: A retrospective

This section revisits Beckmann's mathematical programming (MP) formulation for the user equilibrium (UE) model that endogenously accounts for the flow-dependent route disutility in traffic assignment (Beckmann et al., 1956). To obtain the Beckmann-type MP formulation, the following assumptions are made:

UA1. Link travel disutility is separable, continuously differentiable, nonnegative, and increasing with respect to link flow.

UA2. Path travel disutility is an additive function of link disutility, i.e., $\tau_k^{rs} = \sum_{a \in A_k} \tau_a$.

Given the UE condition that assumes every traveler to be rational and have perfect knowledge of travel disutility, the UE problem is to minimize the path disutility for every unit of incremental OD demand. Figure 5.1 illustrates the UE condition between a single OD pair.

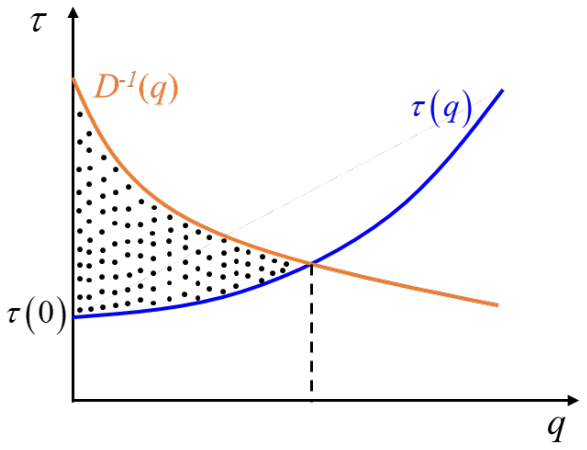

Figure 5.1. Illustration of equilibrium condition

In Figure 5.1, q denotes the trip rate between the OD pair, v denotes the travel disutility. The orange line indicates the demand curve, which is the inverse OD demand

function $D^{-1}(q)$. In the UE problem with elastic demand (UE-ED) in multi-OD networks, the demand function is assumed to be separable, i.e., $D^{rs^{-1}}(q^{rs})$ between OD pair *rs* depends only on q^{rs} and is independent of demands between other OD pairs. The blue line indicates the supply curve as the demand-dependent OD travel disutility function $\tau(q)$, which is defined as the average path travel disutility between the OD pair (Beckmann et al., 1956) and equals to the disutility of each used path under the equilibrium condition. In the multi-OD network, owing to the congestion effect on disutility (e.g., flow-dependent road travel time), the OD travel disutility is a function of demands between all OD pairs, i.e., $\tau^{rs}(\mathbf{q})$, where $\mathbf{q}$ denotes the vector of OD demands. The UE condition is reached when the size of the shaded area in Figure 5.1 is maximized, which is depicted by the shaded area as the difference between the area under demand curve and the blank area under supply curve. This condition is analogous to the solution to competitive equilibrium that maximizes the total aggregate consumer surplus in the transportation network. Hence, the objective of UE problem can be expressed as maximizing the size of the shaded area as follows:

$$\max Z = \sum_{rs \in RS} \int_0^{q^{rs}} D^{rs^{-1}}(\omega)\, d\omega - \int_{C_1} \sum_{rs \in RS} \tau^{rs}(\mathbf{q})\, dq^{rs}, \tag{5.1}$$

where C_1 denotes some integration path with respect to OD demands from (0, …, 0, …, 0) to (q^{11}, q^{12}, …, q^{rs}).

At the UE condition, the following conservation constraints should be satisfied:

$$\sum_{k \in K^{rs}} f_k^{rs} = q^{rs}, \forall rs \in RS, \tag{5.2}$$

where f_k^{rs} denotes the flow on path *k* between OD pair *rs*, K^{rs} denotes the path set between OD pair *rs*. Path flows should satisfy the following nonnegativity constraints:

$$f_k^{rs} \geq 0, \forall k \in K^{rs}, rs \in RS. \tag{5.3}$$

Then we focus on the second term on the right-hand side of Eq. (5.1), which is a line integral that indicates the total area under demand curves. By definition, the supply curve indicates the average path disutility, i.e., $\tau^{rs}(\mathbf{q}) = \sum_{k \in K^{rs}} P_k^{rs} \cdot \tau_k^{rs}(\mathbf{f})$. $\tau_k^{rs}(\mathbf{f})$ is the path disutility function, and **f** denotes the vector of all path flows in the network. P_k^{rs} is the choice proportion of path *k* between OD pair *rs*, such that $f_k^{rs} = P_k^{rs} \cdot q^{rs}$ and $df_k^{rs} = P_k^{rs} \cdot dq^{rs}$. The line integral $\int_{C_1} \sum_{rs \in RS} \tau^{rs}(\mathbf{q}) dq^{rs}$ can then be expressed as follows:

$$\int_{C_2} \sum_{rs \in RS} \sum_{k \in K^{rs}} \tau_k^{rs}(\mathbf{f}) df_k^{rs}, \tag{5.4}$$

where C_2 is some path of integration with respect to path flows between (0, 0, …, 0) and (f_1^{11}, f_2^{11}, …, f_k^{rs}). Hence, the UE objective function can be expressed as:

$$\max Z = \sum_{rs \in RS} \int_0^{q^{rs}} D^{rs^{-1}}(\omega) d\omega - \int_{C_2} \sum_{rs \in RS} \sum_{k \in K^{rs}} \tau_k^{rs}(\mathbf{f}) df_k^{rs}. \tag{5.5}$$

In the problem with fixed OD demands, the term $\sum_{rs \in RS} \int_0^{q^{rs}} D^{rs^{-1}}(\omega) d\omega$ is fixed (i.e., a constant) and can be removed from the maximization problem. Objective function (5.6) can then be equivalently expressed as

$$\min Z = \int_{C_2} \sum_{rs \in RS} \sum_{k \in K^{rs}} \tau_k^{rs}(\mathbf{f}) df_k^{rs}. \tag{5.6}$$

For the dimensions other than route choice, such as the destination choice and mode choice, the separable destination disutility function $\tau^s(q^s)$ and mode disutility function $\tau_m^{rs}(q_m^{rs})$ are often adopted instead of the non-separable disutility term $\tau_k^{rs}(\mathbf{f})$ to formulate the equilibrium trip distribution and modal split model, respectively. Taking the equilibrium modal split problem as an example, the objective function (5.6) can be expressed based on regular integrals as follows:

$$\min Z = \sum_{rs \in RS} \sum_{m \in M^{rs}} \int_0^{q_m^{rs}} \tau_m^{rs}(\omega) d\omega. \tag{5.7}$$

In the route choice problem, the line integral term cannot be derived in a straightforward way as the OD disutility depends on path disutility. By the assumption of additive path disutility (UA2), path disutility is determined by the link disutility that is dependent on link flow x_a.

$$\tau_k^{rs}(\mathbf{f}) = \sum_{rs \in RS} \sum_{k \in K^{rs}} \delta_{a,k}^{rs} \cdot \tau_a\left(x_a(\mathbf{f})\right), \forall k \in K^{rs}, rs \in RS, \tag{5.8}$$

where $\delta_{a,k}^{rs}$ is a binary variable denoting the link-path incidence relationship. $\delta_{a,k}^{rs} = 1$ if link a is on path k between OD pair rs; $\delta_{a,k}^{rs} = 0$, otherwise. The link flow is determined by the path flows based on the following definitional constraint:

$$x_a(\mathbf{f}) = \sum_{rs \in RS} \sum_{k \in K^{rs}} \delta_{a,k}^{rs} \cdot f_k^{rs}, \forall a \in A. \tag{5.9}$$

To obtain the objective function (5.6), we first show that the line integral therein is independent of integration path, where the notation rs is omitted in this paragraph for simplicity. As $\frac{\partial \tau_a}{\partial f_1} = \frac{\partial \tau_a}{\partial f_2} = ... = \frac{\partial \tau_a}{\partial f_k} = \frac{\partial \tau_a}{\partial x_a}$ (for all paths with $\delta_{a,k} = 1$), we have $\frac{\partial \tau_i}{\partial f_j} = \frac{\partial \tau_j}{\partial f_i} = \sum_{a \in A_{i,j}} \frac{\partial \tau_a}{\partial x_a}$ for each pair of paths i and j, where $A_{i,j}$ denotes the set of common links used by paths i and j. Hence, the Jacobian matrix $\nabla_f \boldsymbol{\tau}$ is symmetric, and the line integral in Eq. (5.6) is independent of integration path.

Therefore, by selecting an arbitrary path of integral, e.g., (f_1^{11}, 0, …, 0), (f_1^{11}, f_2^{11}, 0, …, 0), …, (f_1^{11}, f_2^{11}, …, f_k^{rs}), objective function (5.6) can be written as

$$\min Z = \int_0^{f_1^{11}} \tau_1^{11}(\omega, 0, ..., 0)\, d\omega + ... + \int_0^{f_k^{rs}} \tau_k^{rs}\left(f_1^{11}, ..., f_{k-1}^{rs}, \omega\right) d\omega, \tag{5.10}$$

Taking Eq. (5.8) into Eq. (5.10), the objective function can be expressed as

$$\min Z = \sum_{a \in A} \begin{bmatrix} \int_0^{f_1^{11}} \delta_{a,1}^{11} \cdot \tau_a\left(\delta_{a,1}^{11} \cdot \omega + 0 + ... + 0\right) d\omega \\ + ... \\ + \int_0^{f_k^{rs}} \delta_{a,k}^{rs} \cdot \tau_a\left(\delta_{a,1}^{11} \cdot f_{a,1}^{11} + ... + \delta_{a,k-1}^{rs} \cdot f_{a,k-1}^{rs} + \delta_{a,k}^{rs} \cdot \omega\right) d\omega \end{bmatrix}. \tag{5.11}$$

By substituting $\omega_{a,1}^{11} = \delta_{a,1}^{11} \cdot \omega$, …, $\omega_{a,k}^{rs} = \delta_{a,1}^{11} \cdot f_{a,1}^{11} + ... + \delta_{a,k-1}^{rs} \cdot f_{a,k-1}^{rs} + \delta_{a,k}^{rs} \cdot \omega$, Eq. (5.11) can be rewritten as

$$\begin{aligned} \min Z &= \sum_{a \in A} \int_0^{\delta_{a,1}^{11} \cdot f_1^{11}} \tau_a\left(\omega_{a,1}^{11}\right) d\omega_{a,1}^{11} ... + \int_{\delta_{a,1}^{11} \cdot f_1^{11} + ... + \delta_{a,k-1}^{11} \cdot f_{k-1}^{rs}}^{\delta_{a,1}^{11} \cdot f_1^{11} + ... + \delta_{a,k}^{11} \cdot f_k^{rs}} \tau_a\left(\omega_{a,k}^{11}\right) d\omega_{a,k}^{11} \\ &= \sum_{a \in A} \int_0^{\sum_{rs \in RS} \sum_{k \in K^{rs}} \delta_{a,k}^{rs} \cdot f_k^{rs}} \tau_a(\omega) d\omega \end{aligned} . \quad (5.12)$$

Integrating constraints (5.9), Eq. (5.12) can be further expressed as

$$\min Z = \sum_{a \in A} \int_0^{x_a} \tau_a(\omega) d\omega, \quad (5.13)$$

which is the Beckmann transformation for the UE model with fixed OD demand.

5.2 Development of Beckmann-type SUE formulation: Disutility function, composite disutility, and entropy

In the SUE problem, the assumption that travelers have perfect knowledge of travel disutility is relaxed, and travelers' perception error of travel disutility is additionally considered. Under the SUE condition, travelers choose the paths that can minimize their perceived travel disutility. Different from the UE model where the average path travel disutility is used as OD travel disutility, the satisfaction function S^{rs}, i.e., the composite utility/disutility indicating the expectation of the maximum travel utility (or minimum travel disutility) between each OD pair, is used to represent the OD travel utility at SUE. The satisfaction function can be expressed as follows:

$$S^{rs}(\mathbf{q}) = \sum_{k \in K^{rs}} P_k^{rs} \cdot S_{(k)}^{rs}(\mathbf{f}), \forall rs \in RS, \quad (5.14)$$

where $S_{(k)}^{rs}(\mathbf{f})$ is the achieved path utility, i.e., the expected utility conditional on the event that path *k* between OD pair *rs* is chosen. The SUE objective function can be obtained by replacing the deterministic path disutility in Eq. (5.6) with the achieved path disutility. Embedding different RUMs in the SUE problem will lead to different satisfaction and different SUE model formulations.

This section focuses on the entropy-based Beckmann-type MP formulations of the SUE models that integrate RUMs with "Luce-form" choice probabilities (Luce, 1959) and their generalizations. Owing to the invariance property of the "Luce class" error distributions underlying these RUMs, the satisfaction functions have closed-form expressions and satisfy $S^{rs}_{(k)}(\mathbf{f}) = S^{rs}(\mathbf{q}), \forall k \in K^{rs}, rs \in RS$ (Mattsson et al., 2014), which enables the incorporation of stochasticity via entropy terms. This section showcases the formulations of SUE models embedded with commonly used RUMs in literature, including the MNL model, MNW model, and extended logit models that address the correlation among alternatives.

5.2.1 MNL-SUE formulation

We start with the MNL model, which is the mostly used Luce-form model with an additive utility function. Taking the route choice problem as an example, the perceived travel utility of path *k* between OD pair *rs* can be expressed as follows:

$$V^{rs}_k(\mathbf{f}) = -\tau^{rs}_k(\mathbf{f}) + \varepsilon^{rs}_k, \forall k \in K^{rs}, rs \in RS\,. \tag{5.15}$$

V^{rs}_k denotes the perceived travel utility in the MNL model, which is an additive function of the deterministic utility $v^{rs}_k = -\tau^{rs}_k(\mathbf{f})$ and the IID Gumbel random error ε^{rs}_k.

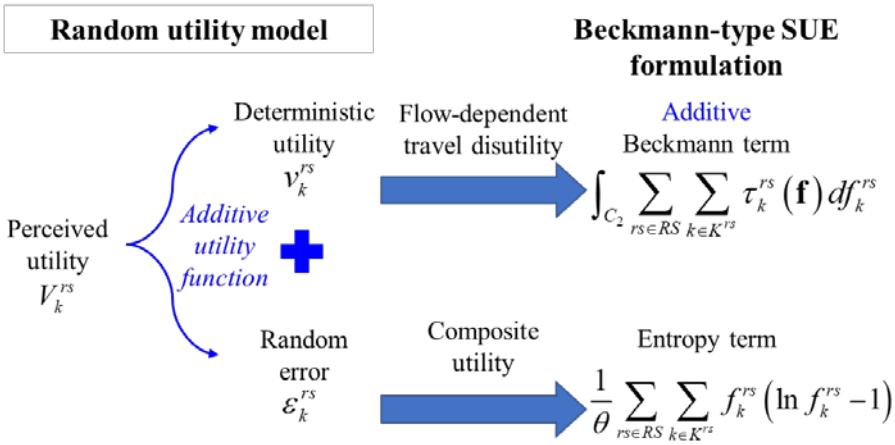

Figure 5.2. Illustration of Beckmann-type MNL-SUE formulation development

The development of the objective function of MNL-SUE model is illustrated in Figure 5.2. Instead of the deterministic path utility, the MNL-SUE model considers the perceived path utility achieved from the MNL model, which is expressed as follows (Anas and Feng, 1988):

$$\begin{aligned} S_{(k)}^{rs}(\mathbf{f}) &= -\tau_k^{rs}(\mathbf{f}) - \frac{1}{\theta}\ln P_k^{rs} \\ &= -\tau_k^{rs}(\mathbf{f}) - \frac{1}{\theta}\ln \frac{f_k^{rs}}{\sum_{k\in K^{rs}} f_k^{rs}}, \forall k \in K^{rs}, rs \in RS \end{aligned} . \tag{5.16}$$

The objective function of the SUE model is then expressed as follows:

$$\begin{aligned} \max Z &= \int_{C_2} \sum_{rs\in RS}\sum_{k\in K^{rs}} S_k^{rs}(\mathbf{f})\, df_k^{rs} \\ &= \int_{C_2} \sum_{rs\in RS}\sum_{k\in K^{rs}} \left[-\tau_k^{rs}(\mathbf{f}) - \frac{1}{\theta}\ln \frac{f_k^{rs}}{\sum_{k\in K^{rs}} f_k^{rs}} \right] df_k^{rs} \end{aligned} . \tag{5.17}$$

Based on the Beckmann transformation introduced in Section 5.1 and the conservation constraint $q^{rs} = \sum_{k\in K^{rs}} f_k^{rs}, \forall rs \in RS$, Eq. (5.17) can be rewritten as the following minimization problem:

$$\begin{aligned} \min Z &= \sum_{a\in A}\int_0^{x_a} \tau_a(\omega)\, d\omega + \sum_{rs\in RS}\sum_{k\in K^{rs}} \int_0^{f_k^{rs}} \frac{1}{\theta}\ln \omega d\omega - \sum_{rs\in RS}\int_0^{q^{rs}} \frac{1}{\theta}\ln \rho d\rho \\ &= \sum_{a\in A}\int_0^{x_a} \tau_a(\omega)\, d\omega + \frac{1}{\theta}\sum_{rs\in RS}\sum_{k\in K^{rs}} f_k^{rs}\left(\ln f_k^{rs} - 1\right) - \frac{1}{\theta}\sum_{rs\in RS} q^{rs}\left(\ln q^{rs} - 1\right) \end{aligned} . \tag{5.18}$$

In the case of fixed OD demand, q^{rs} is constant and can be removed from the objective function, Eq. (5.18) can be rewritten as

$$\min Z = \sum_{a\in A}\int_0^{x_a} \tau_a(\omega)\, d\omega + \frac{1}{\theta}\sum_{rs\in RS}\sum_{k\in K^{rs}} f_k^{rs}\left(\ln f_k^{rs} - 1\right), \tag{5.19}$$

which gives the objective function of Fisk's (1980) MNL-SUE formulation. The conservation, nonnegativity, and definitional constraints of the MNL-SUE model are Eqs. (5.2), (5.3), and (5.9) inherited from the UE model.

Alternatively, the MNL-SUE objective function can be developed based on the additively separable utility function (5.15). Given that the deterministic term is related to the Beckmann term as shown in Section 5.1, we focus on the error term ε_k^{rs}. For travelers choosing path *k* between OD pair *rs*, the value of perceived utility V_k^{rs} is the maximum among all paths, i.e., $\left(\varepsilon_k^{rs}\right)^* = \max_{k \in K^{rs}} \left\{-\tau_1^{rs} + \tau_k^{rs} + \varepsilon_1^{rs}, -\tau_2^{rs} + \tau_k^{rs} + \varepsilon_2^{rs}, ..., \varepsilon_k^{rs}\right\}$. Based on Property 6 of the Gumbel distribution (Table 2.1), $\left(\varepsilon_k^{rs}\right)^*$ is still identically Gumbel distributed with scale parameter θ. The expectation of $\left(\varepsilon_k^{rs}\right)^*$ is

$$\begin{aligned} E\left(\varepsilon_k^{rs}\right) &= \frac{1}{\theta} \ln \sum_{l \in K^{rs}} \exp\left\{\theta \cdot \left[-\tau_l^{rs}\left(\mathbf{f}\right) + \tau_k^{rs}\left(\mathbf{f}\right)\right]\right\} \\ &= -\frac{1}{\theta} \ln \frac{\sum_{l \in K^{rs}} \exp\left[-\theta \tau_l^{rs}\left(\mathbf{f}\right)\right]}{\exp\left[-\theta \tau_k^{rs}\left(\mathbf{f}\right)\right]} \\ &= -\frac{1}{\theta} \ln \frac{\sum_{l \in K^{rs}} f_l^{rs}}{f_k^{rs}} \end{aligned} \quad , \tag{5.20}$$

where the third equality is obtained based on the MNL route choice probability $P_k^{rs} = \frac{f_k^{rs}}{\sum_{l \in K^{rs}} f_l^{rs}} = \frac{\exp\left[-\theta \tau_k^{rs}\left(\mathbf{f}\right)\right]}{\sum_{l \in K^{rs}} \exp\left[-\theta \tau_l^{rs}\left(\mathbf{f}\right)\right]}$. Taking Eq. (5.20) into the integral in Eq. (5.6), the objective function of Fisk's MNL-SUE objective function can be obtained following Eqs. (5.18)–(5.19).

5.2.2 Extended SUE formulations

This section discusses the MP formulation of some extensions to the basic MNL-SUE model. The SUE model development based on the MNW choice model was first introduced as a variant of MNL-SUE model that addresses the heterogeneity issue via the multiplicative disutility function. Development of SUE models is then presented based on two types of extended logit models, which address the correlations among

travel alternatives by introducing either additional correction terms or a nested choice structure.

5.2.2.1 MNW-SUE formulation

In the MNW model, instead of the additive utility function (5.15), the multiplicatively separable disutility function is adopted (Fosgerau and Bierlaire, 2009):

$$V_k^{rs}(\mathbf{f}) = v_k^{rs} \cdot \varepsilon_k^{rs}, \forall k \in K^{rs}, rs \in RS . \tag{5.21}$$

In weibit-based models, V_k^{rs} denotes the perceived travel disutility, $v_k^{rs} = \tau_k^{rs}(\mathbf{f})$ is the deterministic disutility, ε_k^{rs} is the random error assumed to be IID Weibull variables.

The development of the MNW-SUE formulation is analogous to that of the MNL-SUE model. For travelers choosing path *k* between OD pair *rs*, the value of V_k^{rs} is the minimum among all paths, i.e., $\left(\varepsilon_k^{rs}\right)^* = \min_{k \in K^{rs}} \left\{ \frac{\tau_1^{rs}}{\tau_k^{rs}} \cdot \varepsilon_1^{rs}, \frac{\tau_2^{rs}}{\tau_k^{rs}} \cdot \varepsilon_2^{rs}, ..., \varepsilon_k^{rs} \right\}$. Based on Property 6 of the Weibull distribution (Table 2.2), the expectation of $\left(\varepsilon_k^{rs}\right)^*$ is

$$\begin{aligned} E\left[\left(\varepsilon_k^{rs}\right)^*\right] &= \left[\sum_{l \in K^{rs}} \left(\tau_l^{rs}(\mathbf{f}) / \tau_k^{rs}(\mathbf{f})\right)^{-\beta}\right]^{-\frac{1}{\beta}} \\ &= \left[\frac{\sum_{l \in K^{rs}} \left(\tau_l^{rs}(\mathbf{f})\right)^{-\beta}}{\left(\tau_k^{rs}(\mathbf{f})\right)^{-\beta}}\right]^{-\frac{1}{\beta}} \\ &= \left(\sum_{l \in K^{rs}} \left(f_l^{rs}\right)\right)^{-\frac{1}{\beta}} \cdot \left(f_k^{rs}\right)^{\frac{1}{\beta}} \end{aligned} , \tag{5.22}$$

where β is the shape parameter. The third equality is obtained by substituting the MNW route choice probability $P_k^{rs} = \frac{\left[\tau_k^{rs}(\mathbf{f})\right]^{-\beta}}{\sum_{l \in K^{rs}} \left[\tau_l^{rs}(\mathbf{f})\right]^{-\beta}}$. Taking Eq. (5.22) into the

integral in Eq. (5.6) and removing q^{rs} in the case of fixed OD demand, the objective function of MNW-SUE model can be expressed as

$$\begin{aligned}\min Z &= \int_{C_2} \sum_{rs\in RS}\sum_{k\in K^{rs}} S^{rs}_{(k)}(\mathbf{f})\, df^{rs}_k \\ &= \int_{C_2} \sum_{rs\in RS}\sum_{k\in K^{rs}} \left[\tau^{rs}_k(\mathbf{f})\cdot\left(\sum_{l\in K^{rs}}\left(f^{rs}_l\right)\right)^{-\frac{1}{\beta}}\cdot\left(f^{rs}_k\right)^{\frac{1}{\beta}}\right] df^{rs}_k \end{aligned}. \qquad (5.23)$$

Alternatively, the MNW-SUE model formulation can be obtained based on the logarithmic transformation relationship between weibit and logit models (Figure 5.3).

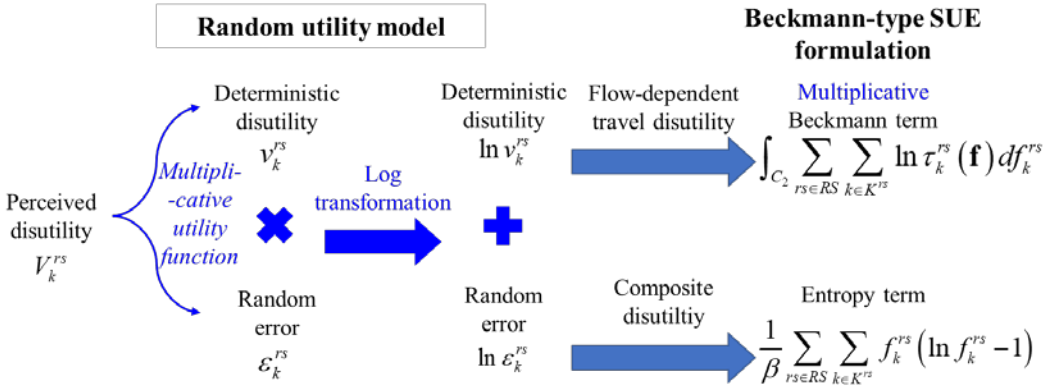

Figure 5.3. Illustration of Beckmann-type MNW-SUE formulation development

The weibit multiplicative disutility function (5.21) can be transformed to an additive one by taking the log on both sides of the equation as follows:

$$\ln\left[V^{rs}_k(\mathbf{f})\right] = \ln\left[\tau^{rs}_k(\mathbf{f})\right] + \ln\varepsilon^{rs}_k, \forall k\in K^{rs}, rs\in RS\,. \qquad (5.24)$$

As ε^{rs}_k follows the Weibull distribution with shape parameter β, $-\ln\varepsilon^{rs}_k$ is Gumbel distributed with scale parameter equal to β. Following the development of the MNL-SUE model formulation shown in Section 5.2.1, the objective function of the MNW-SUE model can be obtained as follows:

$$\min Z = \int_{C_2}\sum_{rs\in RS}\sum_{k\in K^{rs}}\ln\tau^{rs}_k(\mathbf{f})\,df^{rs}_k + \sum_{rs\in RS}\sum_{k\in K^{rs}}\int_0^{f^{rs}_k}\frac{1}{\theta}\ln\omega\, d\omega\,, \qquad (5.25)$$

where the term regarding q^{rs} is removed in the fixed-demand problem. $\ln \tau_k^{rs}(\omega)$ is the multiplicative Beckmann term (Kitthamkesorn and Chen, 2013).

In a higher-level travel demand analysis, such as trip distribution and modal split problems, the destination and mode disutility are functions only dependent on the corresponding destination and mode demands and Eq. (5.25) can be derived based on regular integrals with respect to the demand. Taking the modal split problem as an example, let q_m^{rs} and $\tau_m^{rs}\left(q_m^{rs}\right)$ denote the mode demand and demand-dependent disutility function, the objective function can be written as

$$\min Z = \sum_{rs\in RS}\sum_{m\in M^{rs}}\int_0^{q_m^{rs}} \ln \tau_m^{rs}(\omega) d\omega + \frac{1}{\theta}\sum_{rs\in RS}\sum_{m\in M^{rs}} q_m^{rs}\left(\ln q_m^{rs} - 1\right), \qquad (5.26)$$

While in the traffic assignment problem, the path disutility cannot be directly expressed based on the path flows. However, it is difficult to separate the path disutility into link disutility owing to the inconsistency between the multiplicative disutility function and the assumption (UA2) of additive path disutility. To obtain an MP formulation, Kitthamkesorn and Chen (2013) assumes multiplicative path disutility, i.e., $\tau_k^{rs} = \prod_{a\in A_k} \tau_a$. Hence, the log of path disutility is an additive function of the log of link disutility: $\ln \tau_k^{rs} = \sum_{a\in A_k} \ln \tau_a$. Eq. (5.25) can then be expressed as

$$\min Z = \sum_{a\in A}\int_0^{x_a} \ln \tau_a(\omega)\, d\omega + \frac{1}{\theta}\sum_{rs\in RS}\sum_{k\in K^{rs}} f_k^{rs}\left(\ln f_k^{rs} - 1\right). \qquad (5.27)$$

Eq. (5.27) is in accordance with the MNW-SUE formulation with the multiplicative Beckmann transformation (Kitthamkesorn and Chen, 2013).

5.2.2.2 Extended logit SUE formulation with correction terms

Figure 5.4 illustrates the SUE formulation based on the path-size logit (PSL) model, where a path-size (PS) factor is incorporated as a correction term that penalizes the correlation (overlap) among paths.

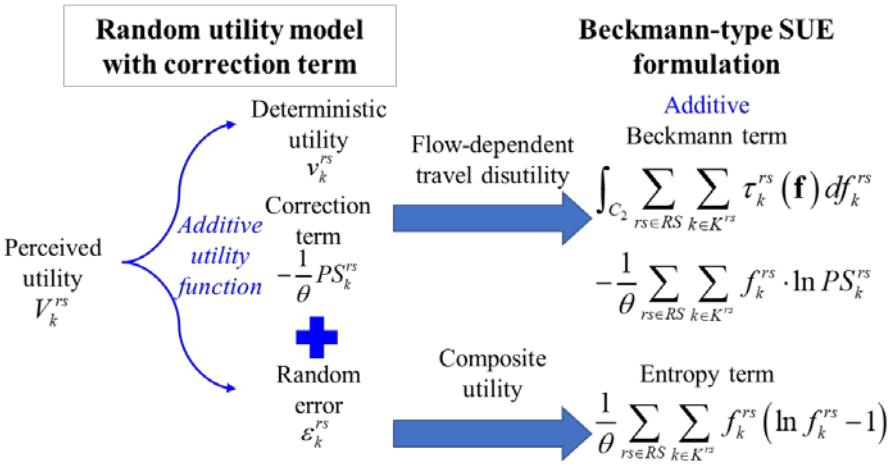

Figure 5.4. Illustration of Beckmann-type PSL-SUE formulation development

The utility function of PSL model is expressed as

$$V_k^{rs}(\mathbf{f}) = -\tau_k^{rs}(\mathbf{f}) + \frac{1}{\theta}\ln PS_k^{rs} + \varepsilon_k^{rs}, \forall k \in K^{rs}, rs \in RS\,. \tag{5.28}$$

The correction term is added to the deterministic utility without influencing the random error; hence, it can be directly integrated into the objective function (5.17):

$$\begin{aligned} \max Z &= \int_{C_2} \sum_{rs\in RS}\sum_{k\in K^{rs}} S_{(k)}^{rs}(\mathbf{f})\, df_k^{rs} \\ &= \int_{C_2} \sum_{rs\in RS}\sum_{k\in K^{rs}} \left[-\tau_k^{rs}(\mathbf{f}) - \frac{1}{\theta}\ln PS_k^{rs} - \frac{1}{\theta}\ln \frac{f_k^{rs}}{\sum_{k\in K^{rs}} f_k^{rs}} \right] df_k^{rs} \end{aligned}, \tag{5.29}$$

which can be rewritten as follows in the case of fixed OD demand:

$$\min Z = \sum_{a\in A}\int_0^{x_a} \tau_a(\omega)\, d\omega + \frac{1}{\theta}\sum_{rs\in RS}\sum_{k\in K^{rs}} f_k^{rs}\cdot\left(\ln f_k^{rs} - 1\right) - \frac{1}{\theta}\sum_{rs\in RS}\sum_{k\in K^{rs}} f_k^{rs}\cdot\ln PS_k^{rs}\,. \tag{5.30}$$

5.2.2.3 Extended logit SUE formulation with a nested choice structure

This section illustrates the SUE formulation based on the nested logit (NL) model, where the travel choice is considered in a nested structure with multiple choice levels. The two-level NL model with marginal and conditional choice levels is adopted to exemplify the SUE formulation. The utility function of NL model is

$$V_k^{rs}(\mathbf{f},\mathbf{q}) = -\tau_{uk}^{rs}(\mathbf{f}) - \tau_u^{rs}(\mathbf{q}) + \varepsilon_{uk}^{rs} + \varepsilon_u^{rs}, \forall k \in K_u^{rs}, u \in U^{rs}, rs \in RS, \quad (5.31)$$

where τ_{uk}^{rs} and τ_u^{rs} are the utility of individual alternative *k* and common disutility of nest *u*; ε_{uk}^{rs} and ε_u^{rs} are random errors at the conditional and marginal choice levels. Based on the distributional assumptions of NL model (Ben-Akiva and Lerman, 1985), ε_{uk}^{rs} and ε_u^{rs} are independent, ε_{uk}^{rs} are IID Gumbel variables with scale parameter θ_k, $\varepsilon_{uk}^{rs} + \varepsilon_u^{rs}$ are IID Gumbel variables with scale parameter θ_u satisfying $0 < \theta_u < \theta_k$.

The NL choice probability can be expressed as the product of marginal choice probability and conditional choice probability:

$$P_k^{rs} = P_u^{rs} \cdot P_{k|u}^{rs}, \forall k \in K_u^{rs}, u \in U^{rs}, rs \in RS, \quad (5.32)$$

where the conditional choice probability of choosing alternative *k* given nest *u* is chosen can be obtained via the MNL model with scale parameter θ_k:

$$P_{k|u}^{rs} = \frac{f_{uk}^{rs}}{\sum_{l \in K_u^{rs}} f_{ul}^{rs}} = \frac{\exp\left[-\theta_k \tau_{uk}^{rs}(\mathbf{f})\right]}{\sum_{l \in K_u^{rs}} \exp\left[-\theta_k \tau_{ul}^{rs}(\mathbf{f})\right]}, \forall k \in K_u^{rs}, u \in U^{rs}, rs \in RS. \quad (5.33)$$

The marginal choice probability of nest *u* is obtained via the MNL model with scale parameter θ_u:

$$P_u^{rs} = \frac{q_u^{rs}}{q^{rs}} = \frac{\exp\left\{-\theta_u\left[\tau_u^{rs}(\mathbf{q}) - S_u^{rs}(\mathbf{f})\right]\right\}}{\sum_{w \in U^{rs}} \exp\left\{-\theta_u\left[\tau_w^{rs}(\mathbf{q}) - S_w^{rs}(\mathbf{f})\right]\right\}}, \forall u \in U^{rs}, rs \in RS, \quad (5.34)$$

where S_u^{rs} denotes the composite utility of nest *u* between OD pair *rs* obtained at the conditional choice level:

$$S_u^{rs}(\mathbf{f}) = \frac{1}{\theta_k} \ln \sum_{k \in K_u^{rs}} \exp\left[-\theta_k \tau_{uk}^{rs}(\mathbf{f})\right], \forall u \in U^{rs}, rs \in RS. \quad (5.35)$$

The NL-SUE model can thus be obtained following the development of MNL-SUE formulation at different choice levels as illustrated in Figure 5.5.

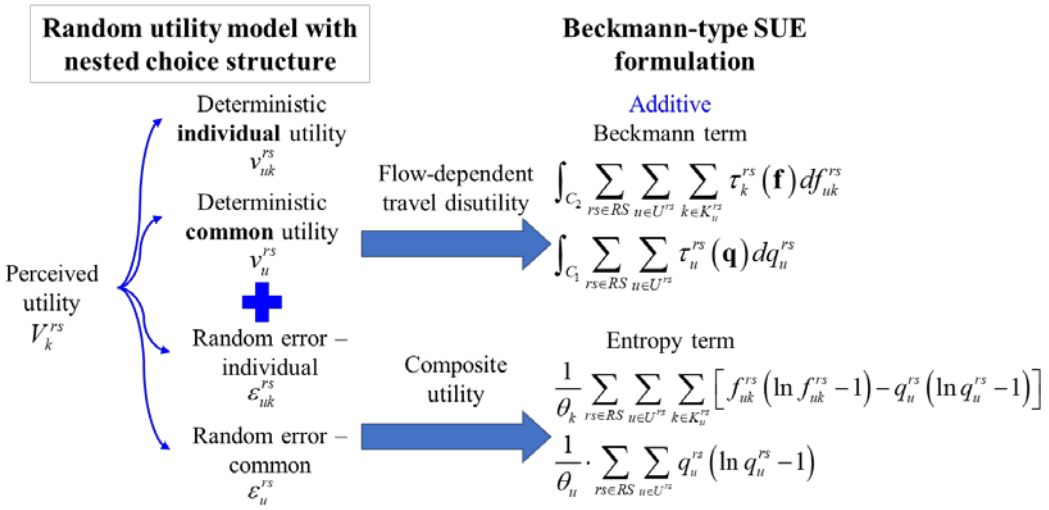

Figure 5.5. Illustration of Beckmann-type NL-SUE formulation development

Based on the distributional assumptions and Property 6 of the Gumbel distribution (Table 2.1), the expectations of error terms can be written as follows:

$$
\begin{aligned}
E\left[\left(\varepsilon_{uk}^{rs}\right)^{*}\right] &= \frac{1}{\theta_k}\ln\frac{\sum_{l\in K_u^{rs}}\exp\left(-\theta_k\tau_{ul}^{rs}(\mathbf{f})\right)}{\exp\left(-\theta_k\tau_{uk}^{rs}(\mathbf{f})\right)} \\
&= -\frac{1}{\theta_k}\ln P_{k|u}^{rs} \qquad , \qquad (5.36)\\
&= -\frac{1}{\theta_k}\ln f_{uk}^{rs} + \frac{1}{\theta_k}\ln\sum_{k\in K_u^{rs}} f_{uk}^{rs}
\end{aligned}
$$

$$
\begin{aligned}
E\left[\left(\varepsilon_{u}^{rs}\right)^{*}\right] &= \frac{1}{\theta_u}\ln\frac{\sum_{w\in U^{rs}}\exp\left[-\theta_u\left(\tau_w^{rs}(\mathbf{q})+S_w^{rs}(\mathbf{f})\right)\right]}{\exp\left[-\theta_u\left(\tau_u^{rs}(\mathbf{q})+S_u^{rs}(\mathbf{f})\right)\right]} \\
&= -\frac{1}{\theta_u}\ln P_{u}^{rs} \qquad . \qquad (5.37)\\
&= -\frac{1}{\theta_u}\ln q_u^{rs} + \frac{1}{\theta_u}\ln\sum_{u\in U^{rs}} q_u^{rs}
\end{aligned}
$$

Substituting Eqs. (5.36) and (5.37) into the integral in Eq. (5.17) gives the objective function of the NL-SUE model:

$$\begin{aligned}\max Z = &\int_{C_2} \sum_{rs\in RS}\sum_{u\in U^{rs}}\sum_{k\in K_u^{rs}}\left[\tau_{uk}^{rs}(\mathbf{f}) - \frac{1}{\theta_k}\ln f_k^{rs} + \frac{1}{\theta_k}\ln\sum_{k\in K_u^{rs}} f_{uk}^{rs}\right] df_k^{rs} \\ &+\int_{C_1} \sum_{rs\in RS}\sum_{u\in U^{rs}}\left[\tau_u^{rs}(\mathbf{q}) - \frac{1}{\theta_u}\ln q_u^{rs} + \frac{1}{\theta_u}\ln\sum_{u\in U^{rs}} q_u^{rs}\right] dq_u^{rs}\end{aligned}, \quad (5.38)$$

where the first integral corresponds to the conditional choice level and the second integral corresponds to the marginal choice level. In Eq. (5.38), C_1 and C_2 denote some integration path between (0, 0, …, 0) and (q_1^{11}, q_2^{11}, …, q_u^{rs}), and between (0, 0, …, 0) and (f_{11}^{11}, f_{12}^{11}, …, f_{uk}^{rs}), respectively. Considering separable nest-specific utility $\tau_u^{rs}\left(q_u^{rs}\right)$ and fixed OD demand q^{rs}, and using link disutility to express path disutility via the Beckmann transformation, Eq. (5.38) can be rewritten as

$$\begin{aligned}\min Z = &\sum_{a\in A}\int_0^{x_a}\tau_a(\omega)\,d\omega + \frac{1}{\theta_k}\sum_{rs\in RS}\sum_{u\in U^{rs}}\sum_{k\in K_u^{rs}} f_{uk}^{rs}\left(\ln f_{uk}^{rs} - 1\right) \\ &+\sum_{rs\in RS}\sum_{u\in U^{rs}}\int_0^{q_u^{rs}}\tau_u^{rs}(\omega)\,d\omega + \left(\frac{1}{\theta_u} - \frac{1}{\theta_k}\right)\sum_{rs\in RS}\sum_{u\in U^{rs}} q_u^{rs}\left(\ln q_u^{rs} - 1\right)\end{aligned}, \quad (5.39)$$

which gives the objective function of the NL-SUE model. Compared with the MNL-SUE model, the NL-SUE model has additional definitional constraints for the relationship between path flow and nest-level demand as follows:

$$q_u^{rs} = \sum_{k\in K_u^{rs}} f_{uk}^{rs}, \forall u \in U^{rs}, rs \in RS\,. \quad (5.40)$$

Alternatively, the NL-SUE formulation can be directly obtained via the satisfaction function. The NL satisfaction function between OD pair *rs* is as follows:

$$\begin{aligned}S^{rs} &= -\frac{1}{\theta_u}\ln\sum_{u\in U^{rs}}\exp\left\{-\theta_u\left[\tau_u^{rs} - \frac{1}{\theta_k}\ln\sum_{k\in K_u^{rs}}\exp\left(-\theta_k\tau_{uk}^{rs}\right)\right]\right\} \\ &= -\frac{1}{\theta_u}\ln\sum_{u\in U^{rs}}\left[\exp\left(-\theta_u\tau_u^{rs}\right)\cdot\left(\sum_{k\in K_u^{rs}}\exp\left(-\theta_k\tau_{uk}^{rs}\right)\right)^{\frac{\theta_u}{\theta_k}}\right]\end{aligned}. \quad (5.41)$$

From the marginal choice probability function in Eq. (5.34), we have the following:

$$\sum_{u\in U^{rs}} \exp\left(-\theta_u \tau_u^{rs}\right)\cdot\left(\sum_{k\in K_u^{rs}} \exp\left(-\theta_k \tau_{uk}^{rs}\right)\right)^{\frac{\theta_u}{\theta_k}} = \frac{q^{rs}\cdot\exp\left(-\theta_u \tau_u^{rs}\right)\cdot\left(\sum_{k\in K_u^{rs}} \exp\left(-\theta_k \tau_{uk}^{rs}\right)\right)^{\frac{\theta_u}{\theta_k}}}{q_u^{rs}} .(5.42)$$

From the conditional choice probability function in Eq. (5.32), we have the following:

$$\sum_{l\in K_u^{rs}} \exp\left(-\theta_k \tau_{ul}^{rs}\right) = \frac{q_u^{rs}\cdot\exp\left(-\theta_k \tau_{uk}^{rs}\right)}{f_{uk}^{rs}} . \quad (5.43)$$

Substitute Eq. (5.43) into Eq. (5.32), we have

$$\sum_{u\in U^{rs}} \exp\left(-\theta_u \tau_u^{rs}\right)\cdot\left(\sum_{k\in K_u^{rs}} \exp\left(-\theta_k \tau_{uk}^{rs}\right)\right)^{\frac{\theta_u}{\theta_k}} = \frac{q^{rs}\cdot\exp\left(-\theta_u \tau_u^{rs}\right)\cdot\left(\frac{q_u^{rs}\cdot\exp\left(-\theta_k \tau_{uk}^{rs}\right)}{f_{uk}^{rs}}\right)^{\frac{\theta_u}{\theta_k}}}{q_u^{rs}} .(5.44)$$

The NL composite utility can be re-expressed by substituting Eq. (5.41) into Eq. (5.38)

$$\begin{aligned} S^{rs} &= -\frac{1}{\theta_u}\ln\frac{q^{rs}\cdot\exp\left(-\theta_u \tau_u^{rs}\right)\cdot\left(\frac{q_u^{rs}\cdot\exp\left(-\theta_k \tau_{uk}^{rs}\right)}{f_{uk}^{rs}}\right)^{\frac{\theta_u}{\theta_k}}}{q_u^{rs}} \\ &= -\frac{1}{\theta_u}\ln q^{rs} + \frac{1}{\theta_u}\ln q_u^{rs} + \tau_u^{rs} - \frac{1}{\theta_k}\ln q_u^{rs} + \frac{1}{\theta_k}\ln f_{uk}^{rs} + \tau_{uk}^{rs} \end{aligned} . \quad (5.45)$$

Following the invariance property, the achieved perceived disutility of path *k* in nest *u* between OD pair *rs* satisfies $S_{(uk)}^{rs} = S^{rs}, \forall k \in K_u^{rs}, u \in U^{rs}, rs \in RS$. Replacing τ_k^{rs} with S_{uk}^{rs} in Eq. (5.6) and removing q^{rs} in the case of fixed OD demand lead to the NL-SUE objective function:

$$
\begin{aligned}
\min Z &= \int_{C_2} \sum_{rs\in RS}\sum_{u\in U^{rs}}\sum_{k\in K_u^{rs}} S_{(uk)}^{rs}(\mathbf{f})\, df_k^{rs} \\
&= \int_{C_2} \sum_{rs\in RS}\sum_{u\in U^{rs}}\sum_{k\in K_u^{rs}} \left[\tau_{uk}^{rs}(\mathbf{f}) - \frac{1}{\theta_k}\ln f_k^{rs} + \frac{1}{\theta_k}\ln q_u^{rs}\right] df_k^{rs} \\
&+ \int_{C_1} \sum_{rs\in RS}\sum_{u\in U^{rs}} \left[\tau_u^{rs}(\mathbf{q}) - \frac{1}{\theta_u}\ln q_u^{rs}\right] dq_u^{rs} \qquad , \qquad (5.46) \\
&= \sum_{a\in A}\int_0^{x_a} \tau_a(\omega)\, d\omega + \frac{1}{\theta_k}\sum_{rs\in RS}\sum_{u\in U^{rs}}\sum_{k\in K_u^{rs}} f_{uk}^{rs}\cdot\left(\ln f_{uk}^{rs} - 1\right) \\
&+ \sum_{rs\in RS}\sum_{u\in U^{rs}}\int_0^{q_u^{rs}} \tau_u^{rs}(\omega)\, d\omega + \left(\frac{1}{\theta_u} - \frac{1}{\theta_k}\right)\sum_{rs\in RS}\sum_{u} q_u^{rs}\cdot\left(\ln q_u^{rs} - 1\right)
\end{aligned}
$$

which is consistent with the objective function developed in Eq. (5.39).

5.3 A partial linearization algorithm for solving the Beckmann-type SUE formulation

Different from the variational inequality or fixed-point formulation, the Beckmann-type MP formulation of equilibrium model is a convex program that enables many readily available convergent and efficient solution algorithms. The objective function can be utilized to obtain appropriate search directions and facilitate the determination of step size and stopping criterion in the solution algorithm. Taking advantage of this property, this section describes a partial linearization algorithm embedded with a self-regulated averaging (SRA) scheme for solving the equilibrium models considered in this research. Compared with the complete linearization algorithm and sequential solution procedure widely used for solving the equilibrium models, the partial linearization algorithm is more efficient while guaranteeing convergence (Evans, 1976; LeBlanc and Farhangian, 1981; Patriksson, 1994).

The partial linearization algorithm involves the search direction finding for deriving auxiliary flow pattern and the line search for determining step size and updating decision variables. The search direction is determined by solving a partial linearized subproblem as a first-order approximation of the original problem. Given the decision variables (travel demands) and corresponding travel disutility at iteration *n-1*,

$\mathbf{q^{n-1}}$ and $\boldsymbol{\tau}\left(\mathbf{f^{n-1}}\right)$, the search direction (i.e., auxiliary travel demand **y**) at iteration *n* is determined the subproblem with following objective function:

$$\begin{aligned} \min\ Z &= Z_{1,sub}\left(\mathbf{y}\right) + Z_2\left(\mathbf{y}\right) \\ &= \sum_i y_i \cdot \tau_i\left(q_i^{n-1}\right) + \sum_i \frac{1}{\theta_i} \cdot y_i\left(\ln y_i - 1\right) \end{aligned} \tag{5.47}$$

The constraints remain the same for the auxiliary demands **y**. In the subproblem, the Beckmann term Z_1 is linearized via a first-order approximation, which fixes the travel disutility $\tau_i\left(q_i^{n-1}\right)$ based on the current demand pattern $\mathbf{q^{n-1}}$. In the multiplicative Beckmann term, the travel disutility is fixed as $\ln \tau_i\left(q_i^{n-1}\right)$. Z_2 represents the entropy terms, where decision variables are directly substituted by auxiliary travel demand **y**. Thus, the subproblem is a convex program with linear inequality constraints. In the line search, the moving step size is determined based on the SRA scheme, which improves the efficiency of the widely used method of successive average scheme (Liu et al., 2009). The procedure of partial linearization algorithm involves the following steps:

Step 0. Initialization.

- Initialize primal variables $\mathbf{q^0=0}$, and the free-flow travel disutility;
- Set outer iteration counter $n = 1$;
- Derive auxiliary flow pattern $\mathbf{y^1}$ by solving the partial linearized subproblem;
- Initialize step size: $\varphi^1 = 1$, $\gamma^1 = 1$. Update primal variables: $\mathbf{q^1=y^1}$.

Step 1. Direction finding.

- Update travel disutility based on the current demand pattern $\mathbf{q^n}$;
- Set $n = n + 1$;
- Derive auxiliary flow pattern $\mathbf{y^n}$ by solving the partial linearized subproblem.

Step 2. Line search.

- Derive the step size φ^n based on the SRA scheme:

$$\varphi^n = 1/\gamma^n \tag{5.48}$$

$$\gamma^n = \begin{cases} \gamma^{n-1} + \sigma_1 & \text{if } \left\| \mathbf{y^n - q^{n-1}} \right\| \geq \left\| \mathbf{y^{n-1} - q^{n-2}} \right\| \\ \gamma^{n-1} + \sigma_2 & \text{otherwise} \end{cases} \tag{5.49}$$

where $\sigma_1 > 1$ and $\sigma_2 < 1$.

Step 3. Update primal variables.

$$\mathbf{q^n} = \mathbf{q^{n-1}} + \varphi^n \cdot \left(\mathbf{y^n} - \mathbf{q^{n-1}} \right).$$

Step 4. Convergence test.

- If $\max \left\{ \left| \mathbf{q^n} - \mathbf{q^{n-1}} \right| \right\} \leq \delta$, terminate the algorithm, where δ is a convergence tolerance at which the procedure stops. Otherwise, go to step 1.

Specifically, the optimality conditions of the MP formulation give rise to analytical expressions of the decision variables based on dual variables, which enables the iterative balancing scheme for direction finding. The iterative balancing scheme is an efficient algorithm to obtain both primal and dual variables, which has been widely used for solving SUE models with side constraints (Bell, 1995; Bell and Iida, 1997; Chen et al., 2009; Ryu et al., 2014). The dual variables associated model constraints are iteratively adjusted based on the primal variables derived from the MP model formulation. The convergence of the iterative balancing scheme has been well proved (Bell and Iida, 1997). As will be described in Chapters 7-9, the partial linearization algorithm is further embedded with an iterative balancing scheme to solve advanced equilibrium models with side constraints (e.g., capacity constraints). The adjustment factor for the dual variable associated with the conservation constraint is derived following Ryu et al. (2014); while the adjustment factor for the dual variable associated with the side constraint is derived following Chen et al. (2009).

Chapter 6 Considering path order and perceptual correlations in a tolled network with ordered GEV model

6.1 Introduction

Based on the ordered path-size generalized extreme value (OPSGEV) model developed in Section 3.1, this chapter proposes an advanced bi-criteria stochastic user equilibrium (BSUE) model for congested road networks with tolls. In equilibrium traffic assignment considering the tradeoff between cost and time, most of existing models are formulated using path flows as the decision variables (Dial, 1996; Yang and Huang, 2004; Huang and Li, 2007; Sun et al., 2019). While few efforts have been made to incorporate the information of ranking of path toll. Leurent (1993) proposed an MP formulation that implicitly considers the order of path toll in the objective function. On this basis, Xie et al. (2021) modified Leurent's MP formulation to consider the path order information by using the cut-off points to distinguish the travel demand assigned to each pair of paths with adjacent orders of tolls. With the integration of path ordering, the model formulation can better capture the time-cost tradeoff among the heterogenous travelers. However, the path order information is mainly introduced at the aggregate level of the MP formulation, which lacks behavioral interpretation at the individual route choice level that can explicitly consider both perceptual and physical correlations.

Furthermore, the equilibrium route choice in tolled networks is often modeled by combining travel time and monetary cost in a generalized travel cost/time term, which cannot fully capture travelers' decision-making behavior. Wang and Ehrgott (2013) proposed a more general concept, i.e., time surplus, which has solid foundation from the decision-making theory and can be adopted in the Beckmann-type MP formulation to flexibly replicate the bi-objective user equilibrium (BUE) condition. However, it assumes travelers have perfect knowledge of the transportation network condition and ignores subjective uncertainties of travelers. Ehrgott et al. (2015) proposed a multi-objective stochastic user equilibrium model to further consider the random perceptions of all path attributes. However, the MNL-based MSUE model cannot capture the

various types of path correlations, and it also lacks an MP formulation that allows for easy interpretation of optimality conditions and development of efficient solution algorithm.

Motivated by the abovementioned issues, this chapter aims to develop an advanced BSUE traffic assignment model while specifically accounting for the effect of path ordering information, which is an important path attribute in tolled networks. A new Beckmann-type MP formulation is developed to bridge the OPSGEV route choice model developed in Section 3.1 to the aggregate time-surplus-based BSUE model. Benefiting from the integrated OPSGEV model, the perceptual correlation associated with ranking of path toll and the physical correlation arising from path overlap can be simultaneously considered. Furthermore, to model subjective uncertainties in the tradeoff between cost and time, the time surplus concept is extended to consider random perception of the path travel time together with physical and perceptual path correlations. In the developed MP formulation, the path order information is explicitly integrated in the decision variables and both types of path correlations are considered in the objective function, which provides a behavioral interpretation of individual route choice behavior in tolled networks following the random utility maximization principle.

6.2 Integrating the OPSGEV model in the time-surplus-based bi-objective equilibrium analysis

6.2.1 Perceived time surplus maximization bi-objective stochastic user equilibrium

This section introduces the perceived time surplus to further account for the tradeoff between cost and time. To start with, we briefly review the concept of time surplus originally proposed by Wang and Ehrgott (2013), which is more general than the commonly used generalized travel cost and has sound economic interpretation for decision making. The time surplus on path *k* between OD pair *rs*, TS_k^{rs}, is defined as

the difference between the maximum travel time travelers willing to spend, $t^{\max}\left(c_k^{rs}\right)$, and the actual travel time t_k^{rs}:

$$TS_k^{rs} = t^{\max}\left(c_k^{rs}\right) - t_k^{rs}, \tag{6.1}$$

where $t^{\max}\left(c_k^{rs}\right)$ can be obtained based on a decreasing indifference curve with respect to the path toll c_k^{rs} (Wang and Ehrgott, 2013). Figure 6.1 provides a simple illustration of time surplus used in the BUE analysis.

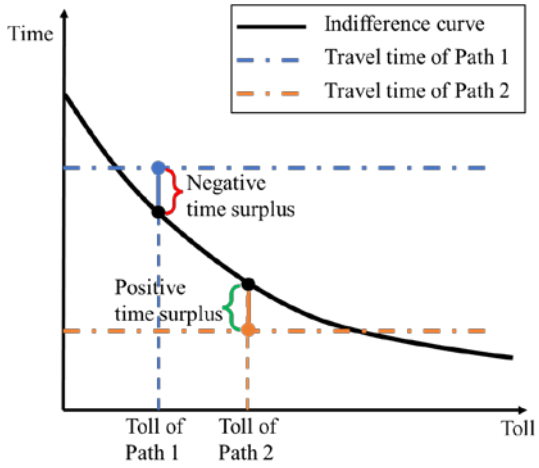

Figure 6.1. Illustration of time surplus in BUE analysis

The above time surplus illustration is constructed based on deterministic monetary cost and travel time, which does not consider the subjective uncertainties of travelers. Although the tolling scheme is predetermined and well disseminated, travelers may have imperfect knowledge of the travel time in the tolled network. In this chapter, we consider travelers have random perception errors on the flow-dependent travel time but know the toll on each path. Hence, the perceived time surplus can be defined as the difference between the maximum travel time willing to spend and the perceived travel time. Consistent with the widely used logit-based travel choice models, the travel time perception is assumed to follow the reversed Gumbel distribution. The perceived time surplus can then be expressed as follows:

$$\begin{aligned} PTS_k^{rs}\left(c_k^{rs},\mathbf{f}\right) &= t^{\max}\left(c_k^{rs}\right) - T_k^{rs}\left(\mathbf{f}\right) \\ &= t^{\max}\left(c_k^{rs}\right) - \left[t_k^{rs}\left(\mathbf{f}\right) - \varepsilon_k^{rs}\right] = TS_k^{rs}\left(\mathbf{f}\right) + \varepsilon_k^{rs}, \forall k \in K^{rs}, rs \in RS \end{aligned} . \quad (6.2)$$

where $T_k^{rs}\left(\mathbf{f}\right)$ denotes the perceived travel time, and ε_k^{rs} is the Gumbel distributed error term. Compared with the time surplus described in Figure 6.1, the perceived time surplus illustrated in Figure 6.2 is no longer deterministic, but Gumbel distributed due to the consideration of random travel time perception.

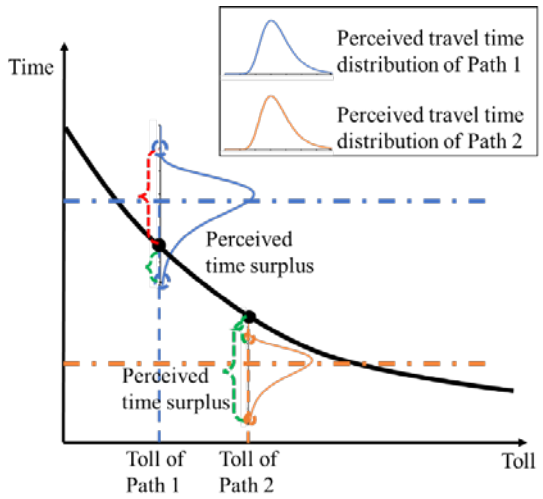

Figure 6.2. Illustration of perceived time surplus

On this basis, we define the perceived time surplus maximization bi-objective stochastic user equilibrium (PTSmaxBSUE) as follows:

Definition 1. Under the PTSmaxBSUE conditions, all individuals are travelling on the path with the maximum perceived time surplus among all the paths between each OD pair, i.e.,

$$f_k^{rs} = q^{rs} \cdot P_k^{rs}\left[PTS_k^{rs}\left(c_k^{rs},\mathbf{f}\right) \geq PTS_l^{rs}\left(c_l^{rs},\mathbf{f}\right), \forall l \neq k \in K^{rs}\right], \forall k \in K^{rs}, rs \in RS . \quad (6.3)$$

The OPSGEV route choice model can then be encapsulated in the PTSmaxBSUE condition to account for both path order correlation and path overlap in the perceived time surplus framework. The utility function (3.1) is substituted with the perceived time

surplus, where the systematic utility v_k^{rs} is represented by time surplus TS_k^{rs}. Owing to Property 4 of the Gumbel distribution (Table 2.1), subtracting a constant from each alternative will not change the logit-based choice probability. An equivalent OPSGEV utility function can be obtained by subtracting $t^{\max}(0)$ from TS_k^{rs} in Eq. (3.1):

$$V_{uk}^{rs} = -\tau_k^{rs} + \frac{1}{\theta_k}\ln PS_k^{rs} + \frac{1}{\theta_u}\ln w_{uk}^{rs} + \varepsilon_{uk}^{rs} + \varepsilon_u^{rs}, \forall k \in K_u, u \in U^{rs}, rs \in RS, \quad (6.4)$$

where the systematic utility v_k^{rs} is represented by TS_k^{rs} and hence replaced with $-\tau_k^{rs}$. τ_k^{rs} is a disutility term introduced to facilitate constructing the equivalent Beckmann-type MP formulation for the PTSmaxBSUE condition:

$$\begin{aligned}\tau_k^{rs} &= -TS_k^{rs} + t^{\max}(0) \\ &= t_k^{rs} + \left[t^{\max}(0) - t^{\max}\left(c_k^{rs}\right)\right],\end{aligned} \quad (6.5)$$

Based on the utility function (6.4), the OPSGEV model can be incorporated into Eq. (3.6) to derive the corresponding route choice probability P_k^{rs}.

6.2.2 Formulation of OPSGEV-based PTSmaxBSUE model

Figure 6.3 demonstrates bridging the OPSGEV individual route choice model to the MP formulation of the aggregate path-correlation-based PTSmaxBSUE model. Based on the utility function (6.4) and choice structure of the OPSGEV model (Figure 3.2), the decision variable f_{uk}^{rs} inherently incorporates path order information based on the path subset *u* determined using the ranking of path tolls. The conservation, definitional, and nonnegativity constraints can be written according to the decision variable. Terms in the objective function can be derived associated with the marginal and conditional choice levels and composite disutility in consistent with the hierarchical choice structure.

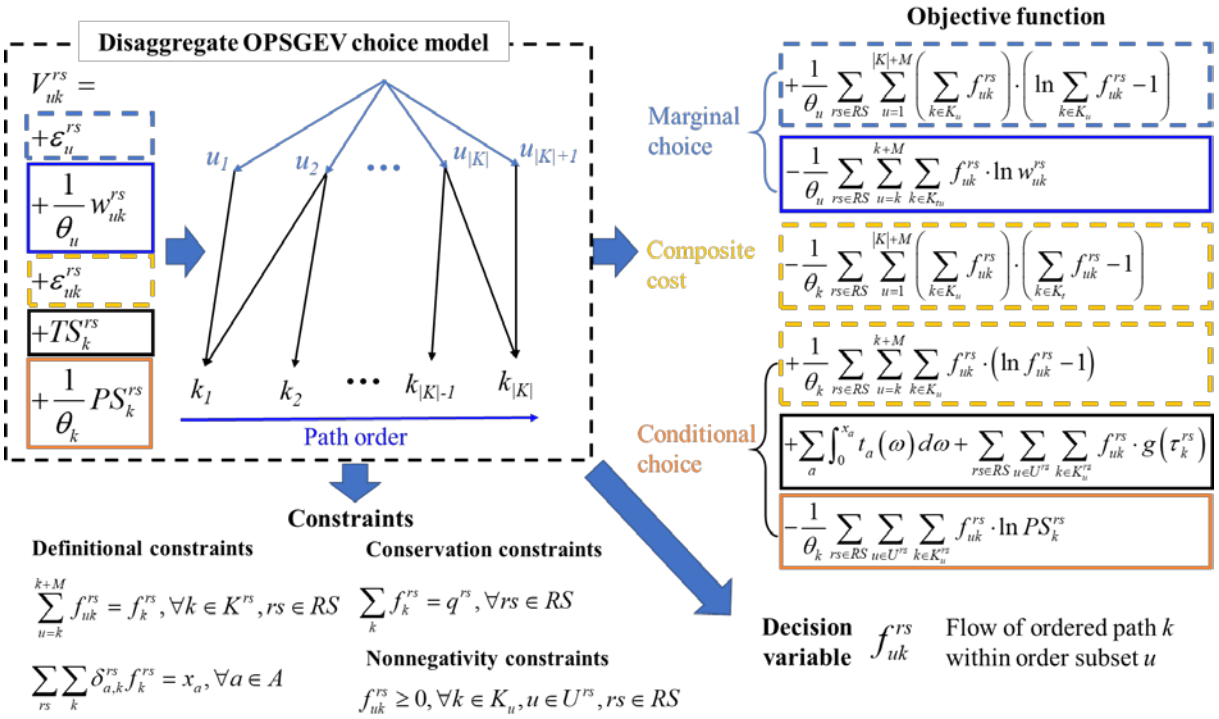

Figure 6.3. Illustration of formulating aggregate traffic assignment model based on OPSGEV route choice model

Following Figure 6.3, the OPSGEV-based PTSmaxBSUE model is formulated as

$$\begin{aligned}\min Z = &\sum_a \int_0^{x_a} t_a(\omega)\,d\omega + \sum_{rs\in RS}\sum_{k\in K^{rs}} f_k^{rs}\cdot g\left(\tau_k^{rs}\right)\\ &+\frac{1}{\theta_k}\sum_{rs\in RS}\sum_{u=1}^{|K^{rs}|+M}\sum_{k\in K_u^{rs}} f_{uk}^{rs}\cdot\left(\ln f_{uk}^{rs}-1\right)\\ &-\frac{1}{\theta_k}\sum_{rs\in RS}\sum_{k\in K^{rs}} f_k^{rs}\cdot\ln PS_k^{rs}\\ &+\left(\frac{1}{\theta_u}-\frac{1}{\theta_k}\right)\sum_{rs\in RS}\sum_{u=1}^{|K^{rs}|+M}\left(\sum_{k\in K_u^{rs}} f_{uk}^{rs}\right)\cdot\left(\ln\sum_{k\in K_u^{rs}} f_{uk}^{rs}-1\right)\\ &-\frac{1}{\theta_u}\sum_{rs\in RS}\sum_{u=1}^{|K^{rs}|+M}\sum_{k\in K_u^{rs}} f_{uk}^{rs}\cdot\ln w_{uk}^{rs}\end{aligned} \tag{6.6}$$

s.t.

$$\sum_{u=k}^{k+M} f_{uk}^{rs} = f_k^{rs},\ \forall k\in K^{rs}, rs\in RS \tag{6.7}$$

$$\sum_{rs\in RS}\sum_{k\in K^{rs}} \delta_{a,k}^{rs} f_k^{rs} = x_a, \forall a \in A \tag{6.8}$$

$$\sum_{k\in K^{rs}} f_k^{rs} = q^{rs}, \forall rs \in RS \tag{6.9}$$

$$f_{uk}^{rs} \geq 0, \forall k \in K_u^{rs}, u \in U^{rs}, rs \in RS \tag{6.10}$$

Objective function (6.6) corresponds to the equilibrium route choice pattern based on the OPSGEV model given in Eq. (3.6). Constraints (6.7) and (6.8) are the definitional constraints. Constraint (6.9) is the conservation constraint. Constraint (6.10) is the nonnegative constraint. To show some qualitative properties of the proposed MP formulation, two propositions are stated as follows:

Proposition 6.1. The proposed MP formulation (6.6)–(6.10) gives the equilibrium path flow pattern of the OPSGEV model.

Proof. See Appendix A1 for detailed proof.

Proposition 6.2. The path and link flow solutions to the MP formulation (6.6)–(6.10) are unique.

Proof. See Appendix B1 for detailed proof.

6.3 Numerical examples

6.3.1 Toy network

This section illustrates the properties of the proposed equilibrium model based on the small network as shown in Figure 6.4. The model parameters are $\theta_k = 0.1$, $\theta_u = 0.05$, $M = 2$, $w_{uk}^{rs} = 0.5$. The travel demand from node 1 to node 6 is 100 veh/hour. The link attributes and path attributes are presented in Tables 6.1 and 6.2. The link travel times are calculated via the Bureau of Public Roads (BPR) function:

$$t_a\left(x_a\right)=t_a^0\cdot\left[1+0.15\left(\frac{x_a}{Cap_a}\right)\right]^4 \tag{6.11}$$

There are three paths connecting nodes 1 and 6, i.e., path 1 with no toll, path 2 with a medium toll \$20, and path 3 with a high toll \$40. The indifference travel times $t^{\max}\left(c_k^{rs}\right)$ are specified at the last column of Table 6.2.

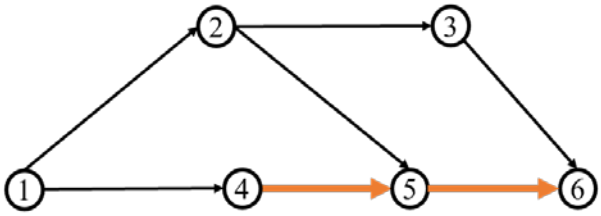

Figure 6.4. Toy network with tolled roads
(adapted from Li et al., 2023)

Table 6.1. Link attributes of toy network

Link	Free-flow travel time (min)	Capacity (veh/hour)	Toll (\$)
1-2	20	50	0
1-4	20	50	0
2-3	20	50	0
2-5	20	50	0
3-6	20	50	0
4-5	10	50	20
5-6	10	50	20

Table 6.2. Path attributes of toy network

ID	Path	Free-flow travel time (min)	Toll (\$)	Rank	$t^{\max}\left(c_k^{rs}\right)$
1	1-2-3-6	60	0	3	70
2	1-2-3-5-6	50	20	2	60
3	1-4-5-6	40	40	1	50

6.3.1.1 Model outcomes

This section presents the outcomes of the proposed OPSGEV-PTSmaxBSUE model and compares it with competing models, including the TSmaxBUE model without considering perception error, the MNL-PTSmaxBSUE model without considering path

correlations, the PSL-PTSmaxBSUE model focusing on the physical correlation only, and the OGEV- PTSmaxBSUE focusing on the perceptual correlation only.

The values of objective terms are summarized in Table 6.3. The objective function is separated into three parts, i.e., $Z_1 = \sum_a \int_0^{x_a} t_a(\omega)\, d\omega + \sum_{rs \in RS} \sum_{k \in K^{rs}} f_k^{rs} \cdot g\left(\tau_k^{rs}\right)$ as the Beckmann term representing deterministic path disutility (opposite of time surplus), $Z_2 = \frac{1}{\theta_k} \sum_{rs \in RS} \sum_{u=1}^{|K^{rs}|+M} \sum_{k \in K_u^{rs}} f_{uk}^{rs} \cdot \left(\ln f_{uk}^{rs} - 1\right) - \frac{1}{\theta_k} \sum_{rs \in RS} \sum_{k \in K^{rs}} f_k^{rs} \cdot \ln PS_k^{rs}$ as the entropy term that corresponds to the conditional choice level considering physical correlations, and $Z_3 = \left(\frac{1}{\theta_u} - \frac{1}{\theta_k}\right) \sum_{rs \in RS} \sum_{u=1}^{|K^{rs}|+M} \left(\sum_{k \in K_u^{rs}} f_{uk}^{rs} \right) \cdot \left(\ln \sum_{k \in K_u^{rs}} f_{uk}^{rs} - 1 \right) - \frac{1}{\theta_u} \sum_{rs \in RS} \sum_{u=1}^{|K^{rs}|+M} \sum_{k \in K_u^{rs}} f_{uk}^{rs} \cdot \ln w_{uk}^{rs}$ as the entropy term that corresponds to the marginal choice level considering perceptual correlations. As can be expected, the consideration of perception error increases the usage of inferior paths and hence increases the values of Z_1 in the four PTSmaxBSUE models. By incorporating different path correlations, the PSL-, OGEV-, and OPSGEV-PTSmaxBSUE models have lower values of Z_1 than the MNL-PTSmaxBSUE model. In particular, the proposed OPSGEV-PTSmaxBSUE model accounts for both physical and perceptual path correlations and has the lowest value of Beckmann term (Z_1) but the highest value of entropy terms ($Z_2 + Z_3$).

Table 6.3. Comparison of objective terms

	TSmaxBUE	MNL-PTSmaxBSUE	PSL-PTSmaxBSUE	OGEV-PTSmaxBSUE	OPSGEV-PTSmaxBSUE
Z_1	6129.644	6157.045	6148.413	6151.492	6144.563
Z_2	\	2523.659	2736.924	1844.468	2054.621
Z_3	\	\	\	3614.754	3613.163

Figure 6.5 further compares the time surplus and flow of each path resulted from the different models. The TSmaxBUE model leads to an equal time surplus for each path, a relatively low traffic flow on Path 2, and relatively high flows on Paths 1 and 3.

The PTSmaxBSUE models tend to have more diverse path flow patterns and different path time surplus. Owing to the incorporation of perception error, Path 2 carries a larger travel demand with lower time surplus. The PSL-, OGEV-, and OPSGEV-PTSmaxBSUE models have more similar time surplus and path flow patterns to the TSmaxBUE model than the MNL-PTSmaxBSUE model. These results are consistent with the observations from Table 6.3, which can be attributed to the consideration of path correlations. The introduction of objective terms with respect to path correlations, including the term related to physical correlation (i.e., $-\frac{1}{\theta_k}\sum_{rs\in RS}\sum_{k\in K^{rs}} f_k^{rs}\cdot\ln PS_k^{rs}$) in Z_2, and term Z_3 related to perceptual correlation, lowers the ratio of the diversification term indicating travelers' completely random choice behavior without considering path disutility (i.e., $\frac{1}{\theta_k}\sum_{rs\in RS}\sum_{u=1}^{|K^{rs}|+M}\sum_{k\in K_u^{rs}} f_{uk}^{rs}\cdot\left(\ln f_{uk}^{rs}-1\right)$).

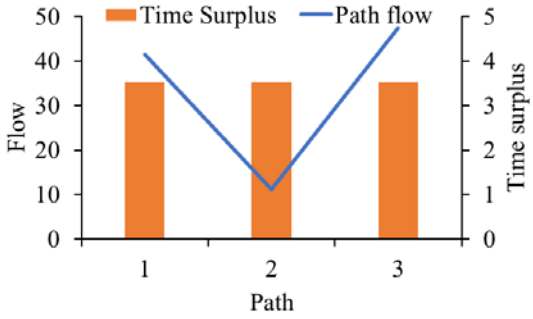

(a) TSmaxBUE

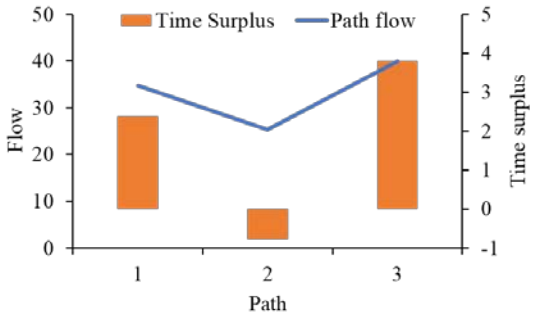

(b) MNL-PTSmaxBSUE

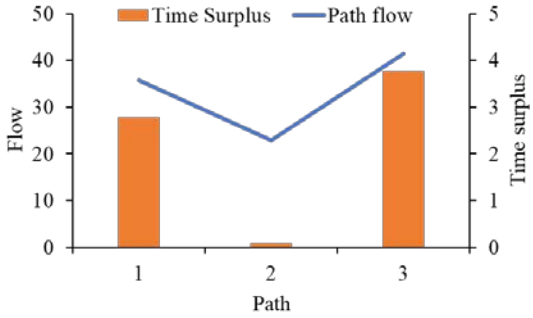

(c) PSL-PTSmaxBSUE

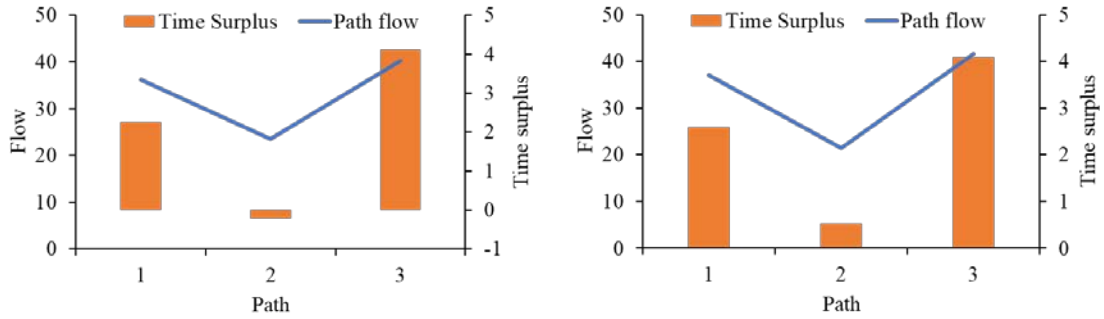

(d) OGEV-PTSmaxBSUE (e) OPSGEV-PTSmaxBSUE

Figure 6.5. Results of different bi-criteria traffic assignment models

6.3.1.2 Effect of path correlations

This section investigates the effect of physical and perceptual path correlations on the equilibrium assignment pattern. Figure 6.6 compares the performances of the four PTSmaxBSUE models in the toy network under varying degrees of physical path correlations (Figure 6.6(a)). With the decrease in path overlap, i.e., increasing value of the PS factor as shown in Figure 6.6(b), the OPSGEV- and PSL-PTSmaxBSUE models degenerate to the OGEV- and MNL-PTSmaxBSUE models, respectively. In the case when path overlap is extremely high (i.e., x=0), the physical correlation dominantly influences the route choice behavior, making the OPSGEV- and PSL-PTSmaxBSUE models result in similar path flows.

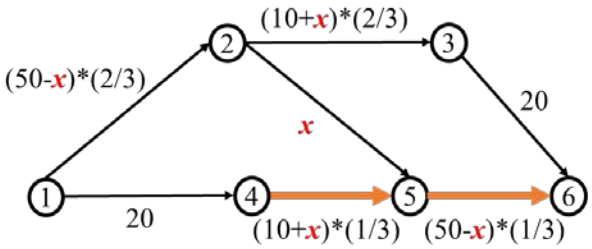

(a) Toy network with varying path overlaps

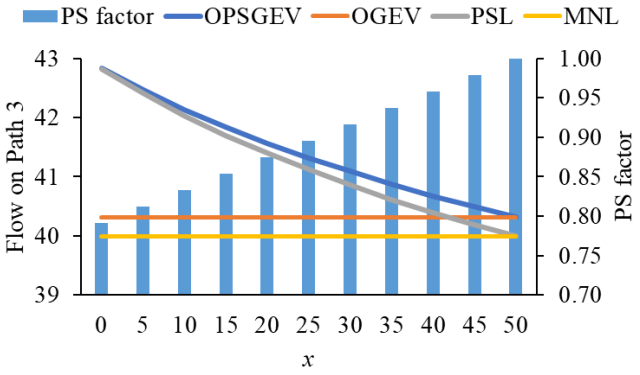

(b) Comparison of flow on Path 3

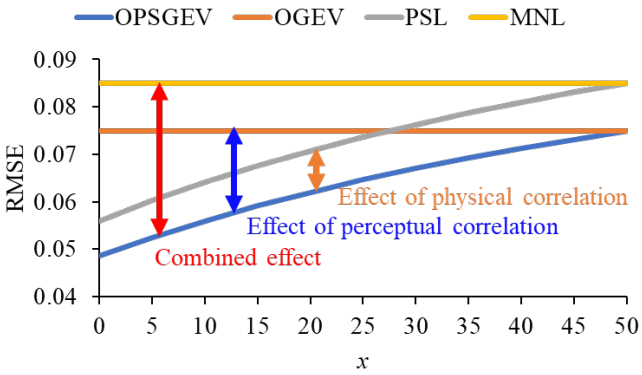

(c) Comparison of time surplus on Path 2

Figure 6.6. Comparison of model outcomes under varying path overlaps

Figure 6.6(c) investigates the difference in link flow patterns between the four PTSmaxBSUE models and the TSmaxBUE model. The root mean square error (RMSE) is adopted to compare the model results:

$$RMSE = \sqrt{\sum_{a \in A} \left(\frac{p_a - p_a^{UE}}{|A|} \right)^2}, \tag{6.12}$$

where p_a and p_a^{UE} denote the choice proportions of link a (ratio between link flow and total demand) that are obtained from the PTSmaxBSUE model and the TSmaxBUE model, respectively. $|A|$ is the number of links in the network. The comparison results are presented in Figure 6.6(c). The OPSGEV- and PSL-PTSmaxBSUE models have varying RMSE values dependent on the degree of path overlap, while the RMSE of OGEV- and MNL-PTSmaxBSUE models owing to the neglect of physical correlation.

The difference between the RMSE values of the four PTSmaxBSUE models implies different effects when considering physical and perceptual path correlations.

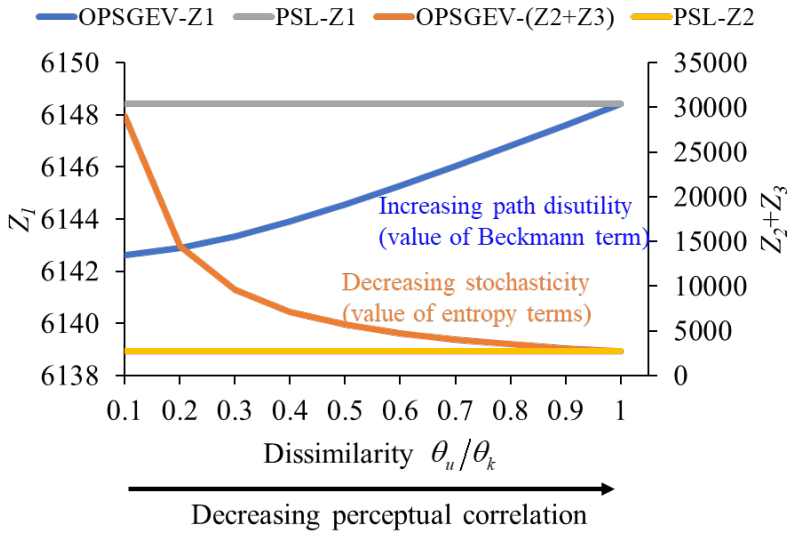

Figure 6.7. Effect of perceptual correlation

Figure 6.7 illustrates the effect of perceptual correlation based on the values of different objective terms. The *x* axis is the ratio between dispersion parameters θ_u/θ_k, which is the dissimilarity parameter in the OPSGEV-PTSmaxBSUE model. A higher value of the dissimilarity parameter implies lower perceptual path correlation and a lower degree of competition among adjacently ranked paths. With an increase in the dissimilarity parameter, the impact of perceptual correlation decreases, as the value of entropy terms decreases while the value of Beckmann term increases. When $\theta_u/\theta_k = 1$, the OPSGEV-PTSmaxBSUE model degenerates to the PSL-PTSmaxBSUE model.

6.3.2 Nguyen-Dupuis network

This section illustrates the applicability of the proposed model in the Nguyen-Dupuis network (Nguyen and Dupuis, 1984) as shown in Figure 6.8. Four OD pairs are considered, i.e., 1-2, 1-3, 4-2, and 4-3, with OD travel demands equal to 400, 800, 600, and 200 vehicles per hour, respectively. The link travel times are calculated as follows:

$$t_a = \alpha_a + \beta_a \cdot x_a . \tag{6.13}$$

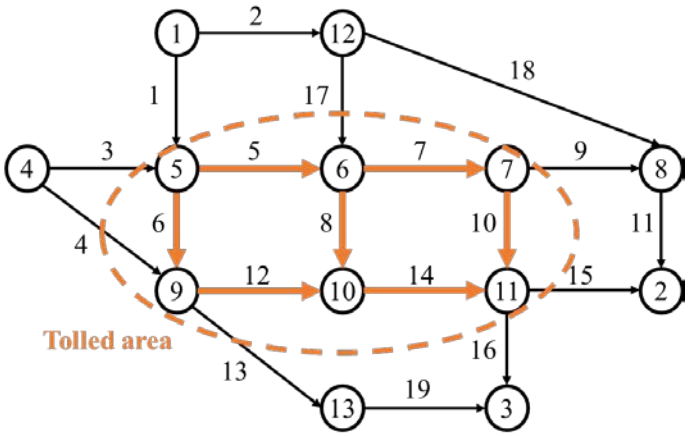

Figure 6.8. Nguyen-Dupuis network

In this experiment, the roads in the city center (i.e., links 5, 6, 7, 8, 10, 12, 14) are tolled. The values of α_a and β_a of each link and link tolls are presented in Table 6.4. Based on the road tolls, the toll on each path can be obtained. Between each pair, the paths are ranked according to path tolls. Attributes of the 25 paths connecting the four OD pairs are shown in Table 6.5.

Table 6.4. Link attributes of Nguyen-Dupuis network

Link	α_a	β_a	Toll ($)	Link	α_a	β_a	Toll ($)
1	7	0.0125	0	11	9	0.0125	0
2	9	0.01	0	12	10	0.005	10
3	9	0.01	0	13	9	0.005	0
4	12	0.005	0	14	6	0.0025	6
5	3	0.0075	3	15	9	0.005	0
6	9	0.0075	9	16	8	0.01	0
7	5	0.0125	5	17	7	0.0125	0
8	13	0.005	13	18	14	0.01	0
9	5	0.0125	0	19	11	0.01	0
10	9	0.0125	9				

Table 6.5. Path attributes of Nguyen-Dupuis network

OD	ID	Path	Free-flow travel time (min)	Toll ($)	Rank	$t^{\max}\left(c_k^{rs}\right)$
1-2	1	2-18-11	32	0	8	50
	2	1-5-7-9-11	29	8	6	46
	3	1-5-7-10-15	33	17	4	41.5
	4	1-5-8-14-15	38	22	2	39
	5	1-6-12-14-15	41	25	1	37.5
	6	2-17-7-9-11	35	5	7	47.5
	7	2-17-7-10-15	39	14	5	43
	8	2-17-8-14-15	44	19	3	40.5
1-3	9	1-6-13-19	36	9	6	45.5
	10	1-5-7-10-16	32	17	4	41.5
	11	1-5-8-14-16	37	22	2	39
	12	1-6-12-14-16	40	25	1	37.5
	13	2-17-7-10-16	38	14	5	43
	14	2-17-8-14-16	43	19	3	40.5
4-2	15	4-12-14-15	37	16	4	42
	16	3-5-7-9-11	31	8	5	46
	17	3-5-7-10-15	35	17	3	41.5
	18	3-5-8-14-15	40	22	2	39
	19	3-6-12-14-15	43	25	1	37.5
4-3	20	4-13-19	32	0	6	50
	21	4-12-14-16	36	16	4	42
	22	3-6-13-19	38	9	5	45.5
	23	3-5-7-10-16	34	17	3	41.5
	24	3-5-8-14-16	39	22	2	39
	25	3-6-12-14-16	42	25	1	37.5

We first investigate the effect of considering perception error on the bi-criteria traffic assignment in tolled networks. The link V/C ratios derived from the TSmaxBUE and MNL-PTSmaxBSUE models are compared in Figure 6.9. As shown in Figure 6.9(a), the TSmaxBUE model considers the deterministic choice of paths with the highest time surplus, which tends to assign traffic volumes on several key roads and lead to high V/C ratios on these links. On the other hand, the PTSmaxBSUE model tends to generate a more diverse path flow pattern, which diverts the flows on extremely congested road to relatively uncongested ones.

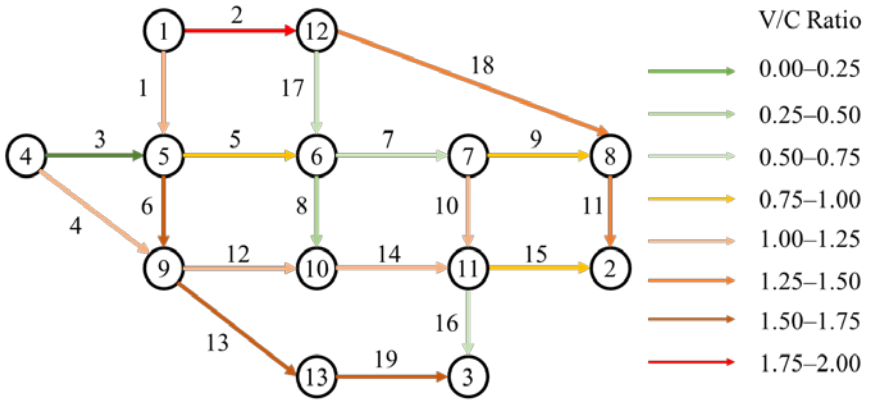

(a) TSmaxBUE model

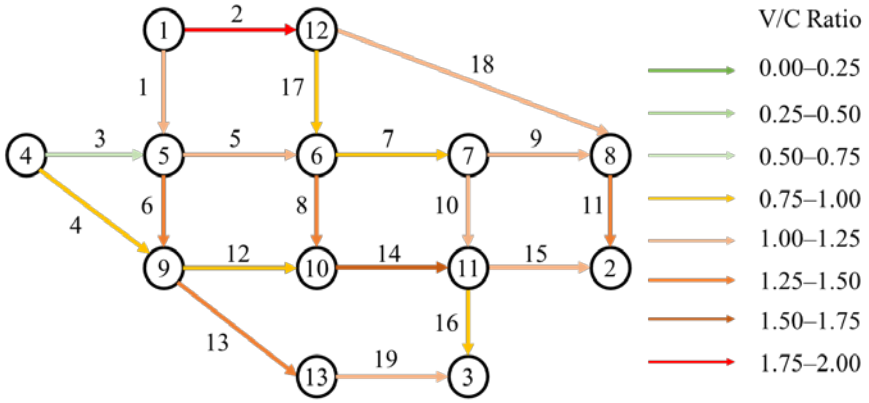

(b) MNL-PTSmaxBSUE model

Figure 6.9. Link V/C ratio patterns from different models

We then investigate the effects of path correlations based on the link flow difference patterns as shown in Figure 6.10. Figure 6.10(a) shows the link flow difference between the OPSGEV- and PSL-PTSmaxBSUE models, which implies the effect of considering the perceptual path correlation. Figure 6.10(b) shows the link flow difference between the OPSGEV- and OGEV-PTSmaxBSUE models, implying the effect of considering the physical path correction. In this experiment, both types of path correlations can significantly influence the model outcomes. The perceptual correlation has a more significant impact than the commonly modeled physical correlation, which implies the importance of considering both correlations in the bi-criteria traffic assignment for tolled networks.

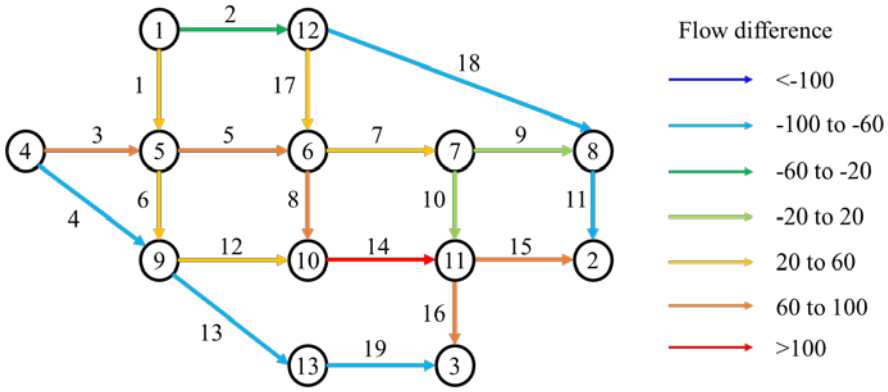

(a) OPSGEV-PTSmaxBSUE – PSL-PTSmaxBSUE

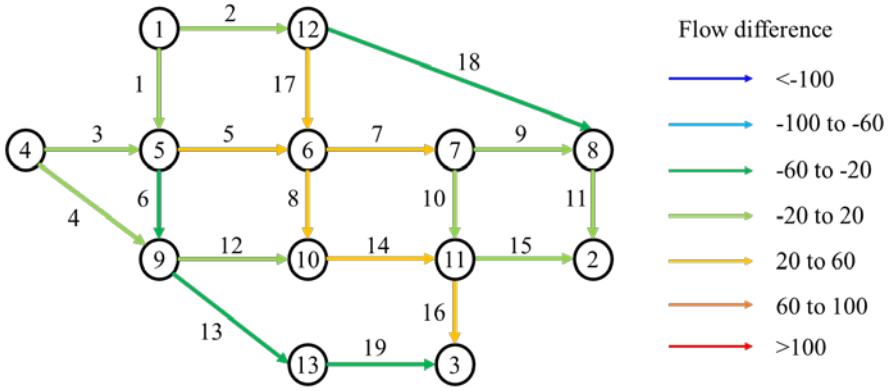

(b) OPSGEV-PTSmaxBSUE – OGEV-PTSmaxBSUE

Figure 6.10. Link flow difference between different models

6.4 Conclusions

This chapter makes an initial effort to introduce the perceptual path correlation in traffic assignment problem and to simultaneously consider the perceptual and physical path correlations in the bi-criteria equilibrium assignment for tolled networks. The two types of path correlations arise from the two important route choice criteria in tolled networks, namely the monetary cost and travel time. The time surplus concept recently proposed for bi-criteria traffic assignment (Wang et al., 2013) is extended to the perceived time surplus that considers the perception error of travel time, which has long been recognized an important concern in the traffic assignment (Sheffi, 1985). In this chapter, we focus on the single-class traffic assignment problem where all travelers are assumed to share the same time surplus function. On this basis, an advanced BSUE

model is proposed that integrates the OPSGEV route choice model (Section 3.1) to consider the travel time perception error as well as perceptual and physical path correlations. An equivalent Beckmann-type MP formulation is developed that facilitates the understanding and evaluation of the proposed BSUE model. Numerical experiments are conducted based on two networks to illustrate the advantages of the proposed model over existing models.

The proposed model could be explored in several other directions in future studies, as follows. (1) Besides the specific perceptual correlation arising from the ranking of path tolls, more types of perceptual correlation in different route choice contexts can be integrated in the proposed modeling framework. For instance, the paths traversing the same important link (e.g., bridge or tunnel) are likely to be perceived as correlated alternatives, which can be an important issue to consider in the traffic assignment (Habib et al., 2013). (2) In addition to focusing on a single user class, it is important to extend the proposed model to consider multiple classes of travelers with heterogeneous values of time (Wang et al., 2013; Li et al., 2023).

Chapter 7 Modeling mode choice of customized bus services with loyalty subscription schemes in multi-modal transportation systems

7.1 Introduction

7.1.1 Background

Based on the dogit-nested weibit (DNW) individual mode choice model developed in Section 3.2, this chapter models the long-term equilibrium mode choice in multi-modal transportation systems with the emerging customized bus (CB) services. In recent years, CB services have been extensively promoted in China to increase transit ridership and alleviate road congestion. CB services were first implemented in 2013 in Qingdao, and have since spread to over 30 Chinese cities, including Beijing, Shenzhen, and Nanjing, where they play important roles in public transportation (Huang et al., 2017). For example, more than 400 CB lines are operated in Beijing to meet commuting, education, and tourism demands, transporting 37,000 passengers per day (China National Radio, 2018). This rapid development of CB services might attract travelers who would otherwise use conventional modes, such as private cars and conventional public transit (PT), thereby influencing the modal demand pattern in urban multi-modal transportation systems. It is therefore imperative to understand the long-term effect of CB services on the modal split patterns of multi-modal transportation systems.

Table 7.1 summarizes innovative characteristics of CB services, which are thus considered a distinct travel mode that should be modeled differently to conventional travel modes (Gu et al., 2018; Huang et al., 2020a). As has been introduced in Section 3.2, CB services are an intermediate mode between conventional PT modes and the private car mode in terms of travel time, travel cost, and in-vehicle congestion. When compared to the conventional PT, CB has shorter travel time, higher fee, and more restricted operating times and lines only serving travelers with similar OD and departure/arrival time choices. When comparing to the private car, CB services are more economical and environmentally friendly and are often allowed to travel in dedicated bus lanes to alleviate road congestion (Liu et al., 2016).

Table 7.1. Characteristics of CB services and other transport modes.

	Conventional PT	Private car	CBs
Access distance	Long	NA	Short
Waiting time	Long	NA	Short
In-vehicle travel time	Long	Short	Medium
In-vehicle congestion	High	None	**None**
Service coverage	Medium	High	Low
Monetary cost	Low	High	Medium
Subscription	Not required	Not required	**Required**
Loyalty scheme	No	No	**Yes**

Note: PT = public transit.

Another unique characteristic of CB services is that they require passengers to subscribe to book a seat. As the number of seats on a CB line are limited, a subscription may not be available if all seats on a CB line are booked. A CB line will be considered as inoperable if the number of subscriptions fails to ensure a profitable occupancy rate. As illustrated in Section 3.2, the passenger loyalty stemming from the loyalty subscription scheme of CB services is also an important determinant of travel behavior. In summary, it is necessary to account for the characteristics of CB services when modeling mode choice in multi-modal systems that encompass conventional travel modes and emerging CB services.

7.1.2 Related studies

An increasing number of studies have been conducted on CB services and similar on-demand modes provided by transportation network companies (TNCs). Table 7.2 summarizes the studies on CB services. Many studies have focused on the tactical or operational level of CB services, and extensive efforts have been devoted to the design and optimization of CB operations, such as the service coverage, routes, stops, timetables, fleet sizes, passenger–vehicle assignment, and pricing of CB services.

Another important stream of studies has considered CB services in the contexts of travel demand analysis and the evaluation of transportation network performance. However, these studies have examined the day-to-day and within-day dynamics of the CB subscription process (i.e., operational aspects), which may not be adequate for modeling the long-term effects of CB services at the strategic level.

Table 7.2. Summary of CB service studies

Aim	References	Consideration	Main feature
Network design and optimization	Tong et al., 2017; Guo et al., 2018; Lyu et al., 2019; Qiu et al., 2019; Huang et al., 2020a; Dou et al., 2021; Ma et al., 2021; Wang et al., 2021b	Service coverage, route, stop, timetable, fleet size, passenger assignment, and fare pricing	Flexible and dynamic service design
Travel demand modeling	Djavadian and Chow, 2017; Gu et al., 2018; Li et al., 2018b; Huang et al., 2020b	Effect of introducing CB services on traffic flow and system performance	Day-to-day and within-day dynamic CB service subscriptions
Empirical choice behavior analysis	Li et al., 2019; Gadepalli et al., 2020; Wang et al., 2019, 2020b	Effect of CB services on travel choice behavior and passenger loyalty	Increased level of service; long-term subscription scheme
Reviews	Liu and Ceder 2015; Liu et al., 2016; Huang et al., 2017	Characteristics and development of CB services	All of the above

To investigate the long-term effects of CB services and other emerging on-demand modes (e.g., ride-hailing and ridesharing) on travelers' travel choice behavior, many studies have adopted statistical methods based on stated- and revealed-preference travel surveys and other supporting data (e.g., Choudhury et al., 2018; Xie et al., 2019; Yan et al., 2019a; Sweet, 2021; Erhardt et al., 2022). Equilibrium modeling framework has

also been developed for on-demand modes which share similar characteristics with the CB services. For instance, Pi et al. (2019) proposed a general dynamic equilibrium assignment model for short-term mode and route choices in the network with both conventional travel modes and emerging on-demand services. Di and Ban (2019) developed a unified equilibrium model focusing on the behavior of drivers and passengers of ridesharing and ride-hailing, where the travel choices are derived based on game theory. The market equilibrium approach has also been used to analyze the customer behavior of conventional and emerging on-demand services, such as taxis and ride-hailing (e.g., Yang et al., 2002; Yang and Yang, 2011; Wang et al., 2020c; Ke et al., 2021). Wang and Yang (2019) provided a systematic review of the ride-sourcing system and the equilibrium models for analyzing transportation systems with this emerging on-demand mode. However, to the best of the authors' knowledge, few equilibrium models have been developed for modeling the long-term mode choice in multi-modal systems with CB services based on the random utility theory. In addition, the effect of passenger loyalty is often not captured in existing equilibrium models.

7.1.3 Objectives and contributions

This chapter aims to make an initial effort to model the long-term modal split in multi-modal transportation systems while specifically considering innovative characteristics of the emerging CB services. As discussed above, the subscription process of CB services calls for the consideration of the limited numbers of available seats and the occupancy rate requirements, which should be regarded as tight constraints on the lower and upper limits of CB demand. Owing to the loyalty CB subscription schemes, passenger loyalty to CB services is to be explicitly considered in the developed equilibrium mode choice model.

A comprehensive mathematical model is developed for the long-term mode choice equilibrium problem in multi-modal transportation systems with emerging shared mobility modes like CB. An equivalent mathematical programming (MP) problem with tight constraints on the lower and upper limits of CB demand is formulated while

retaining consistent with the DNW choice model developed in Section 3.2. Benefiting from the embedded DNW model, various behavioral issues arising from CB services can be simultaneously addressed in the equilibrium analysis, including passenger loyalty, mode correlation, and heterogeneous mode perceptions. This enables the developed equilibrium model to better reproduce the distinct choice behaviors of members of CB loyalty subscription schemes and those who purchase one-time CB subscriptions.

7.2 Problem statement

To facilitate the presentation of the essential ideas without the loss of generality, the main model assumptions and multi-modal transportation system considered in this chapter are presented in Sections 7.2.1 and 7.2.2.

7.2.1 Assumptions

A7.1: This chapter considers three independent travel modes in the urban transportation system: a private car mode, conventional transit mode, and a CB mode.

A7.2: The conventional modes, i.e., private car mode and conventional transit mode, have sufficient capacity to accommodate all potential demand. The generalized travel times of conventional modes are separable, continuous, and monotonically increasing functions of modal demand. Drivers of private cars have demand-dependent in-vehicle travel time and OD-specific monetary costs for parking and fuel consumption. Passengers on conventional transit modes have fixed in-vehicle travel times, waiting times and access (walking) times, but have an in-vehicle crowding disutility dependent on the in-vehicle travel time and number of passengers (Lo et al., 2003; Li and Hensher, 2011; Liu and Lam, 2014; Wang et al., 2018).

A7.3: The in-vehicle travel time of CB is fixed. Because a seat is reserved for each passenger, CB passengers do not experience disutility from in-vehicle crowding. However, this characteristic leads to a tight capacity constraint for CB services, due to

the limited CB fleet size between each OD pair and the limited number of seats per CB. The CB capacity is designed to accommodate all long-term subscriptions but may not be enough for one-time subscriptions. If all CB seats are fully booked, the excess CB passengers will be unable to subscribe to their preferred services and will thus be forced to use less preferable travel modes (Gu et al., 2018; Huang et al., 2020a).

A7.4: Subscribers who purchase long-term CB tickets must pay the entire fare in advance; thus, they will be loyal to CB services, and tend not to consider using other modes (Wang et al., 2020b).

7.2.2 Notations

Set

RS	Set of OD pairs.
U^{rs}	Set of types of modes between OD pair *rs*.
M_u^{rs}	Set of modes of type *U* between OD pair *rs*.
M	Set of all modes.

Inputs and parameters

t_m^{rs}	Generalized travel time of mode *m* between OD pair *rs* (minute).
vot	Value of time (CNY/hour).
fc_{car}^{rs}	Fuel consumption of car between OD pair *rs* (CNY/km).
d^{rs}	Travel distance between OD pair *rs* (km).
pc	Car-parking cost (CNY).
f_m^{rs}	Fare of mode *m* between OD pair *rs* (CNY).
$t_{iv,m}^{rs}$	In-vehicle travel time of mode *m* between OD pair *rs* (minute).
$g\left(q_{PT}^{rs}\right)$	In-vehicle crowding discomfort cost per unit time (CNY/minute).
$t_{wt,m}^{rs}$	Waiting time of mode *m* between OD pair *rs* (minute).
$t_{wk,m}^{rs}$	Access (walking) time of mode *m* between OD pair *rs* (minute).
τ_m^{rs}	Travel disutility of mode *m* between OD pair *rs*.

τ_u^{rs}	Travel disutility of nest *u* between OD pair *rs*.
ψ^{rs}	Required seat-occupation rate of a CB line between OD pair *rs*
n_{seat}	Number of seats on one CB vehicle (persons/vehicle).
$\overline{n}_{CB}^{rs}$	Maximum number of CB vehicles between OD pair *rs* (vehicle).
$n_{CB}^{rs}{}'$	Normal number of vehicles in a CB fleet between OD pair *rs* (vehicle).
cap_m^{rs}	Capacity of mode *m* between OD pair *rs* (person).
ld_{CB}^{rs}	Lower limit of demand for operating CB between OD pair *rs* (person).
q^{rs}	Travel demand between OD *rs* (person).
β_{um}^{rs}	Shape parameter of mode *m* under nest *u* between OD pair *rs*.
β_u^{rs}	Shape parameter of nest *u* between OD pair *rs*.
η_m^{rs}	Loyalty parameter for mode *m* between OD pair *rs* in the dogit-based model.
Acc^{rs}	Utility-based accessibility between OD pair *rs*.
$Acc^{rs,b}$, $Acc^{rs,a}$	Utility-based accessibility between OD pair *rs* before and after implementation of certain policies.
E^{rs}	CO emissions between OD pair *rs* (gram/hour).

Decision variable

q_{um}^{rs}	Travel demand of type *u* mode *m* between OD *rs* (person).
qc_{um}^{rs}	Number of choice passengers choosing mode *m* under nest *u* between OD pair *rs*.
qc_u^{rs}	Number of choice passengers choosing nest *u* between OD pair *rs*.
$\omega_{cap}^{rs}, \omega_{ld}^{rs}$	Lagrangian variables associated side constraints on CB capacity and lower limit of CB demand between OD pair *rs*.
π^{rs}	Lagrangian variables associated with conservation constraints between OD pair *rs*.
q_m^{rs}	Travel demand of mode *m* between OD *rs* (person).

Note: PT = public transit; CB = customized bus.

7.2.3 Multi-modal transportation system with customized bus services

7.2.3.1 Private car

In accordance with A7.2, the generalized travel time of private car drivers between OD *rs* is as follows:

$$t_{car}^{rs} = t_{iv,car}^{rs}\left(q_{car}^{rs}\right) + \left(d_{rs} \cdot fc_{car}^{rs} + pc\right)\Big/vot, \forall rs \in RS, \tag{7.1}$$

where t_{car}^{rs} $t_{iv,car}^{rs}(\cdot)$, q_{car}^{rs}, and fc_{car}^{rs} respectively denote the generalized travel time, in-vehicle travel time, travel demand, and fuel consumption of the car mode between OD pair *rs*; d_{rs} denotes the travel distance between OD pair *rs*; *pc* denotes the car-parking cost; *vot* denotes the value of time, which is measured by cost/time (e.g., CNY/hour). The first term on the right-hand side (RHS) represents the increase in in-vehicle travel time with respect to car demand, and the latter terms give the distance-based cost for fuel consumption and the fixed parking cost (Liu et al., 2016). The car demand q_{car}^{rs} is derived from the equilibrium mode choice model developed in Section 7.3.

7.2.3.2 Conventional PT

In accordance with Assumption A7.2, the generalized travel time of conventional PT between OD pair *rs* is expressed as follows:

$$t_{PT}^{rs} = \left(t_{wk,PT}^{rs} + t_{wt,PT}^{rs}\right) + \left[g\left(q_{PT}^{rs}\right) \cdot t_{iv,PT}^{rs} + f_{PT}^{rs}\right]\Big/vot, \forall rs \in RS, \tag{7.2}$$

where t_{PT}^{rs}, q_{PT}^{rs}, $t_{iv,PT}^{rs}$, and f_{PT}^{rs} respectively denote the generalized travel time, travel demand, in-vehicle travel time, and fare of conventional PT between OD pair *rs*; $t_{wk,PT}^{rs}$ and $t_{wt,PT}^{rs}$ are the access (walking) and waiting time of conventional PT modes between OD pair *rs*; *g*(.) denotes the in-vehicle crowding discomfort cost per unit time. The terms on the RHS separately represent the access and waiting time, and the generalized travel time of in-vehicle traveling, which is affected by in-vehicle crowding discomfort and fare. The in-vehicle crowding discomfort cost is an increasing function with respect

to the in-vehicle travel time and the PT demand (Li and Hensher, 2011; Liu and Lam, 2014; Wang et al., 2018). The derivation of PT demand q_{PT}^{rs} is based on the equilibrium mode choice model developed in Section 7.3.

7.2.3.3 Customized bus

(1) CB operators

As this chapter focuses on the demand analysis rather than the design of CB services, it is assumed that the service characteristics of CB lines (e.g., route, timetable, fleet size, and fare price) are exogenously pre-determined by CB operators. Thus, two operational characteristics of CB services are considered:

(a) CB operators accept subscriptions if there are seats available in their fleet of CBs. A subscription will be rejected if all seats have been booked, i.e., the number of passengers that can subscribe to the CB line between OD pair *rs*, q_{CB}^{rs}, cannot exceed the capacity of the CB line between OD pair *rs*:

$$q_{CB}^{rs} \le cap_{CB}^{rs}, \forall rs \in RS, \tag{7.3}$$

where cap_{CB}^{rs} denotes the CB line capacity, which is given by the maximum fleet size between OD pair *rs*, $\overline{n}_{CB}^{rs}$, and the number of seats on each CB vehicle, n_{seat}, as follows:

$$cap_{CB}^{rs} = \overline{n}_{CB}^{rs} \cdot n_{seat}, \forall rs \in RS. \tag{7.4}$$

(b) A CB line between OD pair *rs* is put into operation only if the demand for this line is profitable, i.e., the number of passengers reaches a lower limit, ld_{rs}^{CB}.

$$q_{CB}^{rs} \ge ld_{CB}^{rs}, \forall rs \in RS, \tag{7.5}$$

In practice, the lower limit is defined by a CB service operator's required threshold of seat-occupation rate:

$$ld_{CB}^{rs} = \psi^{rs} \cdot n_{CB}^{rs\prime} \cdot n_{seat}, \forall rs \in RS, \tag{7.6}$$

where ψ^{rs} is the required seat-occupation rate and $n_{CB}^{rs\prime}$ is the normal size of a CB fleet operated between OD pair *rs*.

(2) CB passengers

The CB travel disutility includes on the generalized travel time, as well as the penalty and incentives incurred by the operational limits stated above, such as the risk of failed subscription owing to the limited capacity and the improved service quality to attract enough passengers. The generalized travel time of CB, t_{CB}^{rs}, can be derived based on the CB in-vehicle travel time, waiting time, access time, and the CB fare:

$$t_{CB}^{rs} = t_{iv,CB}^{rs} + t_{wt,CB}^{rs} + t_{wk,CB}^{rs} + f_{CB}^{rs} / vot, \forall rs \in RS. \tag{7.7}$$

Although the CB generalized travel time is not explicitly dependent on the CB demand for a given in-vehicle travel time and fare price, the travel disutility of CB services is implicitly influenced by the disutility incurred when CB demand violates the upper limit (Eq. (7.3)) or lower limit (Eq. (7.5)). This will be discussed in Section 7.3.2.

7.3 Equilibrium mode choice model with passenger loyalty

7.3.1 Model formulation

This section presents the equivalent MP of the equilibrium mode choice model for the multi-modal transportation system with CB services described in Section 7.2.3. The DNW probability presented in Section 3.2 is adopted in the equilibrium mode choice model because it suitably reflects the period-to-period subscription of loyal passengers to loyalty schemes and provides a direct interpretation of the effect of loyalty. Different from the individual DNW choice model with exogeneous travel disutility, the demand-dependent mode disutility is endogenously reproduced in the equilibrium model to

consider interaction among travelers. Based on the method introduced in Chapter 5, the MP formulation of the equilibrium model is developed as follows:

$$\begin{aligned}\min Z = & \sum_{rs\in RS}\sum_{u\in U^{rs}}\sum_{m\in M_u^{rs}}\int_0^{q_{um}^{rs}} \ln \tau_m^{rs}(\omega)d\omega - \\ & + \sum_{rs\in RS}\sum_{u\in U^{rs}}\sum_{m\in M_u^{rs}} \frac{1}{\beta_{um}^{rs}} \cdot \left(q_{um}^{rs} - \frac{q^{rs}\eta_m^{rs}}{1+\sum_{m\in M_{rs}}\eta_m^{rs}} \right) \left[\ln\left(q_{um}^{rs} - \frac{q^{rs}\eta_m^{rs}}{1+\sum_{m\in M^{rs}}\eta_m^{rs}} \right) - 1 \right] \\ & + \sum_{rs\in RS}\sum_{u\in U^{rs}} \left(\frac{1}{\beta_u^{rs}} - \frac{1}{\beta_{um}^{rs}} \right) \cdot \left[\sum_{m\in M_u^{rs}} \left(q_{um}^{rs} - \frac{q^{rs}\eta_m^{rs}}{1+\sum_{m\in M^{rs}}\eta_m^{rs}} \right) \right] \left[\ln \sum_{m\in M_u^{rs}} \left(q_{um}^{rs} - \frac{q^{rs}\eta_m^{rs}}{1+\sum_{m\in M^{rs}}\eta_m^{rs}} \right) - 1 \right]\end{aligned} \tag{7.8}$$

s.t.

$$\sum_{u\in U^{rs}}\sum_{m\in M_u^{rs}} q_{um}^{rs} = q^{rs}, \forall rs \in RS \tag{7.9}$$

$$q_{CB}^{rs} \le cap_{CB}^{rs}, \forall rs \in RS \tag{7.10}$$

$$q_{CB}^{rs} \ge ld_{CB}^{rs}, \forall rs \in RS \tag{7.11}$$

$$q_{um}^{rs} \ge 0, \forall m \in M_u^{rs}, u \in U^{rs}, rs \in RS \tag{7.12}$$

Objective function (7.8) aims to find the equilibrium modal demand based on the DNW model. The first term in Eq. (7.8) is the multiplicative Beckmann term, which indicates the mode travel disutility. The link-level travel time function is implicitly considered in the mode travel disutility as the route choice dimension is not focused by this chapter. The second and third terms are entropy terms that collectively account for the dogit-based choice behavior of loyal passengers and the nested choice structure of choice passengers. Conservation constraint (7.9) indicates the relationship between modal demand and OD demand. Capacity constraint (7.10) provides the upper limit of the number of CB passengers that can be served by the CB line between each OD pair. The lower limit of demand for maintaining the operation of an existing CB line is given by constraint (7.11). Constraint (7.12) is the nonnegative constraint. To show some

qualitative properties of the proposed MP formulation, the following two propositions are stated.

Proposition 7.1. The proposed MP formulation (7.8)–(7.12) gives the equilibrium mode choice solution of the DNW model presented in Eqs. (3.15)– (3.16).

Proof. See Appendix A2 for the detailed proof.

Proposition 7.2. If Assumptions A7.2 and A7.3 hold, the modal demand solutions to the MP formulation (7.8)–(7.12) are unique.

Proof. See Appendix B2 for detailed proof.

7.3.2 Effect of operational limits of CB lines

Unlike the explicitly demand-dependent generalized travel time of conventional modes, the CB disutility is not only determined by a demand-independent generalized travel time τ_{CB}^{rs} (owing to the fixed fare and in-vehicle travel time), but also implicitly influenced by the limits of CB demand. As shown in the proof of Proposition 7.1, the CB disutility $v_{CB}^{rs}\left(\tau_{CB}^{rs}, \omega_{cap}^{rs}, \omega_{ld}^{rs}\right)$ also includes two Lagrangian variables ω_{cap}^{rs} and ω_{ld}^{rs}, which are related to the tight constraints (7.10) and (7.11) on CB demand, respectively. The effect of the upper and lower limits of CB demand is depicted in Figure 7.1.

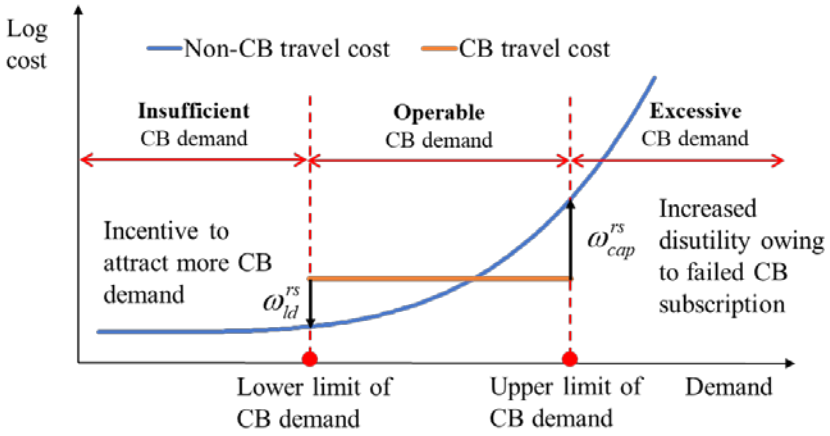

Figure 7.1. Illustration of tight constraints on CB demand

In the proposed model, ω_{cap}^{rs} and ω_{ld}^{rs} can be interpreted as the potential increase and decrease in travel disutility, respectively, when CB demand violates the upper or lower limit. Specifically, ω_{cap}^{rs} represents the potential fare increase or the risk of failed subscription when all seats are booked, i.e., the increased disutility of a passenger being unable to choose his/her preferred CB services, whereas ω_{ld}^{rs} represents the potential incentives set by operators (e.g., a fare decrease) to attract sufficient passengers to make CB line operation viable.

7.3.3 Model degeneration

This section presents the relationship between the developed DNW equilibrium model and other equilibrium choice models shown in Figure 7.2. First, the DNW model can be degenerated by ignoring passenger loyalty: if the loyalty parameter η_m^{rs} is set to zero, the DNW model degenerates to the NW model. This further degenerates to the MNW model if $\beta_u^{rs} / \beta_{um}^{rs} = 1$. Another approach is to ignore mode correlation and heterogeneity. If $\beta_u^{rs} / \beta_{um}^{rs} = 1$, the DNW model degenerates to the dogit-MNW (DMNW) model, which assumes there is no correlation between modes. Alternatively, by assuming the DNW model contains a Gumbel-distributed random error term, the DNW model degenerates to the dogit-NL (DNL) model and the dogit model, which assumes no heterogeneity in mode perceptions (Gaudry and Dagenais, 1979; Wang et al., 2020a). Then, if η_m^{rs} is set to zero, the dogit model further degenerates to the well-known MNL model. Finally, the equilibrium mode choice model collapses to the user equilibrium (UE) model if travelers have no perception error (i.e., $\beta_{um}^{rs} \to +\infty$).

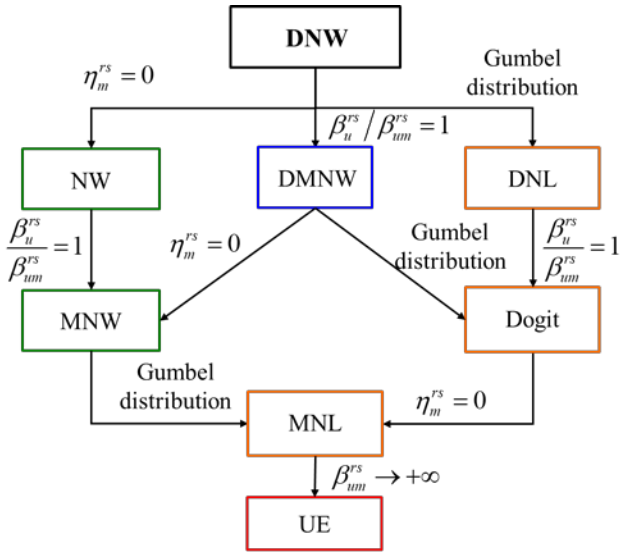

Figure 7.2. Relationship between DNW and other equilibrium choice models

7.3.4 Solution algorithm

The proposed model (7.9)–(7.12) is solved by the partial linearization algorithm as introduced in Section 5.3. An iterative balancing procedure is developed to find the search direction for the equilibrium DNW choice model with side constraints (Ryu et al., 2014). For simplicity, we use $qc_{um}^{rs} = q_{um}^{rs} - \frac{q^{rs}\eta_m^{rs}}{1+\sum_{m\in M}\eta_m^{rs}}$ to represent the choice passengers choosing mode m under nest u, $qc_u^{rs} = \sum_{m\in M_u^{rs}} qc_{um}^{rs}$ to represent the choice passengers choosing nest u, and $qc^{rs} = \sum_{u\in U^{rs}} qc_u^{rs}$ to represent the choice passengers between OD pair rs. The iterative balancing procedure are specified as follows:

Step 0. Initialization.

- Set iteration counter $n = 0$;
- Initialize dual variables associated with constraints (7.9)-(7.11):

  Set $\left(\pi^{rs}\right)^0, \left(\omega_{cap}^{rs}\right)^0, \left(\omega_{ld}^{rs}\right)^0 = 0, \forall rs \in RS$;
- Initialize primal variables based on free-flow mode disutility and dual variables:

$$\left(qc_u^{rs}\right)^0 = \left[\sum_{m\in M_u^{rs}}\left(\tau_{um}^{rs}(0)\cdot e^{\left(\omega_{cap}^{rs}-\omega_{ld}^{rs}\right)}\right)^{-\beta_{um}^{rs}}\right]^{\frac{\beta_u^{rs}}{\beta_{um}^{rs}}}\cdot e^{\beta_u^{rs}\cdot\pi^{rs}},$$

$$\left(qc_{um}^{rs}\right)^0 = \left(\tau_{um}^{rs}(0)\cdot e^{\left(-\pi^{rs}+\omega_{cap}^{rs}-\omega_{ld}^{rs}\right)}\right)^{-\beta_{um}^{rs}}\cdot\left(qc_u^{rs}\right)^{\left(1-\frac{\beta_{um}^{rs}}{\beta_u^{rs}}\right)}$$

Step 1. Update dual variables.

The dual variables can be viewed as corrections to the travel disutility, which can be used to adjust the primal variables (Eqs. (A2.3) and (A2.6)). Specifically, dual variables ω_{cap}^{rs} and ω_{ld}^{rs} are zero if the capacity constraint (7.10) and lower limit of CB demand (7.11) are satisfied by the resulted primal variables. If constraints (7.10)–(7.11) are binding, ω_{cap}^{rs} and ω_{ld}^{rs} will become non-zero. Following equations are used in this step to adjust each dual variable that can steer primal variables to meet constraints (7.9)–(7.11) (Ryu et al., 2014):

- $\left(\pi^{rs}\right)^{n+1} = \left(\pi^{rs}\right)^n + \frac{1}{\beta_u^{rs}}\ln\left(\frac{qc^{rs}}{\sum_{u\in U_{rs}}\left(qc_u^{rs}\right)^n}\right)$
- $\left(\omega_{cap}^{rs}\right)^{n+1} = \text{Max}\left\{0, \left(\omega_{cap}^{rs}\right)^n - \frac{1}{\beta_{um}^{rs}}\ln\left(\frac{cap_{CB}^{rs}}{\left(q_{CB}^{rs}\right)^n}\right)\right\}$
- $\left(\omega_{ld}^{rs}\right)^{n+1} = \text{Max}\left\{0, \left(\omega_{ld}^{rs}\right)^n + \frac{1}{\beta_{um}^{rs}}\ln\left(\frac{ld_{CB}^{rs}}{\left(q_{CB}^{rs}\right)^n}\right)\right\}$

Step 2. Update primary variables.

Based on the Lagrangian of the proposed model, the primal variables can be analytically expressed based on the dual variables (Eqs. (A2.3) and (A2.6)). Following equations are used to update the primal variables using the dual variables:

- $\left(qc_u^{rs}\right)^{n+1} = \left\{\sum_{m\in M_u^{rs}}\left[c_{um}^{rs}\left(\left(q_{um}^{rs}\right)^n\right)\cdot e^{\left(\omega_{cap}^{rs}\right)^{n+1}-\left(\omega_{ld}^{rs}\right)^{n+1}}\right]^{-\beta_{um}^{rs}}\right\}^{\frac{\beta_u^{rs}}{\beta_{um}^{rs}}}\cdot e^{\beta_u^{rs}\cdot\left(\pi^{rs}\right)^{n+1}}$

- $\left(qc_{um}^{rs}\right)^{n+1} = \left[\tau_{um}^{rs}\left(\left(q_{um}^{rs}\right)^{n}\right)\cdot e^{\left(\pi^{rs}\right)^{n+1}+\left(\omega_{cap}^{rs}\right)^{n+1}-\left(\omega_{ld}^{rs}\right)^{n+1}}\right]^{-\beta_{um}^{rs}}\cdot\left[\left(qc_{u}^{rs}\right)^{n+1}\right]^{\left(1-\frac{\beta_{um}^{rs}}{\beta_{u}^{rs}}\right)}$

Step 3. Convergence test.

- First derive the maximum adjustment among all dual variables. If $\text{Max}\left\{\left|\left(\pi^{rs}\right)^{n+1}-\left(\pi^{rs}\right)^{n}\right|,\left|\left(\omega_{cap}^{rs}\right)^{n+1}-\left(\omega_{cap}^{rs}\right)^{n}\right|,\left|\left(\omega_{ld}^{rs}\right)^{n+1}-\left(\omega_{ld}^{rs}\right)^{n}\right|\right\}\le\varepsilon$, terminate the algorithm, where ε is a convergence tolerance (e.g., 10^{-6}) at which the iterative balancing procedure stops. Otherwise, set $n = n + 1$ and go to step 1.

7.4 Numerical experiments

This section illustrates the properties of the proposed model and verifies its applicability using two numerical examples. The first example is a single-OD case and demonstrates the model's ability to consider mode correlation, heterogeneity, and passenger loyalty. The second example is based on the CB services provided in Nanjing, China, and demonstrates the potential applicability of the proposed model for evaluating and designing CB operation schemes.

7.4.1 Example 1: Single OD pair system

7.4.1.1 Experiment setting

In this example, the proposed model is used to investigate the equilibrium mode choice among a private car, conventional PT, and an existing CB line for a single OD pair. The input data for this example are as follows:

q^{rs} = 1,000 (persons), *vot* = 60 (CNY/hour), d^{rs} = 20 (km), $fc_{car}^{rs} = 0.3$ (CNY/km), *pc* = 15 (CNY), $t_{iv,PT}^{rs} = 40$ (minutes), $t_{wt,PT}^{rs} = 3$ (minutes), $t_{wk,PT}^{rs} = 3$ (minutes), $f_{PT}^{rs} = 2$ (CNY), $t_{iv,CB}^{rs} + t_{wt,CB}^{rs} + t_{wk,CB}^{rs} = 32$ (minutes), $f_{CB}^{rs} = 24$ (CNY), $\psi^{rs} = 0.6$, $n_{CB}^{rs\prime} = 10$ (vehicles), $\overline{n}_{CB}^{rs} = 20$ (vehicles), n_{seat} = 20 (persons/vehicle). The in-vehicle travel time

function for private car is $t_{iv,car}^{rs}\left(q_{car}^{rs}\right)=20\cdot\left[1+0.15\left(\frac{q_{car}^{rs}}{600}\right)^{4}\right]$, and the in-vehicle crowding discomfort cost for the PT mode is $g\left(q_{PT}^{rs}\right)\cdot t_{iv,PT}^{rs}=t_{iv,PT}^{rs}\cdot\left[1+0.5\left(\frac{q_{PT}^{rs}}{1000}\right)^{2}\right]$ (Liu and Lam, 2014; Wang et al., 2020a). The default model parameters are $\eta_{CB}^{rs}=0.05$, $\beta_{um}^{rs}=3.7$, and $\beta_{u}^{rs}=1.85$ (Kitthamkesorn and Chen, 2017; Wang et al., 2020a).

Without loss of generality, we adopt the following exponential function as the mode disutility function (Hensher and Truong, 1985; Mirchandani and Soroush, 1987):

$$\tau_{m}^{rs}=\exp\left(0.075t_{m}^{rs}\right),\forall m\in M^{rs},rs\in RS. \tag{7.13}$$

As the logit model is an additive random utility model (RUM), whereas the weibit model is a multiplicative RUM, for comparison we use the following travel disutility function in the logit-based model (Kitthamkesorn and Chen, 2017):

$$h_{m}^{rs}=0.25\cdot t_{m}^{rs},\forall m\in M^{rs},rs\in RS. \tag{7.14}$$

7.4.1.2 Effect of considering mode correlation

This section investigates the effect of considering the correlation between different modes via the nested choice structure. Figure 7.3 shows the choice probability obtained at different values of $\beta_{u}^{rs}/\beta_{um}^{rs}$, where a higher value indicates a lower correlation between modes in the same nest. It is obvious that the consideration of mode correlation significantly influences the estimated share of the CB service. Without considering correlation, the estimated share is lower than the lower limit of demand, which requires CB operators to provide incentives to attract more passengers. However, the estimated CB demand might reach the capacity constraint if there is high correlation between conventional modes, in which case CB operators may increase the fare to decrease the excess demand. Thus, the consideration of mode correlation may have a significant effect on estimated shares and CB services' operation.

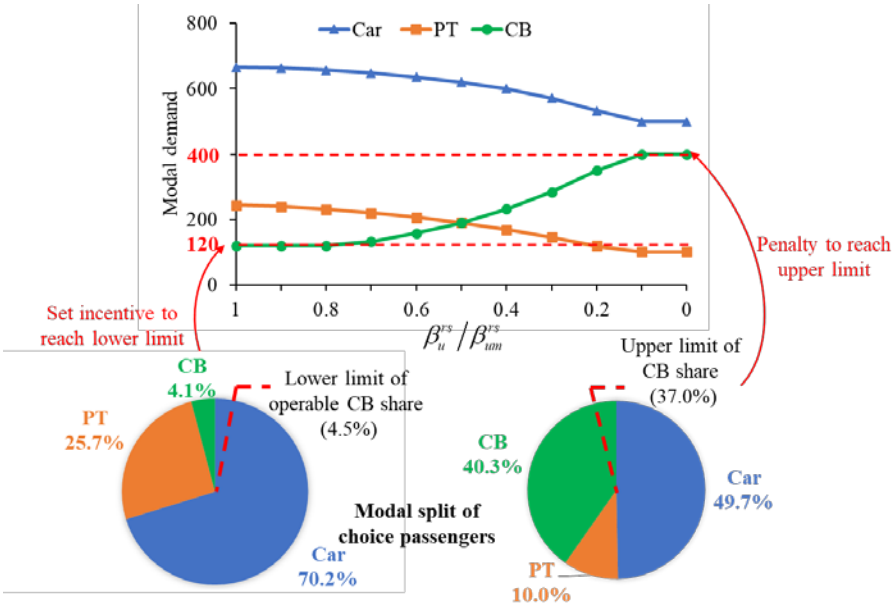

Figure 7.3. Effect of considering mode correlation in equilibrium choice model

7.4.1.3 Effect of considering heterogeneity

The effect of considering the heterogeneity issue is seen from Figure 7.4 by comparing the results from the DNL and the DNW model. In the left panel of Figure 7.4, although the loyalty parameter η_m^{rs} in the dogit-based model can partly account for the heterogeneity issue, the conditional mode choice probability of choice passengers from DNL model remains nearly unchanged due to the homogenous perception variance that is assumed to exist in the same nest. The minor change is attributed to the asymmetric alleviation of congestion effect due to demand shift from conventional modes to CB. This nearly unchanged conditional probability means that there are only minor changes in the CB mode share derived by the DNL model. In contrast, the DNW model accounts for the heterogeneity issue by allowing mode-specific perception variance dependent on mode disutility. As shown by the mode choice probability curve of CB in the right panel of Figure 7.4, this ability of the DNW model and its nested choice structure mean that it can simultaneously account for heterogeneity and mode correlation, thus better reproduce the mode choice behavior of the choice passengers than the commonly used dogit model.

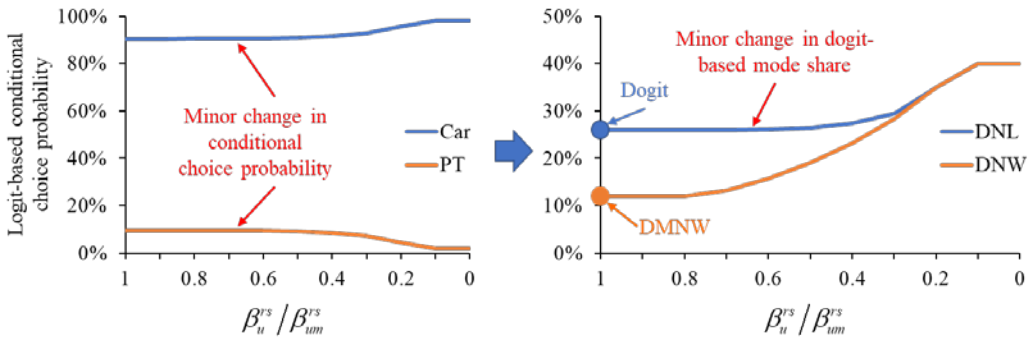

Figure 7.4. Effect of considering heterogeneity issue in equilibrium choice model

7.4.1.4 Effect of passenger loyalty

In this section, we investigate the effect of passenger loyalty on the mode share and the system performances. In addition to the share of the collective mode (conventional PT and CB modes), three other metrics are used to evaluate various aspects of a multi-modal system with CB services. First, the total travel time (TTT) is used to reflect the change in mobility. Second, as accessibility is also an important performance measure that has attracted increasing attention in transportation and urban planning, it is evaluated using the following utility-based measure proposed in Section 2.1.3, which is consistent with the proposed weibit-based choice model:

$$Acc^{rs} = \left[\sum_{u \in U^{rs}} \left(\tau_u^{rs} \right)^{-\beta_u^{rs}} \right]^{-\frac{1}{\beta_u^{rs}}}, \forall rs \in RS, \tag{7.15}$$

where

$$\tau_u^{rs} = \left[\sum_{m \in M_u^{rs}} \left(\tau_{um}^{rs} \right)^{-\beta_{um}^{rs}} \right]^{-\frac{1}{\beta_{um}^{rs}}}, \forall u \in U^{rs}, rs \in RS. \tag{7.16}$$

The weibit-based accessibility measure is then normalized to satisfy both scale and level conditions. Analogous to the normalization of logit-based accessibility measure based on the absolute difference (Dong et al., 2006), the weibit-based accessibility measure is normalized based on the relative difference in weibit expected disutility owing to the property of weibit choice models:

$$\Delta Acc^{rs} = Acc^{rs,b} / Acc^{rs,a}, \forall rs \in RS, \tag{7.17}$$

where $Acc^{rs,b}$ and $Acc^{rs,a}$ denote the weibit-based accessibility measure before and after consideration of passenger loyalty.

Third, environmental friendliness is considered a critical issue for the development of sustainable transportation systems. As such, we use the following expression for carbon monoxide (CO) emissions to evaluate the effect of transportation modes on the environment (Wallace et al., 1998):

$$E^{rs} = \sum_{m \in M^{rs}} q_m^{rs} \cdot 0.2038 \cdot t_m^{rs} \cdot \exp\left(0.7962 \cdot d^{rs} / t_m^{rs}\right), \forall rs \in RS. \tag{7.18}$$

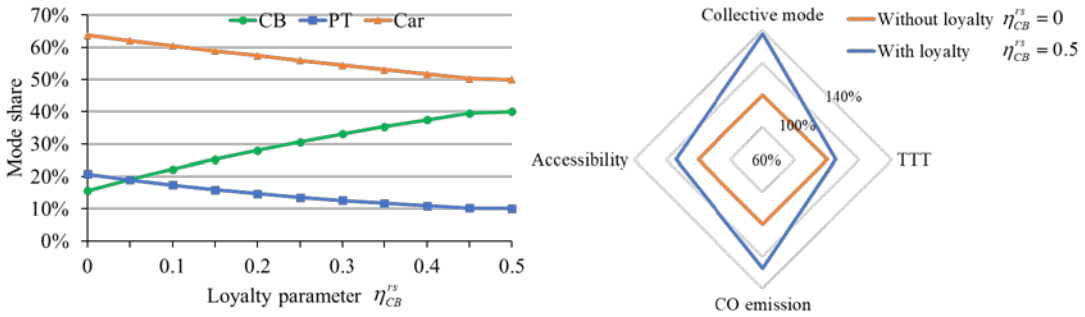

(a) Effect on mode share (b) Effect on system performance

Figure 7.5. Effects of loyalty parameter

Figure 7.5(a) shows the modal shift from conventional modes to the CB mode with an increase in the loyalty to the CB mode (indicated by the value of loyalty parameter η_{CB}^{rs}). Figure 7.5(b) further compares the system performance with and without loyalty to the CB mode. As different performance measures have different magnitudes, we show the ratio between the measures with and without CB loyalty. A higher ratio indicates a lower TTT, lower CO emissions, a higher accessibility, and a higher collective mode share, after consideration of passenger loyalty. A high CB loyalty affords a marginal decrease in mobility (i.e., increase in the TTT), which can be attributed to the significant increase in the share of collective modes that are operated at lower speeds than private cars. However, the CB service can increase accessibility

of its passengers, while the collective modes can transport more travelers in one vehicle than a private car. The increasing collective mode share thus can lead to higher system accessibility and lower total CO emissions.

7.4.1.5 Mode share and CB service profit under different loyalty schemes

This section further investigates how the pricing of CB loyalty schemes affects the CB mode share and the profit of CB services. With the absence of time-series CB ridership data for estimation, we approximate the proportion of loyal CB passengers $\mu_{CB}^{rs}\left(\tau_{CB,ls}^{rs}\right)$ based on the choice probability of loyalty subscription schemes. The choice probability is derived by the NW model adopted in this chapter, which is based on the free-flow disutility of the conventional mode and the disutility of the CB loyalty scheme $\tau_{CB,ls}^{rs}$ given the price of loyalty subscription scheme. On this basis, we can obtain the loyalty parameter η_{CB}^{rs} and investigate the effect of discounts provided by CB loyalty schemes.

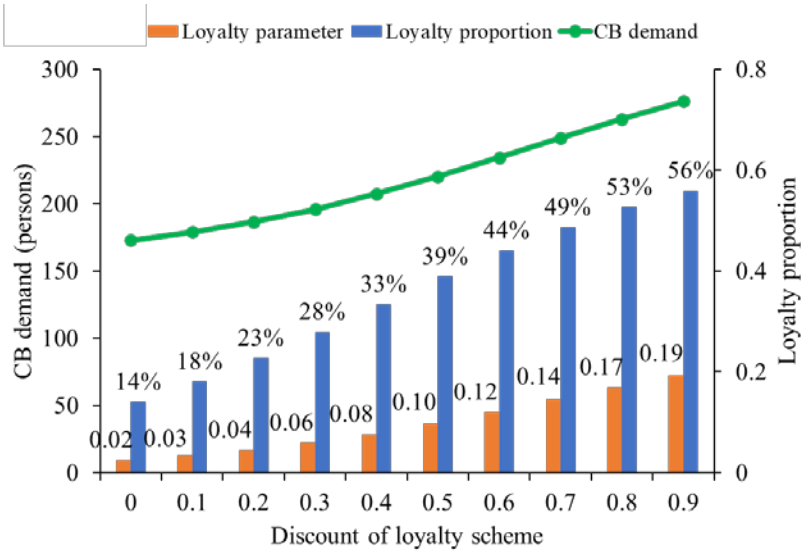

(a) Effect on CB demand and loyalty

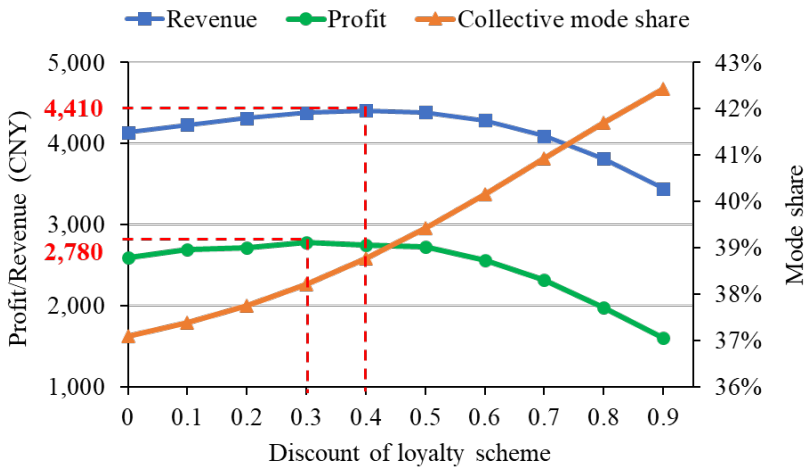

(b) Effect on CB service revenue and profit

Figure 7.6. Effects of pricing of loyalty scheme

Figure 7.6(a) shows that a discounted loyalty scheme greatly increases the proportion of loyal passengers, which leads to an increase in the overall share of CB services. However, the increase in demand does not necessarily lead to an increase in revenue and profit. We assume that the fixed cost of a CB line is CNY 1,000 and that the variable cost of adding a vehicle to the fleet is CNY 60, and then derive the evolution of revenue (from the CB fare) and profit (the difference between the revenue and the cost) with respect to varying loyalty scheme prices, as shown in Figure 7.6(b). This reveals that although a higher discount may increase the share of CB and collective modes, the operator might incline to provide a discount of approximately 30% at which their profit is maximized. This implies that the government may have to subsidize CB operators to provide a higher discount, and thus encourage more drivers of private cars to become CB passengers.

7.4.2 Example 2: Multi-OD pair case study

7.4.2.1 Experiment setting

In this section, the proposed model is applied to a real-world system with CB lines connecting eight OD pairs in Nanjing, China (adapted from Huang et al., 2020a). Figure 7.7 shows the study area and the CB lines selected in this section. Four of the eight CB

lines (indicated by solid lines) are existing lines that have loyal passengers, whereas the remaining four lines (indicated by dotted lines) are new CB lines with no passenger loyalty. The attributes of the eight OD pairs, and the travel time and monetary cost of conventional PT modes between each OD pair, are presented in Table 7.3. The monetary cost of car fuel consumption is $fc_{car}^{rs} = 0.4$ (CNY/km). The in-vehicle travel time function for a car is $t_{iv,car}^{rs}\left(q_{car}^{rs}\right) = 20 \cdot \left[1 + 0.15\left(\frac{q_{car}^{rs}}{cap_{car}}\right)^4\right]$. The value of cap_{car} is 200 for OD pairs 1–4, 2–8, 3–8, 6–7, and 100 for the other OD pairs. The in-vehicle crowding function for PT mode is $g\left(q_{PT}^{rs}\right) \cdot t_{iv,PT}^{rs} = t_{iv,PT}^{rs} \cdot \left[1 + 0.5\left(\frac{q_{PT}^{rs}}{cap_{PT}}\right)^2\right]$. The value of cap_{PT} is 200 for OD pairs 1–4, 2–8, 3–8, 4–7, 6–7, and 500 for the other OD pairs. The other inputs and default model parameters are the same as in Experiment 1.

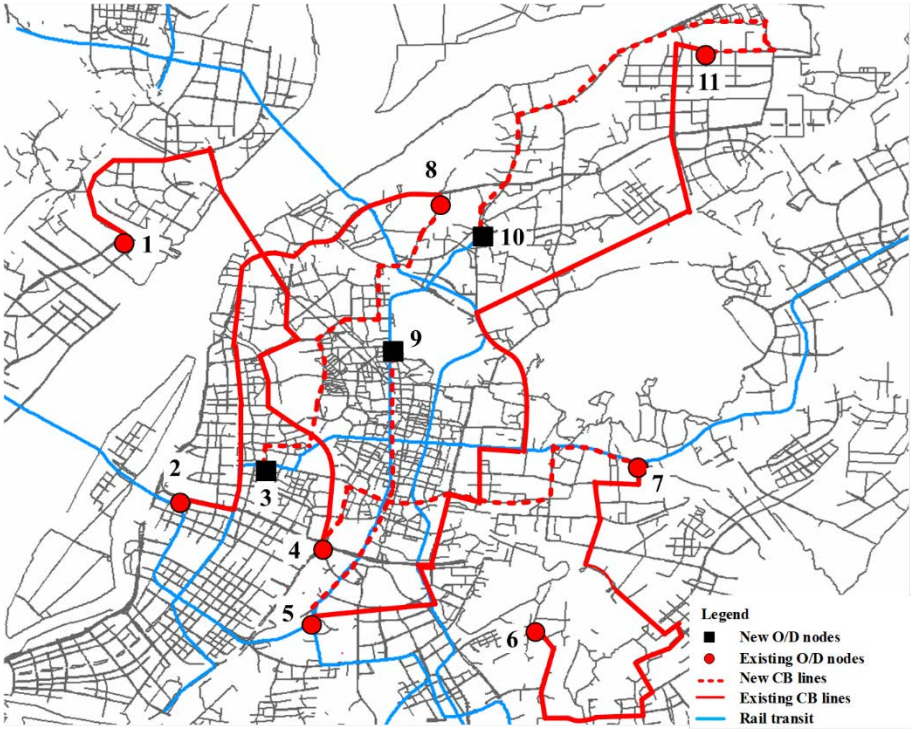

Figure 7.7. Study area with CB services
(adapted from Huang et al., 2020a)

Table 7.3. Inputs of ODs and conventional modes in multi-OD case study

OD pair	Travel demand (persons)	Distance (km)	Private car		Conventional PT			
			In-vehicle time (min)	Parking cost (CNY)	In-vehicle time (min)	Access time (min)	Waiting time (min)	Fare (CNY)
1–4	300	17.6	22	30	65	11	7	3
2–8	420	17.4	21	20	56	22	4	7
3–8	310	11	17	15	55	21	3	4
4–7	300	13.4	17	15	46	22	6	11
5–9	350	14.9	26	20	18	9	1	4
5–11	300	26	40	20	52	10	6	7
6–7	450	5.7	12	10	15	54	5	2
10–11	300	9.1	20	15	30	8	4	2

Table 7.4 presents the attributes of the eight CB lines. The existing CB lines are set to have higher capacity and passenger loyalty: $n_{CB}^{rs\prime}$ is set as five vehicles for new lines and six vehicles for existing lines; and $\overline{n}_{CB}^{rs}$ is set as 10 vehicles for new lines and 12 vehicles for existing lines. The lower limit and capacity of CB demands are then obtained based on $\psi^{rs} = 0.6$ and $n_{seat} = 20$ (persons/veh). The loyalty parameters for CB services are $\eta_{CB}^{rs} = 0.1$ for all OD pairs with existing CB lines and $\eta_{CB}^{rs} = 0$ for all OD pairs with new CB lines. The fixed cost of operating a CB line is set as CNY 1,200, whereas the variable cost of adding a CB vehicle is CNY 100. The model parameters and inputs used in the numerical examples are selected consistent with previous studies (Kitthamkesorn and Chen 2017; Huang et al., 2020a; Wang et al., 2020a) since the empirical model calibration and validation are not the focus of this chapter. The quantitative insights discussed in this section are to illustrate the proposed model is able to consider the effects of passenger loyalty, mode correlation, and heterogeneity, and is potential to be used for the evaluation of CB planning scenarios with different CB lines and pricing policies.

Table 7.4. Inputs of CB services in multi-OD case study

Line ID	OD pair	In-vehicle time (min)	Fare (CNY)	Lower limit	Capacity	Existing line?	Loyalty η_{CB}^{rs}
1	1–4	44	31	54	180	Existing	0.1
2	2–8	42	31	54	180	Existing	0.1
3	3–8	28	22	45	150	New	0
4	4–7	34	25	45	150	New	0
5	5–9	38	27	45	150	New	0
6	5–11	46	32	54	180	Existing	0.1
7	6–7	18	20	54	180	Existing	0.1
8	10–11	30	20	45	150	New	0

7.4.2.2 Evaluation of CB operation plans

Table 7.3 shows that most of the CB lines are operated between OD pairs with poor conventional PT services, i.e., the OD pairs have either an excessive in-vehicle travel time (e.g., OD pair 1–4) or an excessive access time (e.g., OD pair 6–7). The exceptions are OD pairs 5–9 and 10–11, between which the conventional PT modes provide a relatively high level of service. The proposed model is first applied to perform a cost–effectiveness analysis of whether to open new CB lines for OD pairs 5–9 and 10–11. The following four plans are considered:

Plan 1: All CB lines are operated.

Plan 2: CB line No. 5 for OD pair 5–9 is not operated.

Plan 3: CB line No. 8 for OD pair 10–11 is not operated.

Plan 4: CB lines Nos. 5 and 8 are not operated.

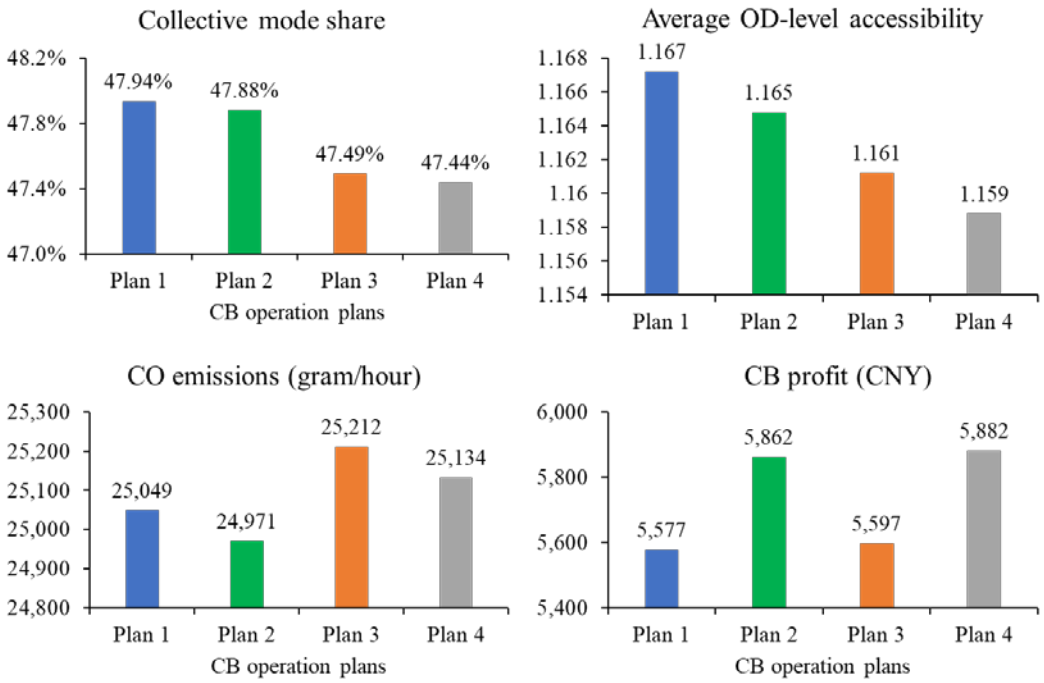

Figure 7.8. Comparison of different CB operation plans

The plans are evaluated in terms of the CB profit and system performance measures, i.e., the share of collective modes (CB and conventional PT services), the average OD-level accessibility, and CO emissions. The results, shown in Figure 7.8, reveal that Plan 2 has similar performance to Plan 1 in terms of collective mode share and accessibility, but has higher environmental friendliness. This is because the PT service for OD pair 5−9 is superior to that of private car mode and can thus attract the majority of the OD demand. The operation of CB services mainly attracts passengers from the more environmentally friendly conventional PT modes rather than the drivers of private cars. In addition, Plan 2 obtains a significantly higher profit than Plan 1, as CB line No. 5 cannot attract sufficient passengers to cover its cost of opening. In contrast, the PT service level for OD pair 10−11 is insufficient, and the CB service serves as an effective supplement for this OD pair. In summary, this experiment shows the applicability of the proposed model in evaluating different CB operations for the service design. The results indicate that Plan 2 is the most cost-effective plan; thus, this plan is adopted in this case study.

7.4.2.3 Effect of passenger loyalty and pricing of loyalty scheme

This section investigates the effect of passenger loyalty to existing CB lines and new CB lines. Figure 7.9 shows the CB revenue and system performance with respect to the evolution of loyalty parameter η_{CB}^{rs} for existing CB lines. Figure 7.9(a) shows that an increase in passenger loyalty may lead to increased CB demand and hence increased revenue for CB operators. The increase in CB demand mainly comprises former drivers of private cars, as the mode share of conventional PT remains nearly unchanged when the CB share increases rapidly. This modal shift results in increased accessibility, increased accessibility-based equity (a lower modified Gini index indicates higher equity), and a reduction in CO emissions (as shown in Figure 7.9(b)).

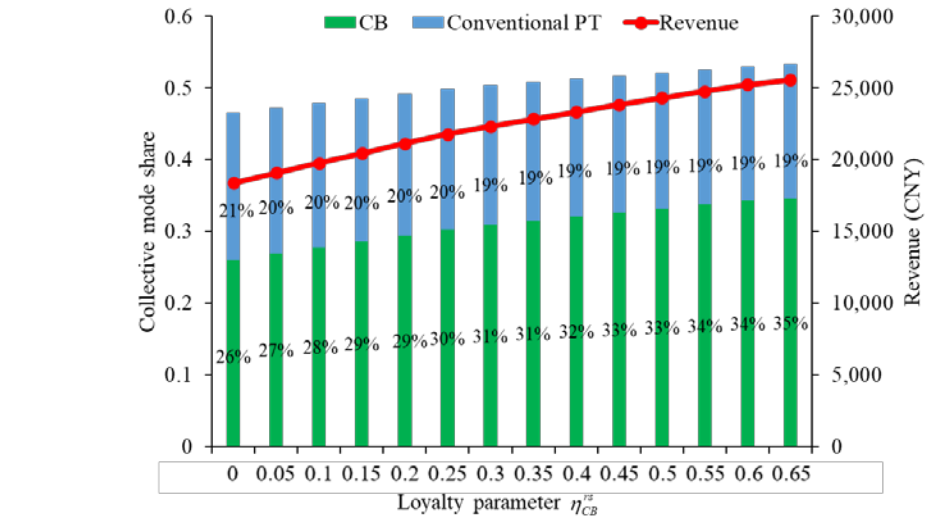

(a) Effect on mode share and CB revenue

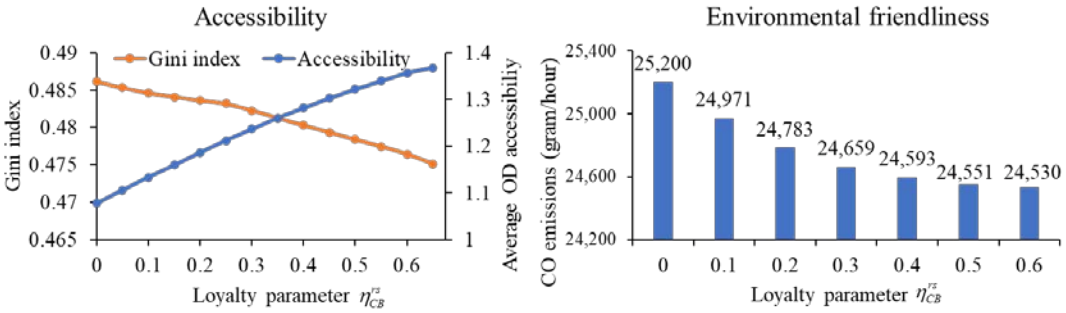

(b) Effect on system performances

Figure 7.9. Effect of passenger loyalty on existing CB lines

We further investigate the effect of a pricing policy (i.e., the discount applied to a loyalty scheme) on passenger loyalty and profit for the new CB lines, which need to attract loyal passengers to increase their mode share. As presented in Figure 7.10, a higher discount leads to an increase in the proportion of loyal passengers compared to choice passengers. This may increase CB demand and enhance system performance, as revealed in Figure 7.9. However, a discounted loyalty scheme may not necessarily result in increased profits. For example, Figure 7.10 indicates that a 10%–30% discount may generate a relatively high profit, which is consistent with the practical pricing of loyalty schemes (Liu and Ceder, 2015). On the other hand, discounts greater than 50% may lead to a rapid decrease in the profit, as the revenue is reduced by the discounted fare and operation costs are increased due to the need to run additional vehicles to meet the increased CB demand.

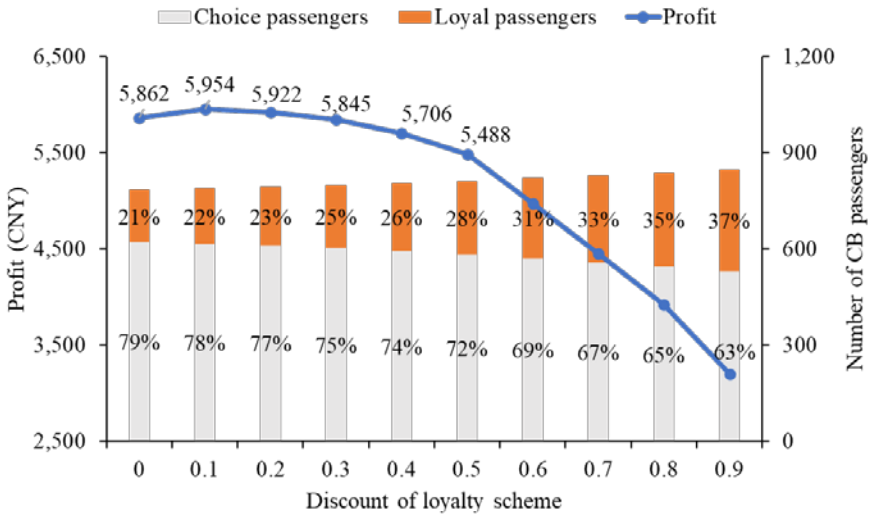

Figure 7.10. Effect of loyalty scheme pricing of new CB lines

7.5 Conclusions

This chapter presents an initial effort to model the effect of emerging CB services on long-term mode choice equilibrium in multi-modal transportation systems. The characteristics of CB services, such as the lower and upper limits of demand for operating a CB line and the passenger loyalty resulting from long-term loyalty subscription schemes, are specifically considered in the proposed model. To model

passenger loyalty, travelers are categorized as loyal passengers and choice passengers to reflect their distinct choice behaviors. Specifically, the mode choice behavior of loyal passengers is modeled as the repeated choice of CB services without considering other modes, which is interpreted using a dogit-based discrete choice model. In contrast, the behavior of choice passengers is modeled based on the disutility minimization rule by considering all modes in the transportation system, which is reproduced using a weibit-based model to account for the effects of mode correlation and heterogeneity.

This chapter can be extended to address several limitations. First, the input and parameters of the proposed model used for the numerical experiments are set only for illustrative purposes. Further empirical studies are required to calibrate and validate the proposed model based on real-world dataset. Second, besides considering the penalty of limited CB to service capacity choice passengers, the proposed model can be extended to further account for the effect of possibly denied booking (when CB demands exceed CB capacity) on loyal CB passengers. Third, the proposed model aims to evaluate long-term equilibrium after introducing CB services, while the short-term operations of CB services, including flexible timetable and adjustable vehicle routing, are not considered. It will be interesting to develop short-term mode choice model to consider and optimize these real-time CB operations (Huang et al., 2020a).

Chapter 8 Equilibrium analysis for emerging mobility services with loyalty bundle schemes

8.1 Introduction

This chapter proposes an advanced equilibrium analysis framework for emerging mobility services based on the dogit-cross-nested weibit (DCNW) individual choice model developed in Section 3.3. Many network equilibrium models have been developed for the analysis and optimization of multi-modal transportation systems with emerging mobility services, where travel choices are reproduced based on the embedded choice model with endogenous travel disutility dependent on the aggregate travel demand. Table 8.1 summarizes the choice modeling in the equilibrium analyses for emerging mobility services. Most of the existing equilibrium models focus on the mode and route choice dimensions, while few explicitly consider the bundle choice dimension (Xi et al., 2022). Many equilibrium analyses model travel choices based on the user equilibrium (UE) principle, which assumes deterministic choice behavior and fails to capture the subjective uncertainty of travelers. The stochasticity in choice behavior is mainly considered via logit models, which have closed-form choice probabilities but may be inadequate to account for travelers' heterogeneous mode disutility perceptions and the correlations among modes (e.g., commonality among modes in the same platform/bundle). Extended logit models, e.g., the nested logit (NL) and cross-nested logit (CNL) models, have been adapted to consider different correlations among modes, including the correlation between the driver and passenger roles in ridesharing, correlation among modes in the same trip, and correlation among modes belonging to same service type. However, the correlation among modes in the same mobility bundle has not been explicitly considered. Also, the extended logit models adopted in existing equilibrium analyses are still inadequate to address the heterogeneous perceptions of conventional and emerging mobility services. Furthermore, equilibrium analyses often ignore the effect of traveler loyalty, which can be cultivated by the long-term loyalty bundle schemes and increase the usage of

bundled mobilities (Nguyen-Phuoc et al., 2020; Tang et al., 2023). Gu and Chen (2023) made an initial effort to consider passenger loyalty to customized bus (CB) services in the mode choice equilibrium analysis via a dogit-nested weibit (DNW) model (see Section 3.2 and Chapter 7). The heterogeneous mode disutility perceptions and correlations among conventional modes can be considered together while retaining a closed-form choice probability. However, Gu and Chen (2023) focused on a single emerging mobility service (i.e., CB) without considering the behavioral impacts of the bundling of various travel modes, including the choice of mobility bundles, flexible mode correlations stemmed from different bundling strategies, and repeated choice of mobility bundles owing to bundle loyalty.

Table 8.1. Summary of choice modeling considered in equilibrium analyses for emerging mobility services

Study	Choice dimension	Mode choice	Perception error	Heterogeneity	Mode correlation considered	Loyalty
Di and Ban, 2019	Mode choice, route choice	Deterministic	\	\	\	\
Ban et al., 2019	Trip choice					
Xi et al., 2022	Bundle choice					
Wang et al., 2022	Mode choice					
Najmi et al., 2022	Trip choice					
Li et al., 2015	Mode choice	MNL	√	\	\	\
Zhu et al., 2022	Mode choice, route choice					
Bahat and Bekhor, 2016	Mode choice, route choice	NL	√	\	Correlation among roles in ridesharing	\
Pi et al., 2019					Correlation among modes within the same type of service	
Li et al., 2022					Correlation between pooling and non-pooling ride-hailing services	
Mori et al., 2022					Correlation among access modes to rail	
Du et al., 2022		CNL			Correlation among modes used in the same intermodal trip	
Gu and Chen, 2023	Mode choice	Dogit-NW	√	√	Correlation among conventional modes	Single mode
This chapter	**Bundle choice**, mode choice	**Dogit-Cross-nested weibit**	√	√	**Flexible correlation structure among all modes based on bundling strategies**	**Mobility bundle**

Note: MNL = multinomial logit, NL = nested logit, NW = nested weibit, CNL = cross-nested logit

This chapter aims to propose an equilibrium analysis framework, including an equilibrium demand model and a system performance analysis for emerging mobility services with consideration of following effects of mobility bundling: (1) travelers' loyalty to the subscription-based mobility bundles; (2) heterogeneous perceptions and correlations among mobility services in different bundles provided by different operators; and (c) effects of different mobility services on system performances. In particular, the DCNW model developed in Section 3.3 is integrated in the equilibrium model for reproducing the joint bundle and mode choices while considering the complex behavioral issues stemmed from mobility bundling and the interactions among individual travelers. A multi-modal transportation system analysis method is then developed based on the equilibrium model to assess bundling effect (c). The overall structure of the proposed equilibrium analysis framework is demonstrated in Figure 8.1.

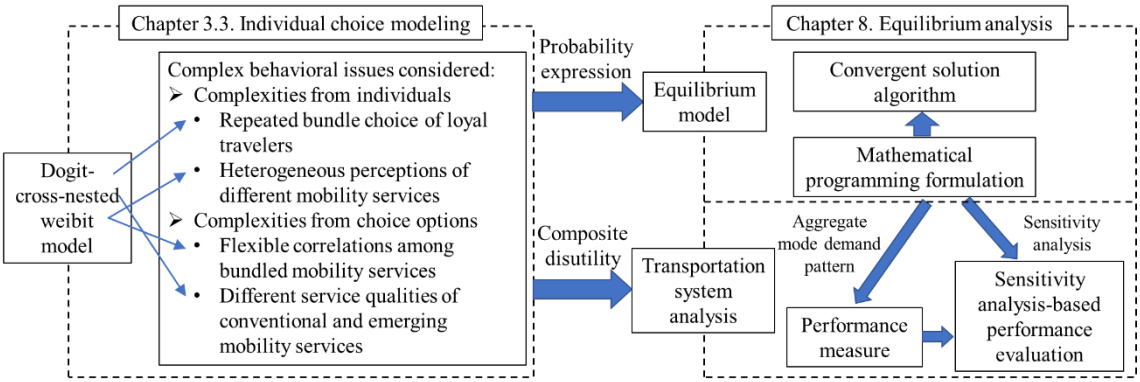

Figure 8.1. Overall structure of the proposed equilibrium analysis framework for emerging mobility services with loyalty bundle schemes

The contributions of the proposed analysis framework are as follows:

(a) Benefiting from the DCNW choice model, the repeated choice behavior of loyal travelers to mobility bundles is explicitly considered together with the disloyal travelers. As for disloyal travelers, the heterogeneous mode, flexible correlations among bundled modes, and interaction between bundle and mode choices are simultaneously modeled based on the random utility theory.

(b) An equilibrium model is developed consistent with the DCNW choice model. The equilibrium model is formulated as a mathematical programming (MP) problem, which guarantees solution equivalence and uniqueness, facilitates understandable interpretation, and is solved by a convergent and efficient solution algorithm.

(c) An effective analysis method is developed for multi-modal transportation systems with emerging mobility services based on the sensitivity analysis of the developed equilibrium model. The analysis outcomes can facilitate the evaluation of mode demand pattern and its impact on system performance in different scenarios, which provide insights into the planning and operations of emerging mobility services.

8.2 Multi-modal transportation system with both conventional and emerging mobility services

To facilitate the presentation of the essential ideas, the notations used in this paper are presented in Section 8.2.1. The travel disutility and physical characteristics of considered conventional and emerging mobility services are described in Section 8.2.2.

8.2.1 Notations

Sets

R	Set of origin zones.
S	Set of destination zones.
U^{rs}	Set of mobility bundles/mode nests between OD pair *rs*.
M^{rs}	Set of modes operated between OD pair *rs*.
M_u^{rs}	Set of modes in nest *u* between OD pair *rs*.

Inputs

τ_m^{rs}	Travel disutility of mode *m* between OD pair *rs.*
t_m^{rs}	Generalized travel time of mode *m* between OD pair *rs.*
$t_{iv,m}^{rs}$	In-vehicle travel time of mode *m* between OD pair *rs.*
$t_{wt,m}^{rs}$	Waiting time of mode *m* between OD pair *rs.*
$t_{a,m}^{rs}$	Access (walking) time of mode *m* between OD pair *rs.*
$c_{i,m}^{rs}$	Monetary cost *i* for mode *m* between OD pair *rs.*
g_{PT}	In-vehicle crowding discomfort of conventional transit mode.
g_{BK}	Discomfort from the physical fatigue of riding bike.
vot	Value of time.
cap_m^{rs}	Capacity of mode *m* between OD pair *rs*.
d^{rs}	Travel distance between OD pair *rs*.
q^{rs}	Travel demand between OD pair *rs*.

Parameters

β_{um}^{rs}	Shape parameter at the conditional choice level between OD pair *rs*.

β_u^{rs}	Shape parameter at the marginal choice level between OD pair *rs*.
μ_{um}^{rs}	Membership of mode *m* in bundle *u* between OD pair *rs*.
η_u^{rs}	Loyalty parameter for bundle *u* between OD pair *rs* in the dogit model.

System performance measures

TTT	System total travel time.
E^{rs}	CO emission between OD pair *rs*.
Acc_u^{rs}	Accessibility of nest *u* between OD pair *rs*.
Acc^{rs}	Accessibility of OD pair *rs*.

Primal and dual variables

q_{um}^{rs}	Travel demand of mode *m* in nest *u* between OD *rs*.
q_m^{rs}	Travel demand of mode *m* between OD *rs*.
q_u^{rs}	Travel demand of nest *u* between OD pair *rs*.
qc_u^{rs}	Number of choice travelers choosing nest *u* between OD pair *rs*.
λ	Dual variables with respect to definitional constraints.
ω_m^{rs}	Dual variables with respect to capacity constraints on mode *m* between OD pair *rs*.

8.2.2 Description of conventional modes and emerging mobility services

This chapter considers a multi-modal transportation system with both conventional travel modes (i.e., private car, private bike, conventional transit, and street-hailing taxi) and emerging mobilities (i.e., e-hailing services, bike sharing, and customized bus). Each type of shared and on-demand mobility can be offered by different service providers, and each mobility service can be integrated in different bundles provided by different platforms. Travelers can either subscribe to long-term loyalty bundle schemes or choose pay-as-you-go (PAYG) schemes for one-time rides. The subscribers of long-term schemes are assumed to be loyal and tend to repeatedly use the subscribed bundle due to the pre-paid subscription fee (Matyas and Kamargianni, 2019) and different levels of incentives for bundled modes (Nguyen-Phuoc et al., 2020). The PAYG users are open to consider all bundles and modes in the transportation system and make choices to minimize the perceived travel disutility. The travel disutility and physical characteristics of mobility services considered in this chapter are described in Figure 8.2 and introduced in detail in Sections 8.2.2.1-8.2.2.5

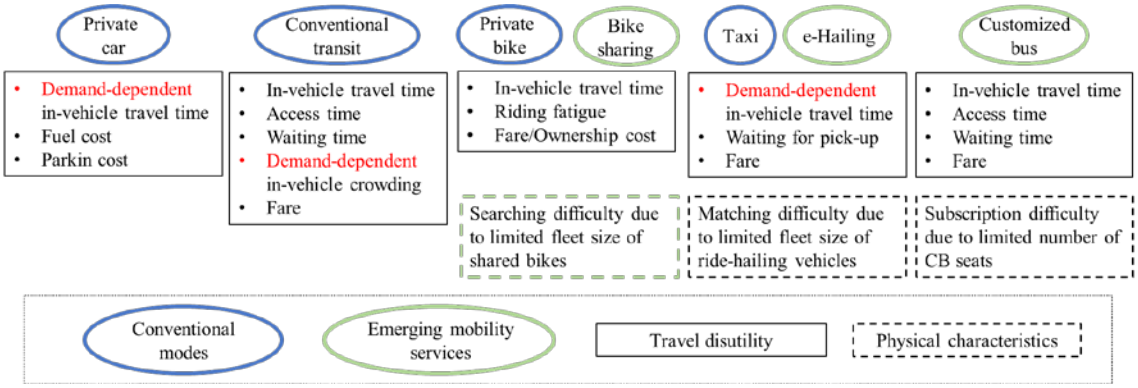

Figure 8.2. Travel disutility and physical characteristics of considered conventional and emerging mobility services in Chapter 8

8.2.2.1 Private car

The disutility of private car trips is composed of monetary costs and in-vehicle travel time. The in-vehicle travel time of private car is assumed to be a separable, continuous, and monotonically increasing function of car demand. The generalized travel time of private car between OD *rs* is expressed as

$$t_{car}^{rs} = t_{iv,rd}^{rs}\left(q_{rd}^{rs}\right) + \frac{1}{vot}\cdot\left(d^{rs}\cdot c_{fl,car}^{rs} + c_{p,car}^{rs}\right), \forall rs \in RS\,, \tag{8.1}$$

where t_{car}^{rs}, $t_{iv,car}^{rs}(\cdot)$, $c_{fl,car}^{rs}$, and $c_{p,car}^{rs}$ respectively denote the generalized travel time, demand-dependent in-vehicle travel time, fuel cost, and parking cost of driving between OD pair *rs*; d^{rs} is the travel distance between OD pair *rs*; *vot* is the value of time; q_{rd}^{rs} denotes the road traffic volume comprised by the volumes of private car and ride-hailing vehicles, which is derived from the equilibrium model presented in Section 8.3.

8.2.2.2 Conventional transit

The generalized travel time of conventional transit modes (e.g., bus) between OD pair *rs*, t_{PT}^{rs}, is expressed as follows:

$$t_{PT}^{rs} = t_{iv,PT}^{rs} + t_{a,PT}^{rs} + t_{wt,PT}^{rs} + \frac{1}{vot}\cdot\left[g\left(q_{PT}^{rs}, t_{iv,PT}^{rs}\right) + c_{f,PT}^{rs}\right], \forall rs \in RS\,, \tag{8.2}$$

where $t_{iv,PT}^{rs}$, $t_{a,PT}^{rs}$, $t_{wt,PT}^{rs}$, q_{PT}^{rs}, and $c_{f,PT}^{rs}$ respectively denote the generalized travel time, in-vehicle travel time, access (walking) time, waiting time, travel demand, and fare of the conventional transit service between OD pair *rs*. $g(.)$ denotes the in-vehicle

crowding discomfort cost, which is an increasing function with respect to the in-vehicle travel time and the transit demand (Li and Hensher, 2011).

8.2.2.3 Customized bus

The disutility of CB services is considered to include the generalized travel time and risk of failed subscription. The generalized travel time of CB, t_{CB}^{rs}, can be derived based on the trip travel time and the CB fare f_{CB}^{rs} as follows:

$$t_{CB}^{rs} = t_{iv,CB}^{rs} + t_{a,CB}^{rs} + t_{wt,CB}^{rs} + \frac{1}{vot} \cdot c_{f,CB}^{rs}, \forall rs \in RS, \tag{8.3}$$

where the trip travel time is the summation of fixed in-vehicle travel time, waiting time, and access time of CB, i.e., $t_{CB}^{rs} = t_{iv,CB}^{rs} + t_{wt,CB}^{rs} + t_{a,CB}^{rs}$.

As demonstrated in Section 7.3.2, although the CB generalized travel time is not explicitly dependent on the number of CB passengers, it is implicitly influenced by the risk of failed subscription incurred when the demand of CB reaches its capacity, i.e., the number of subscribers to the CB line between OD pair *rs* (q_{CB}^{rs}) cannot exceed the capacity of CB line between OD pair *rs* (cap_{rs}^{CB}):

$$q_{CB}^{rs} \le cap_{CB}^{rs}, \forall rs \in RS. \tag{8.4}$$

8.2.2.4 Ride-hailing services

This chapter considers both the conventional street-hailing taxi and the internet-based e-hailing service. The disutility of ride-hailing services is considered to include the generalized travel time and delay due to matching difficulty. The generalized travel time of both ride-hailing services, t_{RH}^{rs}, is obtained based on the demand-dependent in-vehicle travel time $t_{iv,rd}^{rs}$, waiting time for pick-up $t_{wt,RH}^{rs}$, and a distance-based fee $c_{f,RH}^{rs}\left(d^{rs}\right)$ (Pi et al., 2019; Wang et al., 2022):

$$t_{RH}^{rs} = t_{iv,rd}^{rs}\left(q_{rd}^{rs}\right) + t_{wt,RH}^{rs} + \frac{1}{vot} \cdot c_{f,RH}^{rs}\left(d^{rs}\right). \tag{8.5}$$

The delay due to matching difficulty is considered depending on the supply and demand of the ride-hailing services in the origin zone, which is modeled as the dual

variable associated with the capacity constraint of ride-hailing service at origin (Ban et al., 2019). The capacity of street-hailing taxi at origin *r* is expressed as

$$\sum_{s\in S} q_{sh}^{rs} \le Cap_{sh}^{r}, \forall r \in R. \tag{8.6}$$

There can be multiple e-hailing services operated by different providers at each origin. The capacity of e-hailing service at origin *r* by provider *i* is expressed as

$$\sum_{s\in S} q_{eh,i}^{rs} \le Cap_{eh,i}^{r}, \forall u \in U, r \in R. \tag{8.7}$$

8.2.2.5 Bicycles

The disutility of cycling is considered to include the generalized travel time and difficulty to search for an available shared bike (for bike sharing services). As an active travel mode, the generalized travel time of cycling is considered to include the in-vehicle cycling time $t_{iv,BK}^{rs}$ and riding fatigue disutility $g_{BK}\left(t_{iv,BK}^{rs}\right)$ during cycling (Li et al., 2015). Two cycling modes are considered in this chapter, namely the conventional private bike and the emerging bike sharing service. The generalized travel times of the two modes are respectively written as follows:

$$t_{PB}^{rs} = t_{iv,BK}^{rs} + \frac{1}{vot}\cdot\left[g_{BK}\left(t_{iv,BK}^{rs}\right) + c_{PB}^{rs}\right], \tag{8.8}$$

$$t_{BS}^{rs} = t_{iv,BK}^{rs} + \frac{1}{vot}\cdot\left[g_{BK}\left(t_{iv,BK}^{rs}\right) + c_{f,BS}^{rs}\left(t_{iv,BK}^{rs}\right)\right], \tag{8.9}$$

where c_{PB}^{rs} denotes the cost of owning of private bike; $c_{f,BS}^{rs}\left(t_{iv,BK}^{rs}\right)$ is the time-dependent fare of bike sharing. Similar to the ride-hailing service, there is limited bike sharing supply at each zone. Thus, a capacity constraint on the zonal demand of bike sharing is considered:

$$\sum_{s\in S} q_{BS}^{rs} \le Cap_{BS}^{r}, \forall u \in U, r \in R. \tag{8.10}$$

The associated dual variable acts as an additional travel disutility of the bike sharing service, which can be interpreted as difficulty to search for an available shared bike due to the insufficient supply in the origin zone.

8.3 Joint bundle and mode choice equilibrium analysis

8.3.1 Equilibrium model formulation

As described in Section 8.2.2, the disutility of mobility services considered in this chapter are dependent on the travel demand. Directly deriving the aggregate demand pattern from the DCNW model choice model developed in Section 3.3 may lead to a bias, as the mode choice probability derived based on exogenous free-flow disutility will be inconsistent with the mode disutility dependent on traveler interactions in the transportation system. In this section, an equilibrium DCNW choice model is developed to obtain the aggregate mode demand pattern dependent on the endogenous travel disutility. Following the method described in Chapter 5, the equilibrium model is formulated as an equivalent MP problem as follows:

$$
\begin{aligned}
\min Z &= Z_1 + Z_2 + Z_3 + Z_4 + Z_5 \\
&= \sum_{rs\in RS}\sum_{m\in M^{rs}} \int_0^{q_m^{rs}} \ln \tau_m^{rs}(\omega)\, d\omega \\
&+ \frac{1}{\beta_{um}^{rs}} \cdot \sum_{rs\in RS}\sum_{u\in U^{rs}}\sum_{m\in M_u^{rs}} q_{um}^{rs} \cdot \left(\ln q_{um}^{rs} - 1\right) \\
&- \frac{1}{\beta_{u}^{rs}} \cdot \sum_{rs\in RS}\sum_{u\in U^{rs}}\sum_{m\in M_u^{rs}} q_{um}^{rs} \cdot \ln \mu_{um}^{rs} \\
&- \frac{1}{\beta_{um}^{rs}} \cdot \sum_{rs\in RS}\sum_{u\in U^{rs}} \left(\sum_{m\in M_u^{rs}} q_{um}^{rs}\right) \cdot \left(\ln \sum_{m\in M_u^{rs}} q_{um}^{rs} - 1\right) \\
&+ \frac{1}{\beta_{u}^{rs}} \cdot \sum_{rs\in RS}\sum_{u\in U^{rs}} \left(\sum_{m\in M_u^{rs}} q_{um}^{rs} - \frac{\eta_u^{rs}\cdot q^{rs}}{1+\sum_{w\in U^{rs}} \eta_w^{rs}}\right) \cdot \left[\ln\left(\sum_{m\in M_u^{rs}} q_{um}^{rs} - \frac{\eta_u^{rs}\cdot q^{rs}}{1+\sum_{w\in U^{rs}} \eta_w^{rs}}\right) - 1\right]
\end{aligned}
\tag{8.11}
$$

s.t.

Eqs. (8.4), (8.6), (8.7), (8.10),

$$
\sum_{u\in U^{rs}}\sum_{m\in M_u^{rs}} q_{um}^{rs} = q^{rs}, \forall rs \in RS, \tag{8.12}
$$

$$
. \sum_{u\in U^{rs}} q_{um}^{rs} = q_m^{rs}, \forall m \in M^{rs}, rs \in RS, \tag{8.13}
$$

$$
q_{um}^{rs} > 0, \forall m \in M_u^{rs}, u \in U^{rs}, rs \in RS. \tag{8.14}
$$

Objective function (8.11) aims to obtain the mode demand pattern consistent with the proposed DCNW choice probability derived from endogenous mode disutility. The first term Z_1 is the multiplicative Beckmann term for considering the demand-dependent mode disutility (Kitthamkesorn and Chen, 2013). Terms Z_2 and Z_3 are entropy terms which together determine the DCNW conditional choice probability. Term Z_4 corresponds to the interaction between the marginal and conditional choice levels of the DCNW model. Term Z_5 determines the marginal choice probability of choice travelers while considering the effect of bundle loyalty via the dogit model. Eqs. (8.12) and (8.13) are conservation and definitional constraints, respectively. Eq. (8.14) guarantees the positivity of decision variables. Eqs. (8.4), (8.6), (8.7), (8.10) are incorporated as explicit constraints on the capacities of corresponding mobility services. Two propositions are stated below for illustrating qualitative properties of the proposed equilibrium model:

Proposition 8.1. The solutions to the proposed MP model formulation give the equilibrium mode demand pattern consistent with the DCNW model.

Proof. See Appendix A3 for detailed proof.

Proposition 8.2. The solutions to the proposed MP model formulation are unique.

Proof. See Appendix B3 for detailed proof.

8.3.2 Solution algorithm

Benefiting from the developed MP formulation, the relationship between primal and dual variables of the equilibrium model can be analytically derived (as shown in Appendix A3), and the value of objective function can be easily evaluated to find the search direction for updating solution variables. Making use of these desirable properties, the proposed equilibrium model is solved based on the partial linearization method embedded with an iterative balancing scheme for direction finding and the self-regulated averaging scheme for step size determination as introduced in Section 5.3.

The iterative balancing procedure is specified as follows to obtain the auxiliary variables **y** for direction finding:

Step 0. Initialization. Set number of iterations l=1. Set initial primal variables $\mathbf{y}^{(0)}=\mathbf{0}$, and dual variables $\boldsymbol{\omega}^{(0)}=\mathbf{0}$, $\boldsymbol{\lambda}^{(0)}=\mathbf{0}$.

Step 1. Update primal variables.

$$yc_u^{rs(n)} = e^{\beta_u^{rs}\cdot\lambda^{rs(n-1)}}\cdot\left[\sum_{m\in M_u^{rs}}\left(\tau_{um}^{rs}\cdot e^{\omega_m^{rs(n-1)}}\right)^{-\beta_{um}^{rs}}\cdot\left(\mu_{um}^{rs}\right)^{\frac{\beta_{um}^{rs}}{\beta_u^{rs}}}\right]^{\frac{\beta_u^{rs}}{\beta_{um}^{rs}}},$$

$$y_u^{rs(n)} = yc_u^{rs(n)} + \frac{\eta_u^{rs}\cdot q^{rs}}{1+\sum_{w\in U^{rs}}\eta_w^{rs}},$$

$$y_{um}^{rs\,(n)} = y_u^{rs(n)}\cdot\left(yc_u^{rs(n)}\right)^{-\frac{\beta_{um}^{rs}}{\beta_u^{rs}}}\cdot\left(\tau_m^{rs}\cdot e^{\omega_m^{rs(n-1)}}\right)^{-\beta_{um}^{rs}}\cdot\left(\mu_{um}^{rs}\right)^{\frac{\beta_{um}^{rs}}{\beta_u^{rs}}}\cdot e^{\beta_{um}^{rs}\lambda^{rs(n-1)}}.$$

Step 2. Update dual variables.

$$\omega_m^{rs(n)} = \max\left\{0, \omega_m^{rs(n-1)} - \frac{1}{\beta_{um}^{rs}}\ln\left(\frac{cap_m^{rs}}{y_m^{rs}}\right)\right\},$$

$$\lambda^{rs(n)} = \lambda^{rs(n-1)} + \frac{1}{\beta_u^{rs}}\ln\left(\frac{\sum_{u\in U^{rs}} yc_u^{rs(n-1)}}{yc_u^{rs(n-1)}}\right).$$

Step 3. Convergence test.

If certain convergence criterion (e.g., $\max\left\{\left|\boldsymbol{\omega}^{(n)}-\boldsymbol{\omega}^{(n-1)}\right|, \left|\boldsymbol{\lambda}^{(n)}-\boldsymbol{\lambda}^{(n-1)}\right|\right\}\le\varepsilon$) is met, stop. Otherwise, go to Step 1.

8.3.3 Sensitivity analysis-based multi-modal transportation system analysis

The proposed equilibrium model is applied to the decision-making in multi-modal transportation systems with various emerging mobilities. The infrastructure planning and mobility operation strategies can be evaluated by comparing the system performances in different planning scenarios measured based on the equilibrium demand pattern. Instead of repeatedly solving the proposed model in different scenarios, the sensitivity-analysis-based method is an effective post-analysis tool that can approximate the changes in system performance under perturbations in model inputs/parameters (Yang and Chen, 2009; Du and Chen, 2022). The analysis outcomes can reveal the effects of managing supply and demand of mobility services and the criticality of different planning/operation strategies. The sensitivity analysis of the proposed model is first introduced in Section 8.3.3.1, followed by the illustration of the

sensitivity analysis-based multi-modal transportation system performance evaluation in Section 8.3.3.2.

8.3.3.1 Sensitivity analysis of equilibrium DCNW model

Benefiting from the properties of the developed MP formulation, the sensitivity analysis for nonlinear program can be applied to the proposed model (Fiacco, 1983; Yang and Chen, 2009; Du and Chen, 2022). The definitional constraint $q_u^{rs} = \sum_{m \in M_u^{rs}} q_{um}^{rs}$ is introduced to represent the decision variable at the nest/bundle choice level, the Lagrangian of the proposed MP can then be expressed as

$$L = Z + \lambda^{rs} \cdot \left[\sum_{rs \in RS} \sum_{u \in U^{rs}} q_u^{rs} - q^{rs} \right] + \lambda_u^{rs} \cdot \left[\sum_{m \in M_u^{rs}} q_{um}^{rs} - q_u^{rs} \right] + \sum_{rs \in RS} \sum_{m \in M^{rs}} \omega_m^{rs} \cdot \left(q_m^{rs} - cap_m^{rs} \right), \quad (8.15)$$

where λ^{rs} and λ_u^{rs} are dual variable with respect to the definitional constraints; for simplicity, we use ω_m^{rs} to denote the OD-level dual variable with respect to the capacity constraint of each mode. The partial derivatives of the Lagrangian with respect to primal and dual variables are as follows:

$$\nabla_{q_u^{rs}} L = \frac{1}{\beta_u^{rs}} \cdot \ln \left(q_u^{rs} - \frac{\eta_u^{rs} \cdot q^{rs}}{1 + \sum_{w \in U^{rs}} \eta_w^{rs}} \right) - \frac{1}{\beta_{um}^{rs}} \cdot \ln q_u^{rs} + \lambda^{rs} - \lambda_u^{rs}, \quad (8.16)$$

$$\nabla_{q_{um}^{rs}} L = \ln \tau_m^{rs} + \frac{1}{\beta_{um}^{rs}} \cdot \ln q_{um}^{rs} - \frac{1}{\beta_u^{rs}} \cdot \ln \mu_{um}^{rs} + \lambda_u^{rs} + \omega_m^{rs}, \quad (8.17)$$

$$\nabla_{\omega_m^r} L = \sum_{s \in S} q_m^{rs} - cap_m^r, m = BS, EH \; ; \; \nabla_{\omega_{CB}^{rs}} L = q_{CB}^{rs} - cap_{CB}^{rs}, \quad (8.18)$$

$$\nabla_{\lambda_u^{rs}} L = \sum_{m \in M_u^{rs}} q_{um}^{rs} - q_u^{rs}, \quad (8.19)$$

$$\nabla_{\lambda^{rs}} L = \sum_{rs \in RS} \sum_{u \in U^{rs}} q_u^{rs} - q^{rs}. \quad (8.20)$$

Let J_1 denote the Jacobian of Eqs. (8.16)–(8.20) with respect to the primal and dual variables, which can be expressed as

$$J_1 = \begin{bmatrix} \nabla^2_{q_u^{rs}} L & 0 & 0 & -I & \Gamma^T \\ 0 & \nabla^2_{q_{um}^{rs}} L & \Phi & \Lambda^T & 0 \\ 0 & \Phi^T & 0 & 0 & 0 \\ -I & \Lambda & 0 & 0 & 0 \\ \Gamma & 0 & 0 & 0 & 0 \end{bmatrix}, \tag{8.21}$$

where I denotes the identity matrix; Φ denotes the incidence relationship between the decision variable q_{um}^{rs} and activated capacity constraints; Γ and Λ are the incidence matrix between OD pair and nest, and that between nest and mode, respectively. The second partial derivatives $\nabla^2_{q_u^{rs}} L$ and $\nabla^2_{q_{um}^{rs}} L$ are obtained as follows:

$$\nabla^2_{q_u^{rs}} L = \frac{1}{\beta_u^{rs}} \cdot diag\left(\frac{1}{q_u^{rs} - \dfrac{\eta_u^{rs} \cdot q^{rs}}{1 + \sum\limits_{w \in U^{rs}} \eta_w^{rs}}} \right) - \frac{1}{\beta_{um}^{rs}} \cdot diag\left(\frac{1}{q_u^{rs}} \right), \tag{8.22}$$

$$\nabla^2_{q_{um}^{rs}} L = \frac{1}{\tau_m^{rs}} \cdot \nabla_{q_{um}^{rs}} \tau_m^{rs} + \frac{1}{\beta_{um}^{rs}} \cdot diag\left(\frac{1}{q_{um}^{rs}} \right). \tag{8.23}$$

Let J_2 denote the Jacobian of Eqs. (8.16)–(8.20) with respect to perturbation ξ in the model inputs or parameters, which can be referred to as changes in the supply and demand of mobility services, such as infrastructure capacity, fleet size, fare price, travel time, bundle loyalty, and travel demand. J_2 can be written as

$$J_2 = \begin{bmatrix} \nabla_{q_u^{rs},\xi} L & \nabla_{q_{um}^{rs},\xi} L & \nabla_{\omega_m^{rs},\xi} L & \nabla_{\lambda_u^{rs},\xi} L & \nabla_{\lambda^{rs},\xi} L \end{bmatrix}^T. \tag{8.24}$$

Let $\mathbf{y} = \begin{bmatrix} q_u^{rs} & q_{um}^{rs} & \omega_m^{rs} & \lambda_u^{rs} & \lambda^{rs} \end{bmatrix}^T$ indicate the vector of solution variables, the derivatives of $\mathbf{y}$ with respect to perturbation ξ can be obtained (Yang and Chen, 2009):

$$\nabla_{\xi} \mathbf{y} = -J_1^{-1} \cdot J_2 . \tag{8.25}$$

8.3.3.2 Sensitivity analysis-based transportation system performance evaluation

(1) System performance measures

In this chapter, the performance of multi-modal transportation system is measured from different perspectives based on the bundle and mode demand patterns derived from the proposed equilibrium model. The performance measures include mobility, accessibility, and environmental friendliness. The mobility is measured by the system total travel time (TTT) expressed as follows:

$$TTT = \sum_{rs \in RS} \sum_{m \in M^{rs}} q_m^{rs} \cdot t_m^{rs}(\mathbf{q}). \tag{8.26}$$

The accessibility is evaluated using the utility-based measure introduced in Section 2.1.3, which is consistent with the developed choice model and obtained as the weibit-based composite disutility (i.e., the expected minimum disutility from the CNW model) at each choice level. The bundle-level accessibility measure, Acc_u^{rs}, is obtained via Eq. (3.41) using the endogenous travel disutility $\tau_m^{rs}(\mathbf{q})$. The OD-level accessibility measure Acc^{rs} is obtained as

$$Acc^{rs} = \left[\sum_{u \in U^{rs}} \left(Acc_u^{rs} \right)^{-\beta_u^{rs}} \right]^{-\frac{1}{\beta_u^{rs}}}, \forall rs \in RS. \tag{8.27}$$

The accessibility at each level can then be evaluated based on the relative difference in normalized weibit-based composite disutility:

$$\Delta Acc = \frac{Acc}{Acc'(\xi)}, \forall rs \in RS, \tag{8.28}$$

where $Acc'(\xi)$ denotes the weibit-based composite disutility after a perturbation ξ in the examined model inputs or parameters, which is derived based on the sensitivity analysis outcomes as will be illustrated below.

The environmental friendliness is measured based on CO emission. The OD-level CO emission is derived as follows (Wallace et al., 1998):

$$E^{rs} = \sum_{m \in M^{rs}} e_m \cdot q_m^{rs} \cdot 0.2038 \cdot t_m^{rs} \cdot \exp\left(0.7962 \cdot d^{rs} / t_m^{rs}\right), \forall rs \in RS, \tag{8.29}$$

where e_m denotes the passenger car unit of mode *m*, d^{rs} is the travel distance between OD pair *rs*.

(2) Sensitivity analysis-based evaluation of performance measures

As all the performance measures are demand-dependent, the system performances after the implementation of a certain plan or policy can be obtained given the corresponding equilibrium demand pattern under the perturbation in corresponding model inputs/parameters. The derivatives of mode demand, total travel time, accessibility, and CO emission can be obtained based on the sensitivity analysis of decision variable q_{um}^{rs} (as derived in Section 8.3.3.1) and the chain rule as follows:

$$\nabla_{\xi} q_m^{rs} = \sum_{u \in U^{rs}} \nabla_{\xi} q_{um}^{rs}$$

$$\nabla_{\xi} TTT = \sum_{rs \in RS} \sum_{m \in M^{rs}} \nabla_{\xi} q_m^{rs} \cdot \left(t_m^{rs} + q_m^{rs} \cdot \nabla_{q_m^{rs}} \tau_m^{rs} \right)$$

$$\nabla_{\xi} Acc_u^{rs} = \left[\sum_{m \in M_u^{rs}} \left(\mu_{um}^{rs \, -\frac{1}{\beta_u^{rs}}} \cdot \tau_m^{rs} \right)^{-\beta_{um}^{rs}} \right]^{-\frac{1}{\beta_{um}^{rs}}-1} \cdot \sum_{m \in M_u^{rs}} \nabla_{\xi} q_m^{rs} \cdot \left(\mu_{um}^{rs} \right)^{\frac{\beta_{um}^{rs}}{\beta_u^{rs}}} \cdot \nabla_{q_m^{rs}} \tau_m^{rs} \cdot \left(\tau_m^{rs} \right)^{-\beta_{um}^{rs}-1}$$

$$\nabla_{\xi} Acc^{rs} = \left[\sum_{u \in U^{rs}} \left(Acc_u^{rs} \right)^{-\beta_u^{rs}} \right]^{-\frac{1}{\beta_u^{rs}}-1} \cdot \sum_{u \in U^{rs}} \nabla_{\xi} Acc_u^{rs} \cdot \left(Acc_u^{rs} \right)^{-\beta_u^{rs}-1}$$

$$\nabla_{\xi} E^{rs} = \sum_{m \in M^{rs}} e_m \cdot \nabla_{\xi} q_m^{rs} \cdot 0.2038 \cdot \exp\left(\frac{0.7962 \cdot d^{rs}}{t_m^{rs}} \right) \cdot \left[t_m^{rs} + q_m^{rs} \cdot \nabla_{q_m^{rs}} \tau_m^{rs} \cdot \left(1 - \frac{0.7962 \cdot d^{rs}}{t_m^{rs}} \right) \right]$$

(8.30)

The corresponding performance measure $X'(\varepsilon)$ (X can indicate mode demand, total travel time, accessibility, or CO emission) after a perturbation ξ can be approximated based on the first-order Taylor expansion:

$$X'(\xi) = X(\xi_0) + \nabla_{\xi} X\big|_{\xi_0} \cdot (\xi - \xi_0), \tag{8.31}$$

where $\nabla_{\xi} X\big|_{\xi_0}$ denotes the derivatives of performance measure X evaluated at the original perturbation level ξ_0.

8.4 Numerical experiments

This section applies the proposed equilibrium model and sensitivity analysis-based system analysis method to two transportation systems with multiple emerging

mobilities. The mobility services and bundles considered in the numerical experiments are as shown in Figure 8.3. A single-OD example is first conducted to illustrate the properties of the proposed equilibrium analysis framework. A multi-OD case study is then carried out to verify the applicability of the proposed framework in real-world scenarios with different OD-level mobility service qualities and multiple bundle loyalty schemes.

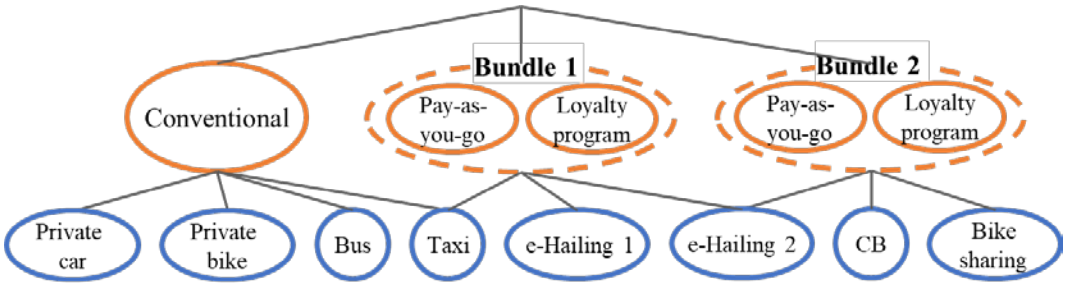

Figure 8.3. Mobility services and bundles considered in numerical experiments

8.4.1 Single-OD system example

In this example, the effectiveness and features of the proposed methods are demonstrated in a single-OD transportation system with two mobility bundles and a single loyalty scheme for each bundle. The model parameters are $\eta_{b_1}=0.1$, $\eta_{b_2}=0.05$, $\beta_{um}^{rs}=3.7$, $\beta_{u}^{rs}=1.85$ (Kitthamkesorn and Chen, 2017; Wang et al., 2020a). The input data for this example are as follows:

$q=1000$ (travelers), $vot=60$ (CNY/h), $d^{rs}=10$ (km), $c_{fl,car}^{rs}=0.6$ (CNY/km), $c_{p,car}^{rs}=15$ (CNY); $t_{iv,PT}^{rs}=25$ (min), $t_{wt,PT}^{rs}=5$ (min), $t_{a,PT}^{rs}=5$ (min), $c_{f,PT}^{rs}=2$ (CNY); $t_{iv,CB}^{rs}=20$ (min), $t_{a,CB}^{rs}=3$ (min), $t_{wt,CB}^{rs}=3$ (min), $c_{f,CB}^{rs}=12$ (CNY); $t_{wt,RH}^{rs}=2$ (min), $c_{f,RH}^{rs}\left(d^{rs}\right)=c_{0,m}^{rs}+\alpha_m\cdot\left(d^{rs}-3\right)$, where $c_{0,SH}^{rs}=9$ (CNY), $c_{0,RH1}^{rs}=10$ (CNY), $c_{0,m}^{rs}=15$ (CNY), $\alpha_{SH}=2.2$ (CNY/km), $\alpha_{RH1}=1.6$ (CNY/km), $\alpha_{RH2}=1.1$ (CNY/km); $t_{iv,BK}^{rs}=34$ (min), $c_{PB}^{rs}=4$ (CNY), $c_{f,BS}^{rs}\left(t_{iv,BK}^{rs}\right)=1.5+\dfrac{t_{iv,BK}^{rs}-15}{15}$ (CNY).

The road in-vehicle travel time is given by the BPR function:

$$t_{iv,rd}^{rs}\left(q_{rd}^{rs}\right)=t_{rd,0}^{rs}\cdot\left[1+0.15\left(\frac{q_{rd}^{rs}}{600}\right)^4\right], \tag{8.32}$$

where $t_{rd,0}^{rs} = 12$ (min) is the free-flow travel time.

The in-vehicle crowding in bus is computed as (Wang et al., 2020a):

$$g\left(q_{PT}^{rs}, t_{iv,PT}^{rs}\right) = t_{iv,PT}^{rs} \cdot \left[1 + 0.5\left(\frac{q_{PT}^{rs}}{1000}\right)^2\right]. \tag{8.33}$$

The riding fatigue during cycling is expressed as (Li et al., 2015):

$$g_{BK}\left(t_{iv,BK}^{rs}\right) = \alpha_1 \cdot t_{iv,BK}^{rs} + \alpha_2 \cdot \left(t_{iv,BK}^{rs}\right)^2, \tag{8.34}$$

where $\alpha_1 = 2$ (HK$/hour), $\alpha_2 = 4$ (HK$/hour^2).

Without loss of generality, we adopt the following function for evaluating mode travel disutility (Hensher and Truong, 1985; Mirchandani and Soroush, 1987):

$$\tau_m^{rs} = \exp\left(0.075 \cdot t_m^{rs}\right), \forall m \in M_{rs}, rs \in RS\,. \tag{8.35}$$

8.4.1.1 Numerical results and evaluation

This section shows model outputs and corresponding system performance measures under sufficient supplies of mobilities (i.e., capacity constraints (8.4), (8.6), (8.7), (8.10) are not activated). The model outputs in terms of the equilibrium bundle and mode demands are presented in Figure 8.4 (where e-hailing 1 and e-hailing 2 are abbreviated as EH1 and EH2).

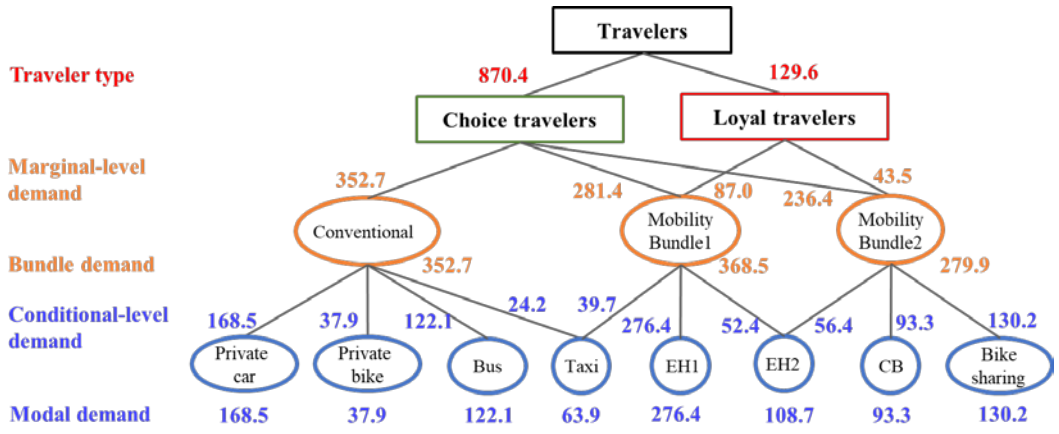

Figure 8.4. Travel demand pattern of single-OD example at each choice level

The bundle and mode shares are respectively summarized in the left and right panels of Figure 8.5. The effect of bundling is reflected in the results. Owing to a larger bundle loyalty, bundle 1 attracts more loyal travelers than bundle 2. Due to the correlations among modes within nests/bundles, the street-hailing taxi and e-hailing 2 services attract much fewer passengers than e-hailing 1 in mobility bundle 1. Their demands are diverted by travel modes in other bundles/nests because of the higher degrees of competition therein.

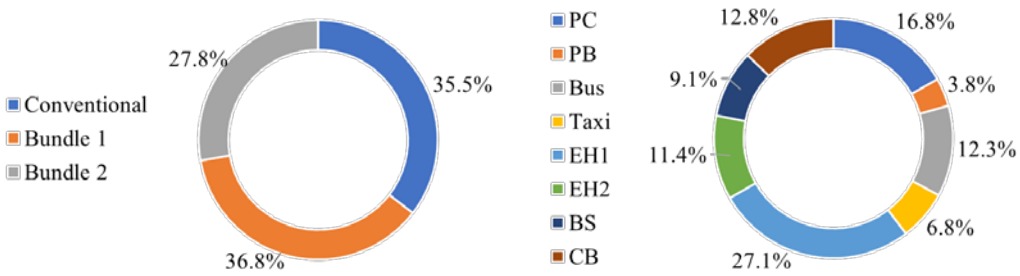

Figure 8.5. Shares of mobility bundles and individual modes in single-OD example

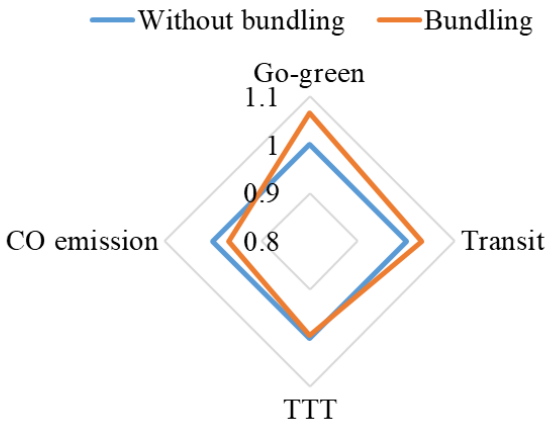

Figure 8.6. Effect of bundling in system performances

The system performance measures, including shares of transit services (i.e., bus and CB) and go-green modes (i.e., private bike, bus, CB, and bike sharing), system total travel time, and system CO emission, are analyzed in Figure 8.6 to further demonstrate the effect of bundling. For comparison, the equilibrium travel demand pattern in the same system but with no mobility bundle is derived using the basic multinomial weibit equilibrium model (Kitthamkesorn and Chen, 2013). From Figure 8.6, the mobility bundling with corresponding loyalty schemes can enhance the attractiveness of bundled

modes, which significantly increases the shares of transit and go-green modes. This leads to a slight reduction in the system travel time by alleviating road congestion and a significant enhancement in environmental friendliness.

8.4.1.2 Sensitivity analysis with respect to inputs and parameters

The section examines the effects of different parameters and inputs on model outcomes through the sensitivity analysis method introduced in Section 8.3.3.1. In this section, the emerging mobilities are considered to have sufficient capacities, such that the differences in attractiveness among bundles and modes are entirely based on the demand-dependent travel disutility.

Figure 8.7 shows the increase in share of bundles and modes under a unit increase in the OD travel demand. E-hailing service 1 will attract more incremental demand due to its superior service quality compared with other ride-hailing services. Compared with the mode share pattern of the existing demand (as shown in Figure 8.5), the sensitivity analysis results show that the go-green modes, such as bus, customized bus, and bike sharing, will attract relatively larger proportion of the incremental travel demand as they are less influenced by the increased road congestion.

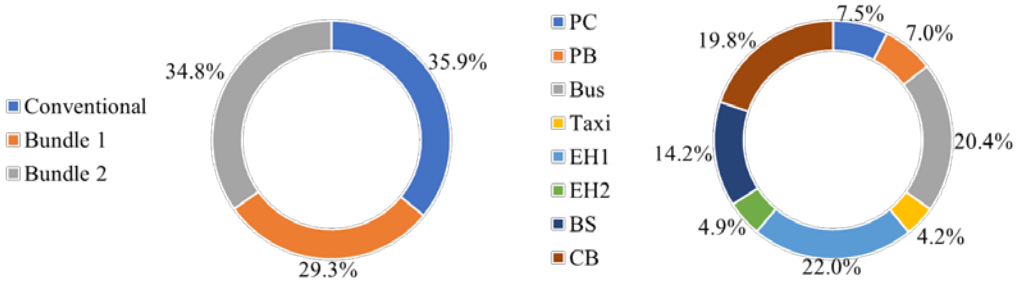

Figure 8.7. Sensitivities to total travel demand

Figure 8.8 investigates the sensitivities of bundle and mode demands with respect to bundle loyalty. Compared with other parameters and inputs, the increase in bundle loyalty can exert a much more significant impact on the equilibrium bundle demand pattern. This implies that loyalty is an important factor to be considered in the travel demand analysis. As for decision-makers, promoting policies/strategies for improving the loyalty to bundles of shared mobilities (e.g., Bundle 2) shows great potential to reduce road traffic and encourage the usage of active (cycling) and go-green modes.

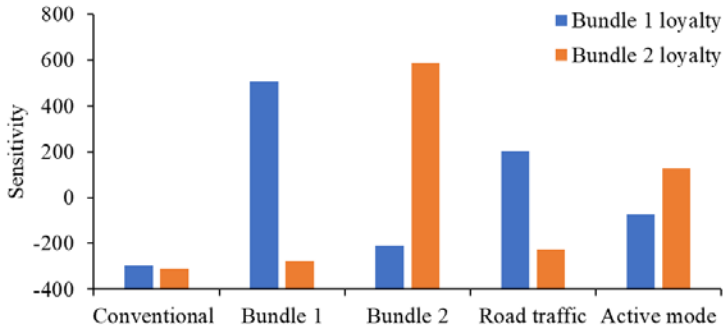

Figure 8.8. Sensitivities to loyalty parameter of each mobility bundle

Figure 8.9 examines the sensitivities to the dissimilarity parameter $\varphi_u^{rs} = \beta_u^{rs} / \beta_{um}^{rs}$, which associates with the degree of competition among modes in the same nest/bundle. An increase in the dissimilarity parameter implies a lower competition among modes within the same bundle. The results indicate that in this example, the ride-hailing modes are more sensitive to the competition between each other. Specifically, taxi and e-hailing 2 are most negatively influenced by the competition as they are bundled/nested with more competitive modes that can divert more demands from them. While e-hailing 1 benefits most from the competition as it has the most significant advantage in service quality compared to the other modes in the same bundle.

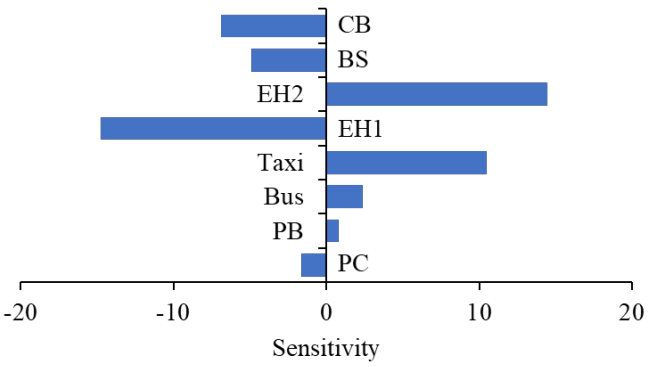

Figure 8.9. Sensitivities to dissimilarity parameter

8.4.1.3 Sensitivity analysis considering mobility supplies

This section uses the sensitivity analysis-based method to investigate the effects of supplies, i.e., capacities of both conventional and emerging travel modes. Figure 8.10 investigates the effect of considering emerging mobility capacity on the sensitivities

with respect to the loyalty parameter η. When the capacities of emerging mobilities are insufficient (capacities of all on-demand modes are set as 100 travelers), the effects of enhancing bundle loyalty significantly decrease. Compared to the results in Figure 8.8, the improvement of loyalty cannot influence the go-green mode share and road traffic as the limited supply becomes the bottleneck of shared mobility attractiveness.

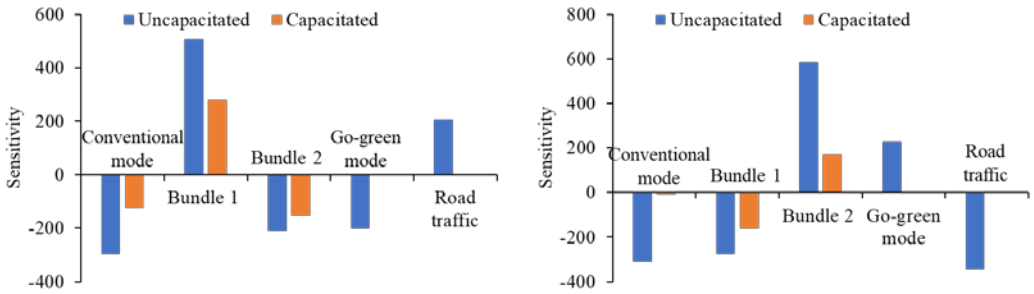

(a) Loyalty to bundle 1 (b) Loyalty to bundle 2

Figure 8.10. Sensitivities of modal demands under different capacitated conditions

Figure 8.11 further investigates the sensitivities to road capacity, which indirectly influences road traffic via road congestion instead of directly restricting modal demands. As can be expected, the improvement in road capacity can reduce congestion, enhance attractiveness of car modes, and divert travel demand from shared mobilities and active modes. Specifically, the private car can attract more demands in the case where on-demand modes are capacitated and ride-hailing services cannot benefit from the enhancement of attractiveness.

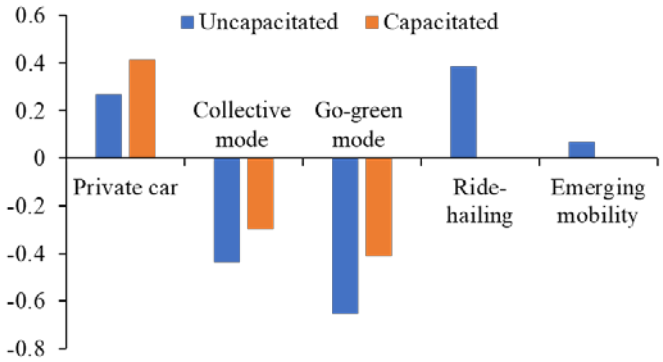

Figure 8.11. Sensitivities of modal demands with respect to road capacity

We further investigate and compare the sensitivities of system performance measures with respect to capacities of both conventional and emerging modes. The outcomes are shown in Figure 8.12, which reflects the criticality of supply improvement for each mobility service. Increasing road capacity still has the most significant positive impacts on system travel time and accessibility. It can even slightly reduce CO emissions by alleviating road congestion. On the other hand, it is worthy to note that comparing to road capacity, the capacity of emerging shared mobilities, i.e., bike sharing and customized bus, can have comparable or even greater positive effect on accessibility and CO emission. Considering the relatively lower cost of increasing capacities of shared mobilities, this result implies that providing enough shared mobility supplies may have higher priority in the planning of future transportation systems. Furthermore, adding capacity of ride-hailing services can have negative effects on the examined performance measures, implying that promoting ride-hailing services may not be a good choice in congested transportation systems.

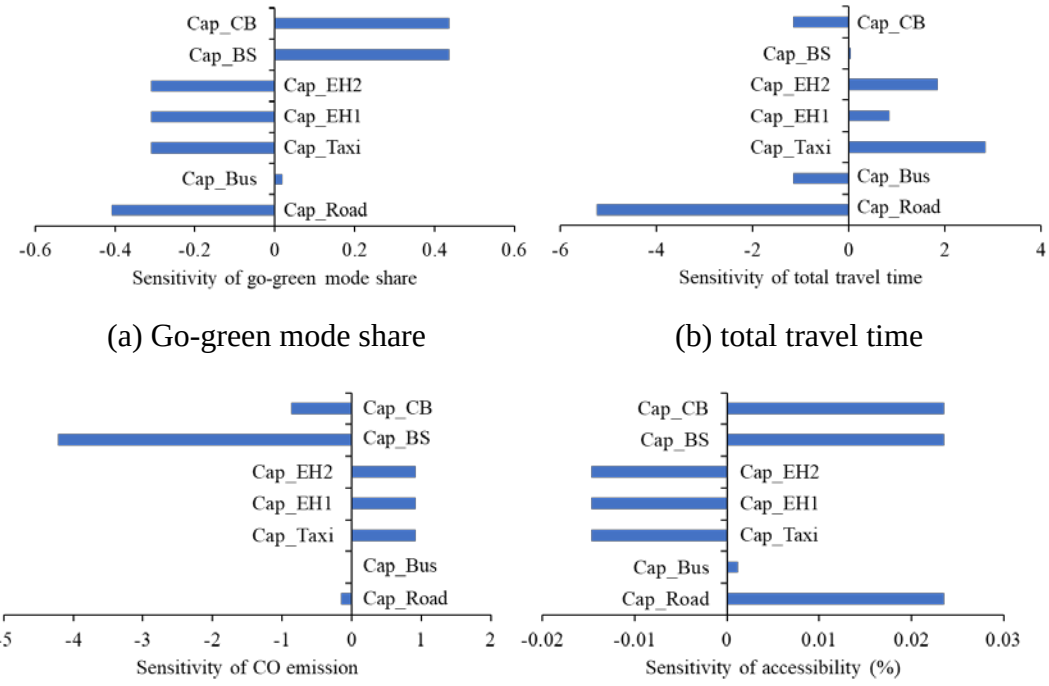

(a) Go-green mode share (b) total travel time

(c) CO emission (d) Accessibility

Figure 8.12. Sensitivities of system performances with respect to capacities

8.4.2 Case study in multi-OD transportation system

This section verifies the application of the proposed model in a multi-OD case study based on a multi-modal network extracted from Nanjing, China (Huang et al., 2020a). The study area is shown in Figure 8.13, where eleven zones, eight OD pairs are considered in the case study.

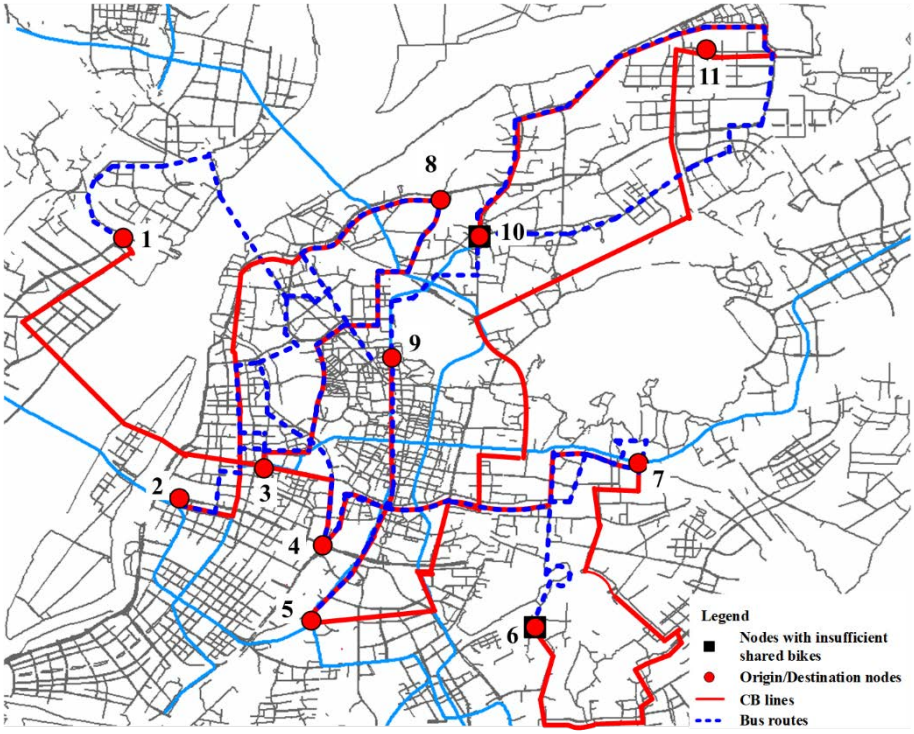

Figure 8.13. Study area with emerging mobility services
(adapted from Huang et al., 2020a)

Table 8.2. Inputs of multi-OD case study

OD pair	Travel demand (person)	Distance (km)	Car Time (min)	Road Capacity (veh)	Bus Time (min)	Bus Capacity (person)	Bike Time (min)	CB Time (min)	CB Fare (CNY)
1-4	300	17.6	22	200	65	300	70.4	44	10
2-8	420	17.4	21	200	56	300	69.6	42	10
3-8	310	11	15	200	41	300	44	33	8
4-7	300	13.4	17	100	46	300	53.6	40	8
5-9	350	14.9	26	100	48	500	59.6	43	8
5-11	300	26	40	100	50	500	104	52	14
6-7	450	5.7	10	200	15	300	22.8	18	6
10-11	300	9.1	15	100	30	500	36.4	30	6

The input data used in the numerical experiments are presented in Table 8.2. The model parameters and computations of mode travel disutility are consistent with

Section 8.4.1. All eight mobility services and three mobility bundles shown in Figure 8.3 are operated between each OD pair with different service qualities and are considered to have the same degree of loyalty and sufficient capacity in Section 8.4.2.1. The effects of pricing of multiple loyalty bundle schemes and capacity of emerging mobilities are then investigated in Section 8.4.2.2.

8.4.2.1 Model outcomes and system performances

Figure 8.14 shows the equilibrium mode shares between each OD pair. Consistent with the insights from existing studies, CB services tend to have higher attractiveness when travel distance is long (e.g., OD pair 5-11), while cycling modes (both private bike and bike sharing) have higher attractiveness in trips with short distance (e.g., OD pairs 10-11 and 6-7). The performances of bus and CB highly depend on the service quality. For instance, the bus and CB lines between OD pairs 4-7 and 5-9 have less detour than those between 1-4 and 2-8, and thus can attract much more demands in the competition with private car and ride-hailing services.

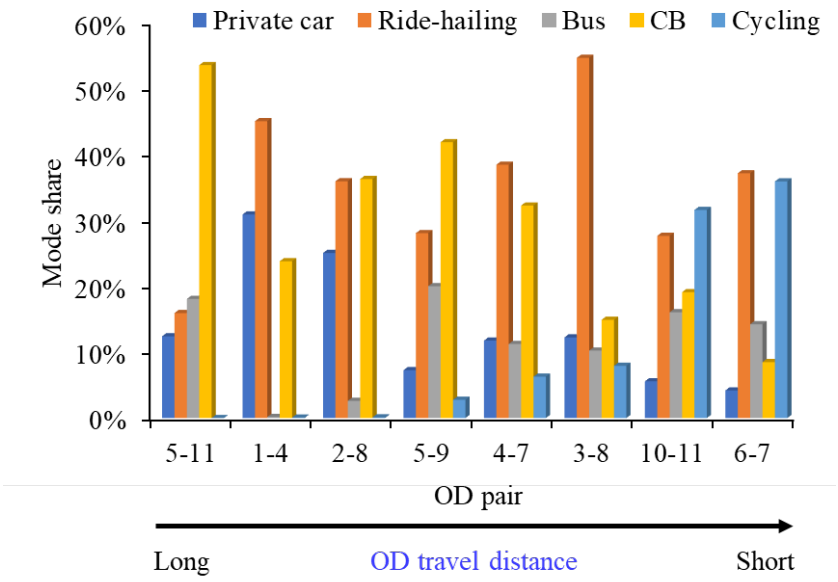

Figure 8.14. Mode share between each OD pair in multi-OD case study

Figure 8.15 examines the sensitivity of performance measures with respect to the free-flow in-vehicle travel time of each mode. Cycling modes and CB services have a more significant impact on the CO emission and system travel time, respectively. Consistent with the discussions on Figure 16, cycling modes are more important for

accessibility of short-distance OD pairs (6-7), while CB services play a critical role in the accessibility of distant OD pairs (5-11). In addition, the reduction in bus travel time has similar but slightly larger effects on CO emission and accessibility. These outcomes can provide insights for deciding the implementation and priority of infrastructure design and policymaking for different mobilities in transportation planning.

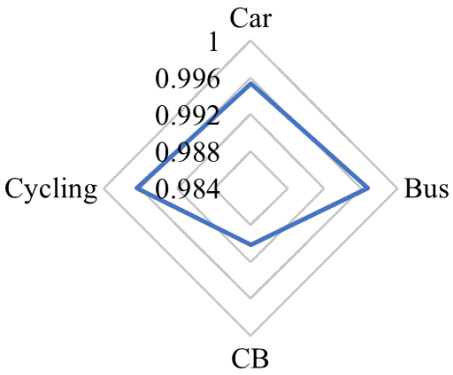

(a) System travel time

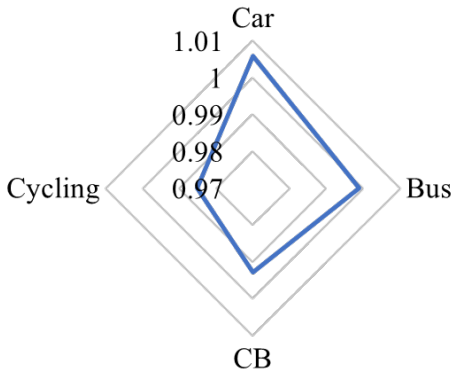

(b) CO emission

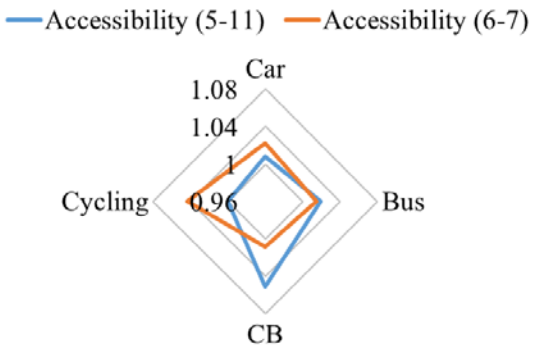

(c) OD-level accessibility

Figure 8.15. Effect of a unit reduction in mode travel time

8.4.2.2 Effect of emerging mobility supply

This section evaluates the effect of supplies of emerging mobilities in terms of service capacity and pricing of loyalty bundle scheme. Figure 8.16 shows the cycling demands and CO emissions between the two short-distance OD pairs (6-7, 10-11) with the evolution of bike sharing capacity. Nodes 6 and 10 are schools and transit hubs that are considered to have insufficient bike sharing supply (capacity = 50 bikes). Before accommodating all potential bike sharing requests, increasing bike sharing capacity can stably increase cycling demand and reduce CO emissions.

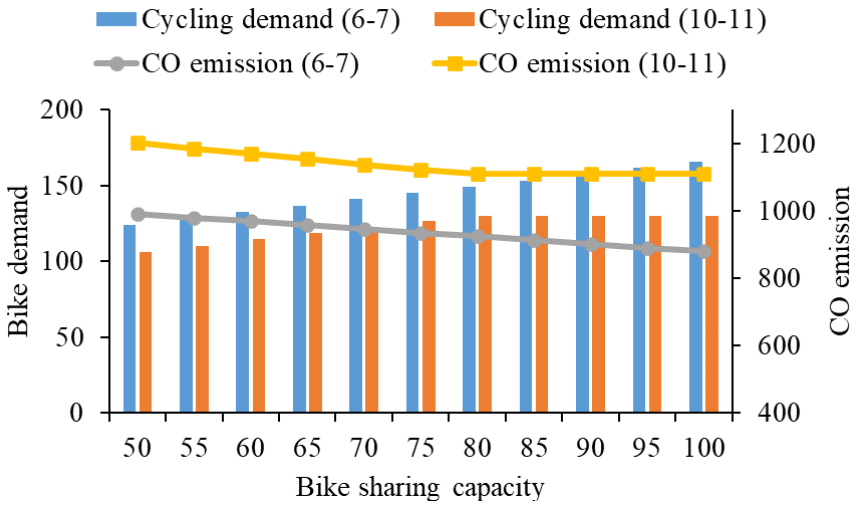

Figure 8.16. Effect of bike sharing capacity

We further consider the case when bike sharing and customized bus services are newly introduced to OD pairs 5-9 and 10-11, where travelers have no loyalty to the corresponding mobility bundle 2. A discount on CB and bike sharing fares is to be implemented to enhance loyalty to bundle 2. In this case, Eqs. (3.51)–(3.52) are used to obtain the loyalty parameter based on the preference to loyalty scheme when previous mode choice probabilities are absent. The bundle demands and OD-level accessibility are evaluated in Figure 8.17 under varying levels of discounts.

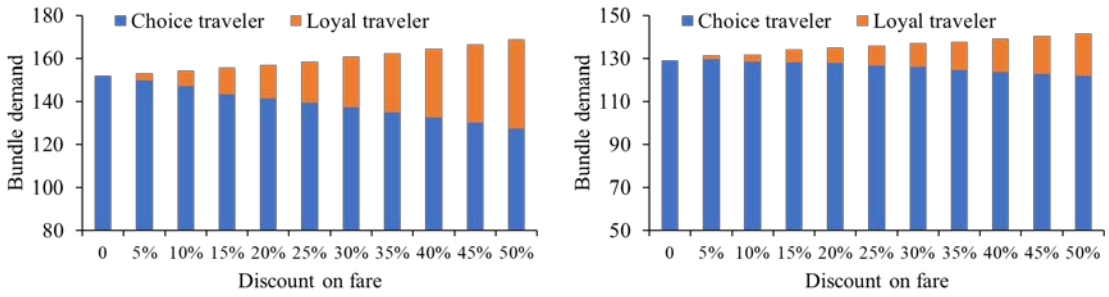

(a) OD pair 5-9 (b) OD pair 10-11

Figure 8.17. Effect of loyalty scheme pricing on demand of mobility bundle 2

From Figure 8.17, the effect of discounts is more significant between OD pair 5-9 where the CB service is preferred. Although bike sharing plays a critical role between OD pair 10-11, the decrease in bike sharing fare has a lower impact than CB fare. It is because that the attractiveness of bike sharing depends more on the cycling time. Unlike

bike sharing, the CB fare is a greater concern for CB passengers Thus, fare discount can have a more significant impact on the bundle preference, leading to a larger increase in bundle loyalty and bundle demand. Compared to fare discount, reducing in-vehicle travel time and riding fatigue might be more effective for the bike sharing service. This implies that the incentives for different emerging mobilities need to be customized based on the service features.

8.5 Conclusions

This chapter proposes an equilibrium analysis for the joint bundle and mode choice in multi-modal transportation systems with emerging mobilities. The loyalty to mobility bundles and correlations among different modes are specifically considered. To derive the aggregate demand pattern, an equilibrium model is developed and formulated as an equivalent MP problem, which guarantees equivalence and uniqueness of solutions and enables the application of convergent and efficient solution algorithms. The sensitivity analysis of the proposed equilibrium model is developed based on the MP model formulation, which facilitates the post-analysis of transportation systems via various performance measures.

Various numerical experiments are conducted to illustrate the proposed choice model and sensitivity analysis-based system evaluation method in a single-OD system and a real-world case study extracted from Nanjing, China. The results show the effect of bundle loyalty and mode correlations can be effectively considered by the proposed model. Mobility bundling and bundle loyalty are found to be important influencing factors of the demand distribution and system performance. The sensitivity analysis-based method can efficiently reveal the effects of different model parameters and inputs on model outcomes, which facilitates understanding the criticalities of different mobility service planning/operation schemes. The outcomes can provide insights for the decision-making on emerging mobility services. For example, the capacity of shared mobility services and incentives to loyalty schemes of shared mobility bundles are found to play an important role in the alleviation of road congestion and the improvement of environmental friendliness and accessibility. The discount on fares is an effective but not necessarily the most appropriate way to enhance the effect of bundle loyalty. The incentives to loyalty bundle schemes should be customized by decision-makers dependent on the features of different emerging mobilities.

Chapter 9 Modeling shared parking services at spatially correlated locations through a weibit-based combined destination and parking choice equilibrium model

9.1 Introduction

This chapter develops an equilibrium model for the emerging shared parking services based on the spatially correlated weibit (SCW) destination choice model and parking-size weibit (PSW) parking choice model developed in Section 3.4. Unlike most conventional curbside parking services, shared parking services allow travelers to circumvent the inconvenience of cruising-for-parking, which is a notable factor in modeling parking choice equilibrium (e.g., Leurent and Boujnah, 2014; Boyles et al., 2015; Pel and Chaniotakis, 2017). Zhang et al. (2020) considered this feature of shared parking and proposed a user equilibrium (UE) model to examine the choice equilibrium between conventional curbside parking and emerging shared parking services. Despite of focusing on the parking choice equilibrium problem (Liu et al., 2022), few efforts have been devoted to modeling the equilibrium of joint destination and parking choice with shared parking services that accounted for the impact of parking service quality on the location attractiveness and destination demand pattern (Liu et al., 2021).

Many combined travel demand models (Oppenheim, 1995; Yang and Meng, 1998; Yao et al., 2014) have been proposed using logit-based models to reproduce the destination and travel choices together, which is similar to the joint destination and parking choice considered in this chapter. However, existing combined travel demand models typically adopt the multinomial logit (MNL) model for reproducing choice behaviors at the individual level. As illustrated in Section 3.4, the MNL model is inadequate to capture the heterogeneity in perceived destination and parking disutility, or the similarity among spatially correlated alternatives, which are important concerns in modeling destination and parking choice behaviors.

To address the abovementioned research gaps, this chapter proposes an advanced equilibrium model for investigating the effect of shared parking services on joint destination and parking choices. Benefiting from the SCW-PSW choice model developed in Section 3.4, travelers' random perceptions of travel disutility are consistently considered based on the random utility theory at both the destination and parking choice dimensions. Furthermore, the heterogeneity and spatial correlation

issues can be simultaneously addressed in each choice dimension. The proposed equilibrium model is formulated as an equivalent mathematical programming (MP) problem consistent with the SCW-PSW choice model. The developed MP formulation ensures high interpretability and enables the application of readily available convergent and efficient solution algorithms.

9.2 Problem statement

To facilitate the presentation of the essential ideas without loss of generality, Sections 9.2.1 and 9.2.2 introduce the notations and main model assumptions, respectively. The travel disutility at each choice dimension is described in Section 9.2.3.

9.2.1 Notations

Sets

R	Set of origins.
S	Set of destinations.
ST	Set of destination pairs.

Inputs and parameters

ψ_s	Attractiveness of destination *s*.
t_s^r	In-vehicle travel time between OD pair *rs*.
vot	Value of time.
c_s^r	In-vehicle travel cost between OD pair *rs*.
$c_{s,sp}, c_{s,cp}$	Cost of shared parking/curbside parking at destination *s*.
$pc_{s,sp}, pc_{s,cp}$	Parking fee of shared parking/curbside parking at destination *s*.
$\alpha_{s,st}^r$	Allocation parameter indicating the proportion of destination *s* in destination pair *st*.
β^r	Shape parameter with respect to the marginal destination choice level.
β_s	Shape parameter with respect to the conditional destination choice level.
μ	Dissimilarity parameter.
w_{st}	Spatial correlation between locations *s* and *t*.
$PS_{s,sp}, PS_{s,cp}$	Parking-size factor of shared/curbside parking at destination *s*.
β_m	Shape parameter with respect to the parking choice.
$Cap_{s,sp}$, $Cap_{s,cp}$	Capacity of shared parking/curbside parking service at destination *s*.

Intermediate variables

τ_s^r	Total disutility of traveling from origin *r* to destination *s*.
$\tau_{s,sp}^r, \tau_{s,cp}^r$	Total disutility of traveling from origin *r* to destination *s* using shared parking/curbside parking.
$\tau_{s,sp}, \tau_{s,cp}$	Disutility of using shared parking/curbside parking at destination *s*.
$\tau_{s,st}^r$	Deterministic part of individual disutility of destination *s* in destination pair *st*.
τ_{st}^r	Common disutility of destination pair *st*.
$t_{s,sp}, t_{s,cp}$	Parking searching time of shared/curbside parking at destination *s*.
A_s^r	Accessibility between OD pair *rs*.

Decision variables

$f_{s,sp}^r$, $f_{s,cp}^r$	Flow of shared parking/curbside parking between OD pair *rs*.
$q_{s,st}^r$	Travel demand at destination *s* belonging to destination pair *st* from origin *r*.
q_{st}^r	Travel demand of destination pair *st* from origin *r*.
q_s^r	Travel demand between OD pair *rs*.

9.2.2 Assumptions

A9.1: Travelers make destination and parking choices together to minimize their total perceived disutility. The random disutility perception errors follow the Weibull distribution (Castillo et al., 2008; Kitthamkesorn and Chen, 2017).

A9.2: The total disutility of travelers resulting from the combined destination and parking choice consists of the destination utility, travel disutility, and parking disutility (including parking searching time and parking fee). The disutility function has a multiplicative form, which is consistent with the psychophysical laws on how different magnitudes of travel disutility is perceived and has better behavioral interpretations than the commonly used additive utility function adopted in logit models (Fosgerau and Bierlaire, 2009; Chakroborty et al., 2021).

A9.3: At the parking choice level, travelers choose from two types of parking services, i.e., shared parking and curbside parking. Shared parking users do not spend any time searching for parking but may fail to reserve a shared parking slot when the shared parking demand reaches the capacity. The searching time for curbside parking is an increasing function with respect to the parking occupancy rate (i.e., the ratio of the parking demand to the parking capacity). The curbside parking capacity is sufficient to accommodate all parking demands (Zhang et al., 2020; Liu et al., 2021, 2022).

9.2.3 Destination utility and parking disutility

The proposed model considers both the destination utility and travel disutility resulting from joint destination and parking choices. Let τ_s^r denote the total disutility of traveling from origin *r* to destination *s*. In the weibit-based choice model, τ_s^r is expressed in the following multiplicative form:

$$v_s^r = A_s^r \cdot \left(\psi_s\right)^{-1}, \forall r \in R, s \in S . \tag{1}$$

ψ_s denotes the utility of destination *s*, which is represented by the attractiveness of *s* that can be calibrated exogenously. A_s^r denotes the accessibility between OD pair *rs*, which is a composite disutility (i.e., the expected minimum travel disutility) derived based on the parking choice model as illustrated in Section 2.1.3.

The travel disutility consists of the in-vehicle travel cost c_s^r and parking disutility $v_{s,m}$. The in-vehicle travel cost between OD pair *rs* is associated with the in-vehicle OD travel time:

$$c_s^r = vot \cdot t_s^r, \forall r \in R, s \in S , \tag{2}$$

where *vot* denotes the value of time. t_s^r is assumed to be exogenously given because on-trip congestion is not the focus of this model (Zhang et al., 2020; Liu et al., 2021). The parking disutility is considered to include the parking cost and difficulty to reserve a vacant shared parking slot (for shared parking services). The parking cost at destination *s* consists of the parking searching time and parking fee:

$$\tau_{s,m} = vot \cdot t_{s,m} + pc_{s,m}, \forall r \in R, s \in S, m = sp, cp . \tag{3}$$

$pc_{s,sp}$ and $pc_{s,cp}$ denote the monetary fee of shared parking and curbside parking at destination *s*. $t_{s,cp}$ is the curbside parking searching time, which is an increasing function of curbside parking demand $f_{s,cp}$ (i.e., $t_{s,cp}\left(f_{s,cp}\right)$). The shared parking service has a constant searching time $t_{s,sp}$ but limited number of parking slots, i.e., there exists a tight capacity constraint on the shared parking space. When the capacity constraint is activated, there exists a positive dual variable that increases the shared parking disutility,

which can be interpreted as the penalty induced by the difficulty to reserve a vacant shared parking slot.

9.3 Combined destination and parking choice equilibrium model

9.3.1 Mathematical programming model formulation

As described in Section 9.2.3, the parking disutility is demand-dependent, it is thus necessary to consider the congestion effect when modeling the equilibrium destination and parking choices. This section presents the equilibrium SCW-PSW model to obtain the aggregate travel demand pattern based on the endogenous parking disutility while consistent with the individual choice probability from the SCW-PSW model developed in Section 3.4. Thus, the equilibrium destination and parking choice behaviors are consistently modeled based on the random utility theory, which addresses the behavioral inconsistency in the joint destination and parking equilibrium model proposed by Liu et al. (2021).

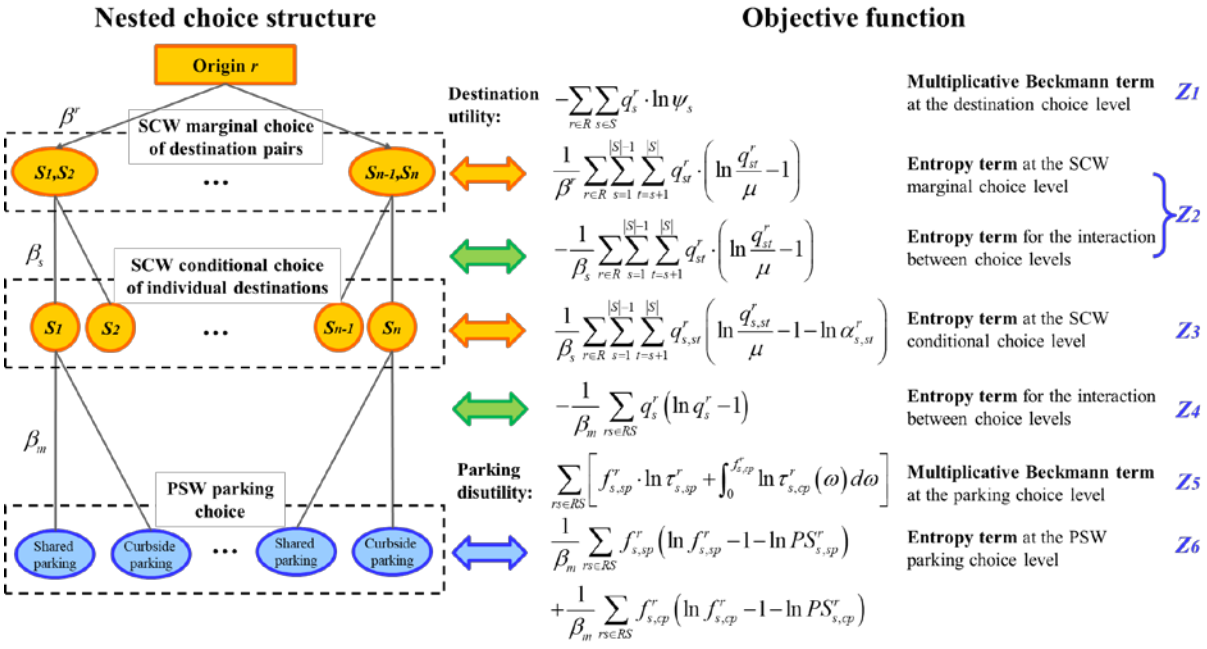

Figure 9.1. Construction of the MP objective function for the equilibrium combined destination and parking choice model

Based on the method introduced in Chapter 5, an equivalent MP formulation of the equilibrium SCW-PSW model is developed, which leads to analytical expressions of primal variables and can be solved by readily available convergent and efficient

algorithms. Figure 9.1 illustrates the construction of the objective function according to the hierarchical structure of the joint destination and parking choice (Figure 3.13) and the nested structure of the SCW model (Figure 3.15). Due to the multiplicative disutility function used by the weibit-based models, the multiplicative Beckmann terms are adopted for representing the destination utility and parking disutility (Kitthamkesorn and Chen, 2013). Entropy terms are constructed individually for the SCW probabilities at the marginal and conditional destination choice levels, PSW probabilities at the parking choice level, and interactions among different choice levels.

By normalizing $\beta^r = 1$, $\beta_s = 1/\mu$ and substituting $q_{st}^r = q_{s,st}^r + q_{t,st}^r$ into term Z_2, the MP model formulation can be written as follows:

$$
\begin{aligned}
\min\ Z &= Z_1 + Z_2 + Z_3 + Z_4 + Z_5 + Z_6 \\
&= \sum_{rs\in RS}\left[f_{s,sp}^r \cdot \ln \tau_{s,sp}^r + \int_0^{f_{s,cp}^r} \ln \tau_{s,cp}^r(\omega)\, d\omega \right] \\
&+ \frac{1}{\beta_m} \sum_{rs\in RS}\left[f_{s,sp}^r \left(\ln f_{s,sp}^r - 1 - \ln PS_{s,sp}^r \right) + f_{s,cp}^r \left(\ln f_{s,cp}^r - 1 - \ln PS_{s,cp}^r \right) \right] \\
&- \frac{1}{\beta_m} \sum_{rs\in RS} q_s^r \left(\ln q_s^r - 1 \right) \\
&- \sum_{r\in R}\sum_{s\in S} q_s^r \cdot \ln \psi_s \\
&+ \mu \sum_{r\in R}\sum_{s\in S}\sum_{t\neq s\in S} q_{s,st}^r \left(\ln \frac{q_{s,st}^r}{\mu} - 1 \right) - \sum_{r\in R}\sum_{s\in S}\sum_{t\neq s\in S} q_{s,st}^r \ln \alpha_{s,st}^r \\
&+ (1-\mu) \sum_{r\in R}\sum_{s=1}^{|S|-1}\sum_{t=s+1}^{|S|} \left(q_{s,st}^r + q_{t,st}^r \right) \left(\ln \frac{q_{s,st}^r + q_{t,st}^r}{\mu} - 1 \right)
\end{aligned}
\tag{9.4}
$$

s.t.

$$f_{s,sp}^r + f_{s,cp}^r = q_s^r, \forall r \in R, s \in S \tag{9.5}$$

$$\sum_{s\in S} q_s^r = q^r, \forall r \in R \tag{9.6}$$

$$\sum_{st\in ST} q_{s,st}^r = q_s^r, \forall r \in R, s \in S \tag{9.7}$$

$$\sum_{r\in R} f_{s,sp}^r \le Cap_{s,sp}, \forall s \in S \tag{9.8}$$

$$q_{s,st}^r \ge 0 \quad \forall r \in R, st \in ST, s \in S \tag{9.9}$$

$$f_{s,sp}^{r},\ f_{s,cp}^{r} \geq 0, \forall r \in R, s \in S \tag{9.10}$$

Objective function (9.4) aims to find the equilibrium destination and parking demand based on the SCW-PSW model. Conservation constraints (9.5) and (9.6) indicate the relationship between the parking flow and OD demand and between the OD demand and zonal production, respectively. Constraint (9.7) is the definitional constraint. Capacity constraint (9.8) specifies the limited shared parking space. Constraints (9.9) and (9.10) are nonnegative constraints. The following two propositions are defined to show the qualitative properties of the proposed MP formulation.

Proposition 9.1. The proposed MP formulation (9.4)–(9.10) yields the equilibrium destination and parking choice solution of the SCW-PSW model.

Proof. Construct the Lagrangian of the proposed MP problem and let its partial derivatives with respect to solution variables equal to zero, we can obtain the analytical expression of decision variables $f_{s,m}^{r}$, q_{s}^{r}, q_{st}^{r}, and $q_{s,st}^{r}$:

$$f_{s,m}^{r} = e^{-\beta_m \cdot \left(\pi_s^r + \omega_{s,m}\right)} \cdot PS_{s,m} \cdot \left(\tau_{s,m}^{r}\right)^{-\beta_m}, \tag{9.11}$$

$$-\frac{1}{\beta_m} \ln q_s^r = \ln A_s^r + \pi_s^r, \tag{9.12}$$

$$\frac{q_{s,st}^{r}}{\mu} \cdot \left(\frac{q_{s,st}^{r} + q_{t,st}^{r}}{\mu}\right)^{\frac{1-\mu}{\mu}} = \left[\alpha_{s,st}^{r} \cdot \left(\tau_s^r\right)^{-1} \cdot e^{-\lambda^r}\right]^{\frac{1}{\mu}}, \tag{9.13}$$

$$q_{st}^{r} = q_{s,st}^{r} + q_{t,st}^{r} = \mu \cdot e^{-\lambda^r} \cdot \left\{\left[\alpha_{s,st}^{r}\left(\tau_s^r\right)^{-1}\right]^{\frac{1}{\mu}} + \left[\alpha_{t,st}^{r}\left(\tau_t^r\right)^{-1}\right]^{\frac{1}{\mu}}\right\}^{\mu}. \tag{9.14}$$

In Eq. (9.11), $e^{-\omega_{s,m}}$ can be considered as a penalty on the risk of failed subscription to shared parking services and can be integrated with the parking disutility $\tau_{s,m}^{r}$. Hence, substituting Eq. (9.11) into Eq. (9.5) leads to the PSW parking choice probability:

$$\frac{f_{s,sp}^{r}}{q_s^r} = \frac{e^{-\beta_m \cdot \pi_s^r} \cdot PS_{s,sp} \cdot \left(\tau_{s,sp}^{r}\right)^{-\beta_m}}{e^{-\beta_m \cdot \pi_s^r} \cdot \left[PS_{s,sp} \cdot \left(\tau_{s,sp}^{r}\right)^{-\beta_m} + PS_{s,cp} \cdot \left(\tau_{s,cp}^{r}\right)^{-\beta_m}\right]}. \tag{9.15}$$

Substitute Eqs. (9.12)–(9.14) into Eq. (9.6), we can obtain the marginal and conditional destination choice probabilities of the SCW model as follows:

$$\frac{q_{s,st}^r + q_{t,st}^r}{\sum_{s=1}^{|S|-1}\sum_{t=s+1}^{|S|}\left(q_{s,st}^r + q_{t,st}^r\right)} = \frac{e^{-\lambda^r}\cdot\left\{\left[\alpha_{s,st}^r\left(\tau_s^r\right)^{-1}\right]^{\frac{1}{\mu}} + \left[\alpha_{t,st}^r\left(\tau_t^r\right)^{-1}\right]^{\frac{1}{\mu}}\right\}^{\mu}}{\sum_{s=1}^{|S|-1}\sum_{t=s+1}^{|S|} e^{-\lambda^r}\cdot\left\{\left[\alpha_{s,st}^r\left(\tau_s^r\right)^{-1}\right]^{\frac{1}{\mu}} + \left[\alpha_{t,st}^r\left(\tau_t^r\right)^{-1}\right]^{\frac{1}{\mu}}\right\}^{\mu}}, \quad (9.16)$$

$$\frac{q_{s,st}^r}{q_{s,st}^r + q_{t,st}^r} = \frac{e^{-\frac{\lambda^r}{\mu}}\cdot\left[\alpha_{s,st}^r\cdot\left(\tau_s^r\right)^{-1}\right]^{\frac{1}{\mu}}}{e^{-\frac{\lambda^r}{\mu}}\cdot\left\{\left[\alpha_{s,st}^r\cdot\left(\tau_s^r\right)^{-1}\right]^{\frac{1}{\mu}} + \left[\alpha_{t,st}^r\cdot\left(\tau_t^r\right)^{-1}\right]^{\frac{1}{\mu}}\right\}}. \quad (9.17)$$

For detailed proof, see Appendix A4.

Proposition 9.2. The destination flow and parking demand solutions to the MP formulation (9.4)–(9.10) are unique.

Proof. See Appendix B4.

9.3.2 Solution algorithm

Benefiting from the developed MP formulation, the relationship between primal and dual variables of the equilibrium model can be analytically derived (Eqs. (9.11)–(9.14)), which can be used to find the search direction in the solution algorithm. Taking advantage of this property, the partial linearization algorithm introduced in Section 5.3 is adapted for solving the proposed equilibrium model. The solution algorithm is described in Sections 9.3.2.1 and 9.3.2.2.

9.3.2.1 Partial linearization algorithm

Given the decision variables and corresponding travel disutility at iteration *k-1*, i.e., $\mathbf{f}^{\mathbf{k\text{-}1}}, \mathbf{q}^{\mathbf{k\text{-}1}}$ and $\boldsymbol{\tau}\left(\mathbf{f}^{\mathbf{k\text{-}1}}\right)$, the search direction (i.e., auxiliary parking flow **g** and auxiliary destination demand **y**) at iteration *k* is determined by solving a partial linearized subproblem as follows:

$$
\begin{aligned}
\min\ Z &= Z_{1,sub}(\mathbf{g}) + Z_2(\mathbf{g}) + Z_3(\mathbf{y}) + Z_4(\mathbf{y}) + Z_5(\mathbf{y}) + Z_6(\mathbf{y}) \\
&= \sum_{rs\in RS} g^r_{s,sp}\cdot \ln \tau^r_{s,sp} + g^r_{s,cp}\cdot \ln \tau^r_{s,cp}\left[\left(f^r_{s,cp}\right)^{n-1}\right] \\
&+ \frac{1}{\beta_m}\sum_{rs\in RS}\left[g^r_{s,sp}\left(\ln g^r_{s,sp} - 1 - \ln PS^r_{s,sp}\right) + g^r_{s,cp}\left(\ln g^r_{s,cp} - 1 - \ln PS^r_{s,cp}\right)\right] \\
&- \frac{1}{\beta_m}\sum_{rs\in RS} y^r_s\left(\ln y^r_s - 1\right) \\
&- \sum_{r\in R}\sum_{s\in S} y^r_s\cdot \ln \psi_s \\
&+ \mu\sum_{r\in R}\sum_{s\in S}\sum_{t\neq s\in S} y^r_{s,st}\left(\ln\frac{y^r_{s,st}}{\mu} - 1\right) - \sum_{r\in R}\sum_{s\in S}\sum_{t\neq s\in S} y^r_{s,st}\ln\alpha^r_{s,st} \\
&+ (1-\mu)\sum_{r\in R}\sum_{s=1}^{|S|-1}\sum_{t=s+1}^{|S|}\left(y^r_{s,st} + y^r_{t,st}\right)\left(\ln\frac{y^r_{s,st} + y^r_{t,st}}{\mu} - 1\right)
\end{aligned}
\tag{9.18}
$$

s.t.

$$g^r_{s,sp} + g^r_{s,cp} = y^r_s, \forall r \in R, s \in S \tag{9.19}$$

$$\sum_{s\in S} y^r_s = y^r, \forall r \in R \tag{9.20}$$

$$\sum_{st\in ST} y^r_{s,st} = y^r_s, \forall r \in R, s \in S \tag{9.21}$$

$$\sum_{r\in R} g^r_{s,sp} \le Cap_{s,sp}, \forall s \in S \tag{9.22}$$

$$y^r_{s,st} \ge 0 \quad \forall r \in R, st \in ST, s \in S \tag{9.23}$$

$$g^r_{s,sp}, g^r_{s,cp} \ge 0, \forall r \in R, s \in S \tag{9.24}$$

In the subproblem, the flow-dependent parking disutility in objective term Z_1 is linearized via a first-order approximation, which fixes the curbside parking searching time based on the current parking flow $\mathbf{f}^{k-1}$. The subproblem is a convex program with linear inequality constraints (i.e., capacity constraints (9.22)). In this chapter, the iterative balancing scheme is adapted to solve the subproblem (Bell, 1995; Ryu et al., 2014). In the line search, the moving step size is determined based on the advanced self-regulated averaging (SRA) scheme. The procedure of partial linearization algorithm involves the following steps:

Step 0. Initialization.

- Initialize primal variables $\mathbf{f^0=0}$, $\mathbf{q^0=0}$, and the free-flow parking disutility;
- Set outer iteration counter $k = 1$;
- Derive auxiliary flow pattern $\mathbf{g^1}$ and $\mathbf{y^1}$ by solving the partial linearized subproblem (9.18)–(9.24) based on the iterative balancing scheme;
- Initialize step size: $\varphi^1 = 1$, $\gamma^1 = 1$. Update primal variables: $\mathbf{f^1=g^1}$, $\mathbf{q^1=y^1}$.

Step 1. Direction finding.

- Update travel disutility based on the current flow pattern $\mathbf{f^k}$ and $\mathbf{q^k}$;
- Set $k = k + 1$;
- Derive auxiliary flow pattern $\mathbf{g^k}$ and $\mathbf{y^k}$ by solving the partial linearized subproblem (9.18)–(9.24) based on the iterative balancing scheme.

Step 2. Line search.

- Derive the step size φ^k based on the SRA scheme:

$$\varphi^k = 1/\gamma^k \tag{9.25}$$

$$\gamma^k = \begin{cases} \gamma^{k-1} + \sigma_1 & \text{if } \left\|\mathbf{g^k} - \mathbf{f^{k-1}}\right\| \geq \left\|\mathbf{g^{k-1}} - \mathbf{f^{k-2}}\right\| \\ \gamma^{k-1} + \sigma_2 & \text{otherwise} \end{cases} \tag{9.26}$$

where $\sigma_1 > 1$ and $\sigma_2 < 1$.

Step 3. Update primal variables.

$$\mathbf{f^k} = \mathbf{f^{k-1}} + \varphi^k \cdot \left(\mathbf{g^k} - \mathbf{f^{k-1}}\right);$$

$$\mathbf{q^k} = \mathbf{q^{k-1}} + \varphi^k \cdot \left(\mathbf{y^k} - \mathbf{q^{k-1}}\right).$$

Step 4. Convergence test.

- If $\max\left\{\left|\mathbf{f^k} - \mathbf{f^{k-1}}\right|, \left|\mathbf{q^k} - \mathbf{q^{k-1}}\right|\right\} \leq \varepsilon_1$, terminate the algorithm, where ε_1 is a convergence tolerance at which the procedure stops. Otherwise, go to step 1.

9.3.2.2 Iterative balancing scheme

This section describes the iterative balancing scheme used for finding the search direction in step 1 of the partial linearization algorithm. At each iteration of the iterative balancing scheme, one of the dual variables (λ^r and $\omega_{s,sp}$) is adjusted to make primal variables satisfy the corresponding constraint. The procedure of the iterative balancing scheme is specified as follows:

Step 0. Initialization.

- Set inner iteration counter $n = 0$;
- Initialize the dual variables: $\left(\omega_{s,sp}\right)^n, \left(\lambda^r\right)^n = 0, \forall r \in R, s \in S$.

Step 1. Update the primary variables.

- Based on dual variables, derive primal variables via Eqs. (9.11)–(9.14):

$$\left(y_{st}^r\right)^n = \mu \cdot e^{-\left(\lambda^r\right)^n} \cdot \left\{ \left[\alpha_{s,st}^r \left(\tau_s^r\right)^{-1} \right]^{\frac{1}{\mu}} + \left[\alpha_{t,st}^r \left(\tau_t^r\right)^{-1} \right]^{\frac{1}{\mu}} \right\}^{\mu}, \forall r \in R, st \in ST,$$

$$\left(y_{s,st}^r\right)^n = \mu \cdot \left[\frac{\left(y_{st}^r\right)^n}{\mu} \right]^{-\frac{1-\mu}{\mu}} \cdot \left[\alpha_{s,st}^r \cdot \left(\tau_s^r\right)^{-1} \cdot e^{-\left(\lambda^r\right)^n} \right]^{\frac{1}{\mu}}, \forall r \in R, s \in S,$$

$$\left(y_s^r\right)^n = \sum_{st \in ST} \left(y_{s,st}^r\right)^n, \forall r \in R, s \in S,$$

$$\left(g_{s,sp}^r\right)^n = e^{-\beta_m \cdot \left[\left(\pi_s^r\right)^n + \left(\omega_{s,sp}\right)^n \right]} \cdot PS_{s,sp} \cdot \left(\tau_{s,sp}^r\right)^{-\beta_m}, \forall r \in R, s \in S,$$

$$\left(g_{s,cp}^r\right)^n = e^{-\beta_m \cdot \left(\pi_s^r\right)^n} \cdot PS_{s,cp} \cdot \left(\tau_{s,cp}^r\right)^{-\beta_m}, \forall r \in R, s \in S,$$

where $\left(\pi_s^r\right)^n = -\frac{1}{\beta_m} \ln\left(y_s^r\right)^n - \ln\left(A_s^r\right)^n$.

Step 2. Update the dual variables.

$$\left(\lambda^r\right)^{n+1} = \left(\lambda^r\right)^n - \ln\left(\frac{q^r}{\sum_{st \in ST} \left(y_{st}^r\right)^n} \right)$$

$$\left(\omega_{s,sp}\right)^{n+1} = \max\left\{ 0, \left(\omega_{s,sp}\right)^n - \frac{1}{\beta_m} \ln\left(\frac{cap_{s,sp}}{\sum_{r \in R} \left(g_{s,sp}^r\right)^n} \right) \right\}$$

Step 3. Convergence test.

- Calculate the maximum adjustment among all dual variables. If $\max\left\{ \left| \left(\omega_{s,sp}\right)^{n+1} - \left(\omega_{s,sp}\right)^n \right|, \left| \left(\lambda^r\right)^{n+1} - \left(\lambda^r\right)^n \right| \right\} \le \varepsilon_2$, terminate the algorithm, where ε_2 is a convergence tolerance for the iterative balancing scheme. Otherwise, set $n = n + 1$ and go to step 1.

In Step 2, the adjustment factor for each dual variable is obtained based on the analytical relationships between primal and dual variables. The adjustment factor Δ^r associated with dual variable λ^r is derived by substituting the analytical expression of y_{st}^r (following Eq. (9.14)) in the conservation constraint (9.24):

$$\begin{aligned}
&\sum_{st\in ST} \mu \cdot e^{-\left(\lambda^r+\Delta^r\right)} \cdot \left\{ \left[\alpha_{s,st}^r \left(\tau_s^r\right)^{-1} \right]^{\frac{1}{\mu}} + \left[\alpha_{t,st}^r \left(\tau_t^r\right)^{-1} \right]^{\frac{1}{\mu}} \right\}^{\mu} = q^r \\
&\Rightarrow e^{-\Delta^r} \cdot \sum_{st\in ST} y_{st}^r = q^r \qquad (9.27) \\
&\Rightarrow \Delta^r = -\ln\left(\frac{q^r}{\sum_{st\in ST} \left(y_{st}^r\right)^n} \right)
\end{aligned}$$

The adjustment factor $\Delta_{s,sp}$ associated with dual variable $\omega_{s,sp}$ is derived by substituting the the analytical expression of $g_{s,sp}^r$ and $g_{s,cp}^r$ (Eq. (following 9.11)) into the capacity constraint (9.22):

$$\begin{aligned}
&\sum_{r\in R} e^{-\beta_m \cdot \left(\pi_s^r + \omega_{s,sp} + \Delta_{s,sp}\right)} \cdot PS_{s,sp} \cdot \left(\tau_{s,sp}^r\right)^{-\beta_m} = Cap_{s,sp} \\
&\Rightarrow e^{-\beta_m \cdot \Delta_{s,sp}} \cdot \sum_{r\in R} g_{s,sp}^r = Cap_{s,sp} \qquad (9.28) \\
&\Rightarrow \Delta_{s,sp} = -\frac{1}{\beta_m} \ln\left(\frac{cap_{s,sp}}{\sum_{r\in R} \left(g_{s,sp}^r\right)^n} \right)
\end{aligned}$$

9.4 Numerical experiments

9.4.1 Toy network

This section designs a numerical example to illustrate the properties of the proposed model. The model parameters are and $\mu = 0.5$ (Kitthamkesorn and Chen, 2017). An exponential parking searching time function is used for congested urban areas (Belloche, 2015):

$$t_{s,cp} = 0.2 \cdot \exp\left(7 \cdot \frac{\sum_{r\in R} f_{s,cp}^r}{cap_{s,cp}} \right), \forall s \in S . \qquad (9.29)$$

A toy network with one origin and six destinations (Figure 9.2) is considered. The travel demand from origin r is q^r = 1,000 (veh). The six destinations S1–S6 are located in two areas. There are five pairs of adjacent destinations: (S1, S3), (S2, S3), (S4, S5), (S4, S6), and (S5, S6). The travel time to each destination is assumed to be 10 min, and all destinations have the same utility $\psi_s = 30$ (HK$). The shared parking cost is HK$ 5 for each destination. The capacities of shared and curbside parking are $Cap_{s,sp}$ = 100 (veh) and $Cap_{s,sp}$ = 300 (veh), respectively. The value of time is vot = 60 (HK$/h).

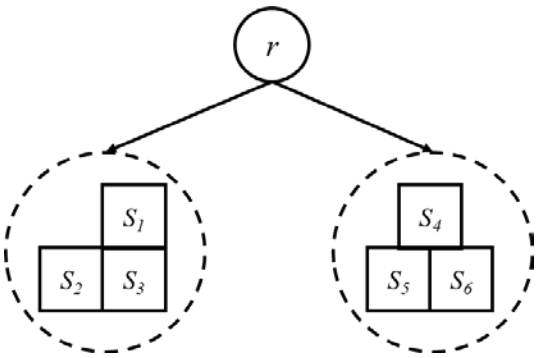

Figure 9.2. Toy network with one origin and six destinations

Table 9.1 summarizes the distribution of parking space. The digits associated with each destination indicate the independent shared parking space (e.g., 82 for S1) and curbside parking space (e.g., 246 for S1) at that destination. The digits associated with each pair of destinations (e.g., 26 and 78 for (S2, S3), respectively) denote the overlapped shared and curbside parking space jointly used by that destination pair.

Table 9.1. Distribution of parking spaces at each destination in toy network

Destination	S1	S2	S3	(S1, S2)	(S1, S3)	(S2, S3)	(S1, S2, S3)
Parking space (veh)	82	62	62	6	6	26	6
	246	126	126	16	18	78	18
Destination	S4	S5	S6	(S4, S5)	(S4, S6)	(S5, S6)	(S4, S5, S6)
Parking space (veh)	80	60	60	10	10	30	0
	240	180	180	30	30	90	0

9.4.1.1 Model outcomes

This section describes the outcomes of the proposed equilibrium choice model. The equilibrium flow at each choice level (i.e., q_{st}^r, $q_{s,st}^r$, q_s^r, and $f_{s,sp}^r$, $f_{s,cp}^r$ from the top down) is shown in Figure 9.3, where SP and CP denote shared parking and curbside parking, respectively. Although the two destination clusters (S1–S3 and S4–S6) have the same number of destinations with the same destination utility, the choice structure of the SCW model leads to different distributions of travel demands. Destinations S1–S3 are considered less spatially correlated than destinations S4–S6 (the former has only two pairs of adjacent destinations whereas the latter has three pairs) and can thus attract slightly higher travel demands. According to the proposed model, S1–S3 attract 51% of the total demand. In contrast, the models that do not consider the spatial correlation (e.g., MNL and MNW) assign half of the demand to S1–S3.

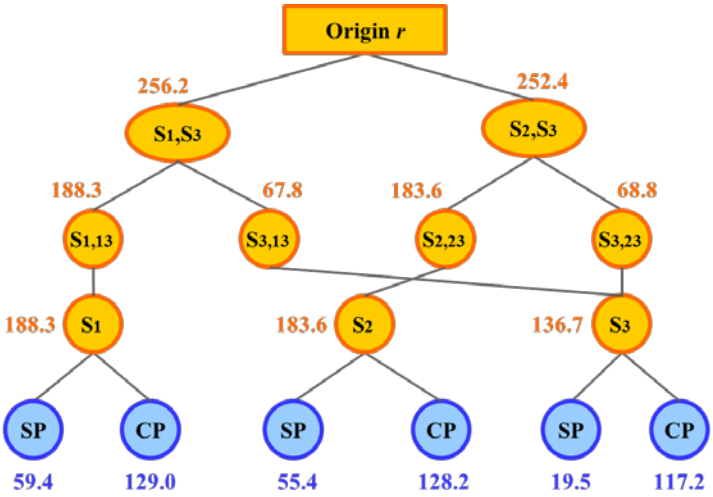

(a) Equilibrium flows to destinations S1–S3

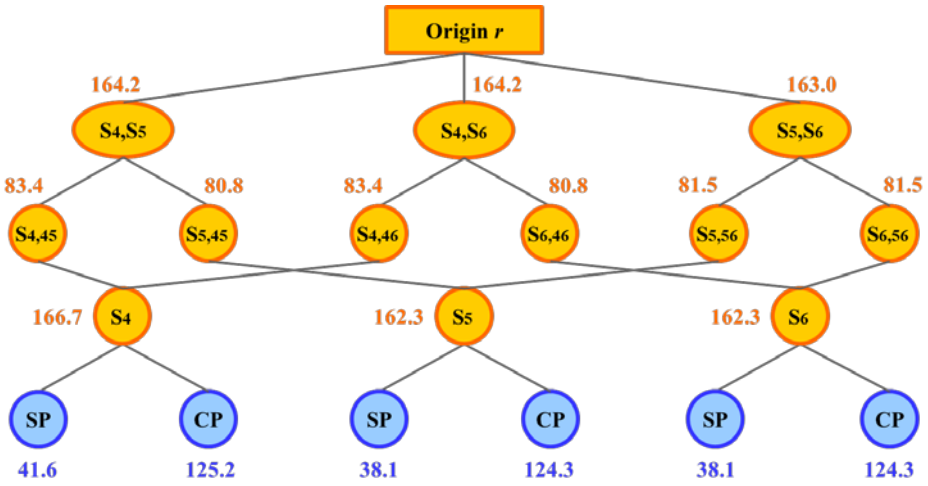

(b) Equilibrium flows to destinations S4–S6

Figure 9.3. Equilibrium flow pattern of toy network at each choice dimension

The model outcomes are summarized in Figure 9.4. Figure 9.4(a) illustrates the effect of considering the correlation issues on destination choice. Within the S1–S3 cluster, S1 and S2 are less spatially correlated (adjacent to fewer locations) and have significantly higher destination demands than S3. Destinations S4–S6, which have symmetric spatial distributions, share the same spatial correlation and have similar travel demands. The slight difference in the destination demand is attributable to the different degrees of overlap among the parking spaces. The parking spaces at S5 and S6 have a higher degree of overlap, leading to higher parking disutility than that of S4. The same reasoning holds for the difference in the demands at S1 and S2.

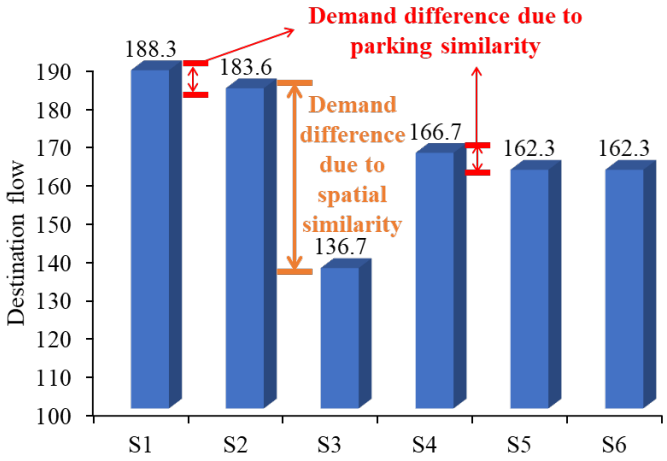

(a) Destination choice

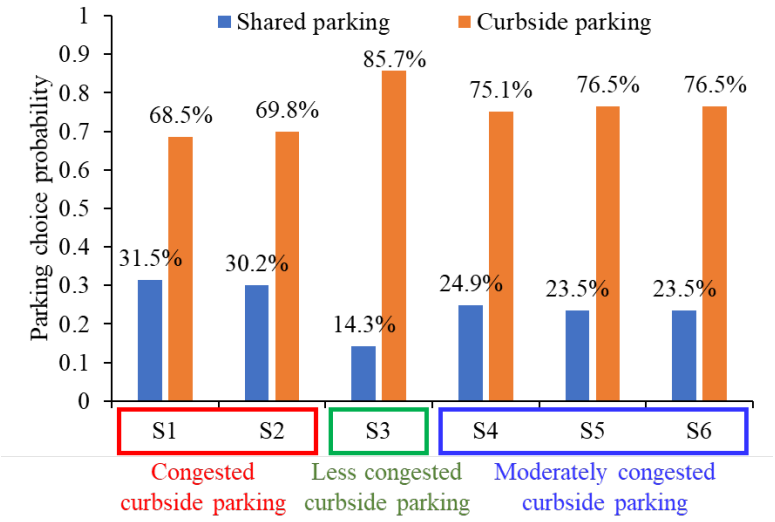

(b) Parking choice

Figure 9.4. Summary of equilibrium choice patterns

Figure 9.4(b) shows the distinct parking choice patterns at different destinations. The choice probability of shared parking is considerably higher at S1–S2 than that at

S3, owing to the effect of congestion on searching for curbside parking. Compared with the uncongested S3, the parking searching time is longer at S1 and S2 due to the higher parking demand, which encourages travelers to shift to the shared parking service.

9.4.1.2 Effects of introducing shared parking service

This section discusses the ability of the proposed model to clarify the effect of introducing shared parking services. Figure 9.5 depicts the relationship between the change in destination/parking choice and variation in the shared parking space at S2. As expected, the changes in the shared parking supply at S2 influence the destination and parking choices not only at S2 but also at the other destinations. Increasing the shared parking space can help increase the choice for shared parking services and decrease parking disutility, thereby increasing travel demand at S2. Moreover, the travel demand at the other locations will be diverted, which will help decrease the curbside parking demand and alleviate parking congestion, thereby lowering the shared parking choice probability at other destinations. This effect is more notable at S1 and S3, which are in the vicinity of S2, especially at S3, which is directly adjacent to S2.

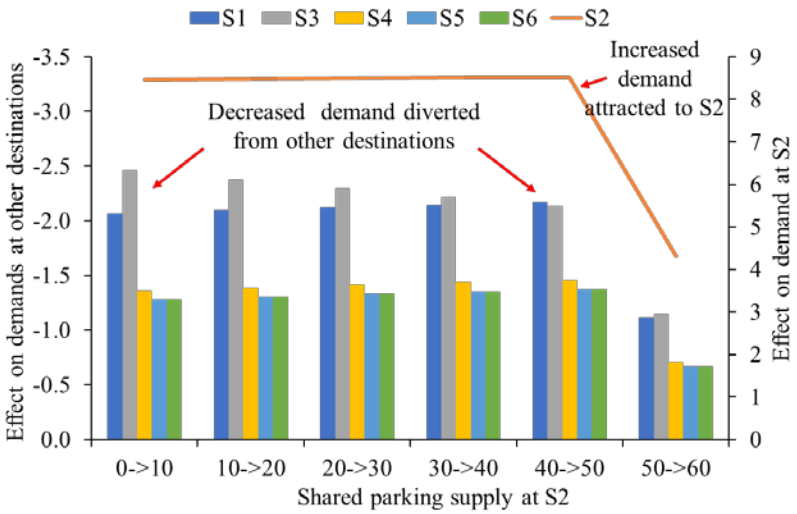

(a) Effect on destination choice

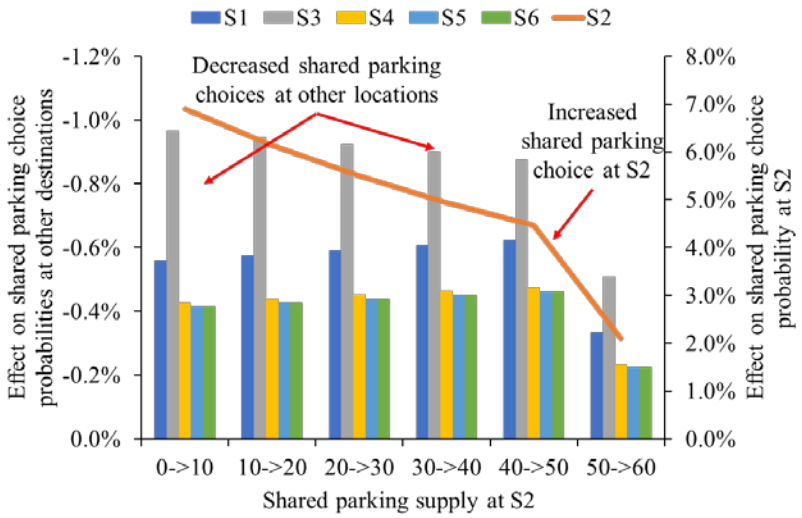

(b) Effect on parking choice

Figure 9.5. Effects of shared parking supply

Next, we illustrate the capability of the proposed model to evaluate different transportation planning scenarios involving shared parking services. Consider the following three planning scenarios with different parking supplies.

- Basic scenario: Only curbside parking (capacity = 300 veh) for each destination.
- Scenario 1: Curbside parking capacity expansion at destinations S1, S2, and S3 (from 300 to 400 veh).
- Scenario 2: Introduction of shared parking at destinations S1, S2, and S3 (curbside parking capacity = 300 veh at each destination and shared parking capacity = 100 veh at S1, S2, and S3)

Figure 9.6 shows the enhancement in the destination accessibility (derived by Eq. (3.69)) in Scenarios 1 and 2 compared with that in the basic scenario. The addition of curbside parking lots has a moderate effect on each destination because the congestion effects are evenly relieved at S1–S3, and the demands at destinations S4–S6 can be diverted to S1–S3. The introduction of shared parking can increase the degree of accessibility enhancement at almost all the destinations. New parking alternatives can provide the travelers with higher utility, and the congestion effect can be relieved because of the avoidance of searching for parking spaces. Notably, these effects may not be as significant at destinations that are originally uncongested (e.g., S3).

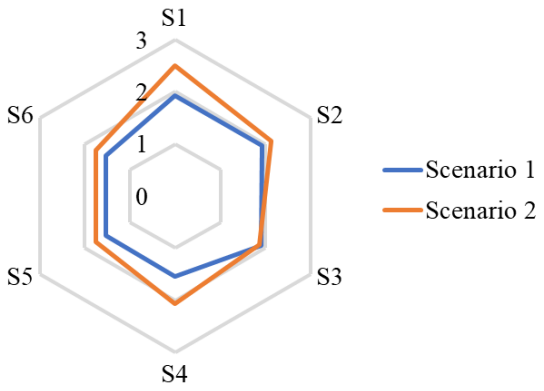

Figure 9.6. Comparison of destination accessibility enhancement in different scenarios

Figure 9.7 compares the effects of introducing shared parking services and increasing curbside parking supply in terms of enhanced parking efficiency (decrease in parking searching time) and destination attractiveness (increase in destination demand). The comparison results are similar to that of destination accessibility. The effect of simply increasing curbside parking supply is average for each destination, while the introduction of shared parking services significantly improves the parking service and attracts higher demands at S1–S3, especially S1 and S2 which are originally congested.

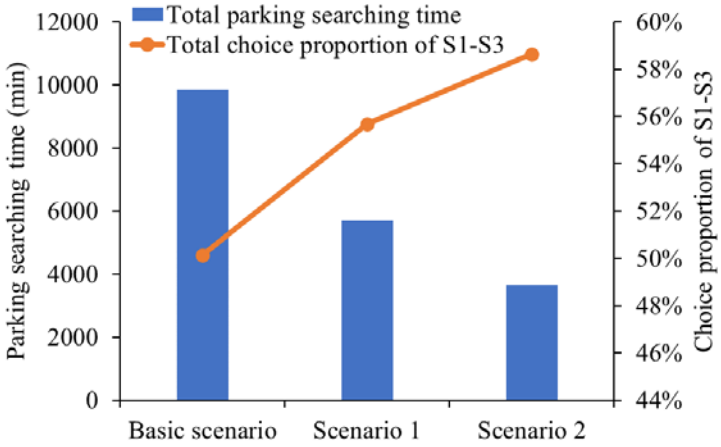

(a) Total parking searching time and destination choice proportions

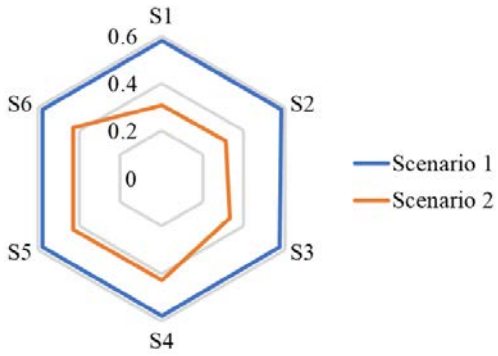

(b) Effect on destination parking time

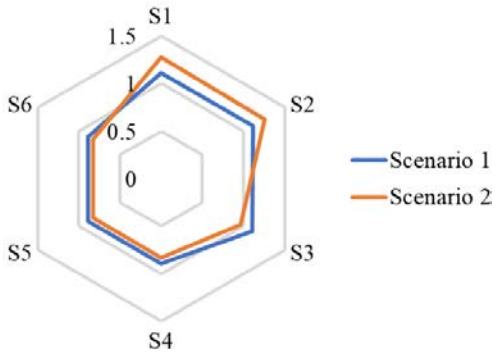

(c) Effect on destination choice proportion

Figure 9.7. Comparison of parking searching time and destination attraction in different scenarios

9.4.1.3 Effect of considering spatial correlation

This section discusses the effect of considering the correlation issue. Figure 9.8 shows the effect of spatial correlation on destination choice probability based on the dissimilarity parameter μ. A larger μ indicates a lower correlation or a higher competition between a pair of adjacent destinations. The SCW model degenerates to the MNW model when $\mu = 1$. Figure 9.8(a) shows the marginal and conditional choice probabilities of the SCW model with variations in μ. As μ decreases, the effect of the spatial correlation between adjacent destinations becomes more notable. The destination pairs including larger fractions of independent destinations (e.g., the pair of S2 and S3) exhibit increasing marginal choice probabilities. A lower μ corresponds to a higher sensitivity of a destination within the same destination pair, which can increase the conditional choice probability of destinations with lower disutility values (e.g., S2 in the pair of S2 and S3). These effects lead to the variations in destination demands shown in Figure 9.8(b). Unlike the evenly distributed demand observed when the correlation is not considered (at the points at which $\mu = 1$), destinations with lower spatial correlations (e.g., S2, which is adjacent only to S3) are modeled to attract higher demands than destinations with higher spatial correlations (e.g., S3, which is adjacent to both S1 and S2). Furthermore, the clusters of destinations with lower spatial correlation (e.g., S1–S3) are expected to attract higher demands.

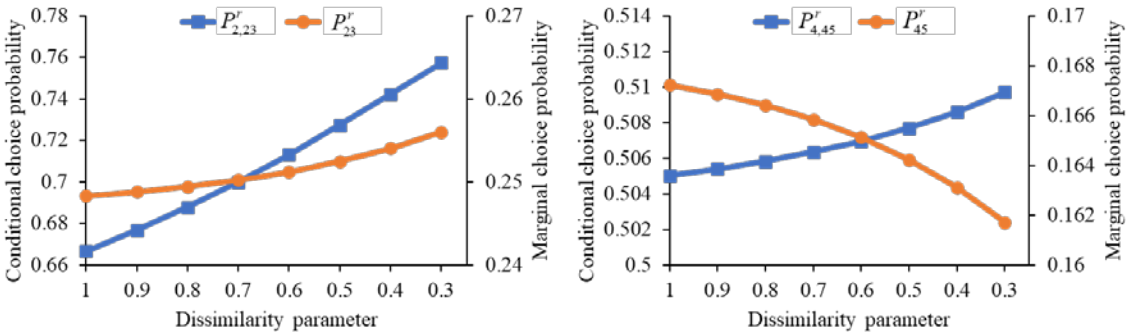

(a) Effect of the dissimilarity parameter on the marginal and conditional choice probabilities

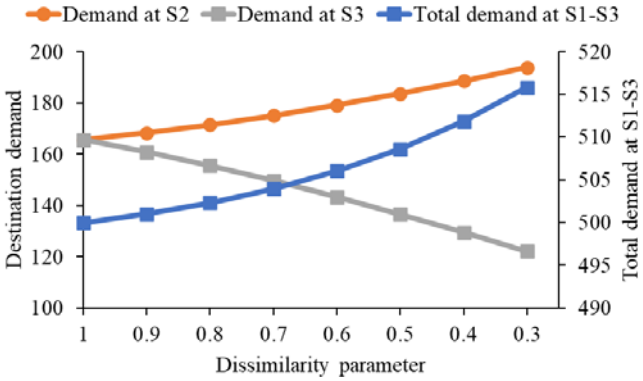

(b) Effect of the dissimilarity parameter on the destination demand

Figure 9.8. Effect of spatial correlation on the destination choice equilibrium

9.4.2 Hong Kong network

This section applies the proposed model to evaluate the potential effect of introducing shared parking services in a multi-origin multi-destination network extracted from Hong Kong (Figure 9.9(a)). Eight residential zones are considered as origins, with trip production values set as 2000, 2000, 3000, 2500, 3000, 2500, 2000, and 2000 veh. Thirty-three adjacently distributed shopping malls in the Kowloon area (blue circle in Figure 9.9(a)) are selected as destinations. The spatial distribution of the destinations and parking lots is shown in Figure 9.9(b). The destinations are divided into eight clusters. Parking lots within 500m of each location are considered the parking space used by that destination. The parking fee and capacity are estimated based on data from the Hong Kong Transport Department (2023). The model parameters are consistent with the analysis described in Section 5.1.

(a) Origins and destinations

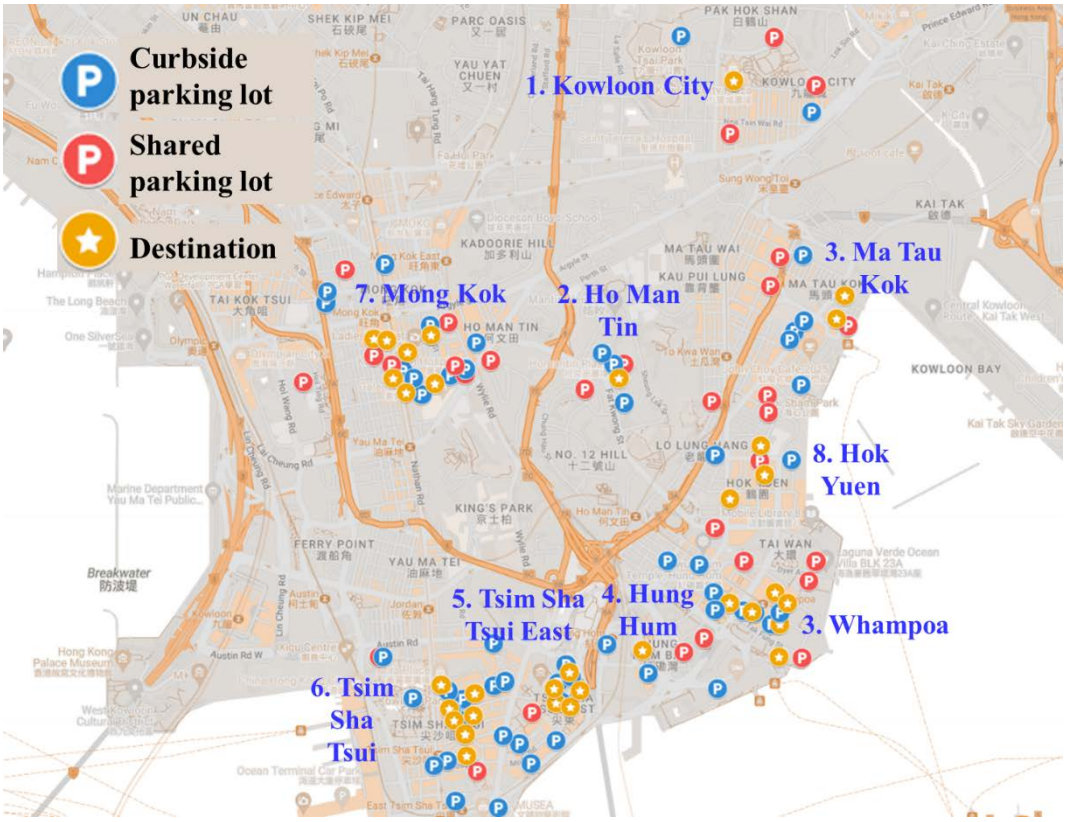

(b) Spatial distribution of the destinations and parking lots

Figure 9.9. Study area in Hong Kong

9.4.2.1 Convergence characteristics

This section examines the algorithmic performance for solving the proposed SCW-PSW equilibrium model in the Hong Kong network. With the step size adjustments set as $\sigma_1 = 1.5$ and $\sigma_2 = 0.1$ in the SRA scheme, the convergence characteristics of the algorithm is shown in Figure 9.10. The center subfigure shows the evolution of step size in partial linearization procedure (outer iteration), which reaches convergence after 46 iterations. The peripheral subfigures demonstrate the convergence of the iterative balancing scheme (inner iteration), which is exemplified by the evolutions of selected dual variables at the first and last outer iterations.

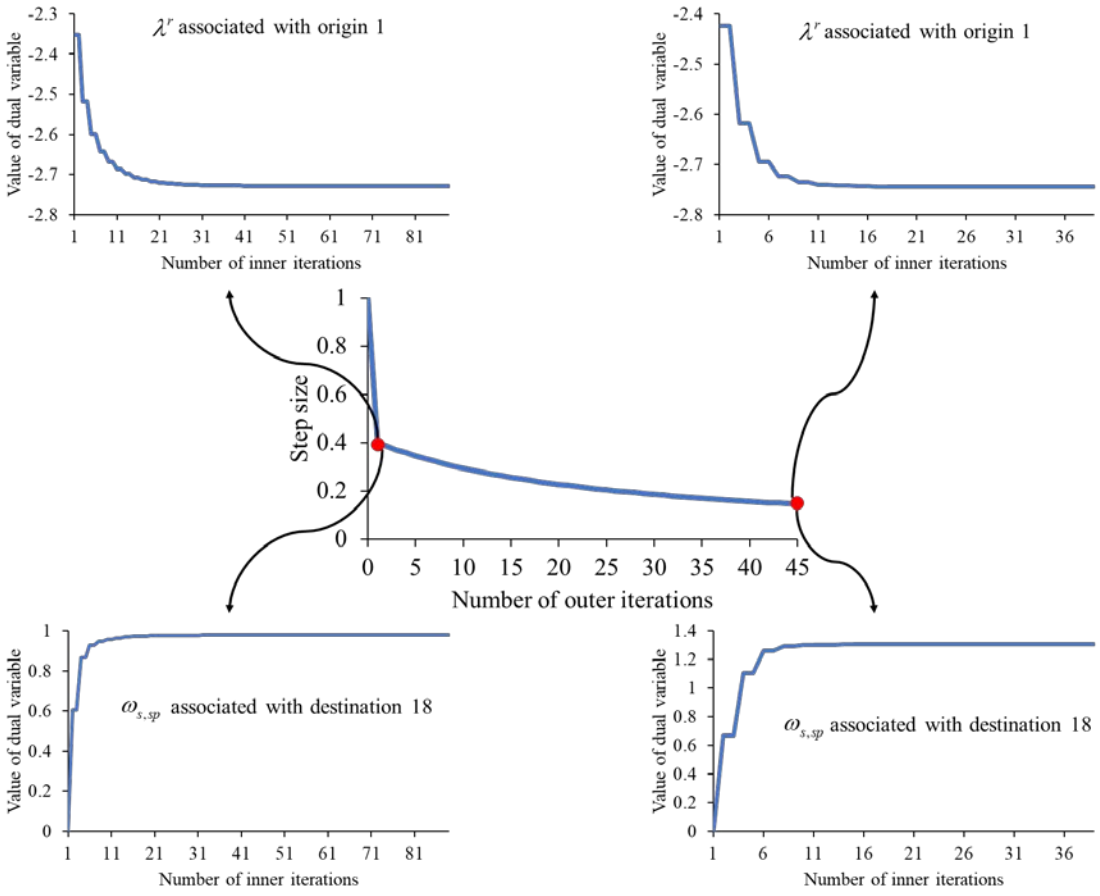

Figure 9.10. Convergence characteristics

9.4.2.2 Equilibrium results

This section presents the aggregate demand pattern from the proposed model, which illustrates its applicability to evaluating and planning the shared parking services in congested urban areas with spatially correlated locations. Figure 9.11 shows the

resulting destination demand pattern in the study area. Even within the same cluster of destinations, the demands of individual destinations may be distinct because of the varying spatial distributions of the destination and parking supplies. For instance, the demands at locations 7, 23, and 33 are relatively higher within the cluster, which is attributable to their lower spatial correlations. Furthermore, the parking supply significantly affects the destination choice. Destinations with more curbside parking spaces (e.g., locations 7, 18, and 22) and sufficient and low-cost shared parking services (e.g., locations in the Mong Kok cluster) attract larger flows even though they do not necessarily provide higher destination utility than the other locations.

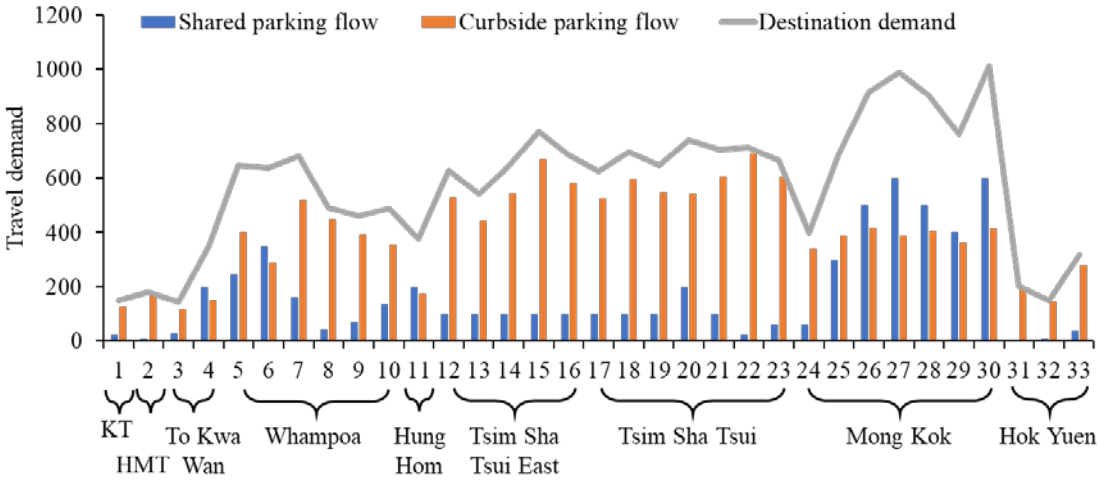

Figure 9.11. Individual destination demand and parking flow pattern in Hong Kong case study

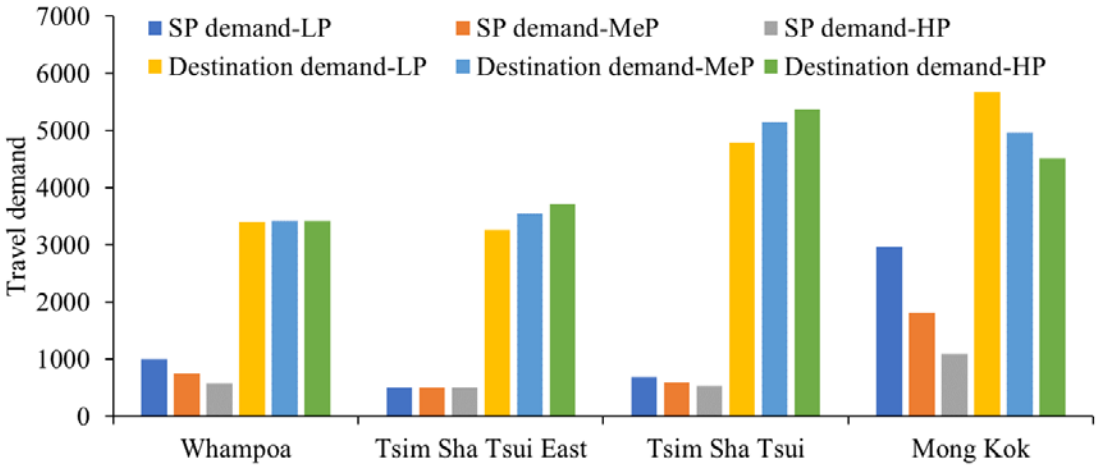

Figure 9.12. Zonal shared parking demands and destination demands with varying shared parking prices

Next, we show the applicability of the proposed model to evaluate different planning scenarios by examining the effect of varying shared parking prices on the destination and parking choices. Figure 9.12 shows the shared parking and destination demand patterns at four major clusters in the study area under three shared parking pricing schemes, i.e., low price (LP: original shared parking price), medium price (MeP: additional profit HK$ 3), and high price (HP: additional profit HK$ 6). An increase in the shared parking price significantly decreases the destination and shared parking demands in areas with sufficient shared parking supplies (e.g., Mong Kok). In contrast, in the Tsim Sha Tsui East region, which has a limited supply of shared parking, the shared parking flows remain almost unchanged as they are mainly restricted by the capacity constraint rather than high cost. The destination demands increase as many travelers are diverted from the destinations dependent on shared parking services (e.g., Mong Kok), where the decrease in the shared parking price can largely lower the destination attractiveness. As for the locations with moderate shared parking supplies, the reduction in shared parking flow is covered by the diversion of destination demand from other locations, making the destination demand nearly unchanged.

9.5 Conclusions

This chapter proposes an equilibrium choice model for assessing the effect of the emerging shared parking services on joint destination and parking choice behaviors while simultaneously considering the heterogeneity and spatial correlation issues. The advanced SCW-PSW choice model developed in Section 3.4 is integrated into the equilibrium model. An equivalent MP formulation is developed that guarantees the existence and uniqueness of solution. Based on the analytical expression of decision variables derived from the MP formulation, a convergent and efficient algorithm is adapted to solve the proposed equilibrium model. Numerical examples demonstrate the capability of the proposed model to capture both heterogeneity and correlation, which cannot be done in the commonly used logit-based combined travel demand models. Moreover, the results of the numerical experiments demonstrate the applicability of the proposed model for evaluating the land use and parking supply in a Hong Kong network with shared parking services.

Chapter 10 Conclusions

10.1 Summary of research contributions

This research develops advanced individual travel choice models and equilibrium models with MP formulation for multi-level travel demand analysis in multi-modal transportation networks with emerging policies and mobility services.

In the first part, five advanced closed-form individual travel choice models are proposed based on the random utility theory. The IID assumptions in the extensively used logit model are relaxed in different ways to consider specific behavioral issues in different choice contexts. Chapter 3 develops four generalized "Luce-form" choice models based on "Luce class" distributional assumptions, which relax the independently distributed assumption to account for varying correlations among travel alternatives at different choice dimensions. Specifically, an OPSGEV model is first developed based on the commonly adopted additive utility function to model route choice in tolled networks with considerations of both physical and perceptual path correlations. Three weibit-based models are then developed based on the multiplicative utility function that can better reflect the way travelers perceive travel disutility consistent with psychophysical laws (Fosgerau and Bierlaire, 2009; Chakroborty et al., 2021). This allows the three weibit-based models to inherently address the heterogeneous perceptions of different travel alternatives. A DNW model is developed for mode choice with CB services considering both the similarity among conventional travel modes and CB passenger loyalty stemmed from the loyalty subscription scheme. A DCNW model is developed to advance the DNW model for joint bundle and mode choice considering the mode correlation due to bundling strategies and traveler loyalty from loyalty bundle schemes. An SCW-PSW model is developed for the joint destination and parking choice with shared parking services. The effects of spatial correlation at the destination and parking choice dimensions are explicitly considered, while the interaction between the two choice dimensions is modeled based on the random utility theory.

Chapter 4 proposes the MNW-O model based on an alternate distributional assumption, which relaxes the identically distributed assumption while retaining the closed-form probability expression. The proposed model can effectively address the "oddball" effect that are likely to take place in future transportation systems, where an oddball alternative with unique service features (e.g., an emerging mobility service)

exists in the travel choice set. The proposed model also inherits the advantage of weibit model to inherently consider heterogenous perception variances with respect to different alternatives and attributes. The proposed model is applied to an empirical mode choice data set to examine its estimation and prediction performances. The results show the superiority of the proposed model against various existing choice models in simultaneously considering the "oddball" effect and the heterogeneity issue.

The second part bridges the "Luce-form" individual choice models developed in Chapter 3 to aggregate-level equilibrium models with MP formulation, which further considers interactions among travelers and operational features of mobility services. The general method to develop the Beckmann-type MP formulation for equilibrium models is first introduced in Chapter 5. On this basis, Chapters 6–9 propose equilibrium analyses consistent with the OPSGEV, DNW, DCNW, and SCW-PSW choice models, respectively. A convergent and efficient partial linearization algorithm is adapted to solve the equilibrium models making use of the appealing properties of developed MP formulations. A sensitivity analysis-based method is also developed in Chapter 8 to evaluate the transportation system performances in different decision-making scenarios. Various numerical experiments are conducted to illustrate the model properties and to verify the applicability to real-world transportation systems. The results indicate that the proposed equilibrium models can facilitate the demand analysis and decision-making in the transition to future transportation systems.

10.2 Directions for future studies

Based on the proposed research, several directions can be found for future research. First, advances can be made in the choice modeling at the individual level:

(1) Existing closed-form random utility-based travel choice models are mainly developed based on the Gumbel and Weibull distributions, which are unlikely to be appropriate for all choice contexts with complex choice behaviors in the era of emerging technologies. More closed-form choice models should be developed based on alternate distributional assumptions, such as the Fréchet distribution, Log-logistic distribution, Pareto distribution, and Kumaraswamy distribution.

(2) This research focuses on the RUMs based on two utility functional forms, i.e., the additive utility function that leads to logit-based models, and the multiplicative disutility function that leads to weibit-based models. However, it could be

restrictive to merely consider two types of functional relationships between the deterministic utility/disutility and random perception errors. Future studies could be conducted to investigate other forms of utility function and explore more error distributions for choice contexts with different behavioral issues.

Second, the equilibrium models could be explored in several directions as follows:

(1) For the planning purpose, the proposed equilibrium models with fixed OD demand could be extended to examining long-term elastic OD demand, as latent travel demands may be induced by the increased service level created by the adoption of innovative transportation policies and emerging mobility services. In addition, other interacting choice dimensions could be integrated in the equilibrium analysis, such as the choice of work from home (WFH), residential location choice, car ownership choice, trip chain choice in intermodal trips, and role choice (driver versus passenger) in ride sharing services.

(2) The proposed equilibrium models and sensitivity analysis could be integrated into bi-level models for the optimization of emerging mobility services, such as the design of parking sharing platforms, allocation of shared bikes, design and adjustment of CB routes, determination of ride-hailing fleet size, and pricing of subscription schemes for emerging mobilities and bundles.

(3) The MP formulations developed in this research use entropy terms to interpret the stochastic choice of travelers (i.e., logit for additive RUM and weibit for multiplicative RUM). It would be interesting to develop alternate forms of MP formulation (e.g., non-entropy-based formulation) for the equilibrium analysis with different behavioral interpretations and different applications.

References

Abbe, E., Bierlaire, M., Toledo, T. (2007) Normalization and correlation of Cross-Nested Logit models. *Transportation Research Part B*, 41(7), 795–808.

Abdulaal, M., and LeBlanc, L.J. (1979). Methods for combining modal split and equilibrium assignment models. *Transportation Science*, 13(4), 292-314.

Anas, A., and Feng, M. (1988). Invariance of expected utilities in logit models. *Economics Letters*, 27, 41-45.

Ardeshiri, A., Safarighouzhdi, F., and Rashidi, T.H. (2021). Measuring willingness to pay for shared parking. *Transportation Research Part A*, 152, 186–202.

Bahat, O., and Bekhor, S. (2016). Incorporating ridesharing in the static traffic assignment model. *Networks and Spatial Economics*, 16, 1125–1149.

Barros, C.P., Buttler, R., and Correia, A. (2008). Heterogeneity in destination choice: Tourism in Africa. *Journal of Travel Research*, 47(2), 235-246.

Beckmann, M., McGuire, C.B., and Winsten, C.B. (1956). *Studies in the Economics of Transportation*. Yale University Press, New Haven, Connecticut.

Bekhor, S., and Prashker, J.N. (1999). Formulations of extended logit stochastic user equilibrium assignments. In *Proceedings of the 14th International Symposium on Transportation and Traffic Theory*, Jerusalem, Israel, 351-372.

Bekhor, S., and Prashker, J.N. (2001) Stochastic user equilibrium formulation for generalized nested logit model. *Transportation Research Record*, 1752, 84-90.

Bell, M.G.H. (1995). Stochastic user equilibrium assignment in network with queues. *Transportation Research Part B*, 29, 125–137.

Bell, M.G.H., and Iida, Y. (1997). *Transportation Network Analysis*. John Wiley & Sons, New York.

Belloche, S. (2015). On-street parking search time modelling and validation with survey-based data. *Transportation Research Procedia*, 6, 313–324.

Ben-Akiva, M.E., Bierlaire, M. (1999). Discrete choice methods and their applications to short term travel decisions. In: Hall, R.W. (Ed.), *Handbook of Transportation Science*. Kluwer, Dordrecht, The Netherlands, 5-34.

Ben-Akiva, M.E., and Lerman, S.R. (1985). *Discrete Choice Analysis: Theory and Application to Travel Demand*. MIT Press.

Berdica, K. (2002). An introduction to road vulnerability: What has been done, is done and should be done. *Transport Policy*, 9, 117-127.

Bhat, C.R. (1995). A heteroscedastic extreme-value model of intercity mode choice. *Transportation Research*, 29B, 6, 471-483.

Bhat, C.R., and Guo, J., (2004) A mixed spatially correlated logit model: formulation and application to residential choice modeling. *Transportation Research Part B*, 38, 147–168.

Bierlaire, M., Axhausen, K., and Georg, A. (2001). The acceptance of modal innovation: The case of Swissmetro. Paper presented at the *1st Swiss Transport Research Conference*.

Bordley, R.F. (1990). The dogit model is applicable even without perfectly captive buyers. *Transportation Research Part B*, 24(4), 315–323.

Bovy, P.H.L., Bekhor, S., and Prato, C.G. (2008). The factor of revised path size: an alternative derivation. *Transportation Research Record*, 2076, 132-140.

Boyce, D., and Bar-Gera, H. (2004). Multiclass combined models for urban travel forecasting. *Network and Spatial Economics*, 4(1), 115–124.

Boyles, S.D., Tang, S., and Unnikrishnan, A. (2015). Parking search equilibrium on a network. *Transportation Research Part B*, 81, 390-409.

Brathwaite, T., and Walker, J.L. (2018) Asymmetric, closed-form, finite-parameter models of multinomial choice. *Journal of Choice Modelling*, 29, 78–112.

Caiati, V., Rasouli, S., and Timmermans, H.J.P. (2020). Bundling, pricing schemes and extra features preferences for mobility as a service: Sequential portfolio choice experiment. *Transportation Research Part A*, 131, 123–148.

Cantarella, G.E., Velona, P., and Watling, D.P. (2015). Day-to-day dynamics & equilibrium stability in a two-mode transport system with responsive bus operator strategies. *Networks and Spatial Economics*, 15(3), 485-506.

Cascetta, E., Nuzzolo, A., Russo, F., and Vitetta, A. (1996). A modified logit route choice model overcoming path overlapping problems: specification and some calibration results for interurban networks. In: *Proceedings of the 13th International Symposium on Transportation and Traffic Theory, Leon, France*, 697-711.

Castillo, E., Menéndez, J.M., Jiménez, P., and Rivas, A. (2008). Closed form expression for choice probabilities in the Weibull case. *Transportation Research Part B*, 42(4), 373-380.

Chakroborty, P., Pinjari, A.R., Meena, J., and Gandhi, A. (2021). A psychophysical ordered response model of time perception and service quality: Application to level of service analysis at toll plazas. *Transportation Research Part B*, 154, 44–64.

Chang, L-Y., and Hung, S-C. (2013). Adoption and loyalty toward low cost carriers: The case of Taipei–Singapore passengers. *Transportation Research Part E*, 50, 29-36.

Chang, C-H., and Thai, V.V. (2016). Do port security quality and service quality influence customer satisfaction and loyalty? *Maritime Policy & Management*, 43(6), 720-736.

Chen, A., Chootinan, P., and Recker, W. (2009). Norm approximation method for handling traffic count inconsistencies in path flow estimator. *Transportation Research Part B*, 43(8-9), 852-872.

Chen, A., Pravinvongvuth, S., Xu, X., Ryu, S., and Chootinan, P. (2012). Examining the scaling effect and overlapping problem in logit-based stochastic user equilibrium models. *Transportation Research Part A*, 46(8), 1343-1358.

Chen, A., Ryu, S., Xu, X., and Choi, K. (2014) Computation and application of the paired combinatorial logit stochastic traffic equilibrium problem. *Computers and Operations Research*, 43(1), 68-77.

Chen, A., Yang, C., Kongsomsaksakul, S., and Lee, M. (2007). Network-based accessibility measures for vulnerability analysis of degradable transportation networks. *Networks and Spatial Economics*, 7, 241-256.

Cheng, Z., Yao, J., Chen, A., and An, S. (2022) Analysis of a multiplicative hybrid route choice model in stochastic assignment paradox. *Transportmetrica A*, 18(3), 1544-1568.

China National Radio. (2018). Available at: http://www.cnr.cn/bj/jrbj/20181011/t20181011_524381893.shtml [accessed 25 June 2021].

Choudhury, C.F., Yang, L., de Abreu e Silva, J., and Ben-Akiva, M. (2018). Modelling preferences for smart modes and services: a case study in Lisbon. *Transportation Research Part A*, 115, 15–31.

Clarke, K.A. (2003). Nonparametric model discrimination in international relations. *Journal of Conflict Resolution*, 47, 72–93.

Colombo, R., and Morrison, D. (1989). A brand-switching model with implications for marketing strategies. *Marketing Science*, 8(1), 89-99.

Chu, C. (1989). A paired combinatorial logit model for travel demand analysis. In: *Proc. Fifth World Conference on Transportation Research, Ventura, Calif*, 4, 295–309.

Chu, Y-L. (2011). Distribution and assignment of compulsory and discretionary traffic. *Transportation Research Record*, 2263, 73-81.

Daganzo, C. (1979). *Multinomial Probit: The Theory and its Application to Demand Forecasting*. Academic Press, New York.

Daganzo, C.F., and Sheffi, Y. (1977) On stochastic models of traffic assignment. *Transportation Science*, 11(3), 253-274.

Daly, A., and Bierlaire, M. (2006). A general and operational representation of generalised extreme value models. *Transportation Research Part B*, 40(4), 285-305.

de Jong, G., Daly, A., Pieters, M. and van der Hoorn, T. (2007) The logsum as an evaluation measure: Review of the literature and new results. *Transportation Research Part A*, 41(9), 874–889.

Di, X., and Ban, X. (2019). A unified equilibrium framework of new shared mobility systems. *Transportation Research Part B*, 129, 50–78.

Dial, R.B. (1971). A probabilistic multipath traffic assignment model which obviates path enumeration. *Transportation Research*, 5(2), 83-111.

Dial, R.B. (1996). Bicriterion traffic assignment: Basic theory and elementary algorithms. *Transportation Science*, 30(2), 93-111.

Diethelm, K. (2012). The limits of reproducibility in numerical simulation. *Computing in Science & Engineering*, 14(1), 64-72.

Djavadian, S., and Chow, J.Y.J. (2017). An agent-based day-to-day adjustment process for modeling 'Mobility as a Service' with a two-sided flexible transport market. *Transportation Research Part B*, 104, 36-57.

Domencich, T., and McFadden, D. (1975) *Urban Travel Demand*. North Holland, Amsterdam.

Dong, X., Ben-Akiva, M.E., Bowman, J.L., and Walker, J.L. (2006). Moving from trip-based to activity-based measures of accessibility. *Transportation Research Part A*, 40, 163–180.

Dou, X., Meng, Q., and Liu, K. (2021). Customized bus service design for uncertain commuting travel demand. *Transportmetrica A*, 17(4), 1405-1430.

Du, M., and Chen, A. (2022). Sensitivity analysis for transit equilibrium assignment and applications to uncertainty analysis. *Transportation Research Part B*, 157, 175-202.

Du, M., Zhou, J., Chen, A., and Tan, H. (2022). Modeling the capacity of multimodal and intermodal urban transportation networks that incorporate emerging travel modes. *Transportation Research Part E*, 168, 102937.

Duncan, L.C., Watling, D.P., Connors, R.D., Rasmussen, T.K., Nielsen, O.A. (2020). Path size logit route choice models: Issues with current models, a new internally consistent approach, and parameter estimation on a large-scale network with GPS data. *Transportation Research Part B*, 135, 1–40.

Ehrgott, M., Wang, J.Y., and Watling, D.P. (2015). On multi-objective stochastic user equilibrium. *Transportation Research Part B*, 81, 704–717.

Ellinger, A.E., Daugherty, P.J., and Plair, Q.J. (1999). Customer satisfaction and loyalty in supply chain: the role of communication. *Transportation Research Part E*, 35, 121-134.

Erhardt, G.D., Mucci, R.A., Cooper, D., Sana, B., Chen, M., Castiglione, J. (2022). Do transportation network companies increase or decrease transit rider-ship? Empirical evidence from San Francisco. *Transportation*, 49, 313–342.

Evans, S. (1976). Derivation and analysis of some models for combining trip distribution and assignment. *Transportation Research*, 9(12), 241–246.

Feneri, A.M., Rasouli, S., and Timmermans, H.J.P. (2022). Modeling the effect of Mobility-as-a-Service on mode choice decisions. *Transportation Letters*, 14(4), 324-331.

Fiacco, A.V. (1983). *Introduction to Sensitivity and Stability Analysis in Nonlinear Programming*. Academic Press, New York.

Fisk, C. (1980) Some developments in equilibrium traffic assignment. *Transportation Research Part B*, 14(3), 243–255.

Florian, M. (1977). A traffic equilibrium model of travel by car and public transit modes. *Transportation Science*, 11, 166–179.

Florian, M., and Nguyen, S. (1978). A combined trip distribution modal split and assignment model. *Transportation Research*, 12, 241–246.

Fosgerau, M., and Bierlaire, M. (2009). Discrete choice models with multiplicative error terms. *Transportation Research Part B*, 43, 494-505.

Fotheringham, A.S., and O'Kelly, M.E. (1989). *Spatial Interaction Models: Formulations and Applications*. Kluwer Academic Publishers, Boston.

Frejinger, E., and Bierlaire, M. (2007). Capturing correlation with subnetworks in route choice models. *Transportation Research Part B*, 41(3), 363–378.

Friesz, T.L. (1981). An equivalent optimization problem for combined multiclass distribution, assignment and modal split which obviates symmetry restrictions. *Transportation Research Part B*, 15(5), 361–369.

Gadepalli, R., Tiwari, G., and Bolia, N. (2020). Role of user's socio-economic and travel characteristics in mode choice between city bus and informal transit services: Lessons from household surveys in Visakhapatnam, India. *Journal of Transport Geography*, 88, 102307.

Galvez, P.T.E. (2001) El Modelo Powit. In *Actas Del X Congreso Chileno de Ingeniería de Transporte*.

Gao, J., Li, S., and Yang, H. (2022). Shared parking for ride-sourcing platforms to reduce cruising traffic. *Transportation Research Part C*, 137, 103562.

Gaudry, M.J.I., and Dagenais, M.G. (1979). The dogit model. Transportation Research, 13(B), 105 ‑ 111.

Glavic, D., Mladenovic, M., Luttinen, T., Cicevic, S., and Trifunovic, A. (2017). Road to price: User perspectives on road pricing in transition country. *Transportation Research Part A*, 105, 79–94.

Gradshteyn, I.S., and Ryzhik, I.M. (2007). *Table of Integrals, Series, and Products*. Elsevier/Academic Press.

Gu, Y., Fu, X., Liu, Z., Xu, X. and Chen, A. (2020). Performance of transportation network under perturbations: Reliability, vulnerability, and resilience. *Transportation Research Part E*, 133, 101819.

Guo, Q-W., Chow, J.Y.J., Schonfeld, P. (2018). Stochastic dynamic switching in fixed and flexible transit services as market entry-exit real options. *Transportation Research Part C*, 94, 288-306.

Habib, K.N., Morency, C., Trépanier, M., and Salem, S. (2013). Application of an independent availability logit model (IAL) for route choice modelling: Considering bridge choice as a key determinant of selected routes for commuting in Montreal. *Journal of Choice Modelling*, 9, 14-26.

Haghani, M., Bliemer, M.C.J., and Hensher, D.A. (2021) The landscape of econometric discrete choice modelling research. *Journal of Choice Modelling*, 40, 100303.

Han, Y., Pereira, F.C., Ben-Akiva, M.E., and Zegras, C. (2022). A neural-embedded discrete choice model: Learning taste representation with strengthened interpretability. *Transportation Research Part B*, 163, 166-186.

Harris, F.E. (1957). Tables of the Exponential Integral Ei(x). *Mathematical Tables and Other Aids to Computation*, 11, 9-16.

Hensher, D.A., and Truong, T.P. (1985). Valuation of travel times savings. *Journal of Transport Economics and Policy*, 237-260.

Hensher, D.A., Ho, C.Q., and Reck, D.J. (2021). Mobility as a service and private car use: Evidence from the Sydney MaaS trial. *Transportation Research Part A*, 145, 17–33.

Hess, S. and Palma, D. (2019). Apollo: A flexible, powerful and customisable freeware package for choice model estimation and application. *Journal of Choice Modelling*, 32, 100170.

Ho, C.Q., Hensher, D.A., Mulley, C., and Wong, Y.Z. (2018). Potential uptake and willingness-to-pay for Mobility as a Service (MaaS): A stated choice study. *Transportation Research Part A*, 117, 302-318.

Ho, C.Q., Hensher, D.A., and Reck, D.J. (2021). Drivers of participant's choices of monthly mobility bundles: Key behavioural findings from the Sydney Mobility as a Service (MaaS) trial. *Transportation Research Part C*, 124, 102932.

Hong Kong Transport Department. (2023). Carparks, [online] Available at: https://www.td.gov.hk/en/transport_in_hong_kong/parking/carparks/index.html. [Accessed 11 March 2023].

Hoogendoorn-Lanser, S. (2005). Modelling travel behaviour in multi-modal networks, PhD thesis, Delft University of Technology.

Huang, D., Gu, Y., Huang, K., and Liu, Z. (2017). Review and Improving method of Customized Bus. *The 2017 China Urban Planning Annual Conference*.

Huang, D, Gu, Y., Wang, S., Liu, Z., and Zhang, W. (2020a). A two-phase optimization model for the demand-responsive customized bus network design. *Transportation Research Part C*, 111, 1-21.

Huang, D., Tong, W., Wang, L., and Yang, X. (2020b). An analytical model for the many-to-one demand responsive transit systems. *Sustainability*, 12, 298.

Huang, H-J., and Li, Z-C. (2007). A multiclass, multicriteria logit-based traffic equilibrium assignment model under ATIS. *European Journal of Operational Research*, 176, 1464-1477.

Huang, H.-J., Xia, T., Tian, Q., Liu, T., Wang, C., and Li, D. (2020c). Transportation issues in developing China's urban agglomerations. *Transport Policy*, 85, A1-A22.

Ibeas, A., dell'Olio, L., Bordagaray, M., and Ortúzar, J. de D. (2014). Modelling parking choices considering user heterogeneity. *Transportation Research Part A*, 70, 41-49.

Jang, S., Caiati, V., Rasouli, S., Timmermans, H.J.P. and Choi, K. (2021). Does MaaS contribute to sustainable transportation? A mode choice perspective. *International Journal of Sustainable Transportation*, 15(5), 351-363.

Jansuwan, S., and Chen, A. (2015). Considering perception errors in network efficiency measure: an application to bridge importance ranking in degradable transportation networks. *Transportmetrica A*, 11(9), 793-818.

Jenelius, E., Petersen, T., and Mattsson, L.G. (2006). Importance and exposure in road network vulnerability analysis. *Transportation Research Part A*, 40, 537-560.

Jiang, N., Xie, C., Duthie, J.C., and Waller, S.T. (2014). A network equilibrium analysis on destination, route and parking choices with mixed gasoline and electric vehicular flows. *EURO Journal on Transportation and Logistics*, 3, 55–92.

Ke, J., Zhu, Z., Yang, H., and He, Q. (2021). Equilibrium analyses and operational designs of a coupled market with substitutive and complementary ride-sourcing services to public transits. *Transportation Research Part E*, 148, 102236.

Kitthamkesorn, S., and Chen, A., (2013). Path-size weibit stochastic user equilibrium model. *Transportation Research Part B*, 57, 378-397.

Kitthamkesorn, S., and Chen, A. (2014). Unconstrained weibit stochastic user equilibrium model with extensions. *Transportation Research Part B*, 59, 1-21.

Kitthamkesorn, S., and Chen, A. (2017) Alternate weibit-based model for assessing green transport systems with combined mode and route travel choices. *Transportation Research Part B*, 103, 291-310.

Kitthamkesorn, S., Chen, A., Opasanon, S., and Jaita, S. (2021) A P-hub location problem for determining park-and-ride facility locations with the weibit-based choice model. *Sustainability*, 13, 7928.

Kitthamkesorn, S., Chen, A., and Xu, X. (2015) Elastic demand with weibit stochastic user equilibrium flows and application in a motorised and non-motorised network. *Transportmetrica A*, 11(2), 158-185.

Kitthamkesorn, S., Chen, A., Xu, X., and Ryu, S. **(**2016). Modeling mode and route similarities in network equilibrium problem with go-green modes**.** *Networks and Spatial Economics*, 16(1), 33-60.

Koppelman, F.S., and Sethi, V. (2008). Closed form discrete choice models. In: Hensher, D.A., Button, K.J. (Eds.), *Handbook of Transport Modelling*, Elsevier Science, 211–225.

Kriswardhana, W., and Esztergar-Kiss, D. (2023). A systematic literature review of Mobility as a Service: Examining the socio-technical factors in MaaS adoption and bundling packages. *Travel Behaviour and Society*, 31, 232–243.

Kurauchi, F., and Ido, H. (2017) Estimation of the expressway/surface road choice model using Logit-Weibit hybrid model. *Proceedings of the 22nd International Conference of Hong Kong Society for Transportation Studies (HKSTS)*, Hong Kong.

Lam, W.H.K., and Huang, H.J. (1992). A combined trip distribution and assignment model for multiple user classes. *Transportation Research Part B*, 26(4), 275-287.

Lam, W.H.K., Li, Z-C., Huang, H-J., and Wong, S.C. (2006). Modeling time-dependent travel choice problems in road networks with multiple user classes and multiple parking facilities. *Transportation Research Part B*, 40(5), 368-395.

LeBlanc, L.J., and Farhangian, K. (1981). Efficient algorithm for solving elastic demand traffic assignment problems and model split-assignment problems. *Transportation Science*, 15, 306–317.

Lee, C.K.H., and Wong, A.O.M. (2021). Antecedents of consumer loyalty in ride-hailing. *Transportation Research Part F*, 80, 14-33.

Leurent, F. (1993). Cost versus time equilibrium over a network. *European Journal of Operational Research*, 71(2), 205-221.

Leurent, F., and Boujnah, H. (2014). A user equilibrium, traffic assignment model of network route and parking lot choice, with search circuits and cruising flows. *Transportation Research Part C*, 47, 28–46.

Li, B. (2011) The multinomial logit model revisited: A semi-parametric approach in discrete choice analysis. *Transportation Research Part B*, 45, 461–473.

Li, D., Wu, W., and Song, Y. (2020) Comparative study of logit and weibit model in travel mode choice. *IEEE Access*, 8, 63452-63461.

Li, J., Lv, Y., Ma, J., and Ren, Y. (2019). Factor analysis of customized bus attraction to commuters with different travel modes. *Sustainability*, 11, 7065.

Li, L., Bai, Y., Song, Z., Chen, A**.**, and Wu, B. (2018a). Public transportation competitiveness analysis based on current passenger loyalty. *Transportation Research Part A*, 113, 213-226.

Li, M., Jiang, G., and Lo, H.K. (2022). Pricing strategy of ride-sourcing services under travel time variability. *Transportation Research Part E*, 159, 102631.

Li, X., Liu, W., and Yang, H. (2018b). Traffic dynamics in a bi-modal transportation network with information provision and adaptive transit services. *Transportation Research Part C*, 91, 77-98.

Li, Z., and Hensher, D.A. (2011). Crowding and public transport: A review of willingness to pay evidence and its relevance in project appraisal. *Transport Policy*, 18(6), 880–887.

Li, Z., Li, G., Xu, Z., Chen, A. (2023). Multiclass bi-criteria traffic assignment without class-specific variables: An alternative formulation and a subgradient projection algorithm. Transportation Research Part E 176, 103210.

Li, Z.-C., Yao, M.-Z., Lam, W.H.K., Sumalee, A., and Choi, K. (2015). Modeling the effects of public bicycle schemes in a congested multi-modal road network. *International Journal of Sustainable Transportation*, 9, 282–297.

Lindberg, P.O. (2012). *Contributions to probabilistic discrete choice*. Ph.D. Thesis, KTH Royal Institute of Technology, Stockholm.

Liu D., and Lam, W.H.K. (2014). Modeling the effects of population density on prospect theory-based travel mode-choice equilibrium. *Journal of Intelligent Transportation Systems*, 18(4), 379-392.

Liu, H., He X., He, B. (2009). Method of successive weighted averages (MSWA) and self-regulated averaging schemes for solving stochastic user equilibrium problem. *Network and Spatial Economics*, 9(4), 485–503.

Liu, P., Xu, X., Chen, A., Yang, C., and Xiao, L. (2017). A select link analysis based on logit-weibit hybrid model. *Journal of Modern Transportation*, 25(4), 205-217.

Liu, T., and Ceder, A. (2015). Analysis of a new public-transport-service concept: Customized bus in China. *Transport Policy*, 39, 63-76.

Liu, T., Ceder, A., Bologna, R., and Cabantous, B. (2016). Commuting by customized bus: A comparative analysis with private car and conventional public transport in two cities. *Journal of Public Transportation*, 19(2), 55-74.

Liu, W. (2018). An equilibrium analysis of commuter parking in the era of autonomous vehicles. *Transportation Research Part C*, 92, 191–207.

Liu, W., Zhang, F., and Yang, H. (2021). Modeling and managing the joint equilibrium of destination and parking choices under hybrid supply of curbside and shared parking. *Transportation Research Part C*, 130, 103301.

Liu, W., Zhang, F., Wang, X., Shao C., and Yang, H. (2022). Unlock the sharing economy: the case of the parking sector for recurrent commuting trips. *Transportation Science*, 56(2), 338-357.

Liu, Z., Chen, X., Meng, Q., and Kim, I. (2018). Remote park-and-ride network equilibrium model and its applications. *Transportation Research Part B*, 117, 37-62.

Lo, H.K., Yip, C.W., and Wan, K.H. (2003). Modeling transfer and non-linear fare structure in multi-modal network. *Transportation Research Part B*, 37(2), 149–170.

Lu, X-S., Liu, T-L., and Huang, H-J. (2015). Pricing and mode choice based on nested logit model with trip-chain costs. *Transport Policy*, 44, 76-88.

Luce, R.D. (1959). *Individual Choice Behavior: A Theoretical Analysis*. John Wiley & Sons.

Luce, R.D., and Suppes, P. (1965). Preferences, utility, and subjective probability. In: Luce, R.D., Bush, R.R., Galanter, E. (Eds.), *Handbook of Mathematical Psychology*, John Wiley & Sons, 249-410.

Lyu, Y., Chow, C-Y., Lee, V.C.S., Ng., J.K.Y., Li, Y., and Zeng, J. (2019). CB-Planner: A bus line planning framework for customized bus systems. *Transportation Research Part C*, 101, 233-253.

Ma, C., Wang, C., and Xu, X. (2021). A multi-objective robust optimization model for customized bus routes. *IEEE Transactions on Intelligent Transportation System*. 22(4), 2359-2370.

Mabit, S.L. (2017). Empirical analyses of a choice model that captures ordering among attribute values. *Journal of Choice Modelling*, 25, 3-10.

Maher, M.J. (2001). Stochastic user equilibrium assignment with elastic demand. *Traffic Engineering & Control*, 42(5), 163-167.

Masin, S.C., Zudini, V., and Antonelli, M. (2009). Early alternative derivations of Fechner's law. *Journal of the History of the Behavioural Sciences*, 45(1), 56–65.

Mattsson, L.-G., and Jenelius, E. (2015). Vulnerability and resilience of transport systems - a discussion of recent research. *Transportation Research Part A*, 81, 16-34.

Mattsson, L.G., Weibull, J.W., and Lindberg, P.O. (2014) Extreme values, invariance and choice probabilities. *Transportation Research Part B*, 59, 81-95.

Matyas, M., and Kamargianni, M. (2019). The potential of mobility as a service bundles as a mobility management tool. *Transportation*, 46(5), 1951-1968.

McFadden, D. (1978). Modeling the choice of residential location. *Transportation Research Record*, 672, 72-77.

McFadden, D. and Train, K. (2000). Mixed MNL models of discrete response. *Journal of Applied Econometrics*, 15, 447–470.

Meng Q, and Liu Z. (2011). Mathematical models and computational algorithms for probit-based asymmetric stochastic user equilibrium problem with elastic demand. *Transportmetrica*, 8(4), 261-290.

Meng, Q., Liu, Z., and Wang, S. (2012). Optimal distance tolls under congestion pricing and continuously distributed value of time. *Transportation Research Part E*, 48(5), 937-957.

Meng, Q., Liu, Z., and Wang, S. (2014). Asymmetric stochastic user equilibrium problem with elastic demand and link capacity constraints. *Transportmetrica* 10(4), 304-326.

Mirchandani, P., and Soroush, H. (1987). Generalized traffic equilibrium with probabilistic travel times and perceptions. *Transportation Science*, 21(3), 133-152.

Mondal, A., and Bhat, C.R. (2021). A new closed form multiple discrete-continuous extreme value (MDCEV) choice model with multiple linear constraints. *Transportation Research Part B*, 147, 42–66.

Mori, K., Miwa, T., Abe, R., and Morikawa, T. (2022). Equilibrium analysis of trip demand for autonomous taxi services in Nagoya, Japan. *Transportation Research Part A*, 166, 476–498

Najmi, A., Rashidi, T.H., and Waller, T. (2023). A multimodal multi-provider market equilibrium model: A game-theoretic approach. *Transportation Research Part C*, 146, 103959.

Nguyen, S., and Dupuis, C. (1984). An efficient method for computing traffic equilibria in networks with asymmetric transportation costs. *Transportation Science*, 18(2), 185-202.

Nguyen-Phuoc, D.Q., Su, D.N., Tran, P.T.K., Le, D.-T.T., and Johnson, L.W. (2020). Factors influencing customer's loyalty towards ride-hailing taxi services – A case study of Vietnam. *Transportation Research Part A*, 134, 96-112.

Nirmale, S.K., and Pinjari, A.R. (2023). Discrete choice models with multiplicative stochasticity in choice environment variables: Application to accommodating perception errors in driver behaviour models. *Transportation Research Part B*, 170, 169–193.

Oppenheim, N. (1993). Equilibrium trip distribution/assignment with variable destination costs. *Transportation Research Part B*, 27(3), 207 ‑ 217.

Oppenheim N. (1995). *Urban Travel Demand Modelling: From Individual Choices to General Equilibrium*. John Wiley & Sons.

Ortúzar, J.D.D., and Willumsen, L.G. (2011). *Modelling Transport*. John Wiley & Sons.

Patriksson, M. (1994). *The Traffic Assignment Problem: Models and Methods*. Utrecht, The Netherlands: VSP.

Pel, A.J., and Chaniotakis, M. (2017). Stochastic user equilibrium traffic assignment with equilibrated parking search routes. *Transportation Research Part B*, 11, 123-139.

Perez-Lopez, J-B., Novales, M., and Orro, A. (2022). Spatially correlated nested logit model for spatial location choice. *Transportation Research Part B*, 161, 1-12.

Perez-Lopez, J-B., Novales, M., Varela-García, F-A., and Orro, A. (2020). Residential location econometric choice modeling with irregular zoning: Common border spatial correlation metric. *Networks and Spatial Economics*, 20, 785–802.

Pi, X., Ma, W., and Qian, Z. (2019). A general formulation for multi-modal dynamic traffic assignment considering multi-class vehicles, public transit and parking. *Transportation Research Part C*, 104, 369-389.

Prashker, J.N., and Bekhor, S. (2004). Route choice models used in the stochastic user equilibrium problem: a review. *Transport Reviews*, 24(4), 437-463.

Prato, C.G. (2009). Route choice modeling: past, present and future research directions. *Journal of Choice Modelling*, 2(1), 65-100.

Qiu, G., Song, R., He, S., Xu, W., and Jiang, M., (2019). Clustering passenger trip data for the potential passenger investigation and line design of customized commuter bus. *IEEE Transactions on Intelligent Transportation System*. 20(9), 3351-3360.

Qu, K., Xu, X., and Chen, A. (2021) Static congestion pricing considering day-to-day dynamics with weibit-based route flow adjustment. *Transportmetrica B*, DOI: 10.1080/21680566.2021.1985010.

Ramming, M.S. (2002). Network Knowledge and Route Choice. Ph.D. Thesis, Massachusetts Institute of Technology, Cambridge.

Recker, W.W. (1995). Discrete choice with an oddball alternative. *Transportation Research*, 29B, 201-212.

Rosa, A., and Maher, M. J. (2002). Stochastic user equilibrium traffic assignment with multiple user classes and elastic demand. In: *The Proceedings of the 13th Mini-Euro Conference and 9th Meeting of the Euro Working Group on Transportation*, Bari, Italy.

Ryu, S., Chen, A., Xu, X., and Choi, K. (2014). A dual approach for solving the combined distribution and assignment problem with link capacity constraints. *Networks and Spatial Economics*, 14, 245–270.

Safwat, K.N.A., and Magnanti, T.L. (1988). A combined trip generation, trip distribution, modal split, and trip assignment model. *Transportation Science*, 22(1), 14-30.

Schmid, B., Jokubauskaite, S., Aschauer, F., Peer, S., Hössinger, R., Gerike, R., Jara-Diaz, S.R., and Axhausen, K.W. (2019). A pooled RP/SP mode, route and destination choice model to investigate mode and user-type effects in the value of travel time savings. *Transportation Research Part A*, 124, 262–294.

Sener, I.N., Pendyala, R.M., and Bhat C.R. (2011). Accommodating spatial correlation across choice alternatives in discrete choice models: an application to modeling residential location choice behavior. *Journal of Transport Geography*, 19, 294-303.

Sharifi, M.S., Chen, A., Kitthamkesorn, S., and Song, Z. (2015). Link-based stochastic loading methods for weibit route choice model. *Transportation Research Record*, 2497, 84-94.

Sheffi, Y. (1985). *Urban Transportation Networks: Equilibrium Analysis with Mathematical Programming Methods*. Prentice Hall, England Cliffs, NJ.

Shui, C.S., and Szeto, W.Y. (2020). A review of bicycle-sharing service planning problems. *Transportation Research Part C*, 117, 102648.

Sifringer, B., Lurkin, V., Alahi, A. (2020). Enhancing discrete choice models with representation learning. *Transportation Research Part B*, 140, 263-261.

Small, K.A. (1987). A discrete choice model for ordered alternatives. *Econometrica*, 55(2), 409-424.

Song, F. (2019). *Understanding Mode Choice Behaviour When New Modes Come into Play*. PhD thesis, University of Leeds.

Su, D.N., Nguyen-Phuoc, D.Q., and Johnson, L.W. (2021). Effects of perceived safety, involvement and perceived service quality on loyalty intention among ride-sourcing passengers. *Transortation*, 48, 369–393.

Sun, C., Cheng, L., Zhu, S., Han, F., and Chu, Z. (2019). Multi-criteria user equilibrium model considering travel time, travel time reliability and distance. *Transportation Research Part D*, 66, 3-12.

Sweet, M.N. (2021). User interest in on-demand, shared, and driverless mobility: Evidence from stated preference choice experiments in Southern Ontario. *Travel Behaviour and Society*, 23, 120–133.

Tam, M.L., and Lam, W.H.K. (2000). Maximum car ownership under constraint of road capacity and parking space. *Transportation Research Part A*, 34(3), 145–170.

Tang, W., Xie, N., Mo, D., Cai, Z., Lee, D.-H., and Chen, X. (2023). Optimizing subsidy strategies of the ride-sourcing platform under government regulation. *Transportation Research Part E*, 173, 103112.

Taylor, M.A.P. (2017). Vulnerability Analysis for Transportation Networks. Elsevier, Oxford.

Tomlin, J.A. (1971). A mathematical programming model for the combined distribution-assignment of traffic. *Transportation Science*, 5(2), 122-140.

Tong, L. C., Zhou, L., Liu, J., and Zhou, X. (2017). Customized bus service design for jointly optimizing passenger-to-vehicle assignment and vehicle routing. *Transportation Research Part C*, 85, 451-475.

Train, K. (2003). *Discrete Choice Methods with Simulation*, Cambridge University Press, Cambridge.

van den Berg, V.A.C., Meurs, H., and Verhoef, E.T. (2022). Business models for Mobility as an Service (MaaS). *Transportation Research Part B*, 157, 203–229.

van Lierop, D., Badami M.G., and El-Geneidy, A.M. (2018) What influences satisfaction and loyalty in public transport? A review of the literature, *Transport Reviews*, 38(1), 52-72.

van Wee., B. (2016) Accessible accessibility research challenges. *Journal of Transport Geography*, 12(2), 127-140.

Varela, J.M.L., Borjesson, M., and Daly, A. (2018). Quantifying errors in travel time and cost by latent variables. *Transportation Research Part B*, 117, 520 – 541.

Vlachos, I., and Lin, Z. (2014). Drivers of airline loyalty: Evidence from the business travelers in China. *Transportation Research Part E*, 71, 1-17.

Vovsha, P. (1997). Application of cross-nested logit model to mode choice in Tel Aviv, Israel, Metropolitan Area. *Transportation Research Record*, 1607, 6-15.

Vuong, Q.H. (1989). Likelihood ratio tests for model selection and non-nested hypotheses. *Econometrica*, 57, 307–333.

Wallace C.E., Courage K.G., Hadi M.A., and Gan A.G. (1998). *TRANSYT-7 F User's Guide*. Gainesville, FL: University of Florida.

Wang, G., Chen, A., Kitthamkesorn, S., Ryu, S., Qi, H., Song, Z., and Song, J.G. (2020a). A multi-modal network equilibrium model with captive mode choice and path size logit route choice. *Transportation Research Part A*, 136, 293-317.

Wang, G., Tong, K., Chen, A., Qi, H., Xu, X., and Ma, S. (2021a) Impacts of the least perceived travel cost on the Weibit network equilibrium. *Transportmetrica A*, DOI: 10.1080/23249935.2021.1980131.

Wang, H., and Yang, H. (2019). Ridesourcing systems: A framework and review. *Transportation Research Part B*, 129, 122–155.

Wang, J., Yamamoto, T., and Liu, K. (2019). Role of customized bus services in the transportation system: insight from actual performance. *Journal of Advanced Transportation*, 6171532.

Wang, J., Yamamoto, T., and Liu, K. (2020b). Key determinants and heterogeneous frailties in passenger loyalty toward customized buses: An empirical investigation of the subscription termination hazard of users. *Transportation Research Part C*, 115, 102636.

Wang, J-P., Liu, T-L., and Huang, H-J. (2018). Tradable OD-based travel permits for bi-modal traffic management with heterogeneous users. *Transportation Research Part E*, 118, 589-605.

Wang, J.Y., and Ehrgott, M. (2013). Modelling route choice behaviour in a tolled road network with a time surplus maximisation bi-objective user equilibrium model. *Transportation Research Part B*, 57, 342–360.

Wang, S., Li, Z., and Xie, N. (2022). A reservation and allocation model for shared-parking addressing the uncertainty in drivers' arrival/departure time. *Transportation Research Part C*, 135, 103484.

Wang, X., Liu, W., Yang, H., Wang, D., and Ye, J. (2020c). Customer behavioural modelling of order cancellation in coupled ride-sourcing and taxi markets. *Transportation Research Part B*, 132, 358-378.

Wang, Y., Lin, X., He, F., and Li, M. (2022). Designing transit-oriented multi-modal transportation systems considering travelers' choices. *Transportation Research Part B*, 162, 292–327.

Wang, Z., Yu, J., Hao, W., and Xiang, J. (2021b). Joint optimization of running route and scheduling for the mixed demand responsive feeder transit with time-dependent travel times. *IEEE Transactions on Intelligent Transportation System*, 22(4), 2498-2509.

Wardrop, J.G. (1952) Some theoretical aspects of road traffic research. *Proceedings of the Institution of Civil Engineers*, 2(1), 325-378.

Wen, C.H., and Koppelman, F.S. (2001) The generalized nested logit model. *Transportation Research Part B*, 35(7), 627-641.

Wen, K., Xie, J., Chen, A., Wong, S.C., Zhan, S., Lo, S.M., and Qiang, L. (2021) Empirical analysis of scaled mixed itinerary-size weibit model for itinerary choice in a schedule-based railway network. *Transportmetrica A*, DOI: 10.1080/23249935.2021.1912206.

Williams, H.C.W.L. (1977) On the formation of travel demand models and economic evaluation measures of user benefit. *Environment and Planning*, 9A, 285-344.

Wilson, A.G. (1967). A statistical theory of spatial distribution models. *Transportation Research*, 1, 253–269.

Winkler, C. (2016) Evaluating transport user benefits: Adjustment of the logsum difference for constrained travel demand models. *Transportation Research Record*, 2564(1), 118–126.

Wu, Z.X., and Lam, W.H.K. (2003). A combined modal split and stochastic assignment model for congested networks with motorized and non-motorized modes. *Transportation Research Record*, 1831, 57–64.

Xi, H., Tang, Y., Waller, S.T., and Shalaby, A. (2022). Modeling, equilibrium, and demand management for mobility and delivery services in Mobility-as-a-Service ecosystems. *Computer-Aided Civil and Infrastructure Engineering*, 38(11), 1403-1423.

Xiao, H., Xu, M., and Gao, Z. (2018). Shared parking problem: A novel truthful double auction mechanism approach. *Transportation Research Part B*, 109, 40–69.

Xie, J., Wang, Q., Nie, Y.M. (2021). An efficient algorithm for continuous bi-criteria traffic assignment. *Preprint online*.

Xie, J., Wong, S.C., Zhan, S., Lo, S.M., and Chen, A. (2020). Train schedule optimization based on schedule-based stochastic passenger assignment. *Transportation Research Part E*, 136, 101882.

Xie, Y., Danaf, M., Lima Azevedo, C., Akkinepally, A.P., Atasoy, B., Jeong, K., Seshadri, R., and Ben-Akiva, M. (2019). Behavioral modeling of on-demand

mobility services: General framework and application to sustainable travel incentives. *Transportation*, 46 (6), 2017–2039.

Xu, X., Chen, A., Kitthamkesorn, S., Yang, H., and Lo, H. K. (2015) Modeling absolute and relative cost differences in stochastic user equilibrium problem. *Transportation Research Part B*, 81, 686-703.

Xu, X., Qu, K., Chen, A., and Yang, C. (2021) A new day-to-day dynamic network vulnerability analysis approach with weibit-based route adjustment process. *Transportation Research Part E*, 153, 102421.

Yan, X., Levine, J., and Zhao X. (2019a). Integrating ridesourcing services with public transit: An evaluation of traveler responses combining revealed and stated preference data. *Transportation Research Part C*, 105, 683–696.

Yan, Y., Xu, X., and Chen, A. (2019b). Is it necessary to relax the IID assumptions in the logsum-based accessibility analysis? *Journal of the Transportation Research Board*, 2673(4), 84-96.

Yang, C., and Chen, A. (2009). Sensitivity analysis of the combined travel demand model with applications. *European Journal of Operational Research*, 198 (3), 909–921.

Yang, H., and Bell, M.G.H. (1998). Models and algorithms for road network design: A review and some new developments. *Transport Reviews*. 18(3), 257-278.

Yang, H., and Huang, H-J. (2004). The multi-class, multi-criteria traffic network equilibrium and systems optimum problem. *Transportation Research Part B*, 38, 1-15.

Yang, H., and Huang, H-J. (2005). *Mathematical and Economic Theory of Road Pricing*. Elsevier.

Yang, H., and Meng, Q. (1998). An integrated network equilibrium model of urban location and travel choices. *Journal of Regional Science*, 38, 575–598.

Yang, H., Wong, S.C., and Wong, K.I. (2002). Demand-supply equilibrium of taxi services in a network under competition and regulation. *Transportation Research Part B*, 36(9), 799-819.

Yang, H., and Yang, T. (2011). Equilibrium properties of taxi markets with search frictions. *Transportation Research Part B*, 45, 696–713.

Yao, J., and Chen, A. (2014) An analysis of logit and weibit route choices in stochastic assignment paradox. *Transportation Research Part B*, 69, 31-49.

Ye, H. (2022). On stochastic user equilibrium based day-to-day dynamics. *Transportation Science*, 56(1), 203-117.

Yim, K.K.W., Wong, S.C., Chen, A., Wong, C.K., and Lam, W.H.K. (2011). A reliability-based land use and transportation optimization model. *Transportation Research Part C*, 19, 351-362.

Zhang, F., Liu, W., Wang, X., and Yang, H. (2020). Parking sharing problem with spatially distributed parking supplies. *Transportation Research Part C*, 117, 102676.

Zhou, Y., Yang, H., Ke, J., Wang, H., and Li, X. (2022). Competition and third-party platform-integration in ride-sourcing markets. *Transportation Research Part B*, 159, 76–103.

Zhou, Z., Chen, A., and Bekhor, S. (2012). C-logit stochastic user equilibrium model: Formulations and solution algorithm.' *Transportmetrica*, 8(1), 17-41.

Zhou, Z., Chen, A., and Wong, S.C. (2009). Alternative formulations of a combined trip generation, trip distribution, modal split, and trip assignment model. *European Journal of Operational Research*, 198(1), 129-138.

Zhu, L., Wang, J., Yuan, Y., and Wu, W. (2022). Mode split equilibrium microsimulation approach for early-stage on-demand shared automated mobility. *Sensors*, 22, 8020.

Appendix A. Proofs of solution equivalence for equilibrium models

A1. Proof of solution equivalence for OPSGEV equilibrium model (6.6)-(6.10)

The Lagrangian of model (6.6)-(6.10) is:

$$L = Z - \lambda^{rs} \cdot \left(\sum_{k} \sum_{u=k}^{k+M} f_{uk}^{rs} - q^{rs} \right). \tag{A1.1}$$

Take the first derivative with respect to f_{uk}^{rs}:

$$\begin{aligned} \frac{\partial L}{\partial f_{uk}^{rs}} = t_k^{rs} + g\left(\tau_k^{rs}\right) + \frac{1}{\theta_k} \ln f_{uk}^{rs} - \frac{1}{\theta_k} \ln \sum_{k \in K_u} f_{uk}^{rs} - \frac{1}{\theta_k} \ln PS_k^{rs} \\ + \frac{1}{\theta_u} \ln \sum_{k \in K_u} f_{uk}^{rs} - \frac{1}{\theta_u} \ln w_{uk}^{rs} - \lambda^{rs} \end{aligned}. \tag{A1.2}$$

With $c_k^{rs} = t_k^{rs} + \tau_k^{rs}$ denoting the generalized path cost function in Eq. (6.5), we have:

$$\left(f_{uk}^{rs} \right)^{\frac{1}{\theta_k}} \cdot \left(\sum_{k \in K_u^{rs}} f_{uk}^{rs} \right)^{\frac{1}{\theta_u} - \frac{1}{\theta_k}} = \left(PS_k^{rs} \right)^{\frac{1}{\theta_k}} \cdot \left(w_{uk}^{rs} \right)^{\frac{1}{\theta_u}} \cdot \exp\left[-\left(c_k^{rs} - \lambda^{rs} \right) \right], \tag{A1.3}$$

$$\left(f_{uk}^{rs} \right) \cdot \left(\sum_{k \in K_u^{rs}} f_{uk}^{rs} \right)^{\frac{\theta_k}{\theta_u} - 1} = PS_k^{rs} \cdot \left(w_{uk}^{rs} \right)^{\frac{\theta_k}{\theta_u}} \cdot \exp\left[-\theta_k \left(c_k^{rs} - \lambda^{rs} \right) \right]. \tag{A1.4}$$

Summing up both sides of Eq. (A1.4) by path *k* leads to the following expression:

$$\left(\sum_{k \in K_u^{rs}} f_{uk}^{rs} \right)^{\frac{\theta_k}{\theta_u}} = \sum_{k \in K_u^{rs}} PS_k^{rs} \cdot \left(w_{uk}^{rs} \right)^{\frac{\theta_k}{\theta_u}} \cdot \exp\left[-\theta_k \left(c_k^{rs} - \lambda^{rs} \right) \right]. \tag{A1.5}$$

Dividing Eq. (A1.4) by Eq. (A1.5), the conditional OPSGEV route choice probability given in Eq. (3.5) can then be derived:

$$\frac{f_{uk}^{rs}}{\sum_{l \in K_u^{rs}} f_{ul}^{rs}} = \frac{PS_k^{rs} \cdot \left(w_{uk}^{rs} \right)^{\frac{\theta_k}{\theta_u}} \cdot \exp\left(-\theta_k c_k^{rs} \right)}{\sum_{l \in K_u^{rs}} PS_l^{rs} \cdot \left(w_{ul}^{rs} \right)^{\frac{\theta_k}{\theta_u}} \cdot \exp\left(-\theta_k c_l^{rs} \right)}. \tag{A1.6}$$

From Eq. (A1.5), we can also have:

$$\sum_{k \in K_u^{rs}} f_{uk}^{rs} = \exp\left(\theta_u \lambda^{rs} \right) \cdot \left[\sum_{k \in K_u^{rs}} PS_k^{rs} \cdot \left(w_{uk}^{rs} \right)^{\frac{\theta_k}{\theta_u}} \exp\left(-\theta_k c_k^{rs} \right) \right]^{\frac{\theta_u}{\theta_k}}. \tag{A1.7}$$

$$q^{rs} = \exp\left(\theta_u \lambda^{rs}\right) \cdot \sum_{u=1}^{\left|K^{rs}\right|+M} \left[\sum_{l \in K_u^{rs}} PS_l^{rs} \cdot \left(w_{ul}^{rs}\right)^{\frac{\theta_k}{\theta_u}} \exp\left(-\theta_k c_l^{rs}\right) \right]^{\frac{\theta_u}{\theta_k}}. \qquad \text{(A1.8)}$$

Dividing Eq. (A1.7) by Eq. (A1.8) gives the marginal choice probability provided in Eq. (3.4):

$$\frac{\sum_{k \in K_u^{rs}} f_{uk}^{rs}}{q^{rs}} = \frac{\left[\sum_{k \in K_u^{rs}} PS_k^{rs} \cdot \left(w_{uk}^{rs}\right)^{\frac{\theta_k}{\theta_u}} \exp\left(-\theta_k c_k^{rs}\right) \right]^{\frac{\theta_u}{\theta_k}}}{\sum_{u=1}^{\left|K^{rs}\right|+M} \left[\sum_{l \in K_u^{rs}} PS_l^{rs} \cdot \left(w_{ul}^{rs}\right)^{\frac{\theta_k}{\theta_u}} \exp\left(-\theta_k c_l^{rs}\right) \right]^{\frac{\theta_u}{\theta_k}}}. \qquad \text{(A1.9)}$$

This completes the proof.

A2. Proof of solution equivalence for DNW equilibrium model (7.8)-(7.12)

The Lagrangian of model (7.8)-(7.12) is:

$$\begin{aligned} L = Z &+ \sum_{rs\in RS} \pi^{rs} \cdot \left(\sum_{u\in U_{rs}} \sum_{m\in M_u^{rs}} q_{um}^{rs} - q^{rs} \right) \\ &+ \sum_{rs\in RS} \omega_{cap}^{rs} \cdot \left(q_{CB}^{rs} - cap_{CB}^{rs} \right) \\ &+ \sum_{rs\in RS} \omega_{ld}^{rs} \cdot \left[ld_{CB}^{rs} - q_{CB}^{rs} \right] \end{aligned} \quad . \tag{A2.1}$$

First, take the partial derivative with respect to q_{um}^{rs}:

$$\begin{aligned} \frac{\partial L}{\partial q_{um}^{rs}} = &\ln \tau_m^{rs}(q_{um}^{rs}) + \frac{1}{\beta_{um}^{rs}} \cdot \ln \left(q_{um}^{rs} - \frac{q^{rs}\eta_m^{rs}}{1+\sum_{m\in M}\eta_m^{rs}} \right) \\ &+ \left(\frac{1}{\beta_u^{rs}} - \frac{1}{\beta_{um}^{rs}} \right) \cdot \ln \sum_{m\in M_u^{rs}} \left(q_{um}^{rs} - \frac{q^{rs}\eta_m^{rs}}{1+\sum_{m\in M}\eta_m^{rs}} \right), \\ &+ \pi^{rs} + \left(\omega_{cap}^{rs} - \omega_{ld}^{rs} \right) \end{aligned} \tag{A2.2}$$

where $\frac{\eta_m^{rs}}{1+\sum_{m\in M}\eta_m^{rs}}$ denotes the proportion of the loyal passengers choosing mode *m*, thus

$qc_{um}^{rs} = q_{um}^{rs} - \frac{q^{rs}\eta_m^{rs}}{1+\sum_{m\in M}\eta_m^{rs}}$ denote the choice passengers choosing mode *m*. Let $\frac{\partial L}{\partial q_{um}^{rs}} = 0$, then Eq. (A2.2) gives:

$$\ln\left[\tau_m^{rs}\left(q_{um}^{rs}\right) \cdot e^{\left(\pi^{rs} + \omega_{cap}^{rs} - \omega_{ld}^{rs}\right)} \right] = -\frac{1}{\beta_{um}^{rs}} \cdot \ln qc_{um}^{rs} - \left(\frac{1}{\beta_u^{rs}} - \frac{1}{\beta_{um}^{rs}} \right) \cdot \ln \sum_{m\in M_u^{rs}} qc_{um}^{rs} \, . \tag{A2.3}$$

$e^{\left(\omega_{cap}^{rs} - \omega_{ld}^{rs}\right)}$ is considered as a correction to CB travel disutility arisen from the side constraints, i.e., the risk of subscription failure led by the CB capacity and the subscription incentives given by the lower limit of CB demand. We denote $v_m^{rs} = \tau_m^{rs}\left(q_{um}^{rs}\right) \cdot e^{\left(\omega_{Cap}^{rs} - \omega_L^{rs}\right)}$ as the final mode disutility at optimality. Then the following conditions can be derived from Eq. (A2.3):

$$v_m^{rs} \cdot e^{\pi^{rs}} = \left(\frac{qc_{um}^{rs}}{\sum_{m \in M_u^{rs}} qc_{um}^{rs}} \right)^{-\frac{1}{\beta_{um}^{rs}}} \cdot \left(\sum_{m \in M_u^{rs}} qc_{um}^{rs} \right)^{-\frac{1}{\beta_u^{rs}}} \tag{A2.4}$$

$$\begin{aligned} \sum_{m \in M_u^{rs}} \left(v_m^{rs} \cdot e^{\pi^{rs}} \right)^{-\beta_{um}^{rs}} &= \sum_{m \in M_u^{rs}} \frac{\left(qc_{um}^{rs} \right)}{\sum_{m \in M_u^{rs}} qc_{um}^{rs}} \cdot \left(\sum_{m \in M_u^{rs}} qc_{um}^{rs} \right)^{\frac{\beta_{um}^{rs}}{\beta_u^{rs}}} \\ &= \left(\sum_{m \in M_u^{rs}} qc_{um}^{rs} \right)^{\frac{\beta_{um}^{rs}}{\beta_u^{rs}}} \end{aligned} \tag{A2.5}$$

$$\left[\sum_{m \in M_u^{rs}} \left(v_m^{rs} \cdot e^{\pi^{rs}} \right)^{-\beta_{um}^{rs}} \right]^{-\frac{1}{\beta_{um}^{rs}}} = \left(\sum_{m \in M_u^{rs}} qc_{um}^{rs} \right)^{-\frac{1}{\beta_u^{rs}}} \tag{A2.6}$$

Taking Eq. (A2.6) into Eq. (A2.4) gives the conditional probability of choice passengers choosing mode *m* given nest *u* (i.e., Eq. (3.8) in the NW model):

$$\left(\frac{\left(qc_{um}^{rs} \right)}{\sum_{l \in M_u^{rs}} qc_{ul}^{rs}} \right)^{-\frac{1}{\beta_{um}^{rs}}} = \frac{v_m^{rs} \cdot e^{\pi^{rs}}}{\left[\sum_{l \in M_u^{rs}} \left(v_l^{rs} \cdot e^{\pi^{rs}} \right)^{-\beta_{um}^{rs}} \right]^{-\frac{1}{\beta_{um}^{rs}}}}, \tag{A2.7}$$

$$\lambda_{m|u}^{rs} = \frac{\left(qc_{um}^{rs} \right)}{\sum_{m \in M_u^{rs}} qc_{um}^{rs}} = \frac{\left(v_m^{rs} \right)^{-\beta_{um}^{rs}}}{\sum_{m \in M_u^{rs}} \left(v_m^{rs} \right)^{-\beta_{um}^{rs}}}. \tag{A2.8}$$

From Eq. (3.10), $v_u^{rs} = \left[\sum_{l \in M_u^{rs}} \left(v_l^{rs} \right)^{-\beta_{um}^{rs}} \right]^{-\frac{1}{\beta_{um}^{rs}}}$. The marginal probability of choice passengers choosing nest *u* (i.e., Eq. (3.9) in the NW model) can also be derived based on Eq. (A2.6):

$$\sum_{m \in M_u^{rs}} qc_{um}^{rs} = \left(v_u^{rs} \cdot e^{\pi^{rs}} \right)^{-\beta_u^{rs}}, \tag{A2.9}$$

$$\lambda_u^{rs} = \frac{\sum_{m \in M_u^{rs}} qc_{um}^{rs}}{\sum_{w \in U^{rs}} \sum_{m \in M_w^{rs}} qc_{um}^{rs}} = \frac{\left(v_u^{rs} \right)^{-\beta_u^{rs}}}{\sum_{w \in U^{rs}} \left(v_w^{rs} \right)^{-\beta_u^{rs}}}. \tag{A2.10}$$

Therefore, the mode choice of choice passengers is given by the NW model:

$$\begin{aligned}\lambda_{um}^{rs} &= \lambda_{m|u}^{rs} \cdot \lambda_{u}^{rs} \\ &= \frac{\left(v_m^{rs}\right)^{-\beta_{um}^{rs}} \left[\sum_{m \in M_u^{rs}} \left(v_m^{rs}\right)^{-\beta_{um}^{rs}}\right]^{\frac{\beta_u^{rs}}{\beta_{um}^{rs}}-1}}{\sum_{u \in U^{rs}} \left[\sum_{m \in M_u^{rs}} \left(v_m^{rs}\right)^{-\beta_{um}^{rs}}\right]^{\frac{\beta_u^{rs}}{\beta_{um}^{rs}}}}.\end{aligned} \tag{A2.11}$$

The choice probability considering all passengers can then be derived:

$$P_{um}^{rs} = \frac{q_{um}^{rs}}{q^{rs}} = \frac{qc_{um}^{rs} + \dfrac{q^{rs}\eta_m^{rs}}{1+\sum_{m \in M} \eta_m^{rs}}}{q^{rs}}. \tag{A2.12}$$

Given that:

$$q^{rs} = \sum_{u \in U^{rs}} \sum_{m \in M_u^{rs}} \left(qc_{um}^{rs} + \frac{q^{rs}\eta_m^{rs}}{1+\sum_{m \in M} \eta_m^{rs}} \right), \tag{A2.13}$$

$$\sum_{u \in U^{rs}} \sum_{m \in M_u^{rs}} qc_{um}^{rs} = \frac{q^{rs}}{1+\sum_{m \in M} \eta_m^{rs}}. \tag{A2.14}$$

Substituting Eqs. (A2.11) and (A2.14) into Eq. (A2.12), then we can obtain exactly the DNW choice probability in Eqs. (3.15) and (3.16). This completes the proof.

A3. Proof of solution equivalence for DCNW equilibrium model (8.11)-(8.14)

The Lagrangian of model (8.11)-(8.14) is:

$$\begin{aligned} L = Z - \lambda^{rs} \cdot \left(\sum_{rs \in RS} \sum_{u \in U^{rs}} \sum_{m \in M_u^{rs}} q_{um}^{rs} - q^{rs} \right) \\ + \sum_{rs \in RS} \omega_{CB}^{rs} \cdot \left(q_{CB}^{rs} - cap_{CB}^{rs} \right) + \sum_{s \in S} \sum_{m=BS,EH} \omega_m^r \cdot \left(q_m^r - cap_m^r \right) \end{aligned} . \quad \text{(A3.1)}$$

Take the first derivative with respect to q_{um}^{rs}:

$$\begin{aligned} \frac{\partial L}{\partial q_{um}^{rs}} = \ln \tau_m^{rs} \left(q_m^{rs} \right) + \frac{1}{\beta_{um}^{rs}} \left(\ln q_{um}^{rs} - \ln \sum_{m \in M_u^{rs}} q_{um}^{rs} \right) - \frac{1}{\beta_u^{rs}} \ln \mu_{um}^{rs} \\ + \frac{1}{\beta_u^{rs}} \cdot \ln \left(\sum_{m \in M_u^{rs}} q_{um}^{rs} - \frac{\eta_u^{rs} \cdot q^{rs}}{1 + \sum_{w \in U^{rs}} \eta_w^{rs}} \right) - \lambda^{rs} + \omega_m^{rs} \end{aligned} . \quad \text{(A3.2)}$$

For simplicity we use ω_m^{rs} to denote the dual variable associated with the capacity constraint of each mode between OD pair *rs*, and $qc_u^{rs} = \sum_{m \in M_u^{rs}} q_{um}^{rs} - \frac{\eta_u^{rs} \cdot q^{rs}}{1 + \sum_{w \in U^{rs}} \eta_w^{rs}}$ to denote the choice travelers that choose mobility bundle/type *u*. Letting $\frac{\partial L}{\partial q_{um}^{rs}} = 0$ gives

$$\left(q_{um}^{rs} \right)^{\frac{1}{\beta_{um}^{rs}}} \cdot \left(\sum_{m \in M_u^{rs}} q_{um}^{rs} \right)^{-\frac{1}{\beta_{um}^{rs}}} \cdot \left(qc_u^{rs} \right)^{\frac{1}{\beta_u^{rs}}} = \left(\tau_m^{rs} \cdot e^{\omega_m^{rs}} \right)^{-1} \cdot \left(\mu_{um}^{rs} \right)^{\frac{1}{\beta_u^{rs}}} \cdot e^{\lambda^{rs}} , \quad \text{(A3.3)}$$

$$\frac{q_{um}^{rs}}{\sum_{m \in M_u^{rs}} q_{um}^{rs}} \cdot \left(qc_u^{rs} \right)^{\frac{\beta_{um}^{rs}}{\beta_u^{rs}}} = \left(\tau_m^{rs} \cdot e^{\omega_m^{rs}} \right)^{-\beta_{um}^{rs}} \cdot \left(\mu_{um}^{rs} \right)^{\frac{\beta_{um}^{rs}}{\beta_u^{rs}}} \cdot e^{\beta_{um}^{rs} \cdot \lambda^{rs}} . \quad \text{(A3.4)}$$

Taking $e^{\omega_m^{rs}}$ as a correction to the mode disutility, i.e., the additional difficulty of using mobility service *m* between OD pair *rs* caused by the capacity constraints, we denote $v_{um}^{rs} = \tau_{um}^{rs} \cdot e^{\omega_m^{rs}}$ as the final mode disutility at optimality. Summing up both sides of Eq. (A3.4) with respect to *m* leads to the following expression:

$$\left(qc_u^{rs} \right)^{\frac{\beta_{um}^{rs}}{\beta_u^{rs}}} = \sum_{m \in M_u^{rs}} \left(v_{um}^{rs} \right)^{-\beta_{um}^{rs}} \cdot \left(\mu_{um}^{rs} \right)^{\frac{\beta_{um}^{rs}}{\beta_u^{rs}}} \cdot e^{\beta_{um}^{rs} \cdot \lambda^{rs}} . \quad \text{(A3.5)}$$

Dividing Eq. (A3.4) by Eq. (A3.5) leads to:

$$\frac{q_{um}^{rs}}{\sum_{m\in M_u^{rs}} q_{um}^{rs}} = \frac{\left(v_{um}^{rs}\right)^{-\beta_{um}^{rs}} \cdot \left(\mu_{um}^{rs}\right)^{\frac{\beta_{um}^{rs}}{\beta_u^{rs}}} \cdot e^{\beta_{um}^{rs}\cdot\lambda^{rs}}}{\sum_{m\in M_u^{rs}} \left(v_{um}^{rs}\right)^{-\beta_{um}^{rs}} \cdot \left(\mu_{um}^{rs}\right)^{\frac{\beta_{um}^{rs}}{\beta_u^{rs}}} \cdot e^{\beta_{um}^{rs}\cdot\lambda^{rs}}}, \tag{A3.6}$$

which gives the DCNW conditional choice probability presented in Eq. (3.39). From Eq. (A4.5), we can also obtain the following:

$$qc_u^{rs} = e^{\beta_u^{rs}\cdot\lambda^{rs}} \cdot \left[\sum_{m\in M_u^{rs}} \left(v_{um}^{rs}\right)^{-\beta_{um}^{rs}} \cdot \left(\mu_{um}^{rs}\right)^{\frac{\beta_{um}^{rs}}{\beta_u^{rs}}}\right]^{\frac{\beta_u^{rs}}{\beta_{um}^{rs}}}. \tag{A3.7}$$

Define $q_u^{rs} = \sum_{m\in M_u^{rs}} q_{um}^{rs}$ as the total demand of bundle *u*, we have the following:

$$q_u^{rs} = qc_u^{rs} + \frac{\eta_u^{rs}\cdot q^{rs}}{1+\sum_{w\in U^{rs}} \eta_w^{rs}}. \tag{A3.8}$$

$$q^{rs} = \sum_{u\in U^{rs}} q_u^{rs} = e^{\beta_u^{rs}\cdot\lambda^{rs}} \cdot \sum_{u\in U^{rs}} \left[\sum_{m\in M_u^{rs}} \left(v_{um}^{rs}\right)^{-\beta_{um}^{rs}} \cdot \left(\mu_{um}^{rs}\right)^{\frac{\beta_{um}^{rs}}{\beta_u^{rs}}}\right]^{\frac{\beta_u^{rs}}{\beta_{um}^{rs}}} + \frac{\sum_{w\in U^{rs}} \eta_w^{rs}}{1+\sum_{w\in U^{rs}} \eta_w^{rs}} \cdot q^{rs}. \tag{A3.9}$$

Eq. (A3.9) can be rewritten as follows:

$$\begin{aligned} \frac{1}{1+\sum_{w\in U^{rs}} \eta_w^{rs}} \cdot q^{rs} &= e^{\beta_u^{rs}\cdot\lambda^{rs}} \cdot \sum_{u\in U^{rs}} \left[\sum_{m\in M_u^{rs}} \left(v_{um}^{rs}\right)^{-\beta_{um}^{rs}} \cdot \left(\mu_{um}^{rs}\right)^{\frac{\beta_{um}^{rs}}{\beta_u^{rs}}}\right]^{\frac{\beta_u^{rs}}{\beta_{um}^{rs}}} \\ q^{rs} &= \left(1+\sum_{w\in U^{rs}} \eta_w^{rs}\right) \cdot \sum_{u\in U^{rs}} \left[\sum_{m\in M_u^{rs}} \left(v_{um}^{rs}\right)^{-\beta_{um}^{rs}} \cdot \left(\mu_{um}^{rs}\right)^{\frac{\beta_{um}^{rs}}{\beta_u^{rs}}}\right]^{\frac{\beta_u^{rs}}{\beta_{um}^{rs}}} \end{aligned}. \tag{A3.10}$$

Considering Eqs. (A3.7), (A3.8) and (A3.10) leads to the following equation:

$$\begin{aligned} \frac{q_u^{rs}}{q^{rs}} &= \frac{qc_u^{rs} + \frac{\eta_u^{rs}\cdot q^{rs}}{1+\sum_{w\in U^{rs}} \eta_w^{rs}}}{q^{rs}} \\ &= \frac{\eta_u^{rs}}{1+\sum_{w\in U^{rs}} \eta_w^{rs}} + \frac{1}{1+\sum_{w\in U^{rs}} \eta_w^{rs}} \cdot \frac{\left[\sum_{m\in M_u^{rs}} \left(v_{um}^{rs}\right)^{-\beta_{um}^{rs}} \cdot \left(\mu_{um}^{rs}\right)^{\frac{\beta_{um}^{rs}}{\beta_u^{rs}}}\right]^{\frac{\beta_u^{rs}}{\beta_{um}^{rs}}}}{\sum_{u\in U^{rs}} \left[\sum_{m\in M_u^{rs}} \left(v_{um}^{rs}\right)^{-\beta_{um}^{rs}} \cdot \left(\mu_{um}^{rs}\right)^{\frac{\beta_{um}^{rs}}{\beta_u^{rs}}}\right]^{\frac{\beta_u^{rs}}{\beta_{um}^{rs}}}} \end{aligned}, \tag{A3.11}$$

which gives the marginal choice probability in Eq. (3.53). This completes the proof.

A4. Proof of solution equivalence for SCW-PSW equilibrium model (9.4)-(9.10)

The Lagrangian of model (9.4)-(9.10) is:

$$\begin{aligned} L = Z &+ \sum_{rs\in RS} \pi_s^r \cdot \left(f_{s,sp}^r + f_{s,cp}^r - q_s^r \right) \\ &+ \sum_{s\in S} \omega_{s,sp} \cdot \left(\sum_{r\in R} f_{s,sp}^r - Cap_{s,sp} \right) + \sum_{r\in R} \lambda^r \cdot \left(\sum_{s\in S} q_s^r - q^r \right) \end{aligned} . \tag{A4.1}$$

Take the first derivative with respect to $f_{s,m}^r$, *m=sp,cp*:

$$\frac{\partial L}{\partial f_{s,m}^r} = \ln \tau_{s,m}^r + \frac{1}{\beta_m} \left(\ln f_{s,m}^r - \ln PS_{s,m} \right) + \pi_s^r + \omega_{s,m} , \tag{A4.2}$$

where $\omega_{s,cp}^r = 0$ as there is no tight capacity constraint for curbside parking. Let $\frac{\partial L}{\partial f_{s,m}^r} = 0$, then we have:

$$\left(\tau_{s,m}^r \right)^{\beta_m} \cdot \frac{f_{s,m}^r}{PS_{s,m}} = e^{-\beta_m \cdot \left(\pi_s^r + \omega_{s,m} \right)} , \tag{A4.3}$$

$$f_{s,m}^r = e^{-\beta_m \cdot \left(\pi_s^r + \omega_{s,m} \right)} \cdot PS_{s,m} \cdot \left(\tau_{s,m}^r \right)^{-\beta_m} . \tag{A4.4}$$

Eq. (A4.4) gives the analytical expression of $f_{s,m}^r$ in Eq. (9.11). Taking $v_{s,m}^r = e^{\omega_{s,m}} \cdot \tau_{s,m}^r$ as the corrected parking disutility given by the parking cost and the disutility to reserve a shared parking slot due to parking capacity constraint, based on the relationship $f_{s,sp}^r + f_{s,cp}^r = q_s^r$, we can express q_s^r as below:

$$q_s^r = f_{s,sp}^r + f_{s,cp}^r = e^{-\beta_m \cdot \pi_s^r} \cdot \left[PS_{s,sp} \cdot \left(v_{s,sp}^r \right)^{-\beta_m} + PS_{s,cp} \cdot \left(v_{s,cp}^r \right)^{-\beta_m} \right] . \tag{A4.5}$$

The PSW shared parking choice probability given in Eq. (3.68) can then be derived:

$$\begin{aligned} \frac{f_{s,sp}^r}{q_s^r} &= \frac{e^{-\beta_m \cdot \pi_s^r} \cdot PS_{s,sp} \cdot \left(v_{s,sp}^r \right)^{-\beta_m}}{e^{-\beta_m \cdot \pi_s^r} \cdot \left[PS_{s,sp} \cdot \left(v_{s,sp}^r \right)^{-\beta_m} + PS_{s,cp} \cdot \left(v_{s,cp}^r \right)^{-\beta_m} \right]} \\ &= \frac{PS_{s,sp} \cdot \left(v_{s,sp}^r \right)^{-\beta_m}}{PS_{s,sp} \cdot \left(v_{s,sp}^r \right)^{-\beta_m} + PS_{s,cp} \cdot \left(v_{s,cp}^r \right)^{-\beta_m}} \end{aligned} . \tag{A4.6}$$

Similarly, the curbside parking choice probability can be derived by substituting $f_{s,cp}^r$ in Eq. (A4.6).

From Eq. (A4.5), the following relationship can be obtained:

$$-\frac{1}{\beta_m}\ln q_s^r-\pi_s^r=-\frac{1}{\beta_m}\ln\left[PS_{s,sp}\cdot\left(v_{s,sp}^r\right)^{-\beta_m}+PS_{s,cp}\cdot\left(v_{s,cp}^r\right)^{-\beta_m}\right]=\ln A_s^r. \quad \text{(A4.7)}$$

Take the first derivative of the Lagrangian with respect to $q_{s,st}^r$:

$$\frac{\partial L}{\partial q_{s,st}^r}=\left(-\ln\psi_s-\pi_s^r+\lambda^r\right)-\frac{1}{\beta_m}\ln q_s^r+\mu\ln\frac{q_{s,st}^r}{\mu}-\ln\alpha_{s,st}^r+(1-\mu)\ln\frac{q_{s,st}^r+q_{t,st}^r}{\mu}. \quad \text{(A4.8)}$$

Let $\frac{\partial L}{\partial q_{s,st}^r}=0$ and take Eq. (A4.7) into Eq. (A4.8), then we have:

$$\mu\cdot\left[\ln\frac{q_{s,st}^r}{\mu}+\ln\left(\frac{q_{s,st}^r+q_{t,st}^r}{\mu}\right)^{\frac{1-\mu}{\mu}}\right]=\ln\alpha_{s,st}^r-\ln A_s^r+\ln\psi_s-\lambda^r. \quad \text{(A4.9)}$$

As $v_s^r=A_s^r\cdot\left(\psi_s\right)^{-1}$ denotes the disutility of traveling from origin *r* to destination *s*, Eq. (A4.9) can then be arranged as:

$$\frac{q_{s,st}^r}{\mu}\cdot\left(\frac{q_{s,st}^r+q_{t,st}^r}{\mu}\right)^{\frac{1-\mu}{\mu}}=\left[\alpha_{s,st}^r\cdot\left(v_s^r\right)^{-1}\cdot e^{-\lambda^r}\right]^{\frac{1}{\mu}}, \quad \text{(A4.10)}$$

$$\left(\frac{q_{s,st}^r}{\mu}+\frac{q_{t,st}^r}{\mu}\right)\cdot\left(\frac{q_{s,st}^r+q_{t,st}^r}{\mu}\right)^{\frac{1-\mu}{\mu}}=\left[\alpha_{s,st}^r\cdot\left(v_s^r\right)^{-1}\cdot e^{-\lambda^r}\right]^{\frac{1}{\mu}}+\left[\alpha_{t,st}^r\cdot\left(v_t^r\right)^{-1}\cdot e^{-\lambda^r}\right]^{\frac{1}{\mu}}. \quad \text{(A4.11)}$$

Eq. (A4.10) gives the analytical expression of $q_{s,st}^r$ in Eq. (9.13). Dividing Eq.(A4.10) by Eq. (A4.11) gives the SCW conditional probability of choosing destination *s* between the destination pair *st* (i.e., Eq. (3.61)).

Eq. (A4.11) can be arranged as follows:

$$\left(\frac{q_{s,st}^r+q_{t,st}^r}{\mu}\right)^{\frac{1}{\mu}}=\left[\alpha_{s,st}^r\left(v_s^r\right)^{-1}\cdot e^{-\lambda^r}\right]^{\frac{1}{\mu}}+\left[\alpha_{t,st}^r\left(v_t^r\right)^{-1}\cdot e^{-\lambda^r}\right]^{\frac{1}{\mu}}, \quad \text{(A4.12)}$$

$$q_{s,st}^r+q_{t,st}^r=\mu\cdot e^{-\lambda^r}\cdot\left\{\left[\alpha_{s,st}^r\left(v_s^r\right)^{-1}\right]^{\frac{1}{\mu}}+\left[\alpha_{t,st}^r\left(v_t^r\right)^{-1}\right]^{\frac{1}{\mu}}\right\}^{\mu}, \quad \text{(A4.13)}$$

$$\sum_{s=1}^{|S|-1}\sum_{t=s+1}^{|S|}\left(q_{s,st}^{r}+q_{t,st}^{r}\right)=\sum_{s=1}^{|S|-1}\sum_{t=s+1}^{|S|}\mu\cdot e^{-\lambda^{r}}\cdot\left\{\left[\alpha_{s,st}^{r}\left(v_{s}^{r}\right)^{-1}\right]^{\frac{1}{\mu}}+\left[\alpha_{t,st}^{r}\left(v_{t}^{r}\right)^{-1}\right]^{\frac{1}{\mu}}\right\}^{\mu}. \qquad \text{(A4.14)}$$

Eq. (A4.13) gives the analytical expression of q_{st}^{r} in Eq. (9.14). Dividing Eq. (A4.13) by Eq. (A4.14) gives the SCW marginal probability of choosing destination pair *st* among all destination pairs (i.e., Eq. (3.59)). This completes the proof.

Appendix B. Proofs of solution uniqueness for equilibrium models

B1. Proof of solution uniqueness for OPSGEV equilibrium model (6.6)-(6.10)

Given the convex feasible region restricted by the sets of linear constraints, the proof of the solution uniqueness is equivalent to proving the strict convexity of the objective function (6.6). for simplicity, let $q_u^{rs} = \sum_{k \in K_u^{rs}} f_{uk}^{rs}$ denote the total flow belonging to the path order subset *u* between OD pair *rs*. We first derive the Hessian matrix with respect to q_u^{rs}:

$$\frac{\partial^2 Z}{\partial q_u^{rs} \partial q_y^{rs}} = \begin{cases} \frac{1}{\theta_u} \cdot \frac{1}{q_u^{rs}} - \frac{1}{\theta_k} \cdot \frac{1}{q_u^{rs}} & u = y \\ 0 & Otherwise \end{cases} . \tag{B1.15}$$

By definition, the dispersion parameter at the marginal choice level is smaller than that at the conditional choice level, i.e., $\theta_u \le \theta_k$. Therefore, $\frac{1}{\theta_u} \cdot \frac{1}{q_u^{rs}} - \frac{1}{\theta_k} \cdot \frac{1}{q_u^{rs}} > 0$, the Hessian matrix with respect to q_u^{rs} is positive definite.

The Hessian matrix with respect to f_{uk}^{rs} is

$$\frac{\partial^2 Z}{\partial f_{uk}^{rs} \partial f_{yl}^{rs}} = \begin{cases} \frac{dt_k^{rs}\left(f_k^{rs}\right)}{df_k^{rs}} + \frac{1}{\theta_k} \cdot \frac{1}{f_k^{rs}} > 0 & k = l \\ 0 & otherwise \end{cases} \tag{B1.16}$$

With an increasing link travel time function with respect to link flow, Eq. (B2) implies the positive definite matrix. In summary, the proposed equilibrium model ()-() has a unique solution f_{uk}^{rs}, which leads to unique path flow f_k^{rs} and link flow x_a. This completes the proof.

B2. Proof of solution uniqueness for DNW equilibrium model (7.8)-(7.12)

Given the convex feasible region restricted by the sets of linear constraints, the proof of the unique modal demand outcome is equivalent to proving the strict convexity of the objective function (7.8). We first derive the Hessian matrix with respect to q_{um}^{rs}. For the diagonal elements:

$$\frac{\partial Z^2}{\partial q_{um}^{rs}\partial q_{wl}^{od}} = \frac{\partial \ln\left[\tau_{um}^{rs}(q_{um}^{rs})\right]}{\partial q_{wl}^{od}} + \frac{1}{\beta_{um}^{rs}} \cdot \frac{\partial \ln\left(q_{um}^{rs} - \dfrac{q_{rs}\eta_m^{rs}}{1+\sum_{n\in M}\eta_m^{rs}}\right)}{\partial q_{wl}^{od}} + \left(\frac{1}{\beta_u^{rs}} - \frac{1}{\beta_{um}^{rs}}\right) \cdot \frac{\partial \ln\left[\sum_{m\in M_u^{rs}}\left(q_{um}^{rs} - \dfrac{q^{rs}\eta_{um}^{rs}}{1+\sum_{m\in M}\eta_m^{rs}}\right)\right]}{\partial q_{wl}^{od}} \tag{B2.1}$$

According to Assumptions 7.2 and 7.3, the mode disutility is increasing with the increase of modal demand, thus the matrices with respect to the first term on the right-hand side of Eq. (B2.1) is positive semi-definite. The second and third terms are positive only when $u=w$ and $m=l$; otherwise, they equal to zero. The summation of positive semi-definite and positive definite matrices is positive definite.

In summary, the Hessian of objective function (7.8) is positive definite with respect to q_{um}^{rs}, which proves the uniqueness of the modal demand q_{um}^{rs}. This completes the proof.

B3. Proof of solution uniqueness for DCNW equilibrium model (8.11)-(8.14)

Given the convex feasible region restricted by the linear constraints, the proof of solution uniqueness is equivalent to proving the strict convexity of the objective function (8.11). Denoting $q_u^{rs} = \sum_{m \in M_u^{rs}} q_{um}^{rs}$ and $qc_u^{rs} = \sum_{m \in M_u^{rs}} q_{um}^{rs} - \frac{\eta_u^{rs} \cdot q^{rs}}{1 + \sum_{w \in U^{rs}} \eta_w^{rs}}$, the Hessian matrix with respect to q_u^{rs} is

$$\frac{\partial^2 Z}{\partial q_u^{rs} \partial q_w^{rs}} = \begin{cases} \frac{1}{\beta_u^{rs}} \cdot \frac{1}{qc_u^{rs}} - \frac{1}{\beta_{um}^{rs}} \cdot \frac{1}{q_u^{rs}} & u = w \\ 0 & Otherwise \end{cases}. \qquad \text{(B3.1)}$$

By definition, $qc_u^{rs} < q_u^{rs}$, and the shape parameter at the marginal choice level is smaller than that at the conditional choice level, i.e., $\beta_u^{rs} \le \beta_{um}^{rs}$. Therefore, $\frac{\partial^2 Z}{\partial q_u^{rs} \partial q_w^{rs}} > 0, \forall u = w$, the Hessian matrix with respect to q_u^{rs} is positive definite.

The Hessian matrix with respect to q_{um}^{rs} is

$$\frac{\partial^2 Z}{\partial q_{um}^{rs} \partial q_{un}^{rs}} = \begin{cases} \frac{1}{\tau_m^{rs}} \cdot \frac{d\tau_m^{rs}\left(q_{um}^{rs}\right)}{dq_{um}^{rs}} + \frac{1}{\beta_{um}^{rs}} \cdot \frac{1}{q_{um}^{rs}} > 0 & m = n \\ 0 & otherwise \end{cases}. \qquad \text{(B3.2)}$$

With an increasing mode travel disutility function with respect to modal demand, Eq. (B3.2) implies the positive definite matrix. In summary, the Hessian of objective function (8.11) is positive definite with respect to q_{um}^{rs}, i.e., the objective function is strictly convex. This completes the proof.

B4. Proof of solution uniqueness for SCW-PSW equilibrium model (9.4)-(9.10)

Given the convex feasible region restricted by the sets of linear constraints, the proof of the solution uniqueness is equivalent to proving the strict convexity of the objective function (9.4). We first derive the Hessian matrix with respect to $f_{s,m}^r$, *m=sp,cp*:

$$\frac{\partial^2 Z}{\partial f_{s,m}^r \partial f_{s,l}^r} = \begin{cases} \dfrac{1}{\tau_{s,m}^r\left(f_{s,m}^r\right)} \cdot \dfrac{d\tau_{s,m}^r\left(f_{s,m}^r\right)}{df_{s,m}^r} + \dfrac{1}{\beta_m} \cdot \dfrac{1}{f_{s,m}^r} > 0 & m = l \\ 0 & \text{Otherwise} \end{cases}. \quad \text{(B4.1)}$$

With the assumption that the parking disutility is increasing with respect to parking demand, Eq. (B4.1) implies the positive definite matrix.

Denote $q_{st}^r = q_{s,st}^r + q_{t,st}^r, \forall r \in R, st \in ST$. The Hessian matrix with respect to q_{st}^r is

$$\frac{\partial^2 Z}{\partial q_{st}^r \partial q_{ij}^h} = \begin{cases} \left(1-\mu\right) \cdot \dfrac{1}{q_{st}^r} > 0 & r = h, st = ij \\ 0 & \text{Otherwise} \end{cases}, \quad \text{(B4.2)}$$

which implies the positive definite matrix. The Hessian matrix with respect to $q_{s,st}^r$ is

$$\frac{\partial^2 Z}{\partial q_{s,st}^r \partial q_{i,ij}^h} = \begin{cases} \mu \cdot \dfrac{1}{q_{s,st}^r} - \dfrac{1}{\beta_m} \cdot \dfrac{1}{q_s^r} & r = h, s = i, t = j \\ 0 & \textit{Otherwise} \end{cases}. \quad \text{(B4.3)}$$

By definition, in the nested choice structure, the shape parameter for choices at the upper level should be smaller than the shape parameter for choices at the lower level, which requires the shape parameter for conditional destination choice smaller than that for parking choice i.e., $\beta_s < \beta_m$. Since β_s is normalized as $\frac{1}{\mu}$ in Section 9.3.2.1, we have $\mu > \frac{1}{\beta_m}$, which ensures $\mu \cdot \frac{1}{q_{s,st}^r} - \frac{1}{\beta_m} \cdot \frac{1}{q_s^r} > 0$. Therefore, the Hessian matrix with respect to $q_{s,st}^r$ is positive definite. In summary, the proposed equilibrium SCW-PSW model has a unique solution for both the destination flow q_s^r and parking flow $f_{s,sp}^r$, $f_{s,cp}^r$. This completes the proof.